

The Official Journal of the Chinese Stomatological Association (CSA)



# Chinese Journal of Dental Research

# CJDR

V  
O  
L  
U  
M  
E

**27**

**2  
0  
2  
4**

N  
U  
M  
B  
E  
R

**1**

# A COMPREHENSIVE GUIDE



Konrad Wangerin  
Caroline Fedder (Eds)

## Optimizing Orthognathic Surgery

Diagnosis, Planning, Procedures

416 pages, 1,450 illus

ISBN 978-1-78698-121-9

€228

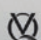
## OPTIMIZING ORTHOGNATHIC SURGERY

Diagnosis • Planning • Procedures


KONRAD WANGERIN  
CAROLINE FEDDER (EDS)

NEW

This book presents interdisciplinary treatment approaches for dysgnathia correction based on considerations of both orofacial function and facial esthetics. Written by international experts with over 30 years of surgical experience, valuable insights are shared through close collaboration with experts from various fields of dentistry and medicine. The integration of intraoral distraction surgery into orthognathic procedures is explored with a special focus on severe cases. The wealth of treatment strategies and solutions presented will navigate readers through the intricate pathways of managing complex craniofacial malformations.

 QUINTESSENZ PUBLISHING



 QUINTESSENZ PUBLISHING





# Chinese Journal of Dental Research

The Official Journal of the Chinese Stomatological Association (CSA)





# Chinese Journal of Dental Research

The Official Journal of the Chinese Stomatological Association (CSA)

## Chinese Stomatological Association Position Statements

- 11 Preserving Natural Teeth to Maintain Oral Health
- 13 Wearing Sports Mouthguards to Prevent Oral and Maxillofacial Trauma

## Reviews

- 17 The Role of DSPP in Dentine Formation and Hereditary Dentine Defects  
Jie JIA, Zhuan BIAN, Yaling SONG
- 29 Review on the Role of *IRF6* in the Pathogenesis of Non-syndromic Orofacial Clefts  
Si Di ZHANG, Yue YOU, Mei Lin YAO, Bing SHI, Zhong Lin JIA
- 39 Characteristic and Import Mechanism of Protein Nuclear Translocation  
Zi Yan SUN, Zhi Peng FAN
- 47 Distinctive Craniofacial and Oral Anomalies in *MN1* C-terminal Truncation Syndrome  
Jing Jia YU, Qiu Yi WU, Qiu Chi RAN, Ying Ya ZHAO, Lin Nan YU, Qing Xin CAO, Xi Meng CHEN, Wen Yang LI, Zhen Jin ZHAO

## Original articles

- 53 *FAM20A*-Associated Amelogenesis Imperfecta: Gene Variants with Functional Verification and Histological Features  
Jia Nan DING, Miao YU, Hao Chen LIU, Kai SUN, Jing WANG, Xiang Liang XU, Yang LIU, Dong HAN



- 
- 65 Integrative Multi-omics Analysis Identifies Genetic Variants Contributing to Non-syndromic Cleft Lip with or without Cleft Palate  
Shu LOU, Jing YANG, Gui Rong ZHU, Dan Dan LI, Lan MA, Lin WANG, Yong Chu PAN
- 75 Knowledge Mapping of Cowden Syndrome: a Bibliometric Analysis  
Qiao PENG, Ning DUAN, Xiang WANG, Wen Mei WANG
- 83 Novel *PTCH1* Mutation Causes Gorlin-Goltz Syndrome  
Hai Tang YUE, Hai Yan CAO, Miao HE
- 89 Clinical and Genetic Analysis of Multiple Idiopathic Cervical Root Resorption  
Yu Meng WANG, Wen Yan RUAN, Dan Dan CHI, Xiao Hong DUAN
- 101 Hub Genes, Possible Pathways and Predicted Drugs in Hereditary Gingival Fibromatosis by Bioinformatics Analysis  
Rong Xia YANG, Fan SHI, Shu Ning DU, Xin Yu LUO, Wan Qing WANG, Zhi Lu YUAN, Dong CHEN

# Chinese Journal of Dental Research

CN 10-1194/R • ISSN 1462-6446 • eISSN 1867-5646 • Quarterly

The Official Journal of the Chinese Stomatological Association

Co-sponsor: Peking University School of Stomatology, Quintessenz Verlag

## Editor-in-Chief

**Chuan Bin GUO** Beijing, P.R. China

## Chief-Editor Emeritus

**Zhen Kang ZHANG** Beijing, P.R. China  
**Xing WANG** Beijing, P.R. China  
**Xu Chen MA** Beijing, P.R. China  
**Guang Yan YU** Beijing, P.R. China  
**Xue Dong ZHOU** Chengdu, P.R. China

## Executive Associate Editor

**Qian Ming CHEN** Hangzhou, P.R. China

## Executive Editors

**Ye Hua GAN** Beijing, P.R. China  
**Hong Wei LIU** Beijing, P.R. China

## Associate Editors

**Li Juan BAI** Beijing, P.R. China  
**Zhuan BIAN** Wuhan, P.R. China  
**Fa Ming CHEN** Xi'an, P.R. China  
**Bin CHENG** Guangzhou, P.R. China  
**Xu Liang DENG** Beijing, P.R. China  
**Xin Quan JIANG** Shanghai, P.R. China  
**Tie Jun LI** Beijing, P.R. China  
**Hong Chen SUN** Changchun, P.R. China  
**Song Ling WANG** Beijing, P.R. China  
**Ling YE** Chengdu, P.R. China  
**Zhi Yuan ZHANG** Shanghai, P.R. China  
**Yi Min ZHAO** Xi'an, P.R. China  
**Yong Sheng ZHOU** Beijing, P.R. China

## Editorial Board

**Tomas ALBREKTSSON**

Gothenburg, Sweden

**Conrado APARICIO**

Barcelona, Spain

**Daniele BOTTICELLI**

Rimini, Italy

**Lorenzo BRESCHI**

Bologna, Italy

**Francesco CAIRO**

Florence, Italy

**Tong CAO**

Singapore

**Jack G. CATON**

Rochester, USA

**Yang CHAI**

Los Angeles, USA

**Wan Tao CHEN**

Shanghai, P.R. China

**Zhi CHEN**

Wuhan, P.R. China

**Bruno CHRCANOVIC**

Malmö, Sweden

**Kazuhiro ETO**

Tokyo, Japan

**Bing FAN**

Wuhan, P.R. China

**Zhi Peng FAN**

Beijing, P.R. China

**Alfio FERLITO**

Udine, Italy

**Roland FRANKENBERGER**

Marburg, Germany

**Xue Jun GAO**

Beijing, P.R. China

**Sufyan GAROUSHI**

Turku, Finland

**Reinhard GRUBER**

Vienna, Austria

**Gaetano ISOLA**

Catania, Italy

**Søren JEPSEN**

Bonn, Germany

**Li Jian JIN**

Hong Kong SAR, P.R. China

**Yan JIN**

Xi'an, P.R. China

**Newell W. JOHNSON**

Queensland, Australia

**Thomas KOCHER**

Greifswald, Germany

**Ralf-Joachim KOHAL**

Freiburg, Germany

**Niklaus P. LANG**

Bern, Switzerland

**Junying LI**

Ann Arbor, USA

**Yi Hong LI**

New York, USA

**Wei LI**

Chengdu, P.R. China

**Huan Cai LIN**

Guangzhou, P.R. China

**Yun Feng LIN**

Chengdu, P.R. China

**Hong Chen LIU**

Beijing, P.R. China

**Yi LIU**

Beijing, P.R. China

**Edward Chin-Man LO**

Hong Kong SAR, P.R. China

**Jeremy MAO**

New York, USA

**Tatjana MARAVIC**

Bologna, Italy

**Claudia MAZZITELLI**

Bologna, Italy

**Mark MCGURK**

London, UK

**Li Na NIU**

Xi'an, P.R. China

**Jan OLSSON**

Gothenburg, Sweden

**Gaetano PAOLONE**

Milan, Italy

**No-Hee PARK**

Los Angeles, USA

**Peter POLVERINI**

Ann Arbor, USA

**Lakshman SAMARANAYAKE**

Hong Kong SAR, P.R. China

**Keiichi SASAKI**

Miyagi, Japan

**Zheng Jun SHANG**

Wuhan, P.R. China

**Song SHEN**

Beijing, P.R. China

**Song Tao SHI**

Guangzhou, P.R. China

**Richard J. SIMONSEN**

Downers Grove, USA

**Manoel Damião de**

**SOUSA-NETO**

Ribeirão Preto, Brazil

**John STAMM**

Chapel Hill, USA

**Lin TAO**

Chicago, USA

**Tiziano TESTORI**

Ann Arbor, USA

**Cun Yu WANG**

Los Angeles, USA

**Hom-Lay WANG**

Ann Arbor, USA

**Zuo Lin WANG**

Shanghai, P.R. China

**Heiner WEBER**

Tuebingen, Germany

**Xi WEI**

Guangzhou, P.R. China

**Yan WEI**

Beijing, P.R. China

**Ray WILLIAMS**

Chapel Hill, USA

**Jie YANG**

Philadelphia, USA

**Quan YUAN**

Chengdu, P.R. China

**Jia Wei ZHENG**

Shanghai, P.R. China

## Publication Department

**Production Manager:** Megan Platt (London, UK)

**Managing Editor:** Xiao Xia ZHANG (Beijing, P.R. China)

**Address:** 4F, Tower C, Jia 18#, Zhongguancun South Avenue, HaiDian District, 100081, Beijing, P.R. China.

**Tel:** 86 10 82195785, **Fax:** 86 10 62173402

**Email:** editor@cjdrcsa.com

**Manuscript submission:** Information can be found on the Guidelines for Authors page in this issue. To submit your outstanding research results more quickly, please visit: <http://mc03.manuscriptcentral.com/cjdr>

**Administered by:** China Association for Science and Technology

**Sponsored by:** Chinese Stomatological Association and Popular Science Press

**Published by:** Popular Science Press

**Printed by:** Beijing ARTRON Colour Printing Co Ltd

**Subscription (domestically)** by Post Office

Chinese Journal of Dental Research is indexed in MEDLINE.

For more information and to download the free full text of the issue, please visit [www.quint.link/cjdr](http://www.quint.link/cjdr)  
<http://www.cjdrcsa.com>

# Acknowledgements

We would like to express our gratitude to the peer reviewers for their great support to the journal in 2023.

Afrashtehfar, Kelvin (Switzerland)	Han, Dong (China)	Ren, Yi Jin (Netherlands)
Agudelo-Suárez, Andrés (Colombia)	Hashimoto, Kenji (Japan)	Ritchie, Helena H. (United States)
Aksoy, Merve (Turkey)	He, Miao (China)	Rodrigues, Gabriel (Oman)
Alkan Aygor, Fehime (Turkey)	Hong, Guang (Japan)	Saber, Shehabeldin Mohamed (Egypt)
Al-Nuaimi, Nassr (United States)	Hourfar, Jan (Germany)	Saddki, Norkhafizah (Malaysia)
An, Na (China)	Hu, Wen Jie (China)	Saito, Hanae (United States)
Ananthaswamy, Akanksha (India)	Hua, Fang (China)	Sarialioglu Gungor, Ayça (Turkey)
Arpornmaeklong, Premjit (Thailand)	Huang, Zhen (China)	Sharma, Rajinder K. (India)
Arslan, Merve (Turkey)	Jayasinghe, Ruwan D (Sri Lanka)	Shi, Song Tao (China)
Ateş, Melis Oya (Turkey)	Ji, Yi (China)	Si, Yan (China)
Ayna, Emrah (Turkey)	Jiang, Hong Bing (China)	Song, Jin Lin (China)
Ballal, Nidambur (India)	Jiang, Jiu Hui (China)	Song, Xiao Meng (China)
Banerjee, Santasree (China)	Ju, Xiang Qun (Australia)	Song, Ya Ling (China)
Bayindir, Funda (Turkey)	Kaklamanos, Eleftherios G (Cyprus)	Sousa-Neto, Manoel D. (Brazil)
Bi, Liang Jia (China)	Karadas, Muhammet (Turkey)	Su, Guan Yue (China)
Bilgili, Dilber (Turkey)	Khan, Sher Alam (Pakistan)	Sui, Bing Dong (China)
Brailo, Vlaho (Croatia)	Khijmatgar, Shah Nawaz (India)	Sulaiman, Ghassan M. (Iraq)
Buldur, Burak (Turkey)	Kinzinger, Gero (Germany)	Sun, Qiang (China)
Cao, Zheng Guo (China)	Kurt, Aysegul (Turkey)	Sun, Yu Chun (China)
Chabbra, Ajay (India)	Li, Gang (China)	Sun, Zhi Peng (China)
Chai, Yang (United States)	Li, Yi Hong (United States)	Taneja, Pankaj (Denmark)
Chen, Bin (China)	Li, Yu (China)	Tang, Qing Ming (China)
Chen, Chen (China)	Li, Ze Han (China)	Tao, Ren Chuan (China)
Chen, Fa Ming (China)	Lin, Min Kui (China)	Topsakal, Kubra Gulnur (Turkey)
Chen, Li (China)	Lin, Xiao Ping (China)	Tsoi, James (HK, China)
Chen, Li Li (China)	Liu, Da Wei (China)	Tuovinen, Olli (United States)
Chen, Peng (China)	Liu, Da Yong (China)	Uzun, Ismail (Turkey)
Chen, Tao (China)	Liu, Hai Bo (China)	Wajid Hussain Chan, Malik (Pakistan)
Chen, Zhi (China)	Liu, Hong Wei (China)	Wang, Chun Li (China)
Chu, Chun Hung (HK, China)	Liu, Huan (China)	Wang, Fu (China)
Cui, Li (United States)	Liu, Jian Zhang (China)	Wang, Lin (China)
Dede, Dogu Omur (Turkey)	Liu, Jia Qiang (China)	Wei, Fu Lan (China)
Dehghanian, Danoosh (Iran)	Liu, Min (China)	Wei, Xi (China)
Desai, Rajiv S (India)	Liu, Yao (China)	Wu, Tao (China)
Ding, Ming Chao (China)	Liu, Ya Wei (China)	Wu, Yi Qun (China)
Dong, Yan Mei (China)	Lu, Yan (China)	Xie, Shang (China)
Eaton, Kenneth (United Kingdom)	Lucchese, Alessandra (Italy)	Xu, Kang (China)
El-Bialy, Tarek (Canada)	Mady, Fatma (Egypt)	Xu, Tian Min (China)
Elias, Carlos N (Brazil)	Mahjabeen, Wajiha (Pakistan)	Yu, Jin Hua (China)
Erber, Ralf (Germany)	Mossey, P. A. (United Kingdom)	Yu, Xi Jiao (China)
Esen, Çağrı (Turkey)	Nassani, Mohammad zakaria (Saudi Arabia)	Yuan, Quan (China)
Fan, Yuan (China)	Nayak, Ullal Anand (Saudi Arabia)	Zadeh, Homayoun H. (United States)
Fan, Zhi Peng (China)	Neves, Lucimara Teixeira das (Brazil)	Zeng, Xiao Juan (China)
Fathy Abo-Elmahasen, Mahmoud M (Egypt)	Niu, Li Na (China)	Zhang, Cheng Fei (HK, China)
Feng, Chen (China)	Özdemir, Burcu (Turkey)	Zhang, Hao (China)
Fu, Kai Yuan (China)	Ozturk, Taner (Turkey)	Zhang, Hong Liang (China)
Gallo, Camila (Brazil)	Pan, Shao Xia (China)	Zhang, Lei (China)
Gan, Ye Hua (China)	Pan, Ya Ping (China)	Zhao, Yu Ming (China)
Gao, Xue Jun (China)	Pan, Yong Chu (China)	Zheng, Shu Guo (China)
Garoushi, Sufyan (Finland)	Park, Joo-Cheol (Korea)	Zheng, Yun Fei (China)
Geduk, Gediz (Turkey)	Pei, Dan Dan (China)	Zhou, Hai Hua (China)
Grigorian, Mircea (Romania)	Pereira, Jefferson Ricardo (Brazil)	Zhou, Hong Mei (China)
Gruber, Reinhard (Austria)	Pugazhendhi, Sathish kumaran (India)	Zhou, Ping (United States)
Gu, Yong Chun (China)	Qin, Li Zheng (China)	Zhu, Xiao Fei (China)
Gündoğar, Mustafa (Turkey)	Ren, Xiu Yun (China)	Zong, Chen (Belgium)

Editorial Office

*Chinese Journal of Dental Research*



## Editorial

**T**ime flies and 2024 is here. I would like to thank all our excellent collaborators in London and Berlin and our colleagues for their great contributions to the development of the journal over the past year.

In the first issue for this year, we have two Chinese Stomatological Association (CSA) position statements. One is entitled “Preserving natural teeth to maintain oral health”, and the other is “Wearing sports mouthguards to prevent oral and maxillofacial trauma”. They both respond to the theme of the 2023 CSA Academic Annual Congress, calling to protect natural teeth and promote oral health.

This is also a special issue on oral and maxillofacial hereditary and rare diseases, with contributions from the Hereditary and Rare Diseases Society of the CSA. There are four reviews and six original articles, all of which provide a comprehensive understanding of many topics in this field.

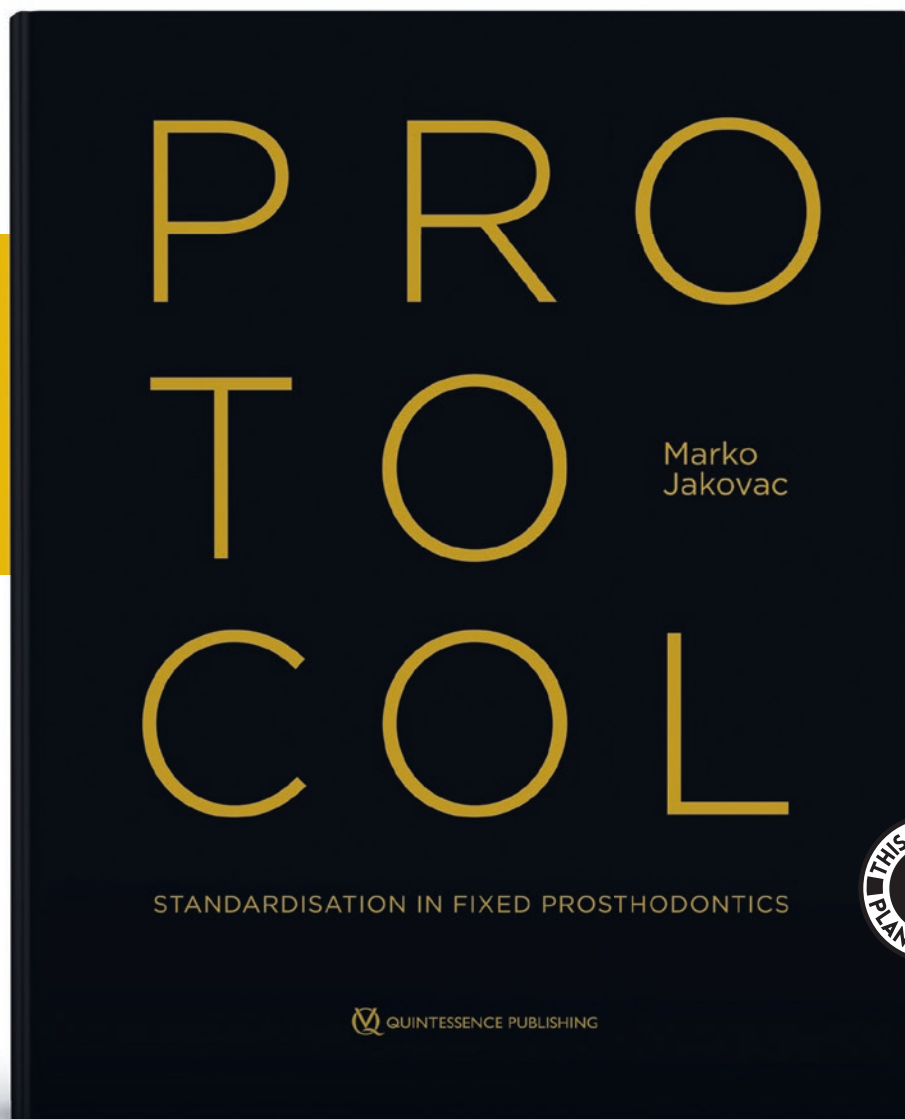
The review entitled “The role of DSPP in dentine formation and hereditary dentine defects” from Prof Song’s team at Wuhan University focuses on recent findings and viewpoints regarding the relationship between dentine sialophosphoprotein (DSPP) and dentinogenesis as well as mineralisation from multiple perspectives, which provide a complete illustration of DSPP in dental research. “Review on the role of *IRF6* in the pathogenesis of non-syndromic orofacial cleft (NSOC)” by Prof Jia’s team at Sichuan University summarises the progress of research into the mechanism of *IRF6* in NSOCs from both genetic and functional aspects. “Characteristic and import mechanism of protein nuclear translocation” by Prof Fan’s team at Capital Medical University provides an overview of the proteins involved in nuclear transport and the mechanisms underlying macromolecular protein transport as well as their potential relation to novel therapeutic strategies. “Distinctive craniofacial and oral anomalies in *MNI* C-terminal truncation syndrome” by Prof Zhao’s team at China Medical University describes this rare condition with their own cases and a detailed review of the reported cases.

The six original articles examine different hereditary and rare oral diseases using different methods of genetic research. Prof Han’s team from Peking University investigated new *FAM20A* gene variants and histological features of amelogenesis imperfecta and further explored the functional impact of these variants, and Prof He’s team from Wuhan University found a novel *PTCH1* mutation causing Gorlin-Goltz syndrome. Both of these articles broaden the spectrum of variants and offer new information on associated diseases. Prof Pan’s team from Nanjing Medical University provide novel insights into the aetiology of non-syndromic cleft lip with or without cleft palate (NSCL/P) by integrating multi-omics data and exploring susceptibility genes, and their findings contribute to a better understanding of the genetic factors involved in NSCL/P. Using a bibliometric analysis, Prof Wang’s team from Nanjing University offer a comprehensive overview of the current knowledge structure of and research hotspots for Cowden syndrome. Prof Duan’s team from The Fourth Military Medical University explored the genetic background and clinical phenotypes of multiple idiopathic cervical root resorption (MICRR) in a Chinese family and found 35 novel potential pathogenic genes, which might be helpful for the clinical and molecular diagnosis. Prof Chen’s team from Zhengzhou University explored potential pathogenic processes of hereditary gingival fibromatosis (HGF) and possible treatment using unbiased and reliable bioinformatic tools, and the research offers some novel insights into molecular pathways and identifies five hub genes associated with cell adhesion. Based on these hub genes, three potential therapeutic miRNAs and small molecule drugs were predicted, which are expected to provide guidance for the treatment of patients with HGF.

I believe our readers will find these reviews and articles highly informative and extremely interesting.

Prof Chuan-bin Guo  
Editor-in-Chief  
President of the Chinese Stomatological Association

# ENHANCE YOUR EXPERTISE



Marko Jakovac

## Protocol: Standardisation in Fixed Prosthodontics

732 pages, 1,200 illus.  
ISBN 978-1-78698-117-2, €300



Fixed prosthodontic therapy is one of the most demanding disciplines in dentistry. This avenue is usually pursued only after other options have been exhausted, often when teeth are missing or show reduced durability, or in the presence of conditions that cannot be treated conservatively. Enhance your expertise with this comprehensive text that presents the key steps to success at every stage of therapy: planning, execution, manufacturing, and finalization. Discover the importance of meticulous treatment planning to meet patients' short- and long-term requirements; learn key principles and techniques for effective

and minimally invasive tooth preparation; avoid mistakes caused by performing procedures without proper guidance; embrace the latest techniques and technologies for creating high-quality prosthetic restorations; explore the intricacies of cementation for optimal adhesion and retention; and learn how to strategize to maintain restoration success and oral health. Whether you are an experienced clinician or a dental professional seeking to expand your practice, the protocol-driven approach advocated in this text will equip you to achieve consistent and exceptional results with fixed prosthodontic therapy.



[www.quint.link/protocol](http://www.quint.link/protocol)



[books@quintessenz.de](mailto:books@quintessenz.de)



+49 (0)30 761 80 667

 **QUINTESSENZ PUBLISHING**

# Preserving Natural Teeth to Maintain Oral Health

Chinese Stomatological Association<sup>1</sup>

*Oral health is an important component of general health, and oral disease is one of the most common human diseases that not only affects oral health and quality of life, but is also closely associated with overall health. Natural teeth are important functional organs and are crucial to oral functions and maintaining a healthy life. The Chinese Stomatological Association (CSA) has released this position statement on “Preserving Natural Teeth to Maintain Oral Health”, which is one of the most important achievements of the 2021 to 2023 CSA Annual Congress themed “Healthy Mouth, Protecting Natural Teeth”, advocating that everyone should take effective measures to protect their natural teeth, maintain oral health and promote general health. Chin J Dent Res 2024;27(1):11–12; doi: 10.3290/j.cjdr.b5139365*

## Taking measures actively to prevent oral diseases

Preventing oral diseases requires a joint effort from the public and oral professionals. The public must take responsibility for maintaining their own oral health, and should take the following preventive measures actively to avoid the occurrence of oral diseases and preserve healthy natural teeth:

- Learn about oral health to adopt healthy behaviours.
- Pay attention to oral cleansing throughout the lifetime to maintain oral hygiene. Avoid risk factors that can lead to oral diseases, for example by following a healthy diet, quitting smoking, limiting alcohol intake and avoiding betel nut.
- Implement topical fluoride application to prevent dental caries. Brush teeth using fluoride toothpaste in the morning and evening for at least 2 minutes each time. People at high risk of dental caries should visit their dental practitioner two to four times a year to receive professional fluoride application.
- Undergo professional tooth scaling once or twice a year to prevent dental caries and periodontal disease.

- Attend an oral examination at least once a year and seek professional advice on prevention and treatment.
- Receive pit and fissure sealant treatment to prevent pit and fissure caries in children and adolescents.
- Wear mouthguards for protection during sport and strenuous exercise to prevent oral maxillofacial trauma.

Oral professionals should fulfil oral health education duties.

They need to implement the concept of “prevention first” and carry out oral health education and promotion activities in depth to build a good oral health platform and create an environment that promotes caring for oral health, and to encourage the public to improve their oral health awareness and adopt good oral health behaviours. To combine the science communication of oral health with regular dental practice, the following recommendations are made:

- Disseminate oral health knowledge widely through the mass media, making full use of oral health-themed or related days, such as World Oral Health Day on 20 March, Children’s Day on 1 June and National Love Your Teeth Day on 20 September.
- Participate in popular science and produce public-friendly popular science works in various forms and styles that are easy to understand and remember.
- Make full use of the public areas in dental institutes to create an oral health education centre, including by

<sup>1</sup> This is authored by Dr Yan SI, Dr Xue Nan LIU, Prof Lin YUE and Prof Guang Yan YU.

Correspondence to: Prof Guang Yan YU and Prof Lin YUE. Email: gyyu@263.net, kqlinyue@bjmu.edu.cn



setting up publicity boards in the registration hall and oral health education corners in the waiting area, and displaying multi-dimensional promotional material in posters, boards, flyers, videos, etc.

- Offer personalised chairside oral health education according to patients' individual problems.
- Encourage the public to receive regular oral health checkups.
- Promote the implementation and application of appropriate technologies for the prevention of oral diseases.

### Early diagnosis and treatment of oral diseases

Oral diseases can be prevented and treated at an early stage. Early detection and treatment could save treatment time and costs and maximise the retention of natural teeth. Methods for early diagnosis and treatment include:

- Preventing the occurrence and development of periodontal diseases by performing regular periodontal examinations and early periodontal basic treatment, and treating gingivitis with supragingival cleaning to prevent the development of periodontitis.
- Treating dental caries and other dental diseases and repairing dental defects to prevent the progression of dental pulp diseases, maxillofacial inflammation and even systemic diseases in a timely manner.
- Correcting malocclusion deformity at an early stage to establish the normal occlusal function, promote the normal development of the maxillofacial region and maintain the health of the oral and maxillary system.
- Preventing serious loss of oral cavity function and reducing the threat to life by performing early screening for oral cancer, and detecting lesions in a timely manner and controlling their progression.

### Trying to preserve natural teeth

Natural teeth are essential for oral function. For teeth suffering from disease, appropriate treatment measures should be taken actively to preserve natural teeth, restore function and maintain the integrity of the dentition. The following measures can be taken:

- Preserving healthy teeth and prolonging the life of natural teeth through supragingival cleaning, subgingival scraping and performing periodontal surgery and endodontic treatment when necessary.
- Carrying out the necessary crown restoration in a timely manner to prevent tooth splitting after large-area tooth defect or root canal treatment.
- Using appropriate orthodontic methods to correct the misalignment of teeth to prevent the aggravation of malocclusion.
- Removing the malpositioned or even impacted wisdom teeth as soon as possible to avoid affecting the health of neighbouring teeth. Normally, there is no need to repair the wisdom teeth after removal. Wisdom teeth that erupt in the right position with an occlusal relationship can be retained.
- Extracting teeth that that oral professionals deem unable to be retained in a timely manner to avoid affecting the health of other teeth and surrounding tissues.
- Restoring missing teeth in a timely manner to maintain the integrity of the dentition, perform normal functions and improve quality of life.

September 2023

# Wearing Sports Mouthguards to Prevent Oral and Maxillofacial Trauma

Chinese Stomatological Association<sup>1</sup>

*The theme of the academic annual conferences held by the Chinese Stomatological Association from 2021 to 2023 was “Protecting Natural Teeth to Maintain Oral Health” and coincided with the 24th Winter Olympic Games that took place in Beijing in 2022, and thus prevention of oral and maxillofacial trauma once again attracted the attention of stomatological experts and the public. The incidence of oral and maxillofacial trauma caused by sports is around 25% to 34%<sup>1-5</sup>, and varies based on the type of sport and other factors, such as age, sex and the skill level of the participants. The risk of oral and maxillofacial trauma is extremely high in high-confrontation and high-speed sports, especially for children and adolescents. Wearing sports mouthguards when participating in sport is an effective way to prevent and reduce the incidence of oral and maxillofacial trauma in such sports, and is the simplest and most practical method of doing so. Sports have developed and gained in popularity significantly in China in recent years, but the awareness and use of sports mouthguards are low. Based on the above background, the Chinese Stomatological Association advocates that athletes and sport participants should wear mouthguards in various confrontational and high-speed sports, and calls on dental practitioners and sports-related organisations to actively support the popularisation and application of sports mouthguards to prevent or alleviate oral and maxillofacial trauma and to raise awareness and increase knowledge of methods to protect natural teeth.*

*Chin J Dent Res 2024;27(1):13–15; doi: 10.3290/j.cjdr.b5139351*

## Role and use of sports mouthguards

### *Protective effect of sports mouthguards*

Sports mouthguards protect the teeth, periodontal tissues, oral soft tissues, jaws, temporomandibular joints and even the brain by cushioning impact force<sup>6</sup>. Wearing a mouthguard can reduce the incidence and severity of oral and maxillofacial trauma experienced in sport significantly. The protective effects include:

- the ability to absorb and disperse the impact force to prevent or mitigate dental traumas, oral soft tissue injuries, and alveolar bone and jaw bone fractures;
- the ability to stabilise the mandible when subjected to traumatic external force to prevent mandibular fracture or reduce the severity of fracture;

- the ability to cushion the upward impact force on the mandible between the maxillary and mandibular teeth to avoid maxillary and mandibular dental trauma, bone fracture, temporomandibular joint injury and even skull base injury, or reduce the degree of trauma;
- the ability to prevent damage to the oral and maxillofacial soft and hard tissues and temporomandibular joint caused by clenching the teeth during sports.

The protective effect of sports mouthguards varies based on the type, material, method of manufacture, thickness, fit, extension and user compliance.

In addition to directly preventing sports injuries, wearing mouthguards may have additional positive effects for the user. For example, they may enhance the athlete's sense of security and increase the strength of the masticatory muscle, which in turn reflexively increases muscle strength throughout the whole body to improve athletic performance.

<sup>1</sup> This is authored by Dr Hong Qiang YE, Prof Lin YUE and Prof Ya Dong YANG.

## *Types and characteristics of sports mouthguards*

### **Prefabricated sports mouthguard**

This type of sports mouthguard is prefabricated by the manufacturer and can be purchased directly, available in multiple sizes and at the cheapest price. The disadvantages include the lack of individual suitability, poor retention and stability, poor protection, bulkiness, impact on breathing and speech, and lack of comfort. It is generally not recommended except for emergency or cost considerations.

### **Mouth-formed sports mouthguard**

This type of mouthguard is prefabricated using elastic resin material with thermoplasticity. After softening in hot water, it can be shaped in the mouth with movements of perioral soft tissue, application of finger pressure and biting. It is the most widely used type and can be purchased directly, and it is affordable and easy to use and has a certain protective effect. However, its fit, retention and stability are not optimal.

### **Customised sports mouthguard**

This type of sports mouthguard is designed and made by dental professionals in accordance with the user's dentition morphology, age, type of sport, intensity of sports confrontation and personal preference. It is the preferred type of mouthguard because it offers good retention, stability, fit, protection and comfort, and causes minimal interference with speech and breathing. Due to the difference in intensity of the impact force on the maxillofacial region in different sports, the characteristics of customised sports mouthguards, such as material, thickness and extension, should be designed differently based on the protective requirements.<sup>7</sup>

### *Indications for use of sports mouthguards*

Confrontational or high-speed sports or recreational activities, such as boxing, sparring, wrestling, ice hockey, basketball, lacrosse, rugby, cycling, ice skating, skiing, car racing, parachuting and extreme sports, present a risk of trauma due to the impact forces on the oral and maxillofacial regions. As a result, participants who practise or compete in these activities should wear mouthguards, preferably customised.

## *Maintenance and replacement of sports mouthguards*

Sports mouthguards and the boxes used to store them should be scrubbed using a soft-bristled toothbrush and toothpaste, then rinsed with cold or lukewarm water. Antibacterial agents or denture cleaning tablets can also be used. Mouthguards can be soaked in rigid containers with clear water after being washed, thus avoiding the high temperature of the storage environment. Ultrasonic cleaners can also be used regularly for cleaning.<sup>8</sup> In the event of obvious abrasion, tears and deformation, the mouthguard should be evaluated by the dental practitioner to evaluate whether it needs to be replaced. It is advisable to replace sports mouthguards every 1 to 2 years. For growing children and adolescents or adolescents undergoing orthodontic treatment, the interval between the replacement of mouthguards should be shortened.

### **Health education and guidance for wearing sports mouthguards**

#### *Public education for sports participants and the public*

The reasons why sports participants rarely wear mouthguards may include a lack of understanding of or negligence towards sports traumas, a lack of understanding of sports mouthguards, poor comfort, high cost, and inappropriate selection. Therefore, there is an urgent need to educate and guide sports participants and the public, with the most critical messages being as follows:

- The risks and consequences of oral and maxillofacial trauma in sport should be understood.
- Wearing sports mouthguards can effectively prevent sports trauma or reduce its extent in the oral and maxillofacial region.
- Wearing sports mouthguards is far better than not wearing them. While customised mouthguards are preferred, other types can certainly be effective when worn properly.

#### *Requirements for dental practitioners*

Dental practitioners play an important role in sports participants' compliance with the use of mouthguards, and compliance directly affects the effectiveness of their use. The requirements for dental practitioners are as follows:

- to pay closer attention to the prevention of oral and maxillofacial sports injuries and recognise the importance of wearing mouthguards for sports participants;
- to provide professional guidance and services relating to the selection, customisation, use, maintenance and replacement of sports mouthguards;
- to enhance the awareness of and ability to publicise sports mouthguards and encourage the public to maintain oral health and protect their natural teeth while actively participating in sports to strengthen their body and mind.

### *Strengthening the health education and management responsibilities of relevant departments*

Government departments related to health, sports and education should strengthen the publicity of knowledge of this statement to schools, organisers of sports games, sports participants, sports coaches and the media. They should vigorously promote the popularisation and correct use of sports mouthguards in sports activities, especially in high-confrontation and high-speed sports.

The relevant management authorities should develop and supervise systems and rules requiring participants to wear sports mouthguards during high-confrontation and high-speed sports and activities.

Sports coaches should possess the ability to provide athletes with knowledge and methods of preventing and rescuing oral and maxillofacial injuries, and to encourage athletes to wear mouthguards during sports.

The public media should actively cooperate with the popularisation of sports mouthguards to create a positive atmosphere in which the public pays attention to sports and sports trauma, cares for sports participants and uses sports mouthguards.

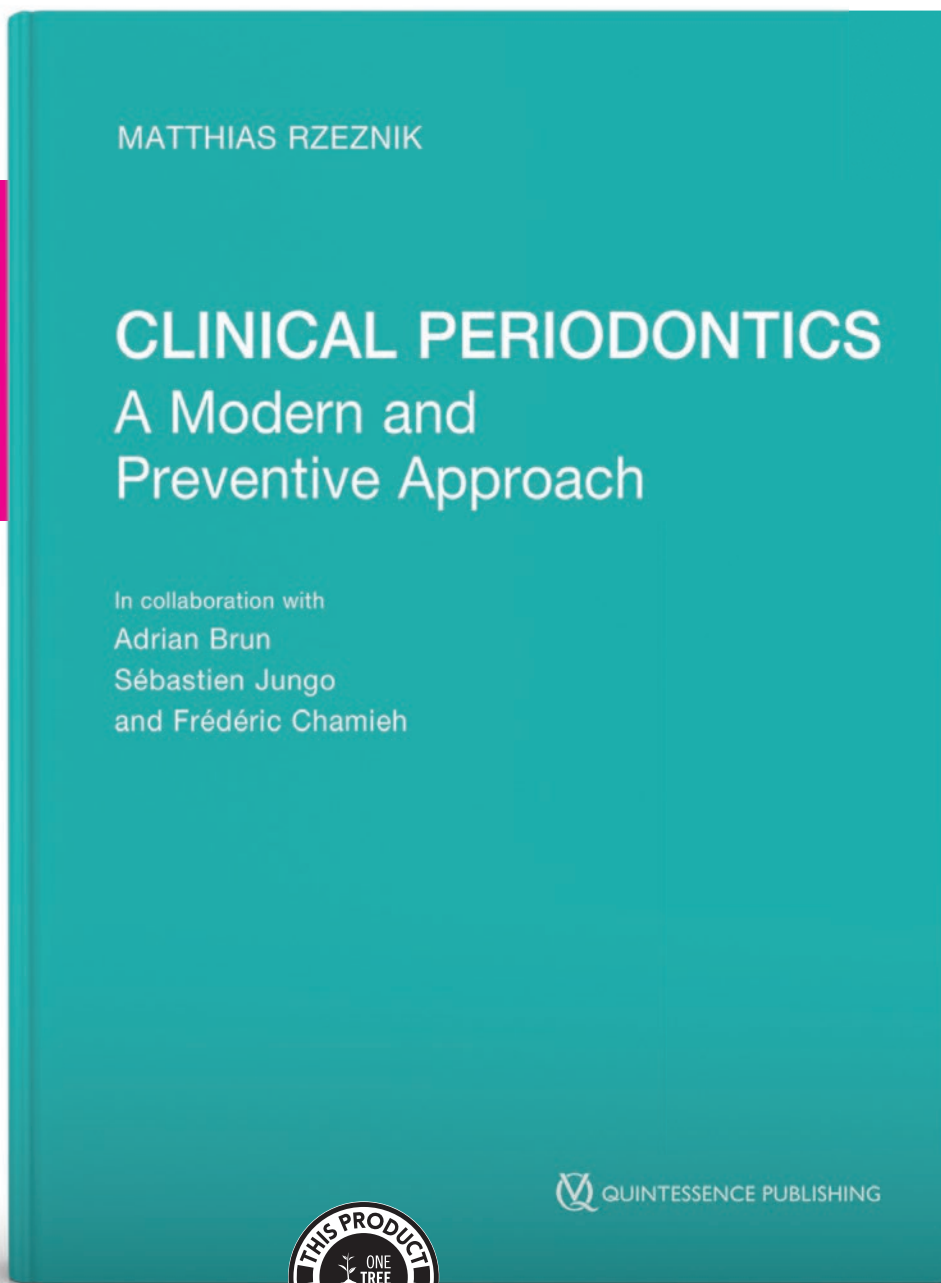
To avoid or mitigate oral and maxillofacial trauma that occurs in sports as much as possible, to reduce the adverse physiological, psychological and economic consequences for individuals caused by sports trauma, and to reduce the burden on the public healthcare system, sports mouthguards should be promoted vigorously as an effective protective device.

September 2023

### References

1. Bojino A, Roccia F, Giaccone E, Cocis S. Comprehensive analyses of maxillofacial fractures due to non-professional sports activities in Italy. *Dent Traumatol* 2020;36:632–640.
2. Sarao SK, Rattai J, Levin L. Dental trauma among hockey players: Preventive measures, compliance and injury types. *J Can Dent Assoc* 2021;87:18.
3. Polmann H, Melo G, Conti Réus J, et al. Prevalence of dentofacial injuries among combat sports practitioners: A systematic review and meta-analysis. *Dent Traumatol* 2020;36:124–140.
4. Chen L, Wang J, Liu P. Epidemiologic study of amateur boxing sport injury in China [in Chinese]. *Zhongguo Yun Dong Yi Xue Za Zhi (Chin J Sports Med)* 2011;30:124–140.
5. Wang Y, Wang H. Investigation on the characteristics and prevention strategies of maxillofacial trauma in Beijing 2022 Olympic Winter Games [in Chinese]. *Zhongguo Ti Yu Ke Ji (China Sport Science and Technology)* 2020;56:65–71.
6. Ge L. *Pediatric Dentistry*, ed 5. Beijing: People's Medical Publishing, 2020:155–156.
7. Roberts HW. Sports mouthguard overview: Materials, fabrication techniques, existing standards, and future research needs. *Dent Traumatol* 2023;39:101–108.
8. Sliwkanich L, Ouanounou A. Mouthguards in dentistry: Current recommendations for dentists. *Dent Traumatol* 2021;37:661–671.

# DETAILED AND THOROUGH



Matthias Rzeznik

## Clinical Periodontics

A Modern and Preventive Approach

Incl 94 Videos, 312 pages, 553 illus

ISBN 978-1-78698-140-0

€178

This book describes a simplified and innovative approach to the prevention and management of periodontal diseases. Learn the keys to success as you follow diverse clinical cases and study the accompanying tips for working with patients and making tailored recommendations for dental hygiene products and protocols. Accurate observations and diagnoses as well as the ability to discuss treatment with your patients so that they understand their important role in the maintenance of periodontal health are critical for providing effective, simple, and pain-free treatment. The details of each step in the management process are thoroughly covered, from first consultation to follow-up maintenance. You will find plenty of photographs and explanatory clinical videos to help you put these therapies into practice right away!



QUINTESSENCE PUBLISHING

QUINTESSENCE PUBLISHING



[www.quint.link/clinical-perio](http://www.quint.link/clinical-perio)



[books@quintessenz.de](mailto:books@quintessenz.de)



+49 (0)30 761 80 667

QUINTESSENCE PUBLISHING



# The Role of DSPP in Dentine Formation and Hereditary Dentine Defects

Jie JIA<sup>1,2</sup>, Zhuan BIAN<sup>1</sup>, Yaling SONG<sup>1</sup>

*The dentine sialophosphoprotein (DSPP) gene is the only identified causative gene for dentinogenesis imperfecta type 2 (DGI-II), dentinogenesis imperfecta type 3 (DGI-III) and dentine dysplasia type 2 (DD-II). These three disorders may have similar molecular mechanisms involved in bridging the DSPP mutations and the resulting abnormal dentine mineralisation. The DSPP encoding proteins DSP (dentine sialoprotein) and DPP (dentine phosphoprotein) are positive regulators of dentine formation and perform a function during dentinogenesis. The present review focused on the recent findings and viewpoints regarding the relationship between DSPP and dentinogenesis as well as mineralisation from multiple perspectives, involving studies relating to spatial structure and tissue localisation of DSPP, DSP and DPP, the biochemical characteristics and biological function of these molecules, and the causative role of the proteins in phenotypes of the knockout mouse model and in hereditary dentine defects.*

**Keywords:** dentine mineralisation, dentine sialophosphoprotein, hereditary dentine defects, mutation

*Chin J Dent Res* 2024;27(1):17–28; doi: 10.3290/j.cjdr.b5136791

Mineralised dentine consists of three components: collagen fibrils that determine the spatial structure and directly sustain the process of mineralisation<sup>1,2</sup>; multiple proteins that interact with each other during the process of mineralisation<sup>3</sup>; and carbon-apatite that forms hierarchically flaky ordered crystal structure.<sup>4</sup> A

number of non-collagenous proteins (NCPs), accounting for 5% to 10% of the dentine extracellular matrix (DECM), are responsible for initiating and modulating the mineralisation of collagen fibres when predentine is converted to dentine.<sup>5</sup> Among these DECM proteins, dentine phosphoprotein (DPP) and dentine sialoprotein (DSP) appear to be the major dentine-specific proteins. They are encoded by the signal mRNA transcript of the dentine sialophosphoprotein (DSPP) gene.<sup>6,7</sup> The coding sequences for DSP are in the 5' end of the DSPP gene and those for DPP are in the 3' terminal (Fig 1). The intact DSPP peptide has never been identified<sup>8-10</sup>, which indicates that DSPP would be catalysed after translation. Blocking the proteolytic processing of DSPP generated dentine hypomineralisation defects that are similar to those observed in *Dspp*-deficient mice models<sup>11</sup>, indicating that the proteolytic processing of DSPP into different fragments would be vital in dentinogenesis.

DSPP plays an essential role in dentinogenesis and tissue development; however, there is contradicting evidence regarding the activity of DSPP and particularly its role in mineralisation. The present review presents the recent findings and viewpoints in detail regarding the relationship between DSPP and dentinogenesis as well as mineralisation from multiple perspectives involv-

1 State Key Laboratory of Oral & Maxillofacial Reconstruction and Regeneration, Key Laboratory of Oral Biomedicine Ministry of Education, Hubei Key Laboratory of Stomatology, School & Hospital of Stomatology, Wuhan University, Wuhan, P.R. China.

2 The First Affiliated Hospital of Henan University, Henan University School of Stomatology, Kaifeng, P.R. China.

**Corresponding authors:** Prof Yaling SONG (ORCID: <https://orcid.org/0000-0003-0747-7381>) and Prof Zhuan BIAN, State Key Laboratory of Oral & Maxillofacial Reconstruction and Regeneration, Key Laboratory of Oral Biomedicine Ministry of Education, Hubei Key Laboratory of Stomatology, School & Hospital of Stomatology, Wuhan University, Luoyu Road 237, Wuhan 430079, P.R. China. Tel: 86-27-87686142. Email: [sningya@whu.edu.cn](mailto:sningya@whu.edu.cn); [bianzhuan@whu.edu.cn](mailto:bianzhuan@whu.edu.cn).

This study was supported by the grants No.82370912 from the National Natural Science Foundation of China, No. 2042023kf0231 from the Fundamental Research Funds for the Central Universities and No. 2022020801010499 from the Bureau of Science and Technology of Wuhan, P.R. China.

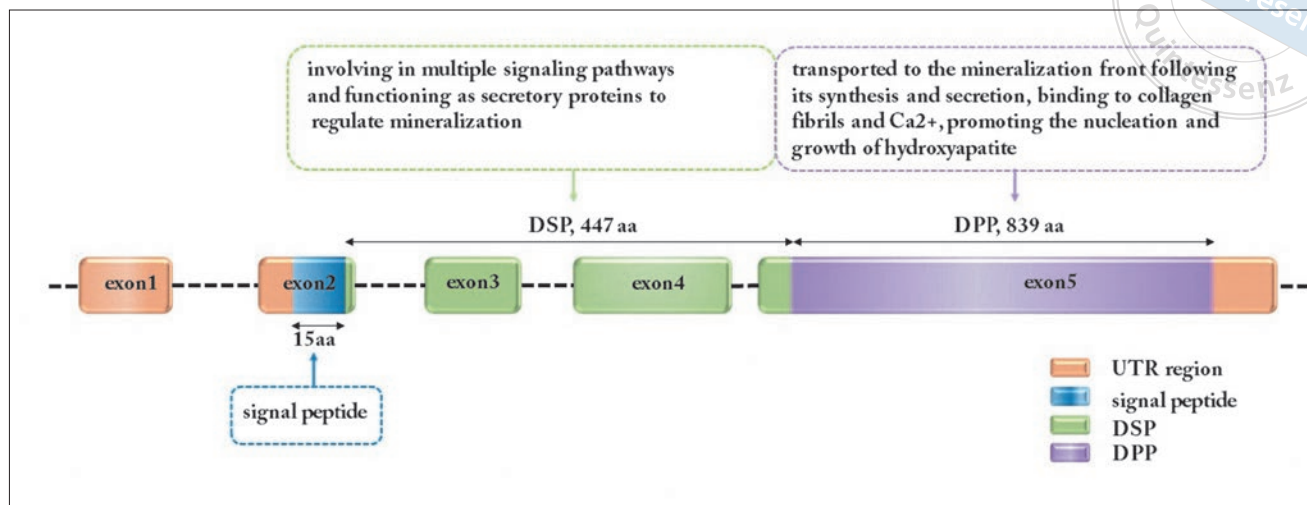


**Fig 1** Diagrammatic representation of DSPP gene structure, encoding proteins and potential function.

ing studies at a molecular and cellular level, in animal models and in human dentine disorders.

### General function of DSPP

DSPP belongs to sialic acid-rich glycoproteins, as a member of the small integrin-binding ligand N-linked glycoproteins (SIBLING) family. Immediately after the translation of full-length DSPP, the DSPP preproprotein in odontoblasts is proteolytically processed into separate daughter proteins with different properties.<sup>12</sup> The two major cleaved products are identified as DSP and DPP, which are secreted to the extracellular matrix by odontoblasts and predominantly but not exclusively expressed in odontoblasts and dentine.<sup>13,14</sup> Dentin glycoprotein (DGP) was found in the middle region of DSPP in porcine<sup>15</sup>, but it had not yet been reported in other species. DSP was found to be specifically expressed in odontoblasts, predentine, dentine and dental pulp<sup>16-21</sup>, and was also detected in osteoblasts within alveolar bone, cellular cementum and periodontal ligament.<sup>22,23</sup> DPP was deposited directly at the advancing mineralisation front of dentine, whereas little phosphoprotein was detected in pulp.<sup>24</sup> DSP and DPP were also found to be expressed transiently in early ameloblasts adjacent to the dentine–enamel junction (DEJ).<sup>25,26</sup>

### DSPP in dentine and pulp

The essential role of DSPP in tooth development and disease occurrence in vivo was analysed in knockout and transgenic mouse models. The *Dspp*<sup>-/-</sup> mice showed tooth defects similar to those seen in patients with DGI-

III (dentinogenesis imperfecta type 3). The defects presented as widened predentine, sporadic unmineralised areas in irregular dentine and frequent pulp exposure, as well as mineralisation defects with globular dentine as a marker of abnormally mineralised dentine.<sup>27</sup> In addition, in the *Dspp*<sup>-/-</sup> mice the compromised DEJ was shown as a gap between enamel and dentine, which suggested a lack of DSPP would result in abnormal epithelial-mesenchymal interactions during early dental development.<sup>28,29</sup> The circular dentine formed within dental pulp and the altered dental pulp cells differentiating into chondrocyte-like cells were observed in the teeth of *Dspp*<sup>-/-</sup> mice.<sup>29</sup> The dosage of DSPP is critical to maintain tooth development and dentine formation. The transgenic mice that expressed *Dspp* mRNA at a level similar to that in wildtype mice can completely rescue the DSPP knockout defect; however, transgenic mouse incisors, with 10% *Dspp* mRNA expression, only partially rescued the DSPP knockout defect in mineral density.<sup>30</sup> *Dspp* heterozygous mice displayed dentine phenotypes similar to DD-II at the age of 12 and 18 months, which was characterised by compromised mineralisation of the dentine.<sup>31</sup> These studies suggested that DSPP would be required for normal pulp cell/odontoblast differentiation as well as dentine development and DEJ formation.

### DSPP in reparative dentine formation

DSPP is mainly expressed in odontoblasts. It is a marker for the differentiation of dental pulp cells into odontoblast cells. *Dspp* expression was absent in the damaged odontoblasts 24 hours after tooth injury, and regenerating odontoblasts began to express *Dspp* at day 5 after

injury.<sup>32</sup> Immunohistochemical analyses in sclerotic dentine revealed a high expression of DSPP inside the tubules in reparative dentine, which was mainly found in the tubules in non-affected dentine of caries lesions and perhaps indicated a preventive defence against carious attack.<sup>33</sup> *Dspp* heterozygous mice (18 months) manifested excessive dentine attrition and excessive formation of reparative dentine, but much weaker DSPP signals within the reparative dentine indicated osteodentine rather than normally formed dentine.<sup>31</sup> Furthermore, DSPP was expressed together with bone sialoprotein (BSP) in the odontoblast-like cells of reparative dentine, which suggests that the newly formed reparative dentine possess both dentinogenic and osteogenic characteristics.<sup>34</sup>

In contrast with pulp capping agent calcium hydroxide, DPP/collagen composite demonstrated more rapid formation of reparative dentine with higher compactness, a greater ability to cover exposed pulp and less pulp inflammation.<sup>35</sup> Decellularised dentine matrix extracts contained DSPP, as pulp capping agents for miniature swine, regenerated complete dentine bridge and reactionary dentine, and this reparative dentine adjacent to pulp tissue showed dentinal tubules that were relatively similar to primary dentine.<sup>36</sup>

At 1 week after pulp capping with calcium hydroxide agent, strong DSPP signals often appeared in the early formed dentine bridge, demonstrating the rapid response of DSPP to the noxious external stimuli.<sup>37</sup> After pulp capping with different capping materials, human odontoblast-like cells and pulpal cells beneath the dentine bridge are capable of differentiating and producing new hard tissue that contains DSPP, ColI or Heme Oxygenase-1; thus, the newly formed hard tissue can be characterised as dentine rather than an unspecific hard organism.<sup>38,39</sup> Three weeks after calcium hydroxide paste was applied to wounded pulp tissue, only anti-DSP staining was visible in newly formed reparative predentine and dentine, indicating that DSPP rapidly performed its function in the formation of reparative dentine.<sup>40</sup>

In general, DSPP is able to respond rapidly to dental injury and could become an excellent biocompatible inducer for the formation of reparative dentine.

#### *Interaction with mineralisation-related proteins*

Tooth development requires the coordinated action of DSPP with other mineralisation-related proteins. TGF- $\beta$ 1, one of the negative regulation factors of DSPP, was reported early on to downregulate DSPP promoter activity. The expression of *Dspp* is significantly downreg-

ulated during tooth development in TGF- $\beta$ 1 transgenic mice with overexpressed active TGF- $\beta$ 1 predominantly in odontoblasts.<sup>41</sup> DPP and DSP binding to TGF- $\beta$ 1 were liberated in association with the degradation of DPP and DSP, and this combination might facilitate reparative dentine formation and affect cell behaviour in the dentine-pulp complex following tissue injury.<sup>42</sup>

DMP1, another member of the SIBLING family, is located on the same chromosome locus as the DSPP gene and shares similar biochemical and genomic DNA features.<sup>43,44</sup> It was proposed that DSPP arose from DMP1 as a result of a gene duplication event.<sup>45</sup> During early differentiation of rat odontoblasts, the COOH-terminal of DMP1 binds specifically with the DSPP promoter in the region between nt -450 and +80 and activates the transcription of DSPP.<sup>46</sup> Studies in mouse models showed that DSPP was reduced in *Dmp1*<sup>-/-</sup> mice at both mRNA and protein levels.<sup>47,48</sup> This finding was in agreement with the results in vitro studies, in which overexpression of *Dmp1* induced *Dspp* expression while blocking DMP1 expression inhibited the expression of *Dspp*.<sup>49</sup> Significantly, in *Dmp1*<sup>-/-</sup> mice, the transgenic *Dspp* expression elevated the expression of molecular markers (BSP, OPN and MEPE) and repaired the defects in dentine and alveolar bone.<sup>48</sup> Taken together, DSPP is not simply a downstream molecule; it also shows the capability of affecting the upstream factors and mineralisation.

Analyses of the mouse *Dspp* gene revealed three *Runx2*-binding sites in *Dspp* promoter.<sup>21</sup> In vitro studies suggested that *Runx2* upregulated DSPP gene expression in mouse preodontoblasts but decreased its activity in mature odontoblasts.<sup>21,50</sup> Overexpression of the *Runx2* gene in mouse dental papilla cells resulted in the downregulation of DSPP expression.<sup>51</sup> Thus, the effects of *Runx2* on DSPP expression depend on stages of cell differentiation, with *Runx2* activating DSPP expression in preodontoblast cells and repressing it at maturation stages.

Mouse *Dspp* promoter also has a BMP2-response element that physically interacts with BMP2. BMP2 upregulated DSPP expression in mouse preodontoblasts.<sup>52</sup> In conditional *Bmp2*<sup>-/-</sup> mice, the gene expression of *Dspp* in odontoblasts was reduced by 90%.<sup>53</sup> In addition, transcription factor *Dlx3* mutations causing tooth defects in humans indicated that DLX3 played a role in tooth development.<sup>54,55</sup> DSPP is directly regulated by DLX3 in odontoblasts and *Dlx3*<sup>-/-</sup> mice also showed major dentine defects and reduced DSPP expression.<sup>56</sup>

Overall, the cooperation between DSPP and other mineralization-related proteins is vital for the process of mineralisation. In summary, DSPP is a positive

regulator of hard tissue mineralisation, acting on both dentine and bone. Because of its unique structure, DSPP would obligatorily be proteolytically processed to segments. A general review of the two main separate daughter proteins of DSPP, DPP and DSP, will now be presented.

## DPP and dentine mineralisation

### *Relationship between DPP conformation and mineralisation*

As the polyanionic macromolecules, DPP is the major noncollagenous DECM protein in dentine<sup>57,58</sup>, which can function in biological mineralisation by binding to the matrix of structural protein, nucleating hydroxyapatite (HA) crystallisation and modulating crystal growth.<sup>2,59</sup> In the majority of species, DPP possesses a unique composition with aspartyl and seryl residues comprising at least 75% of amino acid residues and with 85% to 90% of the phosphorylated seryl residues.<sup>58</sup> DPP isolated from dentine extract was capable of initiating the formation of HA in an in vitro gel diffusion system without HA<sup>60</sup>; however, recombinant full-length PP (rPP-full) required HA co-embedding to induce mineralisation.<sup>61</sup> One interpretation was that rPP might be less phosphorylated than DPP from dentine.<sup>15</sup> It was considered that the length of the serine/aspartic acid-rich repeats (SDrr) of DPP could be associated with phosphorylation and tooth mineralisation<sup>62</sup>; however, inter- and intraspecies length polymorphisms in SDrr have been reported in toothed animals.<sup>15,63</sup> Several recombinant mouse DPP proteins possessing 62.4% and 36.5% of the length of rPP-full induced the precipitation of calcium phosphate similar to rPP-full, whereas the induction ability of the vector without SDrr repeats was significantly lower than that of rPP-full.<sup>61</sup> Thus, interspecies length variation in SDrr may not result in different abilities of individual DPP for tooth mineralisation, but a different phosphorylated extent of DPP determines the capacity for mineralisation.

Comparison of DPP sequences among toothed and toothless animals showed that although there was a significant difference among the species, the BMP1-cleavage motif and RGD (Arg-Gly-Asp) integrin-binding domain were defined in two conservation domains in DPP.<sup>62</sup> The BMP1-cleavage motif is conserved among mammals<sup>62</sup>, and mutations within the BMP1-cleavage site would block, impair or accelerate the efficiency of DSPP cleavage.<sup>9,64</sup> In in vivo studies, the normal DSPP transgene fully repaired the dentine defects of *Dspp*<sup>-/-</sup>

mice, whereas the D452A-DSPP mutant transgene with a mutation in the BMP1-cleavage region failed to do so.<sup>11</sup> These studies imply that the proteolytic processing of DSPP through the BMP1-cleavage motif is indispensable for DSPP to exert its biological function during dentinogenesis.

The RGD motif is another characteristic domain of DSPP. RGD domain in DPP can bind to integrins on the cell surface of undifferentiated mesenchymal stem cells and pulp cells, promoting their terminal differentiation into odontoblast-like cells.<sup>65</sup> In addition, DPP containing RGD motif induced the differentiation and mineralisation of mouse dental papilla cell line 23 (MDPC-23) cells<sup>66</sup>, enhanced the survival and proliferation of rat immortalised preodontoblast cells, and promoted the terminal differentiation of preodontoblasts to functional odontoblasts.<sup>67</sup> Moreover, an RGD peptide derived from porcine DPP promotes cellular migration of human dental pulp cells.<sup>68</sup> All these findings indicate that the RGD motif integrating the surface of dental pulp cells plays a vital role in cell migration or differentiation; however, native rat DPP protein displays no RGD-induced dental pulp cell migration and differentiation.<sup>69</sup>

Conformational analysis suggested that DPP be thought as a unique structure with a nonplanar, folded and modified *trans*-extended backbone chain, in which the repeat aspartic acid/serine/serine (DSS) domain in DPP constituted the extended backbone structures with long ridges of carboxylate and phosphate groups respectively on each side of the peptide backbone, forming two well-defined ionic ridges.<sup>58</sup> Such a specific spatial arrangement could produce highly negatively charged aggregation areas for binding calcium ions. The bound calcium ions on the two ionic ridges could be bridged between the parallel chains or interact with a hydroxyapatite surface array of calcium ions.<sup>58</sup> The spatial structure of DPP directly generated a dual behaviour that is entirely compatible. On one hand, phosphorylated DPP shows an affinity for the surface of hydroxyapatite and octacalciumphosphate and meanwhile maintains the ability to sequester Ca<sup>2+</sup> ions.<sup>70</sup> On the other hand, DPP have an avid affinity for binding the collagen gap zones where collagen fibrils aggregate in the mineralisation front, providing the connecting interfaces for mineralised crystal and collagen fibrils.<sup>71,72</sup> At low DPP concentrations, the Ca<sup>2+</sup> ions might be folded back on themselves, creating partially ordered and internally bridged structures; only at higher concentrations, DPP would adopt an open conformation that provides a structural freedom for interaction as previously mentioned, both with collagen and with

surfaces of cell membranes and mineral crystals.<sup>73</sup> The conformational state of DPP with dual interaction with collagen and crystal might be responsible for facilitating well-defined mineral deposition.

### *Relationship between DPP and collagen and its role in dentine formation*

As the most abundant noncollagenous protein in dentine, DPP is deposited directly at the advancing mineralisation front of dentine while newly synthesised collagen is deposited at the advancing predentine border.<sup>74,75</sup> The key function of DPP is its collagen-binding capacity<sup>75</sup>, and as the concentration of PP increases, more DPP will bind to the collagen fibrils.<sup>76</sup> The close interlinking of DPP and collagen is directly associated with mineral deposition during dentine formation.<sup>77</sup> Previous studies showed that DPP covalently crosslinked to type I collagen (Col1) significantly promoted the growth of hydroxyapatite crystals in vitro.<sup>2,78</sup> Phosphorylated DPP induced highly organised mineralisation of collagen fibrils in which the deposited mineral particles were fully crystalline and organised with their c-axes co-aligned with the collagen fibril axis, whereas non-phosphorylated DPP stabilised amorphous calcium phosphate (ACP) at higher concentrations without organised crystallization.<sup>4,79</sup> Progressive enzymatic removal of immobilised phosphorylorn led to an increase in mineralisation induction time, and when 90% of the phosphate of dentine collagen was removed, mineralisation was no longer induced.<sup>77</sup> These findings definitively suggested that the phosphate esters of DPP correlated with collagen were indispensable for the initiation of mineralisation.

As a mineralisation scaffold, Col1 rarely appears in the mature hypermineralised peritubular dentine<sup>80,81</sup>; however, our previous studies found that amounts of collagen fibres were around dentine tubules in hypomineralised peritubular dentine in DGI specimens with *DSPP* mutation.<sup>82</sup> Higher Col1 expression and lower mineralisation were found in *Dspp* mutation cells than in normal *Dspp* cells.<sup>83</sup> These findings indicate that abnormal DSPP would be associated with the alteration not only of dentine mineralisation but also of the amount of collagen. Altogether, the self-aggregating properties of collagen fibrils contribute to the transition of matrix vesicles forming a larger, mineralised structure.<sup>84,85</sup> In the absence of DPP, collagen fibrils are not directly involved in mineralisation. The interplay between the self-assembled type I collagen matrix and the noncollagenous DPP serves as a template for dentine mineral nucleation and growth.<sup>86,87</sup>

## DSP and mineralisation

### *DSP and its fragments*

DSP is further processed into small molecular fragments that are segregated into specific compartments within odontoblasts and dentine<sup>8</sup>, and later DSP was discovered to be a novel substrate of matrix metalloproteinase 9.<sup>88,89</sup> DSP NH<sub>2</sub>-terminal fragments are highly localised in predentine, whereas the COOH-terminal fragments are mainly distributed to the mineralised dentine.<sup>90</sup> The distinct distribution pattern of the two terminal fragments of DSP in different compartments of teeth suggests that they might play unique functions during dentinogenesis. The C-terminal of recombinant human DSP (rh-DSP<sup>376-462</sup>) was reported to have a novel signalling function of rh-DSP for the promotion of growth, migration and differentiation in HDPCS via the BMP/Smad, JNK, ERK, MAPK and NF- $\kappa$ B signalling pathways.<sup>91</sup> The C-terminal of recombinant mouse DSP (rC-DSP183-457) facilitates attachment, migration, proliferation and differentiation of human periodontal ligament stem cells (PDLSCs) significantly, by regulating gene expression of tooth-/bone-related markers, transcription factors and growth factors.<sup>88</sup> The middle domain (DSPaa183-219) of the N-terminal fragments was bound to integrin  $\beta$ 6, forming a complex to stimulate the phosphorylation of Smad1/5/8 proteins; then, the phosphorylated Smad1/5/8 proteins would be bound to DSPP gene promoter to activate the expression of DSPP and DMP1 and induce dental mesenchymal cell differentiation and biomineralisation.<sup>92</sup>

Few studies clarified the nature of the carbohydrate moieties of DSP. Qin et al<sup>93</sup> first proposed a new concept, high molecular weight DSP (HMW-DSP) from the extracellular matrix of rat dentine, which was an isoform of DSP. HMW-DSP absorbed much more water than DSP, which is consistent with the hypothesis that HMW-DSP contains more carbohydrate than DSP. They found that HMW-DSP possess extremely large amounts of carbohydrates and great heterogeneity in glycosylation, and proposed that HMW-DSP could be the functional form of DSP.<sup>93</sup> In fact, HMW-DSP is the proteoglycan form of DSP and was renamed DSP-PG, which appeared to be more abundant than DSP.<sup>93,94</sup> DSP-PG consists of two glycosaminoglycan (GAG) chains. Investigations have revealed the roles of these GAGs, including binding calcium ions<sup>95</sup> and inhibiting hydroxyapatite crystal growth.<sup>96</sup> The GAG side-chains for the DSP-PG made of chondroitin-sulphate inhibited the formation and growth of hydroxyapatite crystals in collagen gels.<sup>97,98</sup>

In vitro mineralisation analyses showed that DSP without GAG chains did not have a significant effect on mineral formation and growth.<sup>99</sup> *Dspp*/*Dsp*<sup>+</sup> mice showed more severe dentine defects than *Dspp*<sup>-/-</sup> mice.<sup>100</sup> Based on the above investigations, it was suggested that DSP-PG might serve as an antagonist of DPP, preventing the predentine from being mineralised too rapidly during dentinogenesis<sup>100</sup>, and that this proteoglycan might be the functional form of the N-terminal fragment of DSPP during biomineralisation.

Thus, DSP is critical for tooth development and could be processed further into small fragments in odontoblast cells, and some proteolytic processing of DSP could be the activation step of biological function and/or degradation functions.

### *DSP and pulp cell differentiation*

Generally, DSP has similar characteristics to other SIBLING members due to similar amino acid composition. Earlier studies proposed that DSP could nominally affect the formation and growth of hydroxyapatite crystals in vitro<sup>99</sup>; however, recent studies reported new findings on DSP function. Spatially, *DSP-only* transcripts appeared to be localised in cells at the areas subjacent to the odontoblast layer and in the dental pulp rather than expressed in the columnar mature odontoblasts in rats. Stro-1 protein, a stem cell marker, was also identified in cells at the areas subjacent to odontoblasts and in dental pulp.<sup>101</sup> The presence of *DSP-only* transcripts containing no PP sequence was also reported in porcine teeth.<sup>16</sup> DSP was found to enhance the mechanical properties of the DEJ in vivo.<sup>102</sup> The temporal expression of DSP mRNA coincides with odontoblast secretory activity and dentine matrix deposition during dentinogenesis in mouse molars.<sup>103</sup> DSP facilitates initiation of hydroxyapatite formation along or inside the collagen fibrils, leading to the conversion of predentine to dentine at the mineralisation front.<sup>19</sup> The molars in *Dspp*/*Dsp*<sup>+</sup> mice display narrower predentine without any ectopic unmineralised dentine, indicating that the initiation of predentine-dentine conversion is dependent on the expression of DSP.<sup>104</sup> In conclusion, the functions of DSP-only transcripts remain to be determined.

DSP could involve multiple signalling pathways, as well as functioning as secretory proteins to regulate mineralisation. Peptides derived from DSP had the ability to regulate gene expression and protein phosphorylation of BMP-dependent pathway-related molecules, and the signalling function of DSP via the BMP/Smad, JNK, ERK and NF- $\kappa$ B signalling pathways was revealed.<sup>91</sup> DSP was capable of binding to

integrin  $\beta$ 6 and phosphorylated transcription factors Smad1/5/8, which upregulated expression of DSPP and DMP1 genes and induced dental mesenchymal cell attachment, differentiation and mineralisation through P38 and ERK1/2 protein kinases.<sup>92</sup> Furthermore, as a ligand, DSP could also bind to the cell surface receptor Occludin (Ocln) that binds to focal adhesion kinase (FAK), and it induced differentiation and mineralisation of human dental pulp stem cells and mouse dental papilla mesenchymal cells through the Ocln-FAK signalling pathway.<sup>105</sup> Silencing *DSPP* expression altered the levels of signalling molecules Runx2, Numb, Notch1 and Gli1 in developing molars of *Dspp*<sup>-/-</sup> mice.<sup>106</sup> All these findings support the view that the regulatory role of DSP was to orchestrate the process of dentine formation.

DPP binding with collagen improves its structural stability<sup>15</sup>, and similarly, as DSP is the most abundant proteoglycan in dentine, it is also likely to interact with collagen.<sup>42</sup> Recombinant human DSP protein (rhDSP) facilitates human dental pulp stem cell differentiation and induces Col I and endogenous DSPP upregulation.<sup>107</sup> Recombinant mouse DSP fusion protein promotes Col I expression in calvarial bone and osteoblasts.<sup>108</sup> Col I mRNA was downregulated in primary calvarial cells without *Dsp* expression of *Dspp*<sup>-/-</sup> mice in an in vitro culture system.<sup>106</sup> Thus, it is speculated that DSP, as the upstream factor of Col I, ensures the normal differentiation function of odontoblasts.

Although DSP exerts a positive influence in dentine mineralisation, recent studies have shown different results. *Dspp*/*Dsp*<sup>+</sup> mice presented more severe defects in dentine compared to *Dspp*<sup>-/-</sup> mice, indicating that DSP might inhibit dentine mineralisation or restrain the accelerating action of DPP and prevent predentine from being mineralised too rapidly during dentinogenesis.<sup>100</sup> Although studies have shown that DSP is critical for dentine mineralisation, findings concerning the biological roles played by DSP in dentinogenesis are renewed continuously and further studies are warranted to delineate the detailed functions and mechanisms.

To conclude, DSP has the unique biological characteristic of inducing initial dentine mineralisation and participating in differentiation in some mineralisation cells. DSP is involved in multiple signalling transduction pathways in regulating the process of mineralisation.

### **DSPP mutations and human hereditary dentine disorders**

Hereditary dentine disorders are mainly separated into two categories: dentinogenesis imperfecta (DGI) with

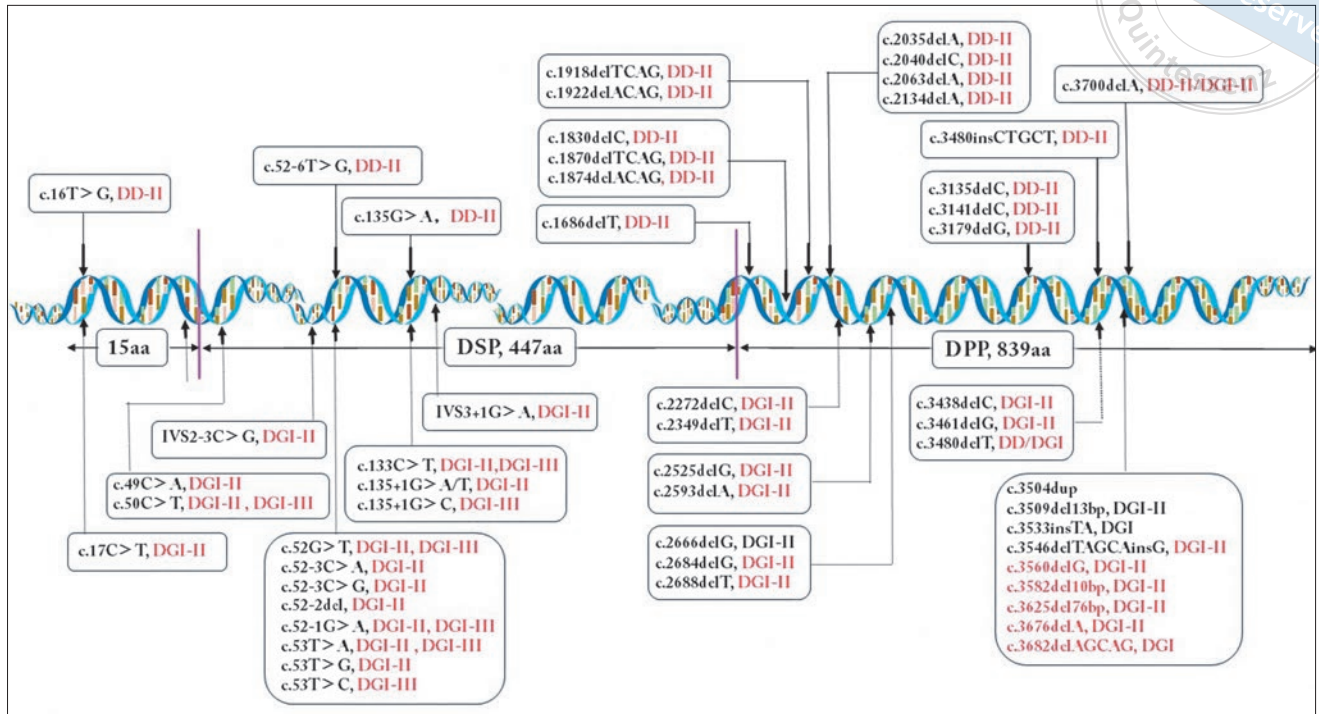


**Fig 2** DSPP gene diagram showing mutations identified in families with dentinogenesis imperfecta.<sup>111-113,115,118,119,121,126-132</sup>

DGI-I, DGI-II and DGI-III subtypes, and dentine dysplasia (DD) with DD-I and DD-II subtypes. Among them, DGI-II, DGI-III and DD-II are isolated dentine disorders usually with an autosomal dominant inheritance, and *DSPP* is the only identified causative gene for them.

Xiao et al<sup>109</sup> and Zhang et al<sup>110</sup> first reported that mutations of the *DSPP* gene are associated with DGI-II. To date, many *DSPP* mutations have been identified in families with dentine disorders.<sup>111,112</sup> A large number of these were in the DSP region, with most being missense, nonsense or splicing mutations. Successful sequencing of the highly repetitive DPP region marked a breakthrough in identifying the mutations in the DPP region in hereditary dentine defects. A previous investigation conducted by our group first revealed frameshift mutations in DPP region resulting in hereditary dentine defects in five Chinese families with DGI-II or DD-II and found 14 in-frame indel polymorphisms and 11 single nucleotide polymorphisms (SNPs) in the DPP region in the normal population.<sup>113</sup> Subsequently, other groups reported similar findings.<sup>114-116</sup> In animal models, mice that deleted a “G” to cause a -1 frameshift following the first four amino acids of DPP exhibited severe dentine defects.<sup>117</sup> The results indicated that the reading frame-preserving length variations and single missense alteration in the DPP coding region had no apparent effects on its function, and functional aberrations would not

take place unless a frameshift or nonsense mutation occurred in DPP.

DSPP can be secreted normally outside the cell, usually requiring the guidance of a signal peptide. Tyrosine to aspartic acid mutations in the signal peptide region of *DSPP* would affect the secretion of both DSP and DPP owing to the significantly reduced ability to translocate the primary translated product into the endoplasmic reticulum (ER).<sup>118</sup> The result is that either the accumulation of the mutant protein in the cytosol or the continued occupation on the ER may indirectly bring about insufficient processing of the normal DSPP with concomitant defective biomineralisation.

Given the proximity to the border of exon 3 and splicing acceptor site, the mutational “hotspot” was suspected to have some influence on normal pre-mRNA splicing, causing skipping of exon 3.<sup>119,120</sup> Closely adjacent to the membrane-associated signal peptide peptidases cleavage site, the first three amino acids of the mature protein DSPP are Ile Pro Val (IPV), which is highly conserved within almost all animal species. Excepting mutations in the signal peptide region, all mutations in this conserved DSP region would result in a change of the proposed IPV domain.<sup>120</sup> The mutations with deleted exon 3 of DSPP, lacking the conserved IPV motif at the N-terminus after cleavage of the signal peptide, would generate varying degrees of clinical

phenotypes. The expression level of the DSPP exon 3 deletion transcript correlated with the severity of the dentine defects, the weaker the quantity of mutant protein, the milder the clinical phenotype.<sup>121</sup> Mutations in or adjacent to the IPV domain would cause mutant protein to be retained within the ER<sup>122</sup>, which can be captured by the autophagy-lysosome system for degradation (ER-phagy).<sup>123</sup> The quantity of mutant protein accumulated in the odontoblast ER was positively associated with the clinical phenotype.<sup>124</sup> Recent studies proposed that the encoding amino acids in the DPP repeat domain with -1bp frameshift mutations result in longer mutant hydrophobic domains that anchor the mutant protein within the rough endoplasmic reticulum (rER) membrane. Meanwhile, the dominant negative effects caused by the retained mutant proteins form entropy-driven, multivalent cation (Ca<sup>2+</sup>) bridges between each other and then entrap WT DSPP through its own calcium-binding domain.<sup>125</sup> In summary, mutations in either the DSP or DPP domain lead to DGI-II or DGI-III and DD-II. A diagram of *DSPP* gene mutations identified in families with dentinogenesis imperfecta is shown in Fig 2.<sup>111-113,115,118,119,121,126-132</sup> The dentine defect phenotype caused by DSPP mutations would contribute to revealing the functional role of DSPP and lead to a better understanding of dentine mineralisation and homeostasis.

## Conclusion and prospects

Since the discovery of DSPP and the degradation products DSP and DPP, considerable progress has been made regarding their biological characteristics. The findings have greatly enhanced our understanding of their function in the process of biomineralisation. The major discoveries to date include the reiwpoints that DSPP was cleaved into DSP, DGP and DPP, and the distinct features of the proteolytic products suggest that these proteins play different roles in biomineralisation; that DPP is transported to the mineralisation front following its synthesis and secretion; that DPP binds to collagen fibrils and Ca<sup>2+</sup>, promoting the nucleation and growth of hydroxyapatite; that the proteoglycan form of DSP is the functional segment of the NH<sub>2</sub>-terminal fragment of DSPP; and that many heterogeneous mutations in the human DSPP gene have been linked to hereditary dentine defects. These discoveries also present challenges, such as whether proteolytic processing of DSPP is an activation step, which components participate in the process of DSPP proteolysis and what biological role they play; what the specific characterisation of the proteoglycan form of DSP is; what the potential roles of DSP/DPP

are in regulating signal pathways and what effect they exert on downstream molecules; and which proteins are associated with biomineralisation in dentine other than DSPP, whether DSP/DPP interacts physically with these proteins and what the precise mechanism is. As such advancements in research enrich our knowledge regarding DSP, DPP and DSPP, they also point to new directions for further exploration.

## Conflicts of interest

The authors declare no conflicts of interest related to this study.

## Author contribution

Drs Jie JIA and Yaling SONG designed the study, drafted and revised the manuscript; Dr Zhuan BIAN supervised the study.

(Received Aug 16, 2023; accepted Oct 23, 2023)

## References

1. Veis A. Mineral-matrix interactions in bone and dentin. *J Bone Miner Res* 1993;8(suppl 2):S493-S497.
2. Saito T, Arsenault AL, Yamauchi M, Kuboki Y, Crenshaw MA. Mineral induction by immobilized phosphoproteins. *Bone* 1997;21:305-311.
3. Goldberg M, Kulkarni AB, Young M, Boskey A. Dentin: Structure, composition and mineralization. *Front Biosci (Elite Ed)* 2011;3:711-735.
4. Lowenstam HA, Weiner S. Transformation of amorphous calcium phosphate to crystalline dahillite in the radular teeth of chitons. *Science* 1985;227:51-53.
5. Qin C, Baba O, Butler WT. Post-translational modifications of sibling proteins and their roles in osteogenesis and dentinogenesis. *Crit Rev Oral Biol Med* 2004;15:126-136.
6. MacDougall M, Simmons D, Luan X, Nydegger J, Feng J, Gu TT. Dentin phosphoprotein and dentin sialoprotein are cleavage products expressed from a single transcript coded by a gene on human chromosome 4. Dentin phosphoprotein DNA sequence determination. *J Biol Chem* 1997;272:835-842.
7. Feng JQ, Luan X, Wallace J, et al. Genomic organization, chromosomal mapping, and promoter analysis of the mouse dentin sialophosphoprotein (Dspp) gene, which codes for both dentin sialoprotein and dentin phosphoprotein. *J Biol Chem* 1998;273:9457-9464.
8. Yamakoshi Y, Hu JC, Iwata T, Kobayashi K, Fukae M, Simmer JP. Dentin sialophosphoprotein is processed by MMP-2 and MMP-20 in vitro and in vivo. *J Biol Chem* 2006;281:38235-38243.
9. von Marschall Z, Fisher LW. Dentin sialophosphoprotein (DSPP) is cleaved into its two natural dentin matrix products by three isoforms of bone morphogenetic protein-1 (BMP1). *Matrix Biol* 2010;29:295-303.
10. Ritchie HH, Yee CT, Tang XN, Dong Z, Fuller RS. DSP-PP precursor protein cleavage by tollid-related-1 protein and by bone morphogenetic protein-1. *PLoS One* 2012;7:e41110.



11. Zhu Q, Gibson MP, Liu Q, et al. Proteolytic processing of dentin sialophosphoprotein (DSPP) is essential to dentinogenesis. *J Biol Chem* 2012;287:30426–30435.
12. Sun Y, Lu Y, Chen S, et al. Key proteolytic cleavage site and full-length form of DSPP. *J Dent Res* 2010;89:498–503.
13. Tsuchiya S, Simmer JP, Hu JC, Richardson AS, Yamakoshi F, Yamakoshi Y. Astacin proteases cleave dentin sialophosphoprotein (Dspp) to generate dentin phosphoprotein. *J Bone Miner Res* 2011;26:220–228.
14. MacDougall M, Simmons D, Luan X, Gu TT, DuPont BR. Assignment of dentin sialophosphoprotein (DSPP) to the critical DGI2 locus on human chromosome 4 band q21.3 by in situ hybridization. *Cytogenet Cell Genet* 1997;79:121–122.
15. Yamakoshi Y, Lu Y, Hu JC, et al. Porcine dentin sialophosphoprotein: Length polymorphisms, glycosylation, phosphorylation, and stability. *J Biol Chem* 2008;283:14835–14844.
16. Yamamoto R, Oida S, Yamakoshi Y. Dentin sialophosphoprotein-derived proteins in the dental pulp. *J Dent Res* 2015;94:1120–1127.
17. Zhu YQ, Song RM, Ritchie HH. Differential expression between “DSP-only” and DSP-PP523 transcripts in rat molar teeth. *Arch Oral Biol* 2017;82:33–37.
18. Butler WT, Bhowm M, Brunn JC, et al. Isolation, characterization and immunolocalization of a 53-kDal dentin sialoprotein (DSP). *Matrix* 1992;12:343–351.
19. Ritchie HH, Wang LH. Sequence determination of an extremely acidic rat dentin phosphoprotein. *J Biol Chem* 1996;271:21695–21698.
20. Bleicher F, Couble ML, Farges JC, Couble P, Magloire H. Sequential expression of matrix protein genes in developing rat teeth. *Matrix Biol* 1999;18:133–143.
21. Chen S, Rani S, Wu Y, et al. Differential regulation of dentin sialophosphoprotein expression by Runx2 during odontoblast cytodifferentiation. *J Biol Chem* 2005;280:29717–29727.
22. Yuan G, Wang Y, Gluhak-Heinrich J, et al. Tissue-specific expression of dentin sialophosphoprotein (DSPP) and its polymorphisms in mouse tissues. *Cell Biol Int* 2009;33:816–829.
23. Figueredo CA, Abdelhay N, Ganatra S, Gibson MP. The role of dentin sialophosphoprotein (DSPP) in craniofacial development. *J Oral Biol Craniofac Res* 2022;12:673–678.
24. Saito T, Yamauchi M, Abiko Y, Matsuda K, Crenshaw MA. In vitro apatite induction by phosphophoryn immobilized on modified collagen fibrils. *J Bone Miner Res* 2000;15:1615–1619.
25. Paine ML, Luo W, Wang HJ, et al. Dentin sialoprotein and dentin phosphoprotein overexpression during amelogenesis. *J Biol Chem* 2005;280:31991–31998.
26. Yamakoshi Y, Hu JC, Fukae M, Zhang H, Simmer JP. Dentin glycoprotein: the protein in the middle of the dentin sialophosphoprotein chimera. *J Biol Chem* 2005;280:17472–17479.
27. Sreenath T, Thyagarajan T, Hall B, et al. Dentin sialophosphoprotein knockout mouse teeth display widened predentin zone and develop defective dentin mineralization similar to human dentinogenesis imperfecta type III. *J Biol Chem* 2003;278:24874–24880.
28. Verdelsis K, Szabo-Rogers HL, Xu Y, et al. Accelerated enamel mineralization in Dspp mutant mice. *Matrix Biol* 2016;52:246–259.
29. Guo S, Lim D, Dong Z, et al. Dentin sialophosphoprotein: A regulatory protein for dental pulp stem cell identity and fate. *Stem Cells Dev* 2014;23:2883–2894.
30. Lim D, Wu KC, Lee A, Saunders TL, Ritchie HH. DSPP dosage affects tooth development and dentin mineralization. *PLoS One* 2021;16:e0250429.
31. Shi C, Ma N, Zhang W, et al. Haploinsufficiency of Dspp gene causes dentin dysplasia type II in mice. *Front Physiol* 2020;11:593626.
32. Nakatomi M, Ida-Yonemochi H, Ohshima H. Lymphoid enhancer-binding factor 1 expression precedes dentin sialophosphoprotein expression during rat odontoblast differentiation and regeneration. *J Endod* 2013;39:612–618.
33. Martini D, Trirè A, Breschi L, et al. Dentin matrix protein 1 and dentin sialophosphoprotein in human sound and carious teeth: An immunohistochemical and colorimetric assay. *Eur J Histochem* 2013;57:e32.
34. Hwang YC, Hwang IN, Oh WM, Park JC, Lee DS, Son HH. Influence of TGF-beta1 on the expression of BSP, DSP, TGF-beta1 receptor I and Smad proteins during reparative dentinogenesis. *J Mol Histol* 2008;39:153–160.
35. Koike T, Polan MA, Izumikawa M, Saito T. Induction of reparative dentin formation on exposed dental pulp by dentin phosphophoryn/collagen composite. *Biomed Res Int* 2014;2014:745139.
36. Chen J, Cui C, Qiao X, et al. Treated dentin matrix paste as a novel pulp capping agent for dentin regeneration. *J Tissue Eng Regen Med* 2017;11:3428–3436.
37. Xie X, Ma S, Li C, et al. Expression of small integrin-binding ligand N-linked glycoproteins (SIBLINGs) in the reparative dentin of rat molars. *Dent Traumatol* 2014;30:285–295.
38. Min KS, Park HJ, Lee SK, et al. Effect of mineral trioxide aggregate on dentin bridge formation and expression of dentin sialoprotein and heme oxygenase-1 in human dental pulp. *J Endod* 2008;34:666–670.
39. Fransson H, Petersson K, Davies JR. Dentine sialoprotein and collagen I expression after experimental pulp capping in humans using emdogain gel. *Int Endod J* 2011;44:259–267.
40. Nakamura Y, Slaby I, Matsumoto K, Ritchie HH, Lyngstadaas SP. Immunohistochemical characterization of rapid dentin formation induced by enamel matrix derivative. *Calcif Tissue Int* 2004;75:243–252.
41. Thyagarajan T, Sreenath T, Cho A, Wright JT, Kulkarni AB. Reduced expression of dentin sialophosphoprotein is associated with dysplastic dentin in mice overexpressing transforming growth factor-beta 1 in teeth. *J Biol Chem* 2001;276:11016–11020.
42. Yamakoshi Y, Kinoshita S, Izuhara L, et al. DPP and DSP are necessary for maintaining TGF-beta1 activity in dentin. *J Dent Res* 2014;93:671–677.
43. Fedarko NS, Fohr B, Robey PG, Young MF, Fisher LW. Factor H binding to bone sialoprotein and osteopontin enables tumor cell evasion of complement-mediated attack. *J Biol Chem* 2000;275:16666–16672.
44. Fisher LW, Torchia DA, Fohr B, Young MF, Fedarko NS. Flexible structures of SIBLING proteins, bone sialoprotein, and osteopontin. *Biochem Biophys Res Commun* 2001;280:460–465.
45. Fisher LW. DMP1 and DSPP: Evidence for duplication and convergent evolution of two SIBLING proteins. *Cells Tissues Organs* 2011;194:113–118.
46. Narayanan K, Gajjerman S, Ramachandran A, Hao J, George A. Dentin matrix protein 1 regulates dentin sialophosphoprotein gene transcription during early odontoblast differentiation. *J Biol Chem* 2006;281:19064–19071.
47. Ye L, MacDougall M, Zhang S, et al. Deletion of dentin matrix protein-1 leads to a partial failure of maturation of predentin into dentin, hypomineralization, and expanded cavities of pulp and root canal during postnatal tooth development. *J Biol Chem* 2004;279:19141–19148.

48. Gibson MP, Zhu Q, Wang S, et al. The rescue of dentin matrix protein 1 (DMP1)-deficient tooth defects by the transgenic expression of dentin sialophosphoprotein (DSPP) indicates that DSPP is a downstream effector molecule of DMP1 in dentinogenesis. *J Biol Chem* 2013;288:7204–7214.
49. Narayanan K, Srinivas R, Ramachandran A, Hao J, Quinn B, George A. Differentiation of embryonic mesenchymal cells to odontoblast-like cells by overexpression of dentin matrix protein 1. *Proc Natl Acad Sci U S A* 2001;98:4516–4521.
50. Napierala D, Sam K, Morello R, et al. Uncoupling of chondrocyte differentiation and perichondrial mineralization underlies the skeletal dysplasia in tricho-rhino-phalangeal syndrome. *Hum Mol Genet* 2008;17:2244–2254.
51. Gaikwad JS, Hoffmann M, Cavender A, Bronckers AL, D'Souza RN. Molecular insights into the lineage-specific determination of odontoblasts: The role of Cbfa1. *Adv Dent Res* 2001;15:19–24.
52. Chen S, Gluhak-Heinrich J, Martinez M, et al. Bone morphogenetic protein 2 mediates dentin sialophosphoprotein expression and odontoblast differentiation via NF- $\kappa$ B signaling. *J Biol Chem* 2008;283:19359–19370.
53. Yang W, Harris MA, Cui Y, et al. Bmp2 is required for odontoblast differentiation and pulp vasculogenesis. *J Dent Res* 2012;91:58–64.
54. Dong J, Amor D, Aldred MJ, Gu T, Escamilla M, MacDougall M. DLX3 mutation associated with autosomal dominant amelogenesis imperfecta with taurodontism. *Am J Med Genet A* 2005;133A:138–141.
55. Lee SK, Lee ZH, Lee SJ, et al. DLX3 mutation in a new family and its phenotypic variations. *J Dent Res* 2008;87:354–357.
56. Duverger O, Zah A, Isaac J, et al. Neural crest deletion of *Dlx3* leads to major dentin defects through down-regulation of *Dspp*. *J Biol Chem* 2012;287:12230–12240.
57. Heuer AH, Fink DJ, Laraia VJ, et al. Innovative materials processing strategies: a biomimetic approach. *Science* 1992;255:1098–1105.
58. George A, Bannon L, Sabsay B, et al. The carboxyl-terminal domain of phosphophoryn contains unique extended triplet amino acid repeat sequences forming ordered carboxyl-phosphate interaction ridges that may be essential in the biomineralization process. *J Biol Chem* 1996;271:32869–32873.
59. Boskey AL, Maresca M, Doty S, Sabsay B, Veis A. Concentration-dependent effects of dentin phosphophoryn in the regulation of in vitro hydroxyapatite formation and growth. *Bone Miner* 1990;11:55–65.
60. Milan AM, Sugars RV, Embery G, Waddington RJ. Adsorption and interactions of dentine phosphoprotein with hydroxyapatite and collagen. *Eur J Oral Sci* 2006;114:223–231.
61. Kobuke S, Suzuki S, Hoshino H, Haruyama N, Nishimura F, Shiba H. Relationship between length variations in Ser/Asp-rich repeats in phosphophoryn and in vitro precipitation of calcium phosphate. *Arch Oral Biol* 2015;60:1263–1272.
62. McKnight DA, Fisher LW. Molecular evolution of dentin phosphoprotein among toothed and toothless animals. *BMC Evol Biol* 2009;9:299.
63. McKnight DA, Hart PS, Hart TC, et al. A comprehensive analysis of normal variation and disease-causing mutations in the human DSPP gene. *Hum Mutat* 2008;29:1392–1404.
64. Yang RT, Lim GL, Yee CT, Fuller RS, Ritchie HH. Site specificity of DSP-PP cleavage by BMP1. *Connect Tissue Res* 2014;55(suppl 1):142–145.
65. Eapen A, Ramachandran A, George A. Dentin phosphoprotein (DPP) activates integrin-mediated anchorage-dependent signals in undifferentiated mesenchymal cells. *J Biol Chem* 2012;287:5211–5224.
66. Tang J, Saito T. Effect of dentine phosphophoryn-derived RGD peptides on odontoblast-like cells. *Int Endod J* 2016;49:670–683.
67. Eapen A, George A. Dentin phosphophoryn in the matrix activates AKT and mTOR signaling pathway to promote preodontoblast survival and differentiation. *Front Physiol* 2015;6:221.
68. Yasuda Y, Izumikawa M, Okamoto K, Tsukuba T, Saito T. Dentin phosphophoryn promotes cellular migration of human dental pulp cells. *J Endod* 2008;34:575–578.
69. Chuang SF, Chen YH, Ma P, Ritchie HH. Phosphophoryn and dentin sialoprotein effects on dental pulp cell migration, proliferation, and differentiation. *Dent J (Basel)* 2018;6:70.
70. Addadi L, Moradian J, Shay E, Maroudas NG, Weiner S. A chemical model for the cooperation of sulfates and carboxylates in calcite crystal nucleation: Relevance to biomineralization. *Proc Natl Acad Sci U S A* 1987;84:2732–2736.
71. Traub W, Jodaikin A, Arad T, Veis A, Sabsay B. Dentin phosphophoryn binding to collagen fibrils. *Matrix* 1992;12:197–201.
72. George A, Hao J. Role of phosphophoryn in dentin mineralization. *Cells Tissues Organs* 2005;181:232–240.
73. Lee SL, Veis A. Cooperativity in calcium ion binding to repetitive, carboxylate-serylphosphate polypeptides and the relationship of this property to dentin mineralization. *Int J Pept Protein Res* 1980;16:231–240.
74. Weinstock M, Leblond CP. Radioautographic visualization of the deposition of a phosphoprotein at the mineralization front in the dentin of the rat incisor. *J Cell Biol* 1973;56:838–845.
75. Weinstock M, Leblond CP. Synthesis, migration, and release of precursor collagen by odontoblasts as visualized by radioautography after (3H)proline administration. *J Cell Biol* 1974;60:92–127.
76. Dahl T, Sabsay B, Veis A. Type I collagen-phosphophoryn interactions: Specificity of the monomer-monomer binding. *J Struct Biol* 1998;123:162–168.
77. Saito T, Yamauchi M, Crenshaw MA. Apatite induction by insoluble dentin collagen. *J Bone Miner Res* 1998;13:265–270.
78. Milan AM, Sugars RV, Embery G, Waddington RJ. Dentine proteoglycans demonstrate an increasing order of affinity for hydroxyapatite crystals during the transition of predentine to dentine. *Calcif Tissue Int* 2004;75:197–204.
79. Deshpande AS, Fang PA, Zhang X, Jayaraman T, Sfeir C, Beniash E. Primary structure and phosphorylation of dentin matrix protein 1 (DMP1) and dentin phosphophoryn (DPP) uniquely determine their role in biomineralization. *Biomacromolecules* 2011;12:2933–2945.
80. Weiner S, Veis A, Beniash E, et al. Peritubular dentin formation: Crystal organization and the macromolecular constituents in human teeth. *J Struct Biol* 1999;126:27–41.
81. Dorvee JR, Deymier-Black A, Gerkowicz L, Veis A. Peritubular dentin, a highly mineralized, non-collagenous, component of dentin: Isolation and capture by laser microdissection. *Connect Tissue Res* 2014;55(suppl 1):9–14.
82. Song Y, Wang C, Peng B, et al. Phenotypes and genotypes in 2 DGI families with different DSPP mutations. *Oral Surg Oral Med Oral Pathol Oral Radiol Endod* 2006;102:360–374.
83. Jia J, Bian Z, Song Y. Dspp mutations disrupt mineralization homeostasis during odontoblast differentiation. *Am J Transl Res* 2015;7:2379–2396.
84. Boyde A, Sela J. Scanning electron microscope study of separated calcospherites from the matrices of different mineralizing systems. *Calcif Tissue Res* 1978;26:47–49.

85. Midura RJ, Vasanthi A, Su X, Wang A, Midura SB, Gorski JP. Calcospherulites isolated from the mineralization front of bone induce the mineralization of type I collagen. *Bone* 2007;41:1005–1016.
86. Veis A. Materials science. A window on biomineralization. *Science* 2005;307:1419–1420.
87. Huq NL, Loganathan A, Cross KJ, et al. Association of bovine dentine phosphophoryn with collagen fragments. *Arch Oral Biol* 2005;50:807–819.
88. Ozer A, Yuan G, Yang G, et al. Domain of dentine sialoprotein mediates proliferation and differentiation of human periodontal ligament stem cells. *PLoS One* 2013;8:e81655.
89. Yuan G, Chen L, Feng J, et al. Dentin sialoprotein is a novel substrate of matrix metalloproteinase 9 in vitro and in vivo. *Sci Rep* 2017;7:42449.
90. Yuan G, Yang G, Song G, Chen Z, Chen S. Immunohistochemical localization of the NH(2)-terminal and COOH-terminal fragments of dentin sialoprotein in mouse teeth. *Cell Tissue Res* 2012;349:605–614.
91. Lee SY, Kim SY, Park SH, Kim JJ, Jang JH, Kim EC. Effects of recombinant dentin sialoprotein in dental pulp cells. *J Dent Res* 2012;91:407–412.
92. Wan C, Yuan G, Luo D, et al. The dentin sialoprotein (DSP) domain regulates dental mesenchymal cell differentiation through a novel surface receptor. *Sci Rep* 2016;6:29666.
93. Qin C, Brunn JC, Baba O, et al. Dentin sialoprotein isoforms: detection and characterization of a high molecular weight dentin sialoprotein. *Eur J Oral Sci* 2003;111:235–242.
94. Sugars RV, Olsson ML, Waddington R, Wendel M. Substitution of bovine dentine sialoprotein with chondroitin sulfate glycosaminoglycan chains. *Eur J Oral Sci* 2006;114:89–92.
95. Embery G, Rees S, Hall R, Rose K, Waddington R, Shellis P. Calcium- and hydroxyapatite-binding properties of glucuronic acid-rich and iduronic acid-rich glycosaminoglycans and proteoglycans. *Eur J Oral Sci* 1998;106(suppl 1):267–273.
96. Chen CC, Boskey AL. Mechanisms of proteoglycan inhibition of hydroxyapatite growth. *Calcif Tissue Int* 1985;37:395–400.
97. Hunter GK, Allen BL, Grynpsas MD, Cheng PT. Inhibition of hydroxyapatite formation in collagen gels by chondroitin sulphate. *Biochem J* 1985;228:463–469.
98. Linde A. Dentin matrix proteins: Composition and possible functions in calcification. *Anat Rec* 1989;224:154–166.
99. Boskey A, Spevak L, Tan M, Doty SB, Butler WT. Dentin sialoprotein (DSP) has limited effects on in vitro apatite formation and growth. *Calcif Tissue Int* 2000;67:472–478.
100. Gibson MP, Liu Q, Zhu Q, et al. Role of the NH2-terminal fragment of dentin sialoprotein in dentinogenesis. *Eur J Oral Sci* 2013;121:76–85.
101. Ritchie HH, Li X. A novel rat dentin mRNA coding only for dentin sialoprotein. *Eur J Oral Sci* 2001;109:342–347.
102. Suzuki S, Sreenath T, Haruyama N, et al. Dentin sialoprotein and dentin phosphoprotein have distinct roles in dentin mineralization. *Matrix Biol* 2009;28:221–229.
103. Quispe-Salcedo A, Ida-Yonemochi H, Nakatomi M, Ohshima H. Expression patterns of nestin and dentin sialoprotein during dentinogenesis in mice. *Biomed Res* 2012;33:119–132.
104. Suzuki S, Haruyama N, Nishimura F, Kulkarni AB. Dentin sialoprotein and dentin matrix protein-1: Two highly phosphorylated proteins in mineralized tissues. *Arch Oral Biol* 2012;57:1165–1175.
105. Li W, Chen L, Chen Z, et al. Dentin sialoprotein facilitates dental mesenchymal cell differentiation and dentin formation. *Sci Rep* 2017;7:300.
106. Chen Y, Zhang Y, Ramachandran A, George A. DSPP is essential for normal development of the dental-craniofacial complex. *J Dent Res* 2016;95:302–310.
107. Yun YR, Kim HW, Kang W, et al. Expression and purification recombinant human dentin sialoprotein in *Escherichia coli* and its effects on human dental pulp cells. *Protein Expr Purif* 2012;83:47–51.
108. Jaha H, Husein D, Ohyama Y, et al. N-terminal dentin sialoprotein fragment induces type I collagen production and upregulates dentinogenesis marker expression in osteoblasts. *Biochem Biophys Res* 2016;6:190–196.
109. Xiao S, Yu C, Chou X, et al. Dentinogenesis imperfecta 1 with or without progressive hearing loss is associated with distinct mutations in DSPP. *Nat Genet* 2001;27:201–204.
110. Zhang X, Zhao J, Li C, et al. DSPP mutation in dentinogenesis imperfecta Shields type II. *Nat Genet* 2001;27:151–152.
111. Simmer JP, Zhang H, Moon SJH, et al. The Modified Shields Classification and 12 families with defined DSPP mutations. *Genes (Basel)* 2022;13:858.
112. Yuan M, Zheng X, Xue Y, He Z, Song G, Song Y. A novel DSPP frameshift mutation causing dentin dysplasia type 2 and disease management strategies. *Oral Dis* 2023;29:2394–2400.
113. Song YL, Wang CN, Fan MW, Su B, Bian Z. Dentin phosphoprotein frameshift mutations in hereditary dentin disorders and their variation patterns in normal human population. *J Med Genet* 2008;45:457–464.
114. Maciejewska I, Chomik E. Hereditary dentine diseases resulting from mutations in DSPP gene. *J Dent* 2012;40:542–548.
115. Li F, Liu Y, Liu H, Yang J, Zhang F, Feng H. Phenotype and genotype analyses in seven families with dentinogenesis imperfecta or dentin dysplasia. *Oral Dis* 2017;23:360–366.
116. Porntaveetus T, Osathanon T, Nowwarote N, et al. Dental properties, ultrastructure, and pulp cells associated with a novel DSPP mutation. *Oral Dis* 2018;24:619–627.
117. Liang T, Hu Y, Zhang H, et al. Mouse Dspp frameshift model of human dentinogenesis imperfecta. *Sci Rep* 2021;11:20653.
118. Rajpar MH, Koch MJ, Davies RM, Mellody KT, Kieley CM, Dixon MJ. Mutation of the signal peptide region of the bicistronic gene DSPP affects translocation to the endoplasmic reticulum and results in defective dentine biomineralization. *Hum Mol Genet* 2002;11:2559–2565.
119. Lee SK, Hu JC, Lee KE, Simmer JP, Kim JW. A dentin sialoprotein mutation that partially disrupts a splice acceptor site causes type II dentin dysplasia. *J Endod* 2008;34:1470–1473.
120. Lee KE, Lee SK, Jung SE, Lee Zh, Kim JW. Functional splicing assay of DSPP mutations in hereditary dentin defects. *Oral Dis* 2011;17:690–695.
121. Kim YJ, Lee Y, Zhang H, et al. Translated mutant DSPP mRNA expression level impacts the severity of dentin defects. *J Pers Med* 2022;12:1002.
122. Nam AS, Yin Y, von Marschall Z, Fisher LW. Efficient trafficking of acidic proteins out of the endoplasmic reticulum involves a conserved amino terminal IleProVal (IPV)-like tripeptide motif. *Connect Tissue Res* 2014;55(suppl 1):138–141.
123. Reggiori F, Molinari M. ER-phagy: Mechanisms, regulation, and diseases connected to the lysosomal clearance of the endoplasmic reticulum. *Physiol Rev* 2022;102:1393–1448.
124. Liang T, Smith CE, Hu Y, et al. Dentin defects caused by a Dspp(-1) frameshift mutation are associated with the activation of autophagy. *Sci Rep* 2023;13:6393.

125. von Marschall Z, Mok S, Phillips MD, McKnight DA, Fisher LW. Rough endoplasmic reticulum trafficking errors by different classes of mutant dentin sialophosphoprotein (DSPP) cause dominant negative effects in both dentinogenesis imperfecta and dentin dysplasia by entrapping normal DSPP. *J Bone Miner Res* 2012;27:1309–1321.
126. Zhu QL, Duan XH, Yu Q. Mutation of dentin sialophosphoprotein and hereditary malformations of dentin [in Chinese]. *Zhonghua Kou Qiang Yi Xue Za Zhi* 2023;58:17–24.
127. Pornaveetus T, Nowwarote N, Osathanon T, et al. Compromised alveolar bone cells in a patient with dentinogenesis imperfecta caused by DSPP mutation. *Clin Oral Investig* 2019;23:303–313.
128. Du Q, Cao L, Liu Y, et al. Phenotype and molecular characterizations of a family with dentinogenesis imperfecta shields type II with a novel DSPP mutation. *Ann Transl Med* 2021;9:1672.
129. Nieminen P, Papagiannoulis-Lascarides L, Waltimo-Siren J, et al. Frameshift mutations in dentin phosphoprotein and dependence of dentin disease phenotype on mutation location. *J Bone Miner Res* 2011;26:873–880.
130. McKnight DA, Simmer JP, Hart PS, Hart TC, Fisher LW. Overlapping DSPP mutations cause dentin dysplasia and dentinogenesis imperfecta. *J Dent Res* 2008;87:1108–1111.
131. Prasad MK, Geoffroy V, Vicaire S, et al. A targeted next-generation sequencing assay for the molecular diagnosis of genetic disorders with orodental involvement. *J Med Genet* 2016;53:98–110.
132. Bloch-Zupan A, Huckert M, Stoetzel C, et al. Detection of a novel DSPP mutation by NGS in a population isolate in Madagascar. *Front Physiol* 2016;7:70.

# Review on the Role of *IRF6* in the Pathogenesis of Non-syndromic Orofacial Clefts

Si Di ZHANG<sup>1</sup>, Yue YOU<sup>1</sup>, Mei Lin YAO<sup>1</sup>, Bing SHI<sup>1</sup>, Zhong Lin JIA<sup>1</sup>

*Non-syndromic orofacial clefts (NSOCs) are the most common craniofacial malformation. In the complex aetiology and pathogenesis of NSOCs, genetic factors play a crucial role and IRF6, located at chromosome 1q32.2, is the best documented NSOC susceptibility gene. IRF6 is a key factor in oral maxillofacial development and known to contribute the most in NSOCs. It is essential to conduct a complete review of the existing results on IRF6 to further understand its role in the pathogenesis of NSOCs. Thus, the present authors summarised the research progress on the mechanism of IRF6 in NSOCs from both genetic and functional perspectives in this review.*

**Keywords:** *IRF6, genetics, non-syndromic orofacial cleft (NSOC)*

*Chin J Dent Res 2024;27(1):29–38; doi: 10.3290/j.cjdr.b5128515*

Non-syndromic orofacial clefts (NSOCs) have a global prevalence of around 1/700 and are the most common craniofacial malformation. The aetiology and pathogenesis are very complex, including genetic factors, environmental factors and their interaction, with genetic factors playing a particularly crucial role<sup>1</sup>. Syndromic orofacial clefts (SOCs) are usually monogenic or oligogenic disease with the characteristics of pedigree inheritance. In contrast, the genetic aspect of NSOCs presents polygenic characteristics.<sup>2</sup> (2 in superscript) Some of the genes may play a major role, whereas most play a minor role, resulting in the occurrence of NSOCs after accumulating to a certain extent.

The aetiology of NSOCs has been investigated using a variety of methods, including linkage analysis, candidate gene association studies, cytogenetics, animal models and expression studies. Since it was first found to be associated with NSOC in 2004<sup>2</sup>, *IRF6* has been recognised as the most contributing and well-documented of dozens of NSOC susceptibility genes/loci identified thus far.

As the encoding gene of interferon regulatory factor (IRF) 6, *IRF6* is located at chromosome 1q32.2 (Fig 1). It first attracted attention in orofacial cleft studies because it was found to be the major pathogenic gene of Van der Woude syndrome (VWS; OMIM 119300), the most common form of SOC characterised by cleft lip and palate and lip pits.<sup>2</sup> This research also demonstrated the involvement of *IRF6* in orofacial development.<sup>2</sup> At present, aetiological *IRF6* variants have been found in at least 70% of patients with VWS.<sup>3</sup> Hypotheses and studies on the association between *IRF6* and NSOCs were thus initiated, and remarkable progress has been made.

Not only is *IRF6* an important factor for craniofacial development<sup>4</sup>, but it has also been suggested that it might even be associated with the severity of orofacial clefts<sup>5</sup>, hence the critical importance of understanding of the existing research on *IRF6* to gain a deeper under-

1 State Key Laboratory of Oral Diseases & National Clinical Research Center for Oral Diseases & Department of cleft lip and palate, West China Hospital of Stomatology, Sichuan University, Chengdu, P.R. China.

**Corresponding author:** Dr Zhong Lin JIA, State Key Laboratory of Oral Diseases, West China Hospital of Stomatology, Sichuan University, No.14, 3rd Section, Renmin Nan Road, Chengdu 610041, P.R. China. Tel: 86-28-85503462. Email: zhonglinjia@sina.com

This project was supported by the major frontier issues of the National Science Funds of China (no. 81271118 and no. 81600849).

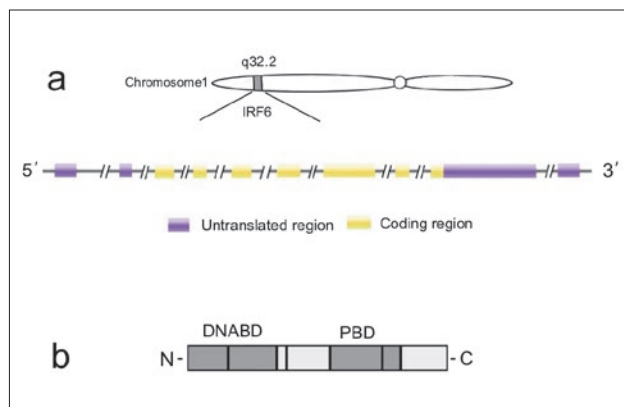


**Fig 1** Diagram of *IRF6* gene. Yellow indicates coding regions and purple indicates untranslated regions (a). DNABD, DNA-binding domain; PBD, protein-binding domain (b).

standing of its function in the mechanism of NSOC. Therefore, the present authors review the research progress of *IRF6* in the pathogenesis of NSOC in genetic and functional studies.

## Genetic studies

Genetic studies have identified many susceptibility variants in the *IRF6* gene that might increase the risk of NSOCs under certain environmental conditions, but the potential influence of these variants on different populations and subtypes leads to a significant difference in their association with NSOCs. In this section, we will review related genetic studies according to the progress of research methods at different stages.

### Linkage analysis

Linkage analysis maps susceptible genes to specific genomic regions by using the relationship between genetic markers (known locations) carried by family members and genetic disease, since susceptible genes associated with the disease are very likely to be linked to genetic markers.<sup>6</sup>

Zuccherro et al<sup>2</sup> proposed that there is a significant association between *IRF6* and the risk of non-syndromic cleft lip with or without cleft palate (NSCL/P). They found that single nucleotide polymorphism (SNP) rs2235371 was significantly associated with the risk of non-syndromic cleft lip and palate (NSCLP) in Asian and South American populations.<sup>2</sup> Located in exon 7 of the *IRF6* gene, rs2235371 is involved in encoding valine or isoleucine at the position 274 amino acid (V274I) in the conserved protein binding domain of IRF6 protein.

In 2005, a linkage disequilibrium between rs2013162 and rs2235375 and NSCL/P was found in an Italian population, confirming the contribution of *IRF6* to the aetiology of NSCL/P in the southern European population for the first time<sup>7</sup>, and later in the white population.<sup>8</sup> In 2007, Jakobsen et al<sup>9</sup> found a 6.5 MB linkage region in the vicinity of *IRF6* within 1q32.1 and q32.2, which may contain genes or non-coding region elements that regulate *IRF6* and increase the risk of NSCL/P.

Due to locus heterogeneity and limitations in the size and number of large multiple families (two or more family members with NSOC), the lack of repeated studies on linkage analysis makes it difficult to achieve genome-wide significant differences in the results of individual studies. Marazita et al<sup>10</sup> conducted a meta-analysis of previous genome-wide linkage studies and found 16 significant linkage regions including 1q32. A subsequent family study identified six chromosomal regions associated with NSOC, of which *IRF6* or its adjacent SNPs were the most significant.<sup>11</sup> Studies conducted on different populations confirmed the contribution of *IRF6* to the aetiology of NSCL/P, suggesting that further study is worthwhile.

### Candidate gene association studies

Incorporating a large number of sporadic cases without relying on large multiple families, candidate gene association studies were conducted to determine whether the candidate gene was associated with NSOC by comparing the allele frequency differences between NSOC and control samples.<sup>12</sup> Considering that the selection of candidate genes is the premise of association study, pathogenic genes of SOC and genes related to cranial and maxillofacial developmental signalling pathways were frequently used as sources for screening candidate genes of NSOC.

*IRF6* initially attracted attention in 2004 as the main pathogenic gene of VWS.2 Subsequent studies explored the association between *IRF6* and NSOC and obtained remarkable results. The first polymorphism found to be associated with NSOC in *IRF6* was rs2235371 and the association was then confirmed in subsequent association studies carried out on different populations.<sup>8,13,14</sup> It was also the first polymorphism that was significantly associated with NSCL/P in Asian and American Indian populations<sup>15,16</sup> and complete left NSCL/P in the Brazilian Caucasian population.<sup>17</sup> In 2008, Suazo et al<sup>18</sup> found a linkage imbalance between SNPs rs2235371, rs764093, rs2236909, rs2235375 and NSCL/P in the Chilean population. The rs2235371 CT and CT/TTP genotypes were associated with a significant reduction

in risk.<sup>19</sup> Larrabee et al<sup>20</sup> proposed that rs2235371 may play a role in the pathogenesis of NSOC by affecting the function of IRF6 protein, and confirmed this association was caused by common rather than rare variants; however, the SNP characteristics of rs2235371 and its effect on protein function still need further exploration, and no association was found between rs642961 and NSOC.<sup>20</sup>

Located in an enhancer of approximately 10,000 base pairs upstream of *IRF6*, rs642961 (G > A) may interfere with *IRF6* expression by disrupting the binding site of AP-2alpha gene which is usually the enhancer of *IRF6*. Rahimov et al<sup>21</sup> found the correlation between this SNP and NSOC in a European population first, and the association was more significant in non-syndromic cleft lip only (NSCLO). Brito et al<sup>22</sup> confirmed that rs642961 was weakly associated with NSCLO in a Brazilian population, but found no association between rs642961 and *IRF6* transcription level in orbicularis oris muscle mesenchymal stem cells (MSCs), suggesting that it may function during a specific period of embryogenesis.

Some studies proposed that A allele at rs642961 was associated with NSCL/P.<sup>2,23</sup> Pan et al<sup>19</sup> found that the AG and AG/AA genotypes of rs642961 were associated with increased risk of NSOC, especially NSCL/P and NSCLP. These findings require further confirmation in subsequent studies; however, studies of different populations or even the same ethnic population may achieve the opposite result. A population study demonstrated a lack of association between the A allele of rs642961 and Swedish NSCLO subset<sup>24</sup>; however, another study suggested that they were associated with NSOC in a Brazilian population and that the G/A haplotype increased the risk for both children and mothers.<sup>16</sup> The complexity of the ethnic mix of the Brazilian population appears to be an important confounding factor for this difference.

Located 27 bp downstream of exon 6 of *IRF6*, rs2235375 may alter the splicing process with functional annotations, suggesting that it is associated with the decrease in *IRF6* expression. It was positively correlated with NSCL/P in Italy<sup>6</sup>, Belgium<sup>14</sup>, China<sup>25</sup>, Norway<sup>26</sup>, Chile<sup>18</sup> and Brazil.<sup>27</sup> C allele at rs2235375 was associated with NSCL/P risk in the Chilean population, and its biological role at the level of craniofacial development needs further investigation<sup>28</sup>; however, in a study of a south Indian population, rs2235375 was associated with an increased risk of non-syndromic cleft palate only (NSCPO) rather than NSCL/P.<sup>29</sup>

The association between NSCL/P and rs2013162 (Ser153Ser) (which is a silent variant located in exon 5 of *IRF6*) was revealed in Belgian and Italian popula-

tions, respectively, in 2005.<sup>14</sup> Xu et al<sup>30</sup> showed that both rs2013162 and rs2235371 were closely associated with an increased risk of NSCL/P in northeast China; however, neither Birnbaum et al<sup>23</sup> nor Huang et al<sup>25</sup> found a significant association between rs2013162 and NSOC, which may be mainly related to population heterogeneity.

Studies on some susceptibility SNPs are limited and the results are controversial, indicating that more validation studies on different population samples are needed. Srichomthong et al<sup>31</sup> found that IRF6 G820A was significantly associated with NSCL/P in a Thai population and was responsible for 16.7% of the genetic contribution to NSCL/P. Tang et al<sup>32</sup> confirmed that A allele at G820A may increase the risk of NSCPO in China, and proposed the possibility of linkage disequilibrium between rs2235371 and other pathogenic variants. In 2009, an association study conducted in western China suggested that rs2235373, rs4844880 and rs2073485 were significantly associated with NSCL/P, whereas rs599021 was associated with NSCPO.<sup>33</sup> These SNPs may be directly involved in transcription or indirectly involved in the replication and transcription of *IRF6* gene through regulatory elements, affecting protein functions and thus regulating oral and maxillofacial development.<sup>33</sup> It is also interesting that there was a gene-environment interaction between rs2235373 GG genotype and maternal history of abortion. Although rs590223 (A > G) regulates the transcription level of *IRF6* in hepatocytes in vivo<sup>34</sup>, its association with NSOC is still controversial.<sup>35,36</sup> In the same year, Nikopensius et al<sup>37</sup> conducted a case-control association study on NSCPO in a northeastern European population and found rs17389541, located about 8kb upstream of *IRF6*, was significantly associated with NSCPO susceptibility.

Several candidate gene association studies have demonstrated that *IRF6* interacts with some genes in the mechanism of NSCLP. A gene-gene interaction analysis in 2013 indicated that the combination of rs2073485, rs2235371 or rs2236909 in *IRF6* and rs17176643 in *PAX9* may increase the risk of NSCL/P.<sup>38</sup>

Some studies combined linkage analyses with candidate gene association studies. Park et al<sup>13</sup> considered the genotype and double risk of specific SNPs in *IRF6* first and identified its association with increased risk of NSCL/P in Asian trios. Diercks et al<sup>39</sup> first demonstrated a strong association between rs2235371, rs1856161, rs2235377 and NSOC in a Honduran population which was enhanced in NSCL/P. Rahimov et al<sup>21</sup> proposed that rs2235371 was not directly related to NSOC, and that there might be pathogenic variants of *IRF6* regulatory element in the region of strong linkage disequilibrium

with rs2235371. The contribution of functional variant rs642961 to the pathogenesis of NSCLO was about 18%.<sup>21</sup> Blanton et al<sup>40</sup> conducted linkage analysis and association studies in Hispanic and non-Hispanic white NSOC families, respectively. They found that the association between rs2235371 and NSOC was more significant in non-Hispanic white single families, whereas the association between rs642961 and NSOC was not confirmed.<sup>40</sup> Jugessur et al<sup>26</sup> confirmed that rs2235371 and rs2013162 were associated with NSOC, which has not been widely confirmed.<sup>24,41</sup> Craniofacial measurements showed that rs2235371, rs2013162 or other pathogenic variants within the linkage disequilibrium region played an important role in the variation of nasolabial soft tissue morphology in a normal range in an East Asian population.<sup>42</sup>

Although linkage analyses and candidate gene association studies are increasingly effective in identifying common loci and speculating genes involved in complex traits, it is difficult to identify specific pathogenic variants. Convincing statistical evidence and functional data are needed to prove that a specific variant in a linkage disequilibrium region containing many strongly correlated SNPs is a pathogenic mutation.

### *Genome-wide association study (GWAS)*

The results of genetic studies of NSOC in the last 10 years varied widely. Complex heterogeneity and confounding factors make linkage analysis and association studies difficult to replicate. The extensive development of the genome-wide association study (GWAS) has brought new breakthroughs to the genetic research of NSOC.

The GWAS can be used for large-scale groups. By selecting genetic markers at the whole genome level, the GWAS compares the differences of SNP allele frequency between NSOC samples and controls, using genetic analysis to identify NSOC-associated SNPs and susceptibility genes by location, linkage disequilibrium and bioinformatics functional annotation.<sup>43</sup> Compared with linkage analysis, the GWAS has lower requirements for research samples and does not require large multiple family samples. Compared with candidate gene association studies, which rely more on the pre-setting of susceptible genes and include a few hundred SNPs at most, GWAS can screen out new susceptible genes and chromosomal regions in the whole genome without prior construction of a hypothesis.<sup>44</sup> Over the past decade, GWAS and correlative meta-analysis have reported more than 40 NSOC susceptibility genes, far surpassing traditional family linkage analyses and candidate gene association studies, and furtherly iden-

tified *IRF6* as a candidate gene for the pathogenesis of NSOC.<sup>45</sup>

In 2010, Beaty et al<sup>46</sup> conducted a GWAS in Asian and European NSOC trios and found four SNPs: rs2013162, rs2073485, rs861020 and rs10863790, which reached genome-wide significance. The first GWAS in a Chinese population was conducted in 2015 and confirmed that 1q32.2 was associated with NSCL/P.<sup>15</sup> CCCTC binding factor (CTCF) chromatin interaction analysis revealed the interaction signal between the regulatory region containing rs2235371 and DNA sequence in multiple cell lines, suggesting that rs2235371 may be involved in chromatin activity. Thus, the role of rs2235371 may be complex and more studies are needed to elucidate its underlying mechanisms.

However, GWAS has limitations: it focuses mainly on common variants and does not involve rare variants. Compared to common variants that have a very limited effect on disease development, rare variants may have a greater effect on the severity and earlier onset of NSOC.<sup>47,48</sup> On the other hand, since SNPs are mainly selected from HapMap data and usually influenced by strong linkage disequilibrium, the candidate genes/loci reported by the GWAS may be different from the actual situation. Therefore, the susceptible regions identified by the GWAS need to be located more accurately.

### *Research progress in the post-GWAS era*

It is gradually realised that known genetic susceptibility genes and loci can only explain a small part of the heritability of NSOC since the complexity and high genetic heterogeneity of NSOC and the limited recognition ability of GWAS. There may be undiscovered genetic factors associated with NSOC in the *IRF6* region, such as rare variants, gene-environment interactions and epigenetic inheritance, which may play a more important role in the development of NSOC.<sup>49</sup> Advances in sequencing technology have resolved this issue.

First-generation sequencing, also known as Sanger sequencing, was developed from the dideoxy terminal termination method and is the gold standard for obtaining nucleic acid sequence information at present; however, it is difficult to carry out on a large scale due to its high operating costs. Next-generation sequencing enables a comprehensive analysis of the genome with the ability to perform massively parallel sequencing at a faster speed and lower cost. Compared with whole genome sequencing, whole exome sequencing (WES) and target region sequencing (TRS) have been more widely used in genetic studies of NSOC due to their economy and efficiency.



Exons and untranslated regions in the human genome only account for 1% to 2% of total sequences, containing up to 85% of disease-related variants. WES screens for pathogenic variants in coding regions that may affect the function of protein products, representing a new breakthrough in the genetic aetiology of NSOC. As it is more efficient, comprehensive and specific than GWAS, WES plays an increasingly important role in the study of the aetiology of genetic diseases with the development of cheap sequencing technology. The combination of WES and GWAS helps to explore the aetiology of NSOC further.

In 2008, Pegelow et al<sup>50</sup> sequenced *IRF6* exons in Swedish multiple NSCL/P families and no disease-related mutation was detected. In 2018, Zhao et al<sup>51</sup> conducted a WES on a Han NSCLP patient and identified a new rare mutation of *IRF6* (c.26G > A; p.Arg9Gln) that affected the structure of *IRF6* to some extent by causing residue changes. A rare synonymous mutation (p.Ser307Ser; g.209963979, G>A; c.921C>T) was identified as a possible aetiology of NSCL/P in a WES in 2020.<sup>52</sup> This mutation is located at exon 7 and may affect the binding of external splicing silencing element to the main splicing regulator. A new *IRF6* pathogenic mutation (c.961C > T; p.Val321Met) was detected in a Chinese Han NSCLP family. As a conserved codon in many species, it also caused changes in residues and altered the structure of *IRF6* to some extent.<sup>53</sup>

TRS, also known as targeted sequencing, provides more comprehensive coverage of targeted regions. It is a cost-effective way to obtain comprehensive information outside the coding area. TRS found a laterality difference in *IRF6*: 26 SNPs were associated with the difference between unilateral and bilateral NSCL/P, which is one of the genetic sources of phenotypic heterogeneity of NSOC.<sup>54</sup> Sequencing of nine exons and untranslated regions at the 5' and 3' ends of *IRF6* in African NSOC patients revealed that 92% of potentially pathogenic exon and splice site mutations occurred in exons 4 and 7.<sup>55</sup> TRS of Chinese, Philippine, American and European trios revealed a G × G interaction between *IRF6* and *MAFB* polymorphisms, which was most significant in European trios.<sup>55</sup>

The susceptibility regions identified by GWAS can be deeply sequenced to mine rare variants and identify functional variants in coding and non-coding sequences. Although TRS can further supplement genetic information in susceptible regions, genome-wide detection can obtain the most complete genomic information and have the potential to fully reveal the molecular changes of NSOC, which is an ideal state for NSOC genetic research; however, large-scale whole genome

sequencing studies of NSOC that have been reported so far are still very limited. Identified variants are believed to be only a part of the overall heritability of NSOC and it is thought that there are other common or rare variants in the *IRF6* region that have not been discovered yet in relation to maxillofacial development and NSOC aetiology.

One of the strategies of NSOC genetics research in the sequencing era is to effectively identify potential susceptibility sites, clarify the biological mechanisms through functional analysis and verify them in large and independent populations. As sequencing throughput and precision increase and costs decrease, the technology will be used more widely. An important trend in NSOC genetics research in the future may be to use sequencing technology to accurately locate susceptible regions based on further mining GWAS data, detect rare and functional variants more comprehensively and conduct in-depth studies on biological mechanisms.

It is important to note that a study published in 2019 found that infants with NSCL/P had a higher methylation level at *IRF6* promoter regions than controls, suggesting that abnormal methylation of the promoter region may contribute to the development of NSCL/P.<sup>56</sup>

## Functional studies

*IRF6* contains 10 exons, among which exons 1, 2 and 10 are not involved in protein coding (Fig 1). As a protein-coding gene, the product protein of *IRF6* is one of nine members of the family of interferon regulatory factor (IRF) proteins and has two conserved domains: a highly conserved DNA-binding domain and a less conserved protein-binding domain termed Smad-interferon regulatory factor-binding domain (SMIR), both of which are critical for its function.<sup>57</sup>

*IRF6* is involved in the normal development of craniofacial structures by regulating epithelial differentiation and palatal fusion

*IRF6* is a key factor in the development of the lip and palate that plays an important role in craniofacial development and participates in the development of skin and external genitalia. Furthermore, as a key determinant in the proliferation-differentiation conversion of keratinocyte, *IRF6* is required for the differentiation of mammalian skin, mammary gland and oral epithelium, and involved in wound healing and migration.

Kondo et al<sup>4</sup> detected high expression of *IRF6* mRNA in fused palate, tooth bud, hair follicle, genitalia and the

medial edge of skin in mice, and found that the haploid deficiency would impair the normal development of the maxillofacial region and lead to orofacial cleft, confirming that *IRF6* is a key factor in the development of the lip and palate and is also involved in the development of the skin and external genitalia.

In 2006, Richardson et al<sup>58</sup> mutated Arg84 to cysteine (R84C) and constructed an *Irf6*<sup>R84C/R84C</sup> homozygous mutant mouse model that showed postnatal death. There were significant abnormalities in epidermal development in *Irf6*<sup>+ /R84C</sup> heterozygous mutant mice: a dense basal layer, less differentiation in the expanded basal layer and no granular layer or keratinised layer, indicating excessive epidermal hyperplasia and an abnormal differentiation process that may lead to epithelial adhesions that block the mouth and cause cleft lip and palate. In the same year, Ingraham et al<sup>59</sup> used a mouse model deficient for *Irf6* and observed abnormal skin, limbs and craniofacial morphology (Fig 2). They then conducted a histological and gene expression analysis on deficient mice and found that the main defect of mouse skin was abnormal proliferation and differentiation of keratinocytes, confirming that *Irf6* is necessary for regulating keratinocyte proliferation and terminal differentiation.<sup>59</sup> In vitro culture experiments supported *IRF6* as a necessary condition for keratinocyte differentiation and the authors speculated that epidermal adhesion in the oral cavity of mice was due to the absence of normal keratinocytes, whereas skeletal abnormalities were secondary to defective epidermal differentiation.<sup>60</sup>

Thompson et al<sup>61</sup> conducted mouse model studies and proposed a different view, suggesting that *IRF6* is involved in regulating bone differentiation and mineralisation during craniofacial bone development. In 2021, Girousi et al<sup>62</sup> used keratinocytes derived from human skin and oral mucosa to construct *IRF6* knockout cell lines. They found that keratinocytes lacking *IRF6* have poor cohesion, and most of the differentially expressed proteins may be related to differentiation, intercellular adhesion and immune response.<sup>62</sup> In 3D skin cultures, loss of *IRF6* resulted in severe keratinocyte differentiation defects while cell growth rates remained constant. These results suggested that *IRF6* deficiency disrupts epithelial homeostasis by altering the colony morphology, migration pattern and differentiation potential of human keratinocytes.<sup>62</sup>

Palatal development in vertebrates involves migration of cranial neural crest, fusion of facial processes and extension of cartilaginous framework, while cleft palate is a structural birth defect resulting from palatal dysplasia. *Irf6* is expressed in ectodermal fusions of

the upper lip and primary palate in mice and chicks, but only in the secondary palate in developing mice.<sup>63</sup> Similar expression patterns also exist in human craniofacial structures. *IRF6* is expressed in bilateral maxillary process chondrocytes and the maxillary processes need to fuse with the lateral nasal process in the centre. Dougherty et al<sup>64</sup> conducted a detailed analysis of palate development in zebrafish and revealed that *IRF6* is involved in palate morphogenesis by regulating the fusion of facial processes.

#### *Exploration of IRF6's participation mechanism in epithelial differentiation and palate fusion*

Given that in vitro and in vivo experiments have confirmed that *IRF6* plays an important role in regulating epithelial differentiation and palatal fusion in craniofacial development, subsequent studies on the molecular mechanism by which *IRF6* functions will help to describe and integrate the molecular pathway of lip and palate morphogenesis further.

Kousa et al<sup>65</sup> constructed a mouse model of *Irf6* gene knockout and restored the expression of *Irf6* in embryonic basal epithelium. They found that severity of the disease was significantly reduced and the death of mice after birth could be prevented, but the adhesion between the palate and tongue could not be saved completely, suggesting the importance of cell-independent *Irf6* expression in peritum.<sup>65</sup> In the same year, another study by Kousa et al<sup>66</sup> confirmed the interaction of *IRF6* and *SPRY4* signals in mouse peridermal development. Through microarray analysis and in vivo transplantation, de la Garza et al<sup>67</sup> proposed that the encoding gene of *Grhl3* is the direct effector of *Irf6* in percutaneous differentiation. In addition, *IRF6* protein interacts directly with *NME1* and *NME2* to regulate the availability or localisation of the *NME1/2* complex and the dynamic behaviour of the epithelia during lip and palate development. Missense mutations in *IRF6* or *NME* can lead to cleft lip and palate by damaging the ability of *IRF6* to bind to *NME* protein 66.<sup>68</sup> Ferretti et al<sup>69</sup> suggested that *IRF6* is involved in the conserved *PBX-Wnt-P63-IRF6* regulatory pathway in mammals that controls facial morphogenesis by promoting epithelial apoptosis. In addition, the integration of *IRF6* and *Jagged2* signalling is essential for controlling palatal adhesion and fusion competence.<sup>70</sup>

Palatal organ culture experiments showed that *IRF6* was involved in the regulation of *TGFβ3* on epithelial mesenchymal transformation and palatal fusion during embryonic palatal development.<sup>71</sup> This result supported the role of *IRF6* in the transforming growth

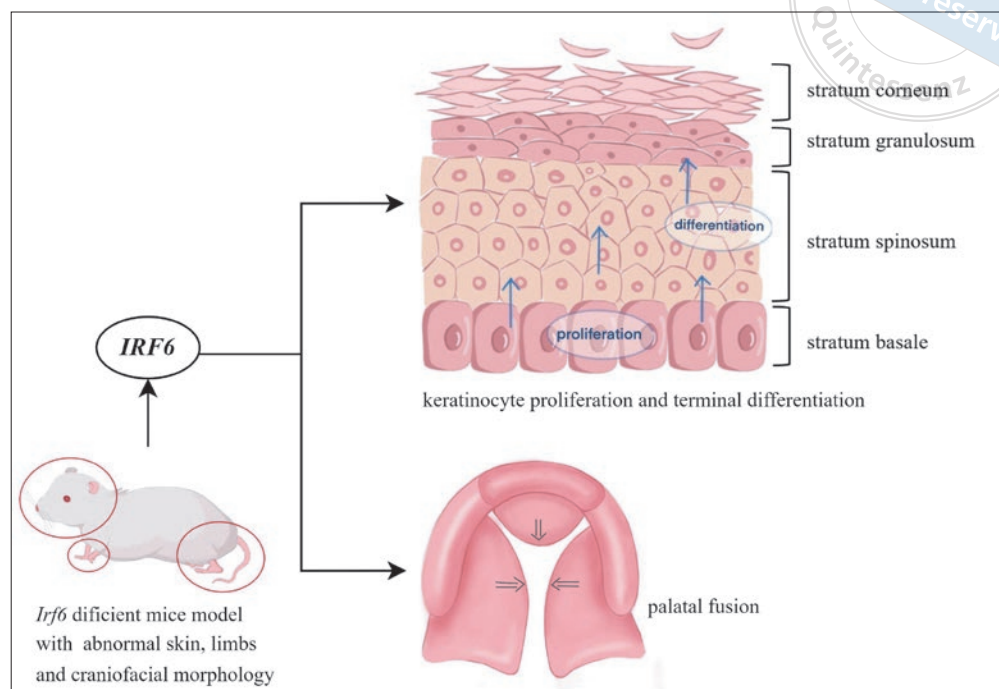


**Fig 2** Function of *IRF6* in the pathogenesis of orofacial cleft.

factor- $\beta$  (*TGF- $\beta$* ) signalling pathway, a fundamental developmental pathway.<sup>12</sup> Considering that deletion of *Irf6* can lead to cranial fracture and mandibular dysplasia in mice while mutations of *Twist1* gene can lead to cranial fracture, mandibular dysplasia and cleft palate, Fakhouri et al<sup>72</sup> constructed monozygotic and double heterozygotic *Irf6* and *Twist1* genes (*Irf6*<sup>+/-</sup>; *Twist1*<sup>+/-</sup>) mouse embryo models, respectively. Homozygous deletion of *Irf6* resulted in multiple bone defects in the mandible and limbs of mice; however, no expression of *Irf6* was detected in bone tissue, suggesting the existence of intercellular communication. Although monozygous mice were almost normal, some dizygous mice (*Irf6*<sup>+/-</sup>; *Twist1*<sup>+/-</sup>) mice developed severe hypoplasia of the mandible, leading to holoacrania and cleft palate. It is suggested that genes encoding IRF6 and Twist1, two transcription factors essential for craniofacial development, may lead to craniofacial diseases through gene-gene interaction.<sup>72</sup> A study in 2019 proposed that IRF6 and TAK1 synergistically promote HIPK2 activation and stimulate apoptosis during palatal fusion.<sup>73</sup> IRF6 can also regulate the expression of ESRP1, which overlaps in mouse oral-facial skin and zebrafish periderm, nasofrontal ectoderm and oral epithelium, and controls vertebrate midfacial morphogenesis through *Irf6*-ESRP1/2 regulatory axis.<sup>74</sup> Another study in 2020 indicated that SPECC1L cytoskeletal protein may function downstream of IRF6 in palatogenesis.<sup>75</sup>

In addition, mice carrying both p63 heterozygous deletion and *Irf6* knockout mutation R84C showed abnormal ectoderm development, which resulted in cleft palate. In vitro culture of primary keratinocytes from patients with cleft palate and functional studies found that P63 is a key regulatory molecule in palate development and binds to the upstream enhancer element to transactivate IRF6.<sup>76,77</sup> Mutations in this enhancer element are associated with increased susceptibility to cleft palate. In mouse and human oral and maxillofacial development, p63 and IRF6 act within a regulatory ring that coordinates epithelial cell proliferation and differentiation during normal palatal development. *IRF6* or p63 mutations cause this ring to break, resulting in fissure.<sup>76,77</sup> On the other hand, Kousa et al<sup>78</sup> found that IRF6 and AP2A interact to regulate epidermal development, and rs642961 located in the enhancer element interferes with its binding with AP2A protein, affecting epithelial cell development and increasing the risk of NSOC. They proposed that P63 and AP-2 $\alpha$  may play a synergistic role in *IRF6* regulation.<sup>78</sup>

### Conclusions and future research

Numerous genetic and functional studies have provided sufficient evidence for the contribution of *IRF6* in the pathogenesis of NSOC; however, studies have been conducted on different ethnic groups and population strati-

fication has become a major source of confounding factors in genetic studies, leading to possible differences in the results of studies of polymorphisms in different ethnic groups. In addition, although many polymorphisms in *IRF6* were associated with NSOC in genetic studies, it is still uncertain which of them are pathogenic due to the existence of linkage disequilibrium. The inclusion of other risk factors and genes would also be useful for the improvement of disease prediction models and occurrence risk assessment of NSOC.

### Conflicts of interest

The authors declare no conflicts of interest related to this study.

### Author contribution

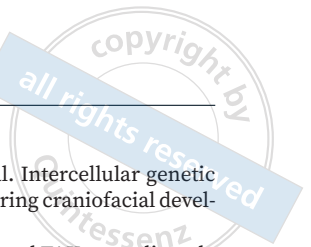
Dr Si Di ZHANG contributed to the literature collection, draft and revision; Dr Yue YOU contributed to the conception and draft; Dr Mei Lin YAO contributed to the draft; Dr Bing SHI contributed to supervision; Dr Zhong Lin JIA contributed to the conception, supervision and manuscript revision. All authors read and approved the final manuscript.

(Received Jun 05, 2023; accepted Oct 23, 2023)

### References

- Grosen D, Chevrier C, Skytthe A, et al. A cohort study of recurrence patterns among more than 54,000 relatives of oral cleft cases in Denmark: Support for the multifactorial threshold model of inheritance. *J Med Genet* 2010;47:162–168.
- Zuccherio TM, Cooper ME, Maher BS, et al. Interferon regulatory factor 6 (IRF6) gene variants and the risk of isolated cleft lip or palate. *N Engl J Med* 2004;351:769–780.
- Leslie EJ, Standley J, Compton J, Bale S, Schutte BC, Murray JC. Comparative analysis of IRF6 variants in families with Van der Woude syndrome and popliteal pterygium syndrome using public whole-exome databases. *Genet Med* 2013;15:338–344.
- Kondo S, Schutte BC, Richardson RJ, et al. Mutations in IRF6 cause Van der Woude and popliteal pterygium syndromes. *Nat Genet* 2002;32:285–289.
- Kerameddin S, Namipashaki A, Ebrahimi S, Ansari-Pour N. IRF6 is a marker of severity in nonsyndromic cleft lip/palate. *J Dent Res* 2015;94(9, suppl):226S–232S.
- Barrett JH, Teare MD. Linkage analysis. In *Silico Tools for Gene Discovery*. Berlin: Springer, 2011:19–33.
- Scapoli L, Palmieri A, Martinelli M, et al. Strong evidence of linkage disequilibrium between polymorphisms at the IRF6 locus and nonsyndromic cleft lip with or without cleft palate, in an Italian population. *Am J Hum Genet* 2005;76:180–183.
- Blanton SH, Cortez A, Stal S, Mulliken JB, Finnell RH, Hecht JT. Variation in IRF6 contributes to nonsyndromic cleft lip and palate. *Am J Med Genet A* 2005;137A:259–262.
- Jakobsen LP, Ullmann R, Kjaer KW, Knudsen MA, Tommerup N, Eiberg H. Suggestive linkage to a neighboring region of IRF6 in a cleft lip and palate multiplex family. *Am J Med Genet A* 2007;143A:2716–2721.
- Marazita ML, Murray JC, Lidral AC, et al. Meta-analysis of 13 genome scans reveals multiple cleft lip/palate genes with novel loci on 9q21 and 2q32–35. *Am J Hum Genet* 2004;75:161–173.
- Marazita ML, Lidral AC, Murray JC, et al. Genome scan, fine-mapping, and candidate gene analysis of non-syndromic cleft lip with or without cleft palate reveals phenotype-specific differences in linkage and association results. *Hum Hered* 2009;68:151–170.
- Ardinger HH, Buetow KH, Bell GI, Bardach J, VanDemark DR, Murray JC. Association of genetic variation of the transforming growth factor-alpha gene with cleft lip and palate. *Am J Hum Genet* 1989;45:348–353.
- Park JW, McIntosh I, Hetmanski JB, et al. Association between IRF6 and nonsyndromic cleft lip with or without cleft palate in four populations. *Genet Med* 2007;9:219–227.
- Ghassibé M, Bayet B, Revencu N, et al. Interferon regulatory factor-6: A gene predisposing to isolated cleft lip with or without cleft palate in the Belgian population. *Eur J Hum Genet* 2005;13:1239–1242.
- Sun Y, Huang Y, Yin A, et al. Genome-wide association study identifies a new susceptibility locus for cleft lip with or without a cleft palate. *Nat Commun* 2015;6:6414.
- de Souza LT, Kowalski TW, Ferrari J, et al. Study of IRF6 and 8q24 region in non-syndromic oral clefts in the Brazilian population. *Oral Dis*. 2016;22:241–245.
- Letra A, Fakhouri W, Fonseca RF, et al. Interaction between IRF6 and TGFA genes contribute to the risk of nonsyndromic cleft lip/palate. *PLoS One* 2012;7:e45441.
- Suazo J, Santos JL, Jara L, Blanco R. Linkage disequilibrium between IRF6 variants and nonsyndromic cleft lip/palate in the Chilean population. *Am J Med Genet A* 2008;146A:2706–2708.
- Pan Y, Ma J, Zhang W, et al. IRF6 polymorphisms are associated with nonsyndromic orofacial clefts in a Chinese Han population. *Am J Med Genet A* 2010 ;152A:2505–2511.
- Larrabee YC, Birkeland AC, Kent DT, et al. Association of common variants, not rare mutations, in IRF6 with nonsyndromic clefts in a Honduran population. *Laryngoscope* 2011;121:1756–1759.
- Rahimov F, Marazita ML, Visel A, et al. Disruption of an AP-2 binding site in an IRF6 enhancer is associated with cleft lip. *Nat Genet* 2008;40:1341–1347.
- Brito LA, Bassi CF, Masotti C, et al. IRF6 is a risk factor for nonsyndromic cleft lip in the Brazilian population. *Am J Med Genet A* 2012;158A:2170–2175.
- Birnbaum S, Ludwig KU, Reutter H, et al. IRF6 gene variants in Central European patients with non-syndromic cleft lip with or without cleft palate. *Eur J Oral Sci* 2009;117:766–769.
- Pegelow M, Koillinen H, Magnusson M, et al. Association and mutation analyses of the IRF6 gene in families with nonsyndromic and syndromic cleft lip and/or cleft palate. *Cleft Palate Craniofac J* 2014;51:49–55.
- Huang Y, Wu J, Ma J, et al. Association between IRF6 SNPs and oral clefts in West China. *J Dent Res* 2009;88:715–718.
- Jugessur A, Rahimov F, Lie RT, et al. Genetic variants in IRF6 and the risk of facial clefts: Single-marker and haplotype-based analyses in a population-based case-control study of facial clefts in Norway. *Genet Epidemiol* 2008;32:413–424.
- Ibarra-Arce A, García-Álvarez M, Cortés-González D, et al. IRF6 polymorphisms in Mexican patients with non-syndromic cleft lip. *Meta Gene* 2015;4:8–16.

28. Suazo J, Recabarren AS, Marín N, Blanco R. Association between IRF6 variants and nonsyndromic cleft lip with or without cleft palate in Chile. *Reprod Sci* 2020;27:1857–1862.
29. Gurramkonda VB, Syed AH, Murthy J, Lakkakula BVKS. IRF6 rs2235375 single nucleotide polymorphism is associated with isolated non-syndromic cleft palate but not with cleft lip with or without palate in South Indian population. *Braz J Otorhinolaryngol* 2018;84:473–477.
30. Xu W, Han WT, Lu YP, Feng WH, Dai M. Association of single-nucleotide polymorphisms, rs2235371 and rs2013162, in the IRF6 gene with non-syndromic cleft palate in northeast China. *Genet Mol Res* 2016;15:(3).
31. Srichomthong C, Siriwan P, Shotelersuk V. Significant association between IRF6 820G->A and non-syndromic cleft lip with or without cleft palate in the Thai population. *J Med Genet* 2005;42:e46.
32. Tang W, Du X, Feng F, et al. Association analysis between the IRF6 G820A polymorphism and nonsyndromic cleft lip and/or cleft palate in a Chinese population. *Cleft Palate Craniofac J* 2009;46:89–92.
33. Jia ZL, Li Y, Li L, et al. Association among IRF6 polymorphism, environmental factors, and nonsyndromic orofacial clefts in western China. *DNA Cell Biol* 2009;28:249–257.
34. Schadt EE, Molony C, Chudin E, et al. Mapping the genetic architecture of gene expression in human liver. *PLoS Biol* 2008;6:e107.
35. Jagomägi T, Nikopensius T, Krjutskov K, et al. MTHFR and MSX1 contribute to the risk of nonsyndromic cleft lip/palate. *Eur J Oral Sci* 2010;118:213–220.
36. Mostowska A, Hozyasz KK, Wojcicki P, Biedziak B, Paradowska P, Jagodzinski PP. Association between genetic variants of reported candidate genes or regions and risk of cleft lip with or without cleft palate in the Polish population. *Birth Defects Res A Clin Mol Teratol* 2010;88:538–545.
37. Nikopensius T, Jagomägi T, Krjutskov K, et al. Genetic variants in COL2A1, COL11A2, and IRF6 contribute risk to non-syndromic cleft palate. *Birth Defects Res A Clin Mol Teratol* 2010;88:748–756.
38. Song T, Wu D, Wang Y, Li H, Yin N, Zhao Z. SNPs and interaction analyses of IRF6, MSX1 and PAX9 genes in patients with non-syndromic cleft lip with or without palate. *Mol Med Rep* 2013;8:1228–1234.
39. Diercks GR, Karnezis TT, Kent DT, et al. The association between interferon regulatory factor 6 (IRF6) and nonsyndromic cleft lip with or without cleft palate in a Honduran population. *Laryngoscope* 2009;119:1759–1764.
40. Blanton SH, Burt A, Garcia E, Mulliken JB, Stal S, Hecht JT. Ethnic heterogeneity of IRF6 AP-2a binding site promoter SNP association with nonsyndromic cleft lip and palate. *Cleft Palate Craniofac J* 2010;47:574–577.
41. Paranaíba LM, Bufalino A, Martelli-Júnior H, de Barros LM, Graner E, Coletta RD. Lack of association between IRF6 polymorphisms (rs2235371 and rs642961) and non-syndromic cleft lip and/or palate in a Brazilian population. *Oral Dis* 2010;16:193–197.
42. Tomita D, Yamaguchi T, Nakawaki T, et al. Interferon regulatory factor 6 variants affect nasolabial morphology in East Asian populations. *Arch Oral Biol* 2018;85:142–147.
43. Cantor RM, Lange K, Sinsheimer JS. Prioritizing GWAS results: A review of statistical methods and recommendations for their application. *Am J Hum Genet* 2010;86:6–22.
44. Manolio TA, Collins FS, Cox NJ, et al. Finding the missing heritability of complex diseases. *Nature* 2009;461:747–753.
45. Beaty TH, Taub MA, Scott AF, et al. Confirming genes influencing risk to cleft lip with/without cleft palate in a case-parent trio study. *Hum Genet* 2013;132:771–781.
46. Beaty TH, Murray JC, Marazita ML, et al. A genome-wide association study of cleft lip with and without cleft palate identifies risk variants near MAFB and ABCA4. *Nat Genet* 2010;42:525–529.
47. Raychaudhuri S. Mapping rare and common causal alleles for complex human diseases. *Cell* 2011;147:57–69.
48. Zuk O, Hechter E, Sunyaev SR, Lander ES. The mystery of missing heritability: Genetic interactions create phantom heritability. *Proc Natl Acad Sci U S A* 2012;109:1193–1198.
49. Eichler EE, Flint J, Gibson G, et al. Missing heritability and strategies for finding the underlying causes of complex disease. *Nat Rev Genet* 2010;11:446–450.
50. Pegelow M, Peyrard-Janvid M, Zucchelli M, et al. Familial non-syndromic cleft lip and palate—analysis of the IRF6 gene and clinical phenotypes. *Eur J Orthod* 2008;30:169–175.
51. Zhao H, Zhang M, Zhong W, et al. A novel IRF6 mutation causing non-syndromic cleft lip with or without cleft palate in a pedigree. *Mutagenesis* 2018;33:195–202.
52. Sylvester B, Brindopke F, Suzuki A, et al. A synonymous exonic splice silencer variant in IRF6 as a novel and cryptic cause of non-syndromic cleft lip and palate. *Genes (Basel)* 2020;11:903.
53. Wang Y, Ma C, Jiang C, Zhang Y, Wu D. A novel IRF6 variant detected in a family with nonsyndromic cleft lip and palate by whole exome sequencing. *J Craniofac Surg* 2021;32:265–269.
54. Carlson JC, Taub MA, Feingold E, et al. Identifying genetic sources of phenotypic heterogeneity in orofacial clefts by targeted sequencing. *Birth Defects Res* 2017;109:1030–1038.
55. Xiao Y, Taub MA, Ruczinski I, et al. Evidence for SNP-SNP interaction identified through targeted sequencing of cleft case-parent trios. *Genet Epidemiol* 2017;41:244–250.
56. Li Y, Deng Y, Deng C, et al. Association of long interspersed nucleotide element-1 and interferon regulatory factor 6 methylation changes with nonsyndromic cleft lip with or without cleft palate. *Oral Dis* 2019;25:215–222.
57. Eroshkin A, Mushegian A. Conserved transactivation domain shared by interferon regulatory factors and Smad morphogens. *J Mol Med (Berl)* 1999;77:403–405.
58. Richardson RJ, Dixon J, Malhotra S, et al. Irf6 is a key determinant of the keratinocyte proliferation-differentiation switch. *Nat Genet* 2006;38:1329–1334.
59. Ingraham CR, Kinoshita A, Kondo S, et al. Abnormal skin, limb and craniofacial morphogenesis in mice deficient for interferon regulatory factor 6 (Irf6). *Nat Genet* 2006;38:1335–1340.
60. Biggs LC, Rhea L, Schutte BC, Dunnwald M. Interferon regulatory factor 6 is necessary, but not sufficient, for keratinocyte differentiation. *J Invest Dermatol* 2012;132:50–58.
61. Thompson J, Mendoza F, Tan E, et al. A cleft lip and palate gene, Irf6, is involved in osteoblast differentiation of craniofacial bone. *Dev Dyn* 2019;248:221–232.
62. Giroussi E, Muerner L, Parisi L, et al. Lack of IRF6 disrupts human epithelial homeostasis by altering colony morphology, migration pattern, and differentiation potential of keratinocytes. *Front Cell Dev Biol* 2021;9:718066.
63. Knight AS, Schutte BC, Jiang R, Dixon MJ. Developmental expression analysis of the mouse and chick orthologues of IRF6: The gene mutated in Van der Woude syndrome. *Dev Dyn* 2006;235:1441–1447.
64. Dougherty M, Kamel G, Grimaldi M, et al. Distinct requirements for wnt9a and irf6 in extension and integration mechanisms during zebrafish palate morphogenesis. *Development* 2013;140:76–81.



65. Kousa YA, Moussa D, Schutte BC. IRF6 expression in basal epithelium partially rescues Irf6 knockout mice. *Dev Dyn* 2017;246:670–681.
66. Kousa YA, Roushangar R, Patel N, et al. IRF6 and SPRY4 signaling interact in periderm development. *J Dent Res* 2017;96:1306–1313.
67. de la Garza G, Schleiffarth JR, Dunwald M, et al. Interferon regulatory factor 6 promotes differentiation of the periderm by activating expression of Grainyhead-like 3. *J Invest Dermatol* 2013;133:68–77 [erratum 2013;133:859].
68. Parada-Sanchez MT, Chu EY, Cox LL, et al. Disrupted IRF6-NME1/2 complexes as a cause of cleft lip/palate. *J Dent Res* 2017;96:1330–1338.
69. Ferretti E, Li B, Zewdu R, et al. A conserved Pbx-Wnt-p63-Irf6 regulatory module controls face morphogenesis by promoting epithelial apoptosis. *Dev Cell* 2011;21:627–641.
70. Richardson RJ, Dixon J, Jiang R, Dixon MJ. Integration of IRF6 and Jagged2 signalling is essential for controlling palatal adhesion and fusion competence. *Hum Mol Genet* 2009;18:2632–2642.
71. Ke CY, Xiao WL, Chen CM, Lo LJ, Wong FH. IRF6 is the mediator of TGF $\beta$ 3 during regulation of the epithelial mesenchymal transition and palatal fusion. *Sci Rep* 2015;5:12791.
72. Fakhouri WD, Metwalli K, Naji A, et al. Intercellular genetic interaction between Irf6 and Twist1 during craniofacial development. *Sci Rep* 2017;7:7129.
73. Ke CY, Mei HH, Wong FH, Lo LJ. IRF6 and TAK1 coordinately promote the activation of HIPK2 to stimulate apoptosis during palate fusion. *Sci Signal* 2019;12:eaav7666.
74. Carroll SH, Macias Trevino C, Li EB, et al. Irf6An - Regulatory axis controls midface morphogenesis in vertebrates. *Development* 2020;147:dev194498.
75. Hall EG, Wenger LW, Wilson NR, et al. SPECC1L regulates palate development downstream of IRF6. *Hum Mol Genet* 2020;29:845–858.
76. Moretti F, Marinari B, Lo Iacono N, et al. A regulatory feedback loop involving p63 and IRF6 links the pathogenesis of 2 genetically different human ectodermal dysplasias. *J Clin Invest* 2010;120:1570–1577.
77. Thomason HA, Zhou H, Kouwenhoven EN, et al. Cooperation between the transcription factors p63 and IRF6 is essential to prevent cleft palate in mice. *J Clin Invest* 2010;120:1561–1569.
78. Kousa YA, Fuller E, Schutte BC. IRF6 and AP2A interaction regulates epidermal development. *J Invest Dermatol* 2018;138:2578–2588.

# Characteristic and Import Mechanism of Protein Nuclear Translocation

Zi Yan SUN<sup>1</sup>, Zhi Peng FAN<sup>2,3</sup>

*Coordination and information exchange among the various organelles ensure the precise and orderly functioning of eukaryotic cells. Interaction between the cytoplasm and nucleoplasm is crucial for many physiological processes. Macromolecular protein transport into the nucleus requires assistance from the nuclear transport system. These proteins typically contain a nuclear localisation sequence that guides them to enter the nucleus. Understanding the mechanism of nuclear import of macromolecular proteins is important for comprehending cellular processes. Investigation of disease-related alterations can facilitate the development of novel therapeutic strategies and provide additional evidence for clinical trials. This review provides an overview of the proteins involved in nuclear transport and the mechanisms underlying macromolecular protein transport.*

**Keywords:** karyopherin, nuclear import, nuclear localisation sequence, nuclear pore complex, nucleocytoplasmic transport

*Chin J Dent Res* 2024;27(1):39–46; doi: 10.3290/j.cjdr.b5136729

Eukaryotic cells are characterised by the presence of a complete nucleus enclosed by a double nuclear membrane and well-defined organelles that ensure the spatial segregation of nuclear DNA replication, gene transcription and protein translation. This structure confers a potent mechanism for regulating gene expression in eukaryotes.<sup>1</sup> After their synthesis in the cytoplasm,

proteins are selectively and efficiently transported to distinct locations where they perform their physiological functions. Karyophilic proteins, including transcription factors, replication factors, DNA repair factors and cell-cycle regulators, require nuclear entry to execute their functions.<sup>2</sup> The nuclear envelope (NE), as a natural selective barrier, separates the nucleus from other organelles and the cytoplasm. The nuclear pore complex (NPC), located on the nuclear membrane, regulates molecular transport between the nucleus and cytoplasm. The transport mechanism used by the NPC depends on the size of the substrate transported: while small molecules diffuse passively through the NPC, larger proteins require active transport by the nuclear transport system (NTS) to enter the nucleus.<sup>3</sup> Karyophilic proteins typically possess a conserved amino acid sequence, known as the nuclear localisation sequence (NLS), that functions as a recognition site for protein nuclear import.<sup>4</sup>

Recent studies on the nuclear transport of NLS-containing proteins have been conducted in the field of oral and maxillofacial diseases.<sup>5,6</sup> PTHrP exerts its effects via intracrine/paracrine signalling or by entering the nucleus. Deletion of the PTHrP NLS leads to dental and mandibular dysplasia in mice and is associated with the p27 pathway.<sup>5</sup> IGFBP2 upregulates

1 Beijing Key Laboratory of Tooth Regeneration and Function Reconstruction, Capital Medical University School of Stomatology, Beijing, P.R. China.

2 Laboratory of Molecular Signaling and Stem Cells Therapy, Beijing Key Laboratory of Tooth Regeneration and Function Reconstruction, Capital Medical University School of Stomatology, Beijing, P.R. China.

3 Research Unit of Tooth Development and Regeneration, Chinese Academy of Medical Sciences, Beijing, P.R. China.

**Corresponding author:** Dr Zhi Peng FAN, Laboratory of Molecular Signaling and Stem Cells Therapy, Beijing Key Laboratory of Tooth Regeneration and Function Reconstruction, Capital Medical University School of Stomatology, No. 4 Tiantanxili, Dongcheng District, Beijing 100050, P.R. China. Tel: 86-10-57099114. Email: zpfan@ccmu.edu.cn

This work was supported by National Key Research and Development Program (2022YFA1104401), CAMS Innovation Fund for Medical Sciences (2019-I2M-5-031) and grants from Innovation Research Team Project of Beijing Stomatological Hospital, Capital Medical University (NO. CXTD202204).

ZEB1 expression in an NF- $\kappa$ B (p65)-dependent manner, thereby promoting epithelial-mesenchymal transition (EMT) in salivary adenoid cystic carcinoma. Mutations in the IGFBP2 NLS effectively prevent EMT and reduce lung and liver metastasis.<sup>6</sup> Based on these findings, NLS-mediated protein nuclear transport plays a crucial role in the occurrence and progression of oral and maxillofacial diseases via various proteases, cytokines and signalling pathways. The investigation of protein nuclear import processes offers potential targets for treating oral and maxillofacial diseases. The present review advances this by focusing on proteins involved in the NTS and elucidates the mechanisms underlying karyophilic protein transport.

## NTS

The NTS, which plays an important role in the nucleocytoplasmic translocation of macromolecular proteins, encompasses the NPC and nuclear transport receptors (NTRs).<sup>7</sup> The NPC is a large macromolecular assembly that spans the NE, forming a central transport channel with an outer diameter of  $\sim 1,200$  Å, an inner diameter of  $\sim 425$  Å and a height of  $\sim 800$  Å. This structure regulates nucleocytoplasmic transport and mediates protein trafficking.<sup>3,8</sup> The NPC comprises  $> 30$  nucleoporins (NUPs), which can be divided into three groups based on their functions: transmembrane proteins, which anchor the NPC to the NE; scaffold proteins, which constitute the inner and outer rings of the NPC; and phenylalanine-glycine (FG) NUPs (FG-NUPs), characterised by their abundant hydrophobic FG repeats. FG-NUPs, intrinsically disordered proteins that comprise approximately one-third of all NUPs, play an important role in precisely mediating cargo protein transport; during nucleocytoplasmic translocation, they exclude nonspecific macromolecular substances from the NPC's central transport channel, forming a dynamic selective barrier.<sup>1,2,8-11</sup>

Based on their structural and functional differences, NTRs can be separated into the Karyopherin  $\alpha$  and  $\beta$  families.<sup>3,4</sup> Karyopherin  $\alpha$ , also known as importin  $\alpha$ , recognises and connects importin  $\beta$  with cargo proteins.<sup>4,11,12</sup> In mammalian cells, the importin  $\alpha$  family comprises six members that are capable of recognising and binding cargo proteins; however, within the NPC, importin  $\alpha$  lacks a shuttle function, and importin  $\beta$  is required to help translocate cargo proteins into the nucleus.<sup>2,13,14</sup> In eukaryotes, the karyopherin  $\beta$  family serves as a ubiquitous NTR; at least 20 distinct isoforms, responsible for most intracellular trafficking between the nucleus and cytoplasm, have been identified in human cells. The karyopherin  $\beta$  family includes the

importin  $\beta$  proteins, which are composed of 11 members that function specifically as import receptors.<sup>14</sup> Most importin  $\beta$  members can bind directly to the NLS and carry it into the nucleus, where they then release the cargo protein.<sup>14-16</sup>

Importin  $\alpha$  has three key domains, the first of which is the central domain, comprising ten Armadillo (ARM) repeats, each 42 to 43 amino acids in length. This domain is responsible for recognising the cargo protein NLS.<sup>4,13,17</sup> The cargo protein binds to two sites in the ARM repeat sequence: the major NLS binding site (ARM repeat sequences 2 to 4) and the minor NLS binding site (ARM repeat sequences 6 to 8).<sup>13</sup>

Second, at its N-terminus, importin  $\alpha$  contains the importin  $\beta$  binding domain (IBB), which can bind to importin  $\beta$ .<sup>12</sup> The IBB, containing an NLS-like sequence, can occupy the NLS binding site in the absence of importin  $\beta$ ; this capability is thought to exert an autoinhibitory effect. This autoinhibition effectively prevents importin  $\beta$  from binding to an empty importin  $\alpha$ , thus ensuring that nuclear transport is not blocked. The autoinhibitory domain competitively occupies the NLS binding site, facilitating the release of the NLS cargo upon transport to the nucleus.<sup>16-18</sup>

The third domain is the C-terminal domain of importin  $\alpha$ , which binds to the nuclear export receptor (cellular apoptosis susceptibility protein [CAS]). CAS has a similar structure to importin  $\beta$ , facilitating importin export of  $\alpha$  into the cytoplasm (Table 1).<sup>2,17,19,20</sup>

Importin  $\beta$  comprises tandem huntingtin, elongation factor 3, A subunit of PP2A, and TOR (HEAT) repeats arranged in a superhelix or ring-like structure to form binding sites for importin  $\alpha$ , FG-NUPs and Ran-GTP.<sup>15,21,22</sup> By altering its own conformation, importin  $\beta$  can provide binding sites for protein-protein interactions (Table 1).<sup>23</sup>

In the karyophilic protein transport cycle, molecular recognition depends crucially on precise spatial and temporal regulation.<sup>16</sup> The binding and release of cargo proteins by the NTR is regulated by the small GTPase Ran. Upon binding to importin  $\beta$ , Ran-GTP triggers the dissociation of the cargo protein from the transport complex. Ran, characterised by an N-terminal globular domain and C-terminal extension structure, participates in various nuclear processes, including maintaining nuclear architecture, facilitating protein import, regulating mRNA processing and export, and controlling cell cycle progression.<sup>8,24,25</sup> Ran occurs as Ran-GDP and Ran-GTP on both sides of the nuclear membrane. The N-terminal globular domain of Ran binds to GTP and facilitates its hydrolysis. Its C-terminal extension structure features a unique acidic tail that binds to its



**Table 1** Structural characterisation of NTRs.

NTR	Structural characterisation	Function
Importin $\alpha$	Armadillo (ARM) repeats	Recognizes the cargo proteins NLS
	Importin $\beta$ binding (IBB) domain	Acts as a competitive inhibitor to regulate cNLS-cargo binding by importin $\beta$ 1
	C-terminal domain of importin $\alpha$	Binds to the export receptor CAS
Importin $\beta$	HEAT repeats	Forms binding sites with importin $\alpha$ , FG-NUPs, Ran-GTP

FG-NUP, phenylalanine-glycine (FG) nucleoporins (FG-NUPS); HEAT, huntingtin, elongation factor 3, A subunit of PP2A and TOR.

**Table 2** Sequence features of cargo proteins with the NLS.

Category	Sequence features		Example
cNLS	Monopartite cNLS	K-K/R-X-K/R	PKKKRRV
	Bipartite cNLS	(K/R)(K/R)X <sub>10-12</sub> (K/R) <sub>3/5</sub>	KRPAATKKAGQAKKKK
ncNLS	PY-NLS	R/K/H-X <sub>2-5</sub> -P-Y or R/K/H-X <sub>2-5</sub> -P- $\Phi$ motif	FGNYNNQSSNFGPMKGGNFGGRSSGPY RSGGNHRRNRGRGGYNNRRNGYHPY
	IK-NLS	K-V/I-X-K-X1-2-K/H/R	None
	RS-repeat NLS	None	None
Other types of NLS	Cryptic NLS	None	None
	Putative NLS	None	None

cNLS, classical NLS; ncNLS, nonclassical NLS; IK-NLS, isoleucine-lysine NLS; PY-NLS, proline-tyrosine NLS; RS-NLS, arginine-serine NLS.

N-terminus when it is bound to GDP, thereby stabilising the structure of Ran-GDP.<sup>15</sup> Ran-GTP is hydrolysed to Ran-GDP by the RAN GTPase-activating protein (RanGAP) and RAN-binding protein-1 (RanBP-1), and can be converted back to Ran-GTP via interactions with the guanine nucleotide exchange factor for Ran (RanGEF). These key regulators exhibit a non-uniform distribution within cells, with RanGAP concentrated in the cytoplasm and RanGEF enriched in the nucleus, resulting in the accumulation of Ran-GTP in the nucleus and enrichment of Ran-GDP in the cytoplasm. The concentration gradient on either side of the NPC is important for directional nuclear transport.<sup>2,15,22,24-26</sup>

### Molecular mechanism of protein nuclear transport

Karyophilic proteins require not only the NTS, but also the NLS. The latter can be located anywhere within a karyophilic protein; upon recognition and binding by NTRs, this complex is transported into the nucleus.<sup>27</sup>

#### Classification of NLSs

Since the discovery of the first NLS in the 1980s (the T-antigen of simian vacuolating virus 40, SV40 TAg), an NLS classification system has gradually been developed.<sup>1,4,20,27</sup> Based on their residue composition, NLSs are currently classified into one of three types: classical (cNLS), nonclassical (ncNLS) or other.<sup>4</sup>

#### Classical NLSs

Classical NLSs contain one (monopartite) or two (bipartite) clusters of basic amino acids rich in positively charged lysine and arginine. A monopartite cNLS comprises 4 to 8 amino acids and has a consensus sequence of K-K/R-X-K/R, where X can be any residue. A representative example is the SV40-TAg cNLS PKKKRRV. A bipartite cNLS comprises two clusters of basic amino acids separated by a 10 to 12 residue linker region; the consensus sequence is (K/R)(K/R)X<sub>10-12</sub>(K/R)<sub>3/5</sub>, where X<sub>10-12</sub> is a linker of 10 to 12 residues and (K/R)<sub>3/5</sub> refers to three basic residues within five consecutive residues. The prototypical bipartite NLS is the *Xenopus* nucleoplasmic NLS (KRPAATKKAGQAKKKK) (Table 2).<sup>2,4,20</sup>

#### Nonclassical NLSs

For many proteins that lack distinct amino acid clustering, the structural characterisation of the NLS has not yet been clearly defined. Such NLSs are considered nonclassical. The most extensively researched ncNLSs, the proline-tyrosine (PY)-NLS, exhibits sequence diversity.<sup>14</sup> It comprises a loose N-terminal hydrophobic or basic motifs and a C-terminal R/K/H-X<sub>2-5</sub>-P-Y or R/K/H-X<sub>2-5</sub>-P- $\Phi$  motif (where  $\Phi$  refers to hydrophobic, H to histidine, P to proline and Y to tyrosine, and X<sub>2-5</sub> is any sequence of 2-5 residues).<sup>14,28,29</sup> PY-NLSs can be divided into two subclasses, depending on the composition of their N-terminal motifs: hydrophobic PY (hPY)-NLSs,

containing  $\Phi$ G/A/S $\Phi\Phi$  motifs (where  $\Phi$  refers to a hydrophobic residue), and basic PY (bPY)-NLSs, which are enriched with basic residues.<sup>14,29</sup> hnRNPA1 and Hrp1 are representative PY-NLSs, with the sequences FGNYN-NQSSNFGPMKGGNFGGRSSGPY and RSGGNHRRNGRG-GRGGYNRRNNGYHPY, respectively.<sup>4</sup> Isoleucine-lysine (IK)-NLS, another ncNLS, has the consensus sequence K-V/I-X-K-X1-2-K /H/R. TNPO3-binding arginine-serine repeat NLS (RS-repeat NLS), is another type of ncNLS (Table 2).<sup>29</sup> Further research into these NLSs is required.

### Other NLSs

Other specialised forms of NLS have been identified. These include cryptic NLSs, which occur in some proteins that do not bind to NTRs. However, upon specific signalling stimulation, these protein structures can undergo transformation and expose their NLS for entry into the nucleus.<sup>4,30</sup> Some NLSs predicted by software exhibit a characteristic NLS amino acid sequence composition (Table 2). Upon verification, some exhibited a nuclear-localisation function, whereas others did not and were therefore classified as putative NLSs.<sup>4,31</sup> This indicates that, despite the regularity of the NLS, there remain uncertainties that require investigation and investment.

### Mechanisms of nuclear transport

#### Nuclear transport of proteins with a cNLS

Importin  $\alpha$  and  $\beta$ 1 participate in the cNLS-mediated nuclear protein import.<sup>4,12,13,32</sup> The ARM domain of importin  $\alpha$  initially recognises and binds to the cNLS of the cargo protein. Monopartite cNLSs bind to the major NLS-binding site, whereas bipartite cNLSs interact with both major and minor NLS binding sites.<sup>16</sup> The IBB domain of importin  $\alpha$  then interacts with importin  $\beta$ 1, forming a trimeric complex (cargo-importin  $\alpha$ -importin  $\beta$ 1) that localises to the NE.<sup>16,20</sup> Finally, the importin  $\beta$ 1 in this complex binds to FG-NUPs, facilitating translocation of the trimeric complex into the nucleus.<sup>16</sup> During cargo-protein transport into the nucleus, nuclear RanGTP binds to importin  $\beta$ 1, inducing conformational change and elongation of its superhelical structure. This leads to the dissociation between importin  $\alpha$  and importin  $\beta$ 1, releasing the IBB domain, which in turn competitively binds to importin  $\alpha$  and promotes cargo-protein dissociation. NUPs such as Nup50 also facilitate the dissociation of the cargo proteins that remain in the nucleus.<sup>8,16,18,33</sup> Importin  $\beta$ 1-RanGTP dimers are transported directly back to the cytoplasm, while

importin  $\alpha$  is exported from the nucleus with the assistance of RanGTP and the nuclear export receptor CAS. Aided by RanBP1, cytoplasmic RanGAP catalyses the conversion of RanGTP to RanGDP, causing the dissociation of the importin  $\beta$ 1-RanGTP dimer and the CAS-RanGTP-importin  $\alpha$  complex, freeing the importin  $\beta$ 1 and importin  $\alpha$  to participate in subsequent nuclear import cycles. RanGDP in the cytoplasm is transported back to the nucleus via its carrier nuclear transport factor-2 (NTF2), replenishing the nucleoplasmic RanGTP and maintaining the RanGTP-RanGDP concentration gradient (Fig 1).<sup>13,16,34</sup>

#### Nuclear transport of proteins with an ncNLS

Most of the ncNLS-mediated nuclear transport proteins are imported via importin  $\beta$ .<sup>15,16</sup> Many karyophilic proteins lack classical monopartite and bipartite NLSs, necessitating other modes of transport into the nucleus. The mechanism of nuclear entry of PY-NLS-carrying proteins has been well investigated. PY-NLS, the best characterised substrate of importin  $\beta$ 2, is directly recognised by importin  $\beta$ 2. Various PY-NLS-containing proteins, including hnRNPA1, hnRNP D, hnRNP M and HCC1, have been identified as importin  $\beta$ 2 cargo proteins. Although the sequence identity of importin  $\beta$ 2 and  $\beta$ 1 is only 24%, they have almost the same structure: while their RanGTP-binding domains are highly similar, they differ substantially in their cargo-protein binding positions.<sup>35</sup>

Importin  $\beta$ 2 can bind directly to cargo proteins in the absence of importin.<sup>14,35</sup> Two major NLS-binding sites have been identified within importin  $\beta$ 2. The first, Site A, corresponds to H8-H13 and exhibits a high affinity for PY-NLS; it plays an indispensable role in recognition. The second, Site B, corresponds to H14-H20 and exhibits a lower affinity for PY-NLS.<sup>36</sup> The interaction between Site B and the NLS governs the overall binding affinity of importin  $\beta$ 2.<sup>36</sup> PY-NLS has three important epitopes involved in importin  $\beta$ 2 binding.<sup>37</sup> Epitope 1 corresponds to the N-terminal hydrophobic/basic motif, epitope 2 to the positively charged residue of the C-terminal R/K/H-X<sub>2-5</sub>-P-Y motif, and epitope 3 to the proline-tyrosine dipeptide of the C-terminal R/K/H-X<sub>2-5</sub>-P-Y motif.<sup>37</sup> Site A of importin  $\beta$ 2 interacts with epitopes 2 and 3, whereas Site B interacts with epitope 1.<sup>35</sup>

Initially, importin  $\beta$ 2 binds to PY-NLS via its C-terminal arch: first, Site A binds to the C-terminal R/K/H-X<sub>2-5</sub>-P-Y motif, triggering structural rearrangement at H13-H14 and inducing Site B to bind to epitope 1. Importin  $\beta$ 2 exhibits biochemical proper-

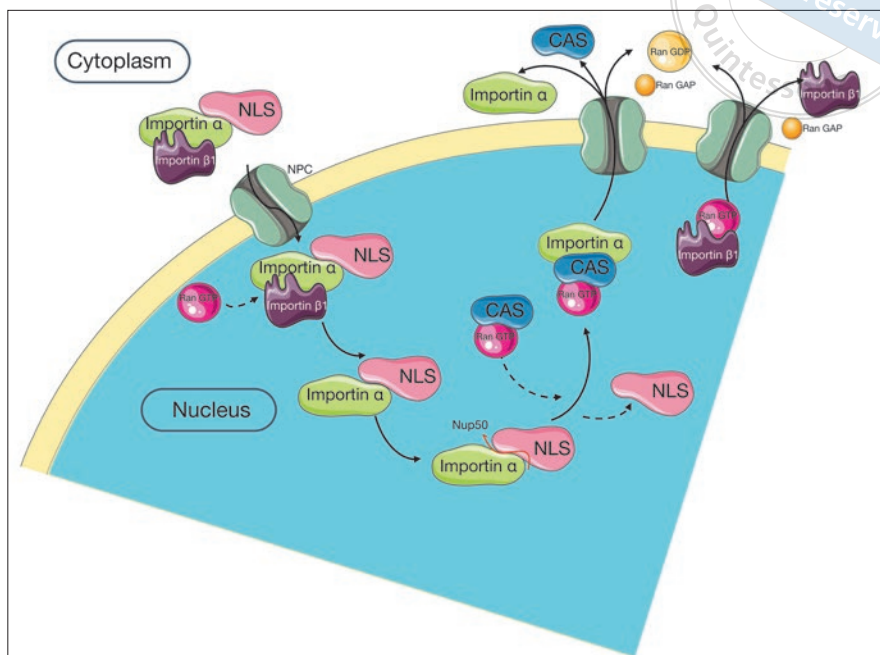


**Fig 1** Nuclear transport guided by a classical NLS (cNLS). The cargo protein containing a cNLS binds to importin  $\alpha$ , which is subsequently recognised and bound by importin  $\beta$  to form the cNLS cargo-importin  $\alpha$ -importin  $\beta$  complex. After the complex enters the nucleus, RanGTP binds to importin  $\beta$ , resulting in the dissociation of the complex. Upon dissociation, importin  $\alpha$  exits the nucleus with the help of CAS and RanGTP, enters the cytoplasm, and is incorporated there. The importin  $\beta$ -RanGTP complex is then returned to the cytoplasm for the next round of transportation.

ties that enable it to interact with FG-NUPs and pass through NPC-selective barriers, ultimately entering the nucleus.<sup>35,36</sup> The abundant RanGTP in the nucleus then binds to importin  $\beta$ -transported cargo proteins, triggering the dissociation of the cargo protein. The complex first disassociates from Site B, and the cargo protein is completely released once Site A has disassociated.<sup>36</sup> Importin  $\beta$ -RanGTP then moves towards and through the NPC. On the cytoplasmic surface of the NPC, RanGTP undergoes hydrolysis and dissociates from importin  $\beta$  upon binding to RanBP and RanGAP. The components are thus released into the cytoplasm for subsequent import cycles (Fig 2).<sup>35</sup>

IK-NLS and RS-NLS, other ncNLSs, are recognised and bound by Kap121 of the Karyopherin  $\beta$  family and by transportin 3, respectively<sup>29</sup>; however, these transport mechanisms require further study.

## Therapeutic application of NLSs

### *Construction of a therapeutic system*

#### Construction of a nuclear-targeted therapy system

Compared to conventional radiotherapy and chemotherapy, targeted therapy is a safer and more efficient form of cancer treatment, targeting pathogenic cellular and molecular targets precisely. As a result, there

have been rapid advances in the development of drug-delivery systems.<sup>38</sup> Drug-delivery systems targeting the nucleus have become a research hotspot because the nucleus is the prime target for multiple cancer-targeting drugs. Barrabés et al<sup>39</sup> assembled a peptide NLS-BN3 drug-carrier system capable of nuclear-targeted delivery of metal-based chemotherapeutic drugs; the use of the NLS-BN3 peptide enhanced targeting efficiency towards gastrin-releasing peptide receptor (GRPR)-over-expressing tumour cells, resulting in increased nuclear accumulation and improved cytotoxic effectiveness.

Nanoparticle (NP)-based delivery systems can interact with biomolecules and access previously inaccessible parts of the body, thereby expanding the possibilities for disease detection and treatment.<sup>40-42</sup> Larger NPs (> 40 nm) require active NLS-assisted transport to pass through the NPC. The main components of NLS peptide nano-drug carrier systems include the NLS peptide; the basic nanomaterials skeleton; antitumour substances (chemotherapy drugs, nucleic acids and photosensitisers); and other substances, such as other drugs that can treat tumours.<sup>43</sup> For instance, Özçelik and Pratz<sup>44</sup> developed a targeted therapy system using arginylglycylaspartic acid (RGD) peptide-gold NPs modified with the NLS peptide (CGYGPKKKRQVGG); this modification resulted in an increased number of nuclear-targeting gold NPs, thus enhancing the radiosensitivity of A549 cells, inhibiting their proliferation, and inducing cell death.

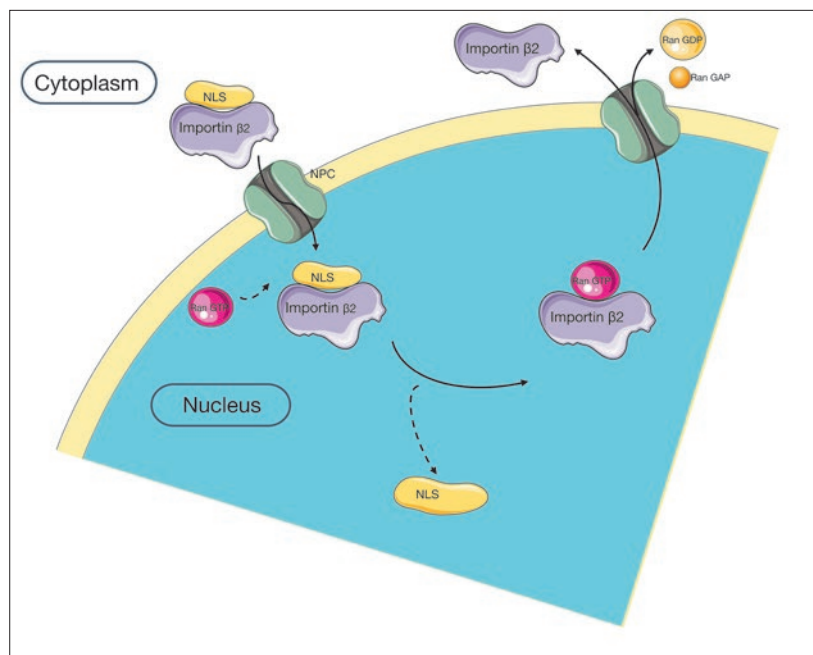


**Fig 2** Nuclear transport guided by a proline-tyrosine NLS (PY-NLS). Importin  $\beta$ 2 binds to the PY-NLS via its C-terminal arch, passes through selective nuclear pore complex (NPC) barriers and enters the nucleus. Once in the nucleus, RanGTP binds to the importin  $\beta$ 2-cargo protein complex, triggering dissociation of the cargo protein. Subsequently, the importin  $\beta$ 2-RanGTP complex approaches and moves through the NPC. On the cytoplasmic surface of the NPC, RanGTP undergoes hydrolysis and dissociates from importin  $\beta$ 2 upon binding to RanBP and RanGAP.

## Generating novel antimicrobial peptides

Since the 1940s, the emergence of antibiotic resistance has posed a worldwide challenge, necessitating the design of improved antimicrobial peptides.<sup>45</sup> The physicochemical parameters of cell-penetrating peptides and antimicrobial peptides overlap, resulting in shared functional characteristics between these peptide groups. Budagavi and Chugh<sup>46</sup> fused an NLS with a laticin-derived peptide (LDP); the LDP-NLS effectively mitigated the cytotoxicity of LDP towards HeLa cells, demonstrated significantly enhanced cellular penetration of methicillin-resistant *Staphylococcus aureus* (MRSA) and successfully inhibited intracellular MRSA infection by entering HeLa cells.

## Gene therapy

The nucleus serves as a regulatory centre for cellular genetics activity and metabolism, and many diseases are associated with disordered gene expression. Consequently, gene therapy has attracted significant attention for the treatment of both acquired and inherited diseases, rendering the nucleus a prominent target for gene therapy. Gene delivery vectors can be classed as viral or non-viral: while viral vectors are highly efficient, their application is limited by problems such as endogenous viral recombination, carcinogenesis and unexpected immune responses; and although non-viral gene vectors are safer, their nuclear delivery efficiency remains

low.<sup>20,47</sup> The incorporation of NLS peptides into non-viral gene delivery systems can significantly enhance their nuclear translocation efficiency, thus augmenting their therapeutic efficacy via diverse systems.

Tarvirdipour et al<sup>47</sup> synthesised an NLS multi-compartment micelles (MCMs) nano-nonviral vector system integrating the minimal NLS (KRKR) into the hydrophilic domain of a peptide backbone carrying a synthetic DNA oligomer (antisense oligonucleotide [ASO]). In MCF-7 cancer cells, this NLS-mediated nuclear translocation machinery improved the nuclear incorporation efficiency of ASO, thus reducing the expression of BCL-2, which is closely associated with solid tumour growth.

## Nuclear localisation probes

### Alterations in nuclear metabolism

The nucleus is a metabolic centre in which the biochemical reactions primarily involve biosynthesis of metabolites that modulate gene expression.<sup>48</sup> Hydrogen peroxide, the foremost indicator of oxidative stress and a crucial mediator in signal transduction, is indispensable role in biological systems. Reactive oxygen species (ROS) generated by abnormal concentrations of hydrogen peroxide can damage cellular structures or biomolecules including proteins, liposomes and DNA. Such damage is closely associated with aging, Alzheimer's disease and cancer. As such, it is crucial to monitor the changes in hydrogen peroxide levels in cells and tissues.<sup>49</sup>

Wen et al<sup>49</sup> developed a multifunctional ratiometric hydrogen peroxide fluorescent probe (NP1). Given the pivotal role of oxidative DNA damage in tumour initiation, NP1 contains a NLS peptide (VQRKRQKLMP-NH<sub>2</sub>) that acts as a transmembrane molecular carrier, facilitating nuclear delivery of the probe to detect DNA-proximal hydrogen peroxide. In HeLa cells, this peptide-based probe effectively localised in the nucleus and achieved quantitative detection of nuclear hydrogen peroxide.

### Subcellular localisation of macromolecular substances

Monitoring dynamic changes in nuclear proteins in living cells and correlating them with changes in cellular behaviour could enhance understanding of the mechanisms and outcomes of cellular invasion behaviour.

For living cells, Sun et al<sup>50</sup> developed a Companion-Probe & Race (CPR) platform capable of real-time detection of nuclear proteins and simultaneous guiding and tracking of cell behaviours such as migration. The CPR platform comprises an intracellular probe region containing two peptide complexes for binding to target proteins, and each complex includes an NLS peptide to guide nuclear entry. This platform was used to validate the expression of the nuclear protein MDM2 and its impact on the migratory behavior of tumour cell lines and primary clinical cells.

The NLS has also been applied in other subcellular localisation probes, such as APEX2-NLS, which detects the nuclear localisation of RNA. These probes offer a potent and versatile approach for exploring the spatial environment and function of macromolecules.<sup>51</sup>

### Conclusion

NLS-mediated nuclear import of karyophilic proteins is crucial for maintaining cellular functionality. Abnormalities in NLSs can disrupt nuclear transport, resulting in aberrant protein localisation, which is closely associated with disease occurrence and progression. A comprehensive understanding of NLS-mediated protein nuclear-import mechanisms will provide valuable therapeutic strategies in the future.

### Conflicts of interest

The authors declare no conflicts of interest related to this study.

### Author contribution

Dr Zi Yan SUN contributed to the literature collection and drafting the manuscript; Prof Zhi Peng FAN supervised and revised the manuscript.

(Received Jun 29, 2023; accepted Nov 09, 2023)

### References

1. Cautain B, Hill R, de Pedro N, Link W. Components and regulation of nuclear transport processes. *FEBS J* 2015;282:445–462.
2. Oka M, Yoneda Y. Importin  $\alpha$ : Functions as a nuclear transport factor and beyond. *Proc Jpn Acad Ser B Phys Biol Sci* 2018;94:259–274.
3. Schmidt HB, Görlich D. Transport selectivity of nuclear pores, phase separation, and membraneless organelles. *Trends Biochem Sci* 2016;41:46–61.
4. Lu J, Wu T, Zhang B, et al. Types of nuclear localization signals and mechanisms of protein import into the nucleus. *Cell Commun Signal* 2021;19:60.
5. Sun W, Wu J, Huang L, et al. PTHrP nuclear localization and carboxyl terminus sequences modulate dental and mandibular development in part via the action of p27. *Endocrinology* 2016;157:1372–1384.
6. Yao X, Wang Y, Duan Y, et al. IGFBP2 promotes salivary adenoid cystic carcinoma metastasis by activating the NF- $\kappa$ B/ZEB1 signaling pathway. *Cancer Lett* 2018;432:38–46.
7. Beck M, Schirmacher P, Singer S. Alterations of the nuclear transport system in hepatocellular carcinoma - New basis for therapeutic strategies. *J Hepatol* 2017;67:1051–1061.
8. Lin DH, Hoelz A. The structure of the nuclear pore complex (an update). *Annu Rev Biochem* 2019;88:725–783.
9. Khan AU, Qu R, Ouyang J, Dai J. Role of nucleoporins and transport receptors in cell differentiation. *Front Physiol* 2020;11:239.
10. Nag N, Sasidharan S, Uversky VN, Saudagar P, Tripathi T. Phase separation of FG-nucleoporins in nuclear pore complexes. *Biochim Biophys Acta Mol Cell Res* 2022;1869:119205.
11. Matsuda A, Mofrad MRK. On the nuclear pore complex and its emerging role in cellular mechanotransduction. *APL Bioeng* 2022;6:011504.
12. Goldfarb DS, Corbett AH, Mason DA, Harreman MT, Adam SA. Importin alpha: A multipurpose nuclear-transport receptor. *Trends Cell Biol* 2004;14:505–514.
13. Miyamoto Y, Yamada K, Yoneda Y. Importin alpha: A key molecule in nuclear transport and non-transport functions. *J Biochem* 2016;160:69–75.
14. Soniat M, Chook YM. Nuclear localization signals for four distinct karyopherin-beta nuclear import systems. *Biochem J* 2015;468:353–362.
15. Chang CC, Hsia KC. More than a zip code: Global modulation of cellular function by nuclear localization signals. *FEBS J* 2021;288:5569–5585.
16. Stewart M. Molecular mechanism of the nuclear protein import cycle. *Nat Rev Mol Cell Biol* 2007;8:195–208.
17. Pumroy RA, Cingolani G. Diversification of importin-alpha isoforms in cellular trafficking and disease states. *Biochem J* 2015;466:13–28.
18. Lange A, Mills RE, Lange CJ, Stewart M, Devine SE, Corbett AH. Classical nuclear localization signals: Definition, function, and interaction with importin alpha. *J Biol Chem* 2007;282:5101–5105.

19. Cook A, Fernandez E, Lindner D, Ebert J, Schlenstedt G, Conti E. The structure of the nuclear export receptor Cse1 in its cytosolic state reveals a closed conformation incompatible with cargo binding. *Mol Cell* 2005;18:355–367.
20. Kim YH, Han ME, Oh SO. The molecular mechanism for nuclear transport and its application. *Anat Cell Biol* 2017;50:77–85.
21. Xu D, Farmer A, Chook YM. Recognition of nuclear targeting signals by Karyopherin-beta proteins. *Curr Opin Struct Biol* 2010;20:782–790.
22. Yoshimura SH, Kumeta M, Takeyasu K. Structural mechanism of nuclear transport mediated by importin beta and flexible amphiphilic proteins. *Structure* 2014;22:1699–1710.
23. Fu X, Liang C, Li F, et al. The rules and functions of nucleocytoplasmic shuttling proteins. *Int J Mol Sci* 2018;19:1445.
24. Lonhienne TG, Forwood JK, Marfori M, Robin G, Kobe B, Carroll BJ. Importin-beta is a GDP-to-GTP exchange factor of Ran: Implications for the mechanism of nuclear import. *J Biol Chem* 2009;284:22549–22558.
25. Scheffzek K, Klebe C, Fritz-Wolf K, Kabsch W, Wittinghofer A. Crystal structure of the nuclear Ras-related protein Ran in its GDP-bound form. *Nature* 1995;374:378–381.
26. Avis JM, Clarke PR. Ran, a GTPase involved in nuclear processes: Its regulators and effectors. *J Cell Sci* 1996;109:2423–2427.
27. Christie M, Chang CW, Róna G, et al. Structural biology and regulation of protein import into the nucleus. *J Mol Biol* 2016;428:2060–2090.
28. Wang L, Li M, Cai M, Xing J, Wang S, Zheng C. A PY-nuclear localization signal is required for nuclear accumulation of HCMV UL79 protein. *Med Microbiol Immunol* 2012;201:381–387.
29. Wing CE, Fung HYJ, Chook YM. Karyopherin-mediated nucleocytoplasmic transport. *Nat Rev Mol Cell Biol* 2022;23:307–328.
30. Gu Y, Hinnerwisch J, Fredricks R, Kalepu S, Mishra RS, Singh N. Identification of cryptic nuclear localization signals in the prion protein. *Neurobiol Dis* 2003;12:133–149.
31. Mallet PL, Bachand F. A proline-tyrosine nuclear localization signal (PY-NLS) is required for the nuclear import of fission yeast PAB2, but not of human PABPN1. *Traffic* 2013;14:282–294.
32. Görlich D, Kutay U. Transport between the cell nucleus and the cytoplasm. *Annu Rev Cell Dev Biol* 1999;15:607–660.
33. Zachariae U, Grubmüller H. Importin-beta: Structural and dynamic determinants of a molecular spring. *Structure* 2008;16:906–915.
34. Stewart M. Function of the nuclear transport machinery in maintaining the distinctive compositions of the nucleus and cytoplasm. *Int J Mol Sci* 2022;23:2578.
35. Mboukou A, Rajendra V, Kleinova R, Tisné C, Jantsch MF, Barraud P. Transportin-1: A nuclear import receptor with moonlighting functions. *Front Mol Biosci* 2021;8:638149.
36. Imasaki T, Shimizu T, Hashimoto H, et al. Structural basis for substrate recognition and dissociation by human transportin 1. *Mol Cell* 2007;28:57–67.
37. Süel KE, Gu H, Chook YM. Modular organization and combinatorial energetics of proline-tyrosine nuclear localization signals. *PLoS Biol* 2008;6:e137.
38. Huang R, Zhou PK. DNA damage repair: Historical perspectives, mechanistic pathways and clinical translation for targeted cancer therapy. *Signal Transduct Target Ther* 2021;6:254.
39. Barrabés S, Ng-Choi I, Martínez MÁ, et al. A nucleus-directed bombesin derivative for targeted delivery of metallodrugs to cancer cells. *J Inorg Biochem* 2020;212:111214.
40. Tran VA, Thuan Le V, Doan VD, Vo GNL. Utilization of functionalized metal-organic framework nanoparticle as targeted drug delivery system for cancer therapy. *Pharmaceutics* 2023;15:931.
41. Doroudian M, Zanganeh S, Abbasgholinejad E, Donnelly SC. Nanomedicine in lung cancer immunotherapy. *Front Bioeng Biotechnol* 2023;11:1144653.
42. Herdiana Y, Wathoni N, Gozali D, Shamsuddin S, Muchtaridi M. Chitosan-based nano-smart drug delivery system in breast cancer therapy. *Pharmaceutics* 2023;15:879.
43. Li B, Shao H, Gao L, Li H, Sheng H, Zhu L. Nano-drug co-delivery system of natural active ingredients and chemotherapy drugs for cancer treatment: a review. *Drug Deliv* 2022;29:2130–2161.
44. Özçelik S, Pratz G. Nuclear-targeted gold nanoparticles enhance cancer cell radiosensitization. *Nanotechnology* 2020;31:415102.
45. Kumari A, Singh M, Sharma R, et al. Apoptin NLS2 homodimerization strategy for improved antibacterial activity and bio-stability. *Amino Acids* 2023;55:1405–1416.
46. Budagavi DP, Chugh A. Antibacterial properties of Latarcin 1 derived cell-penetrating peptides. *Eur J Pharm Sci* 2018;115:43–49.
47. Tarvirdipour S, Skowicki M, Schoenenberger CA, et al. A self-assembling peptidic platform to boost the cellular uptake and nuclear delivery of oligonucleotides. *Biomater Sci* 2022;10:4309–4323.
48. Ruiz-Rodado V, Lita A, Larion M. Advances in measuring cancer cell metabolism with subcellular resolution. *Nat Methods* 2022;19:1048–1063.
49. Wen Y, Xue F, Lan H, Li Z, Xiao S, Yi T. Multicolor imaging of hydrogen peroxide level in living and apoptotic cells by a single fluorescent probe. *Biosens Bioelectron* 2017;91:115–121.
50. Sun H, Dong Z, Zhang Q, et al. Companion-Probe & Race platform for interrogating nuclear protein and migration of living cells. *Biosens Bioelectron* 2022;210:114281.
51. Fazal FM, Han S, Parker KR, et al. Atlas of subcellular RNA localization revealed by APEX-Seq. *Cell* 2019;178:473–490.

# Distinctive Craniofacial and Oral Anomalies in *MN1* C-terminal Truncation Syndrome

Jing Jia YU<sup>1#</sup>, Qiu Yi WU<sup>1#</sup>, Qiu Chi RAN<sup>1</sup>, Ying Ya ZHAO<sup>1</sup>, Lin Nan YU<sup>1</sup>, Qing Xin CAO<sup>1</sup>, Xi Meng CHEN<sup>1</sup>, Wen Yang LI<sup>2</sup>, Zhen Jin ZHAO<sup>1</sup>

*MN1 C-terminal truncation (MCTT) syndrome was first reported in 2020 and only 28 patients have been recorded to date. Since MCTT syndrome is a newly defined and rare syndrome with many clinical features, the present study reviewed the manifestations and management of oral and dental anomalies. Gene variants of MCTT syndrome and their positive phenotypes were summarised. The phenotypes of variants in two exons differed from each other mainly in the craniomaxillofacial region, including brain MRI abnormalities and palatal morphology. Pathogenic mechanisms, especially in craniofacial and oral anomalies, were discussed. Appropriate treatments in the stomatology and respiratory departments could improve the symptoms of MCTT syndrome. The different sites of *MN1* gene variants may influence the clinical symptoms and there may be racial differences in MCTT syndrome. We recommend oral and pulmonary evaluations for the multidisciplinary treatment of MCTT syndrome.*

**Keywords:** craniofacial and oral anomalies, *MN1* C-terminal truncation syndrome, *MN1* gene variant.

*Chin J Dent Res* 2024;27(1):47–52; doi: 10.3290/j.cjdr.b5128655

*MN1* C-terminal truncation (MCTT) syndrome, also known as craniofacial defects, dysmorphic ears, structural brain abnormalities, expressive language delay and impaired intellectual development (CEBALID) syndrome, was first reported by Mak et al<sup>1</sup> and is caused by Meningioma-1 (*MN1*) gene variants.<sup>1,2</sup> The most common features of MCTT syndrome include characteristic facial defects; cranial and brain anomalies; developmental, speech and motor delays; intellectual

disability; hearing loss; and hypotonia. To date, 28 patients with MCTT syndrome have been reported in the literature.<sup>1,3-6</sup> Its clinical phenotype has been established, with some clinical and research studies having been conducted on its aetiology and pathogenesis.<sup>3,4</sup> The present authors reviewed the clinical symptoms, pathogenic gene, pathogenic mechanisms and treatment of patients with MCTT syndrome reported in the literature. The study was approved by the ethics committee of China Medical University, Hospital of Stomatology (approval no. 2021-20).

1 The First Clinic, Department of Orthodontics, School and Hospital of Stomatology, China Medical University, Liaoning Province Key Laboratory of Oral Disease, Shenyang Clinical Medical Research Center of Orthodontic Disease, Shenyang, Liaoning Province, P.R. China.

2 Institute of Respiratory Disease, The First Hospital of China Medical University, Shenyang, Liaoning Province, P.R. China.

# These two authors contributed equally.

**Corresponding author:** Dr Zhen Jin ZHAO, The First Clinic, Department of Orthodontics, School and Hospital of Stomatology, China Medical University, Liaoning Province Key Laboratory of Oral Disease, 117 Nanjing Northern Street, Heping District, Shenyang 110001, Liaoning Province, P.R. China. Email: zjzhao@cmu.edu.cn. ORCID: 0000-0002-9212-6510.

This study was financially supported by the Foundation of Liaoning Education Department (ZF2019030).

## Relationship between clinical symptoms and gene variants

Based on the common symptoms of MCTT syndrome (Table 1), all patients exhibited developmental delay, characteristic facial defects and ear anomalies.<sup>1,3-6</sup> Symptoms with an incidence of more than 90% included speech delay, motor delay, intellectual disability, midfacial hyperplasia, short and upturned nose, and hypertelorism. Other symptoms included oculomotor defects (such as Duane anomaly, nystagmus and strabismus), spinal anomalies (clinical or radiographic abnormalities such as lordosis, scoliosis or kyphosis), atrial or

ventricular septal defects, seizures, hyperphagia, cleft palate and congenital diaphragmatic hernia.<sup>1,3</sup>

*MNI* gene variants lead to MCTT syndrome. *MNI*, located at chromosome 22q12.1, is a transcriptional coregulator composed of two exons and that encodes 1,320 amino acid residues. The t (4;22) *MNI* gene variant was first reported in meningioma and t (12;22) in myeloproliferative diseases.<sup>7,8</sup> *MNI* is closely related to haematological malignant tumours, especially acute myeloid leukaemia, and high expression of *MNI* is related to poor prognosis.<sup>9-11</sup>

Variants in *MNI* at different sites lead to different clinical symptoms. MCTT syndrome is a variant in *MNI* located at the terminal exon or extreme 3' region of exon 1. To date, 16 different variant sites have been identified in MCTT syndrome (Fig 1 and Table 1), resulting in different clinical symptoms (Table 1).<sup>1,3-6</sup> Among the 16 variant sites, six variant sites of six patients were located in the extreme 3' region of exon 1, including all three reported Chinese patients.<sup>4-6</sup> Ten variant sites of 22 patients were located at exon 2. For patients with variants in exon 1, symptoms with an incidence of more than 90% included developmental delay, speech delay, motor delay, intellectual disability, characteristic facial defects, ear anomalies and hypertelorism, which were consistent with those of patients with variants in exon 2 (Table 1). The phenotypes of variants in the two exons differed from each other mainly in the cranio-maxillofacial region. The incidences of brain magnetic resonance imaging (MRI) abnormalities and palatal morphology differed between the two groups.

The incidence of brain MRI abnormalities in exon 2 was 82%, which was 32% higher than that in exon 1. Notably, none of the three Chinese patients had symptoms of brain MRI abnormalities.

All patients with MCTT syndrome showed characteristic facial features, and 93% of patients had maxillary hypoplasia. Consequently, a high-arched palate was commonly observed (Table 1).<sup>1,3-5</sup> In terms of palatal morphology, the incidence of a high-arched/narrow palate in exon 2 was 76% and 50% in exon 1. Among all the reported patients with MCTT syndrome, only three were diagnosed with cleft palate. Two of these were Chinese, and all three variant sites were located in the extreme 3' region of exon 1 and the incidence was 50%. One patient was diagnosed with a submucosal cleft palate with bifid uvula.<sup>1</sup> One Chinese patient was diagnosed with cleft palate.<sup>4</sup> The initial diagnosis of another Chinese patient was submucosal cleft palate<sup>5</sup>, consistent with the previous case reported<sup>1</sup>; however maxillary expansion was performed over 2 years and widened the maxilla, and the cleft secondary palate became visible,

possibly because the maxillary hypoplasia and narrow maxilla resulted in the maxilla and palate adhering to each other.<sup>5</sup> The incidence of cleft palate associated with MCTT syndrome may be related to race or variant location. Although these are uncertain at present due to the small number of reported cases, whether cleft palate should be included as a common symptom of MCTT syndrome merits further research.

Narrowing of the maxilla could influence mandibular development, resulting in reactive mandibular protrusion or retrusion. The clinical symptoms of mandible positions varied in the reported cases, including eight cases of normal mandibular development, six of mandibular protrusion and five of mandibular hypoplasia. These indicated that the development of the maxilla was affected, whereas that of the mandible was normal in MCTT syndrome.<sup>1</sup>

In addition, one patient had obstructive sleep apnoea (OSA) syndrome. Maxillary hypoplasia and mandibular retrusion are significant causes of a narrow upper airway in patients with OSA.<sup>5,12</sup> Hypoxemia and hypercapnia are caused by frequent apnoea and hypopnea in children with OSA. OSA causes damage to various systems, resulting in several complications such as poor memory, impaired growth, learning and behavioural problems, and other cognitive impairments. Children with severe or untreated OSA also suffer from serious cardiovascular complications.<sup>13,14</sup> It aggravates other symptoms such as muscle weakness and developmental delay in patients with MCTT syndrome, which requires immediate attention.

### Possible pathogenic mechanisms

In MCTT syndrome, gene variants lead to C-terminally truncated protein expression. Our unpublished results showed that the mutant *MNI* protein (c. 3760C > T, p. Q1254 \*) leads to the deletion of a terminal helix structure due to the premature stop codon (Fig 2).

Both wild-type and mutant-type *MNI* proteins were localised in the nucleus.<sup>3,4</sup> Mutant *MNI* proteins tended to aggregate more than wild-type *MNI* proteins, possibly due to the increased number of intrinsically disordered regions in *MNI* proteins that cause phase separation; however, the specific pathogenic mechanisms underlying MCTT syndrome remain unclear.

Miyake et al<sup>3</sup> confirmed that the *MNI* variant led to escape nonsense-mediated mRNA decay and the *MNI* protein was degraded by the ubiquitin-proteasome pathway. Mutant *MNI* proteins showed higher stability than the wild-type. The C-terminal region of *MNI* is degraded by the ubiquitin-proteasome pathway. *MNI*



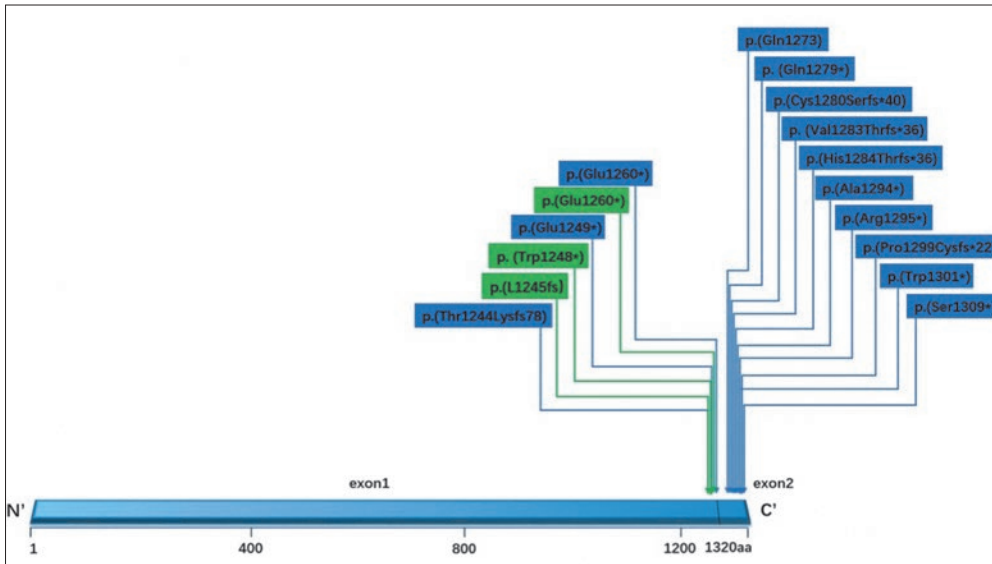


**Fig 1** Variant sites of mutant-type MN1. Blue, other countries' patients; green, Chinese patients. \*Non-sense mutation.

**Table 1** The incidence of different clinical symptoms in the reported MCTT syndrome patients.

Clinical symptoms*	All patients (positive/total) and positive/total %	Patients with different variant sites of mutant-MN1	
		Exon 1 (positive/total) and positive/total %	Exon 2 (positive/total) and positive/total %
Developmental delay	(27/27) 100%	(5/5) 100%	(22/22) 100%
Speech delay	(24/26) 92%	(5/5) 100%	(19/21) 90%
Motor delay	(24/25) 96%	(4/4) 100%	(20/21) 95%
Intellectual disability	(17/18) 94%	(3/3) 100%	(14/15) 93%
Hearing loss	(18/26) 69%	(4/6) 67%	(14/20) 70%
OSA	(1/1) 100%	(1/1) 100%	NR
Brain MRI abnormalities	(17/23) 74%	(3/6) 50%	(14/17) 82%
High-arched/narrow palate	(19/27) 70%	(3/6) 50%	(16/21) 76%
Cleft palate	(3/27) 11%	(3/6) 50%	(0/21) 0%
Hypotonia	(20/23) 87%	(4/5) 80%	(16/18) 89%
Feeding difficulty	(15/24) 63%	(3/5) 60%	(12/19) 63%
Cranial anomaly	(21/27) 78%	(5/6) 83%	(16/21) 76%
Characteristic facial defects	(28/28) 100%	(6/6) 100%	(22/22) 100%
Midface hypoplasia	(25/27) 93%	(4/5) 80%	(21/22) 95%
Mandibular skeletal retrusion	(6/22) 27%	(1/4) 25%	(5/18) 28%
Down slanting palpebral fissures	(16/22) 73%	(3/4) 75%	(13/18) 72%
Ear anomalies	(28/28) 100%	(6/6) 100%	(22/22) 100%
Short and upturned nose	(26/28) 93%	(5/6) 83%	(21/22) 95%
Hypertelorism	(24/26) 92%	(5/5) 100%	(19/22) 90%

NR, not reported.

\*Not all case reports mention all the clinical symptoms, so the "total" number may not be 28.

participates in the transcriptional regulation of target genes by interacting with transcription factors Pre-B-Cell Leukaemia Homeobox 1 (*PBX1*), *PBX/*Knotted Homeobox 1 (*PKNOX1*) and Zinc Finger Protein 450 (*ZBTB24*). The binding of mutant *MN1* to E3 ubiquitin ligase *ZBTB24* and Really Interesting New Gene 1 (*RING1*) protein is impaired, which interferes with the degradation of *MN1* protein resulting in mutant *MN1*

protein aggregation and imbalanced *MN1*-related transcription.<sup>3</sup>

All patients with MCTT syndrome exhibited mid-facial hypoplasia, but the underlying mechanism by which *MN1* affects midfacial development remains unclear. *MN1* plays an important role in maintaining the proliferation, differentiation and function of osteoblasts, and is related to craniofacial development

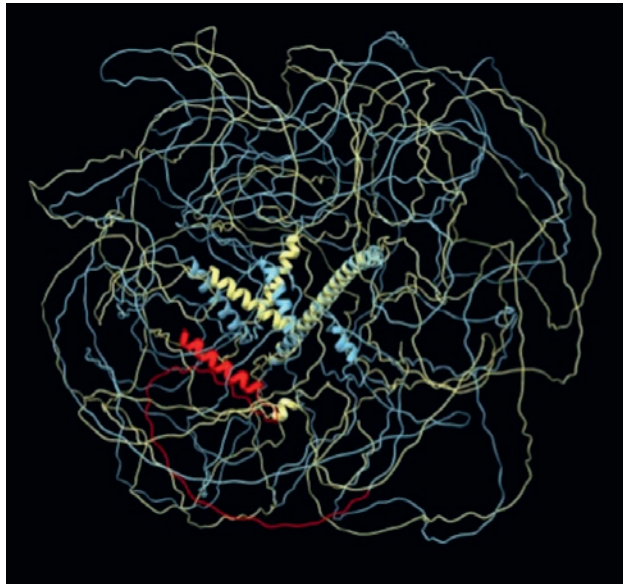


**Fig 2** MN1 protein structure prediction (c.3760C > T, p.Q1254\*). Blue, wild-type MN1; yellow, mutant-type MN1; red, the deletion part of wild-type MN1.

in mice and humans.<sup>15-17</sup> In vitro experiments showed that *MN1* plays a key role in regulating osteoblast proliferation.<sup>16</sup> Moreover, *MN1* is important for intramembranous bone formation. Evolutionary analysis has shown that *MN1* appears at the base of bony vertebrates, where the ossified head emerges.<sup>15</sup> Thus, *MN1* is a key gene involved in skull formation and variations in skull shapes within a population.<sup>15</sup> *MN1* plays an important role in maintaining the normal maturation and function of skull osteoblasts, and is related to brain and craniofacial development in mice and humans.<sup>17</sup>

Half of the patients with variants in exon 1 were reported to have cleft palate but the underlying mechanism was unclear. The deletion of *MN1* affects the development of membranous bone in mice, with some symptoms resembling the human phenotype, such as craniofacial abnormalities (mandibular retrusion is common), cleft palate, speech delay, feeding problems, vestibular schwannomas and corpus callosum agenesis.<sup>18-22</sup> *MN1* is involved in the development of cleft palate in mice.<sup>23,24</sup> Meester-Smoor et al<sup>24</sup> constructed an *MN1* knockout transgenic mouse model and found that *MN1* homozygous knockout mice usually died at birth due to secondary cleft palate, whereas 15% of *MN1* heterozygous knockout mice had mild palate defects and formed a narrow cleft palate. It has been suggested that *MN1* should be considered a candidate gene for cleft palate, prompting us to further investigate the effect of *MN1* gene variants on craniofacial development, espe-



**Fig 3** Image of a typical patient (from Yu et al<sup>5</sup>): maxilla before treatment (a); maxilla after treatment (b); frontal face (c).

cially on cleft palate.

One case of MCTT syndrome was complicated by OSA.<sup>5</sup> Among the reported cases, patients with MCTT syndrome had developmental delays and hypotonia. Miyake et al<sup>3</sup> found that *MN1* is highly expressed in foetal and adult skeletal muscle. Some patients with *MN1* deletions have Pierre-Robin syndrome.<sup>21,22</sup> Homozygous *MN1* knockout mice died of dyspnoea after birth, with no pulmonary function or developmental abnormalities.<sup>24</sup> In the case of *MN1* overexpression, hypoxia-related genes were significantly upregulated in mice carrying Additional Sex Combs-Like Transcriptional Regulator 1 (*ASXL1*) variants compared with those in wild-type mice.<sup>25</sup> OSA causes hypoxia, which usually inhibits osteoblast activation and proliferation.<sup>26</sup> Utting et al<sup>27</sup> noted that exposure to hypoxia delays osteoblast growth and differentiation, and decreases bone formation. In addition to decreased osteoblast production, osteoblast matrix mineralisation is inhibited during hypoxia due to the decreased expression and activity of alkaline phosphatase.<sup>26,28</sup> Hypoxia stimulates an increase in the number and activity of osteoclasts<sup>29</sup>; however, persistent hypoxia can inhibit osteoclast formation and activity due to extensive cell death.<sup>30</sup> Thus, the relationship between OSA and *MN1* variants and the underlying mechanisms warrant further investigation.

## Treatment

Currently, there are no reports on treatment results and the efficacy of treatment in patients with MCTT syndrome. It is advisable to treat the patient's clinical symptoms with rehabilitation, speech training and cardiovascular therapy.<sup>2</sup> Multidisciplinary experts can address

problems such as developmental delays, intellectual disabilities, feeding problems, epilepsy, hearing loss and speech delay, and refer patients to stomatologists for treatment only if there is a malocclusion. Only one study reported the effect of treatment in the orthodontic and respiratory department settings (Fig 3).<sup>5</sup> Using a reverse sector fan-shaped expander, the patient's maxilla was widened to provide space for the development of the mandible, and continuous positive airway pressure was used during this period to improve the patient's respiratory condition.<sup>5</sup> After 2 years of treatment, the OSA and the patient's condition improved, and systemic problems such as developmental delays and muscle weakness were also improved significantly, suggesting that despite the abnormal maxillary development in this patient, the mandibular development conformed to the natural course of growth and development.<sup>5</sup> Therefore, the author recommended oral and pulmonary evaluations for multidisciplinary treatment of MCTT syndrome.<sup>5</sup> For patients with narrow maxillae, the author recommended expanding the arches to enlarge the oral volume in those with the potential for growth and development<sup>5</sup>; however, once the narrowing of the upper airway and hypoxia are observed, it is necessary to conduct appropriate examination and treatment in the respiratory department. At present, there is only one report on therapeutic effect.<sup>5</sup> Thus, it is necessary to conduct further investigation and verification.

## Summary

The different sites of gene variants may influence the clinical symptoms of MCTT syndrome and there may be racial differences. Characteristic features such as dysplasia of the palate and developmental delay suggest the possibility of MCTT syndrome, which can be diagnosed by whole genome sequencing. The craniofacial anomalies and developmental delays attributed to this syndrome would benefit from optimising care with a particular focus on the teeth, palate, maxilla and upper airway. We also recommend oral and pulmonary evaluations for multidisciplinary treatment of MCTT syndrome. Further studies on the clinical characteristics and pathogenic mechanisms may help develop long-term treatment strategies and establish a multidisciplinary treatment system to improve the quality of life of patients with MCTT syndrome.

## Conflicts of interest

The authors declare no conflicts of interest related to this study.

## Author contribution

Dr Jing Jia YU designed the research and drafted the manuscript; Dr Qiu Yi WU revised the manuscript; Drs Qiu Chi RAN and Ying Ya ZHAO made the figures; Drs Lin Nan YU, Qing Xin CAO and Xi Meng CHEN collected data and made tables; Professor Wen Yang LI revised the manuscript; Professor Zhen Jin ZHAO supervised the study and revised the manuscript.

(Received Jul 08, 2023; accepted Nov 19, 2023)

## References

1. Mak CCY, Doherty D, Lin AE, et al. MN1 C-terminal truncation syndrome is a novel neurodevelopmental and craniofacial disorder with partial rhombencephalosynapsis. *Brain* 2020;143:55–68.
2. Mak CCY, Fung JLF, Lee M, et al. MN1 C-terminal truncation syndrome. In: Adam MP, Feldman J, Mirzaa GM, et al (eds). *GeneReviews*. Seattle: University of Washington, 2020.
3. Miyake N, Takahashi H, Nakamura K, et al. Gain-of-function MN1 truncation variants cause a recognizable syndrome with craniofacial and brain abnormalities. *Am J Hum Genet* 2020;106:13–25.
4. Tian Q, Shu L, Zhang P, et al. MN1 neurodevelopmental disease-Atypical phenotype due to a novel frameshift variant in the MN1 gene. *Front Mol Neurosci* 2021;14:789778.
5. Yu J, Li C, Chen J, et al. Diagnosis and treatment of MN1 C-terminal truncation syndrome. *Mol Genet Genomic Med* 2022;10:e1965.
6. Zhao A, Shu D, Zhang D, et al. Novel truncating variant of MN1 penultimate exon identified in a Chinese patient with newly recognized MN1 C-terminal truncation syndrome: Case report and literature review. *Int J Dev Neurosci* 2022;82:96–103.
7. Buijs A, Sherr S, van Baal S, et al. Translocation (12;22)(p13;q11) in myeloproliferative disorders results in fusion of the ETS-like TEL gene on 12p13 to the MN1 gene on 22q11. *Oncogene* 1995;10:1511–1519.
8. Lekanne Deprez RH, Riegman PH, Groen NA, et al. Cloning and characterization of MN1, a gene from chromosome 22q11, which is disrupted by a balanced translocation in a meningioma. *Oncogene* 1995;10:1521–1528.
9. Gopakumar S, McDonald MF, Sharma H, Tatsui CE, Fuller GN, Rao G. Recurrent HGNET-MN1 altered (astroblastoma MN1-altered) of the foramen magnum: Case report and molecular classification. *Surg Neurol Int* 2022;13:139.
10. Grosveld GC. MN1, a novel player in human AML. *Blood Cells Mol Dis* 2007;39:336–339.
11. Li HB, Huang G, Tu J, et al. METTL14-mediated epitranscriptome modification of MN1 mRNA promote tumorigenicity and all-trans-retinoic acid resistance in osteosarcoma. *EBioMedicine* 2022;82:104142.
12. Luzzi V, Ierardo G, Di Carlo G, Saccucci M, Polimeni A. Obstructive sleep apnea syndrome in the pediatric age: The role of the dentist. *Eur Rev Med Pharmacol Sci* 2019;23(1, suppl):9–14.
13. Lo Bue A, Salvaggio A, Insalaco G. Obstructive sleep apnea in developmental age. A narrative review. *Eur J Pediatr* 2020;179:357–365.

14. Savini S, Ciorba A, Bianchini C, et al. Assessment of obstructive sleep apnoea (OSA) in children: An update. *Acta Otorhinolaryngol Ital* 2019;39:289–297.
15. Pallares LF, Carbonetto P, Gopalakrishnan S, et al. Mapping of craniofacial traits in outbred mice identifies major developmental genes involved in shape determination. *PLoS Genet* 2015;11:e1005607.
16. Sutton AL, Zhang X, Ellison TI, Macdonald PN. The 1,25(OH)2D3-regulated transcription factor MN1 stimulates vitamin D receptor-mediated transcription and inhibits osteoblastic cell proliferation. *Mol Endocrinol* 2005;19:2234–2244.
17. Zhang X, Dowd DR, Moore MC, et al. Meningioma 1 is required for appropriate osteoblast proliferation, motility, differentiation, and function. *J Biol Chem* 2009;284:18174–18183.
18. Barbi G, Rossier E, Vossbeck S, et al. Constitutional de novo interstitial deletion of 8 Mb on chromosome 22q12.1-12.3 encompassing the neurofibromatosis type 2 (NF2) locus in a dysmorphic girl with severe malformations. *J Med Genet* 2002;39:E6.
19. Beck M, Peterson JF, McConnell J, et al. Craniofacial abnormalities and developmental delay in two families with overlapping 22q12.1 microdeletions involving the MN1 gene. *Am J Med Genet A* 2015;167A:1047–1053.
20. Breckpot J, Anderlid BM, Alanay Y, et al. Chromosome 22q12.1 microdeletions: Confirmation of the MN1 gene as a candidate gene for cleft palate. *Eur J Hum Genet* 2016;24:51–58.
21. Davidson TB, Sanchez-Lara PA, Randolph LM, et al. Microdeletion del(22)(q12.2) encompassing the facial development-associated gene, MN1 (meningioma 1) in a child with Pierre-Robin sequence (including cleft palate) and neurofibromatosis 2 (NF2): A case report and review of the literature. *BMC Med Genet* 2012;13:19.
22. Said E, Cuschieri A, Vermeesch J, Fryns JP. Toriello-Carey syndrome with a 6Mb interstitial deletion at 22q12 detected by array CGH. *Am J Med Genet A* 2011;155A:1390–1392.
23. Liu W, Lan Y, Pauws E, et al. The Mn1 transcription factor acts upstream of Tbx22 and preferentially regulates posterior palate growth in mice. *Development* 2008;135:3959–3968.
24. Meester-Smoor MA, Vermeij M, van Helmond MJ, et al. Targeted disruption of the Mn1 oncogene results in severe defects in development of membranous bones of the cranial skeleton. *Mol Cell Biol* 2005;25:4229–4236.
25. Hsu YC, Chiu YC, Lin CC, et al. The distinct biological implications of Asx11 mutation and its roles in leukemogenesis revealed by a knock-in mouse model. *J Hematol Oncol* 2017;10:139.
26. Hannah SS, McFadden S, McNeilly A, McClean C. "Take my bone away?" Hypoxia and bone: A narrative review. *J Cell Physiol* 2021;236:721–740.
27. Utting JC, Robins SP, Brandao-Burch A, Orriss IR, Behar J, Arnett TR. Hypoxia inhibits the growth, differentiation and bone-forming capacity of rat osteoblasts. *Exp Cell Res* 2006;312:1693–1702.
28. Stegen S, Carmeliet G. Hypoxia, hypoxia-inducible transcription factors and oxygen-sensing prolyl hydroxylases in bone development and homeostasis. *Curr Opin Nephrol Hypertens* 2019;28:328–335.
29. Knowles HJ, Athanasou NA. Acute hypoxia and osteoclast activity: A balance between enhanced resorption and increased apoptosis. *Pathol* 2009;218:256–264.
30. Ma Z, Yu R, Zhao J, et al. Constant hypoxia inhibits osteoclast differentiation and bone resorption by regulating phosphorylation of JNK and IκBα. *Inflamm Res* 2019;68:157–166.

# FAM20A-Associated Amelogenesis Imperfecta: Gene Variants with Functional Verification and Histological Features

Jia Nan DING<sup>1</sup>, Miao YU<sup>1</sup>, Hao Chen LIU<sup>1</sup>, Kai SUN<sup>1</sup>, Jing WANG<sup>2</sup>, Xiang Liang XU<sup>2</sup>, Yang LIU<sup>1</sup>, Dong HAN<sup>1</sup>

**Objective:** To investigate FAM20A gene variants and histological features of amelogenesis imperfecta and to further explore the functional impact of these variants.

**Methods:** Whole-exome sequencing (WES) and Sanger sequencing were used to identify pathogenic gene variants in three Chinese families with amelogenesis imperfecta. Bioinformatics analysis, in vitro histological examinations and experiments were conducted to study the functional impact of gene variants, and the histological features of enamel, keratinised oral mucosa and dental follicle.

**Results:** The authors identified two nonsense variants c. 406C > T (p.Arg136\*) and c.826C > T (p.Arg176\*) in a compound heterozygous state in family 1, two novel frameshift variants c.936dupC (p.Val313Argfs\*67) and c.1483dupC (p.Leu495Profs\*44) in a compound heterozygous state in family 2, and a novel homozygous frameshift variant c.530\_531insGGTC (p.Ser178Valfs\*21) in family 3. The enamel structure was abnormal, and psammomatoid calcifications were identified in both the gingival mucosa and dental follicle. The bioinformatics and subcellular localisation analyses indicated these variants to be pathogenic. The secondary and tertiary structure analysis speculated that these five variants would cause structural damage to FAM20A protein.

**Conclusion:** The present results broaden the variant spectrum and clinical and histological findings of diseases associated with FAM20A, and provide useful information for future genetic counselling and functional investigation.

**Keywords:** amelogenesis imperfecta, FAM20A, frameshift variants, mutations, nonsense variants

Chin J Dent Res 2024;27(1):53–63; doi: 10.3290/j.cjdr.b5136761

1 Department of Prosthodontics, Peking University School and Hospital of Stomatology & National Center for Stomatology & National Clinical Research Center for Oral Diseases & National Engineering Research Center of Oral Biomaterials and Digital Medical Devices, Beijing, P.R. China.

2 Department of Oral and Maxillofacial Surgery, Peking University School and Hospital of Stomatology & National Center for Stomatology & National Clinical Research Center for Oral Diseases & National Engineering Research Center of Oral Biomaterials and Digital Medical Devices, Beijing, P.R. China.

**Corresponding authors:** Dr Yang LIU and Dr Dong HAN, Department of Prosthodontics, Peking University School and Hospital of Stomatology, No. 22 Zhongguancun South Avenue, Haidian District, Beijing 100081, PR China. Tel: 86-10-82195393. Email: pkussliuyang@bjmu.edu.cn; donghan@bjmu.edu.cn

This study was supported by the National Natural Science Foundation of China (82270944, 82100976, and 81600846).

The teeth are one of the key parts of the stomatognathic system. The teeth, gingiva and periodontal tissue develop from tooth germ.<sup>1</sup> The tooth germ consists of three parts: the enamel organ, dental papilla and dental follicle.<sup>2,3</sup> The enamel organ is the epithelial part of the tooth germ<sup>2</sup>, which gives rise to dental enamel and the epithelial part of the gingiva, whereas the dental papilla and dental follicle are the mesenchymal parts of the tooth germ.<sup>4</sup> The dental papilla develops into dental pulp and dentine, and the dental follicle forms cementum, periodontal ligament and alveolar bone.<sup>5</sup> Many genes participate in the development of tooth germ, and gene variants may lead to malformation of the teeth and adjacent tissue.<sup>6-8</sup>

Enamel is the hardest ectodermal tissue on the surface of the tooth crown.<sup>9</sup> The development of enamel

involves two main processes<sup>10</sup>: matrix formation and mineralisation. Due to some gene variants, it may lead to changes in enamel matrix protein deposition and/or abnormal mineralisation<sup>11</sup>, resulting in amelogenesis imperfecta (AI)<sup>12</sup>. According to the Witkop classification set out in 1988<sup>13</sup>, AI was divided into four categories: hypoplastic (type I: OMIM#104530, OMIM#104500, OMIM#204650, OMIM#301200, OMIM#616270, OMIM#204690, OMIM#616221, OMIM#617297 and OMIM#620104;), hypomaturation (type II: OMIM#204700, OMIM#612529, OMIM#613211, OMIM#614832, OMIM#615887 and OMIM#617217), hypocalcified (type III: OMIM#130900, OMIM#617607 and OMIM#618386) and hypomaturation-hypoplastic with taurodontism (type IV: OMIM#104510).

*FAM20A* (OMIM \* 611062) is one of the members of the *FAM20* gene family (*FAM20A*, *FAM20B* and *FAM20C*) that encode kinases (phosphorylating enzymes) which modify proteins within the secretory pathway.<sup>14</sup> *FAM20A* gene located on human chromosome 17q24.2 consists of 11 exons and contains a highly conserved C-terminal domain.<sup>15</sup> *FAM20A* protein is considered to be a pseudokinase that forms a complex with *FAM20C* and allosterically activates *FAM20C*<sup>15-18</sup>, thereby promoting phosphorylation of *FAM20C* targets.<sup>19,20</sup> *FAM20A* binds directly to *FAM20C*.<sup>17</sup> *FAM20C* protein is a Golgi casein kinase that phosphorylates the Ser-X-Glu/Ser(P) motif of most secretory proteins, including enamel matrix proteins.<sup>21</sup> *FAM20C* variants cause Raine syndrome<sup>22</sup>, exhibiting bone and craniofacial/dental abnormalities.<sup>17</sup> *FAM20B* protein is a xylose kinase regulating proteoglycan synthesis.<sup>19</sup> *FAM20A* variant can lead to enamel hypoplasia (OMIM #204690)<sup>23</sup>, which is inherited as autosomal recessive inheritance. This disease is also known as enamelrenal syndrome (ERS).<sup>24</sup> It is characterised by enamel hypoplasia, dental pulp stones, delayed eruption of permanent teeth, gingival overgrowth and renal calcinosis.<sup>25</sup>

In the present study, screening of the gene variants and histological and functional investigation were performed. Five variants of *FAM20A* were identified in three patients with AI, of which three were novel variants. The clinical phenotypes of the three probands were reported, and histological examinations revealed the dysplastic enamel structure and ectopic mineralisation in the dental follicle and gingival mucosa. The *in vitro* functional assay confirmed subcellular localisation changes and the functional impact of *FAM20A* variants.

## Materials and methods

### *Pedigree construction and patient recruitment*

All the probands and family members of three pedigrees requested treatment advice at the Department of Prosthodontics, Peking University School of Stomatology, Beijing, China. Oral examinations were carried out and panoramic dental radiographs were taken. Informed consent was obtained from all the participants. This study was approved by the Ethics Committee of Peking University School and Hospital of Stomatology (PKUS-SIRB-202162021). A total of three nuclear families were recruited, all of whom denied consanguineous marriage. Three individuals were included in Sanger sequencing for each pedigree. Only the proband in each pedigree showed the enamel hypoplasia phenotype. The mode of inheritance was consistent with autosomal recessive inheritance.

### *Variant detection and analysis*

Genomic DNA from these three probands of the three recruited pedigrees was isolated from peripheral blood lymphocytes using a BioTek DNA Whole-blood Mini Kit (BioTek, Beijing, China) according to the manufacturer's instructions. After polymerase chain reaction (PCR), DNA products were sheared to acquire 150- to 200-bp fragments. Whole-exome sequencing (WES) was performed by Beijing Angen Gene Medicine Technology (Beijing, China) with the Illumina-X10 platform. After this, the detected variants were filtered according to the following methods. Firstly, all genes associated with tooth development were analysed<sup>26,27</sup>, especially for AI-associated genes. Secondly, non-synonymous single nucleotide variants (SNVs) and insertions/deletions (InDels) with a minor allele frequency (MAF)  $\geq 0.01$  in bioinformatic databases, including the single nucleotide polymorphism database (dbSNP, <http://www.ncbi.nlm.nih.gov/projects/SNP/snpsummary.cgi>), the Genome Aggregation Database (gnomAD, <http://gnomad.broadinstitute.org>), the Human Gene Mutation Database (HGMD, <http://www.hgmd.org>) and the 1,000 Genomes Project data in Ensembl ([http://asia.ensembl.org/Homo\\_sapiens/Info/Index](http://asia.ensembl.org/Homo_sapiens/Info/Index)) were excluded. Finally, pathogenicity of the remaining variants was further predicted using the Protein Variation Effect Analyzer (PROVEAN, <https://www.jcvi.org/research/provean>) and polymorphism phenotyping (PolyPhen-2, <http://genetics.bwh.harvard.edu/pph2/>).

### *Sanger sequencing and clone sequencing*

Variants of *FAM20A* (NM\_017565.4) were identified in three affected families. Co-segregation analysis and Sanger sequencing of the probands and their family members were performed to verify the variants of *FAM20A* based on WES results.

For further verification, the related *FAM20A* (NM\_017565.4) fragments were sequenced using Sanger sequencing. Genomic DNA from these family members was isolated according to the procedure described above. We designed the corresponding primers (provided on request) for each variant. The PCR products were sequenced by Ruibio Biotech (Beijing, China). TA clone sequencing was used to confirm the exact status of the frameshift and nonsense variants.

### *Bioinformatics*

To carry out the bioinformatics analysis, we also used a series of bioinformatics databases, such as MutationTaster (<https://www.mutationtaster.org/>) and PROVEAN. The pathogenicity of the three variants was classified according to the American College of Medical Genetics and Genomics (ACMG) guideline.<sup>28</sup>

The secondary structure of wild-type *FAM20A* and five mutated variants was predicted using PsiPred 4.0 (<http://bioinf.cs.ucl.ac.uk/psipred>). An optimum template of *FAM20A* protein was selected for homology modelling analysis through SWISS-MODEL (<https://swiss-model.expasy.org>) and the tertiary structural changes of variants were captured using PyMOL software (Molecular Graphics System, DeLano Scientific, San Carlos CA, USA).

### *Scanning electron microscope (SEM) examination of the affected teeth*

Teeth 25,16 and 65 were extracted from proband 302, then fixed in 10% neutral formaldehyde solution. Tooth 65 was separated to expose the inner surface, then the pieces were etched with 30% phosphate gel, rinsed with distilled water thoroughly and dried in the vacuum drying oven at 37°C overnight. After being coated with gold, the teeth samples were observed under a scanning electron microscope.

### *Hematoxylin-eosin (HE) staining of the patient's gingival mucosa and dental follicle*

A small piece of gingival mucosa was obtained during patient 302's oral surgery. The dental follicle was

obtained during the extraction of impacted tooth 16. The samples were fixed in 10% neutral formaldehyde solution at room temperature for 24 hours, then embedded in paraffin and mounted on the slicing machine and sectioned to a thickness of 5 µm. The sections were stained with hematoxylin and eosin following the routine process and observed under the microscope.

### *Construction of plasmids*

The full-length coding region of the human *FAM20A* gene (NM\_017565.4) was cloned into the pEGFP-C1 expression vector with enhanced GFP to synthesise the wild-type plasmid pEGFP-C1-*FAM20A*. Then, *in vitro* site-directed mutagenesis was performed to generate five mutated plasmids: pEGFP-C1-R136X, pEGFP-C1-S178Vfs\*21, pEGFP-C1-R276X, pEGFP-C1-V313Rfs\*67 and pEGFP-C1-L495Pfs\*44. All plasmids were synthesised by Ruibio Biotech, and the company also confirmed the entire sequence of the mutated constructs.

### *Cell culture and transfection*

Human embryonic kidney 293T cells were cultured in Dulbecco's modified Eagle medium (Invitrogen, Waltham, MA, USA) supplemented with 10% foetal bovine serum and 2 mmol/L L-glutamine in the presence of 5% CO<sub>2</sub>. Following the manufacturer's instructions, transient transfection was carried out using Lipofectamine 3000 (Invitrogen).

### *Subcellular localisation assay*

We transiently transfected 293T cells with pEGFP-C1 expression plasmids containing GFP-wild-type or mutated *FAM20A* cDNA fusion proteins. At 48 hours after transfection, the cells were washed three times with phosphate buffer and fixed with 4% paraformaldehyde for 15 minutes. After washing, the cells were placed in a mounting medium with 4',6-diamidino-2-phenylindole (Solarbio, Beijing, China), mounted and photographed using an LSM 510 Meta confocal microscope (Zeiss, Oberkochen, Germany) with a ×63/1.00 numerical aperture oil objective lens.

### *Co-immunoprecipitation (Co-IP) and immunoblotting*

Human embryonic kidney 293T (HEK-293T) cells were transiently co-transfected with the GFP empty vector, wild-type mutant *FAM20A*-GFP and wild-type *FAM20C*-FLAG plasmids using Lipofectamine 3000. Proteins from each group were harvested 48 hours after co-transfection.

50 µl of each protein sample was removed as input. GFP-Trap Magnetic Agarose (gama, Chromotek, Germany) were pre-treated according to the manufacturer's instructions and added to the other protein supernatants obtained overnight at 4°C. The next day, the beads were washed until the supernatant was clear. The washed beads were resuspended in 2× SDS sample buffer and the supernatant was the IB group. To observe the protein expression, the IB and input samples were assessed through Western blot analysis. After electrophoresis on 10% polyacrylamide gel, the protein was transferred to a PVDF membrane by electrophoresis and then incubated with anti-GFP (ab1218) mouse antibody (Abcam, Cambridge, UK) and anti-Flag (AE092) rabbit antibody (Abclonal, Wuhan, China). The membrane was washed and incubated with peroxidase-conjugate rabbit or mouse anti-mouse secondary antibodies (ab150077, Abcam; ab6728, Abcam).

## Results

### *Clinical findings confirmed AI and eruption defect*

The dental characteristics and panoramic radiographs of the probands are shown in Fig 1. In family 1, the proband (302) was a 19-year-old woman. Intraoral photographs showed mixed dentition, small dental crowns with generally thin enamel and yellow discolouration of teeth (Fig 1a to c). Obviously, her occlusal vertical distance was decreased. Radiographic examination revealed impacted permanent teeth with enamel defect (Fig 1d). The roots of all her teeth were generally short. Her parents both had normal enamel without any disorder. The proband stated that she had been diagnosed as having bilateral medullary nephrosis with small calcifications in both kidneys.

In family 2, the proband (748) was a 24-year-old woman. She had completed most of her dental crown restorations at another hospital when the intraoral pictures were taken. Only teeth 17, 35 and 36 without restoration revealed the original appearance of thin enamel (Fig 1e and f). Radiographic film taken prior to restoration showed no radiopaque enamel, delayed tooth eruption and intrapulpal calcifications (Fig 1g). Unfortunately, her parents had passed away. Her two brothers had normal teeth and well-developed enamel.

In family 3, the proband (914) was a 15-year-old boy. An intraoral scan was taken using a TRIOS intraoral scanner (3Shape, Copenhagen, Denmark). In addition to thin enamel, he also showed an anterior open bite, which may have been caused by an eruption defect and decreased occlusal vertical distance (Fig 1h to j).

The panoramic radiograph showed that he had short roots and impacted teeth (Fig 1k). His parents both had normal dentition.

Notably, as seen on the panoramic radiographs taken of all three patients, the impacted teeth showed enamel defects as well.

### *Sequencing of patients and family members detected FAM20A variants*

The pedigree of three family lines is shown in Fig 2a to c. Using whole-exome sequencing (WES), we identified five variants of the *FAM20A* gene in these families and confirmed them through Sanger sequencing (Fig 2d to h). The two nonsense variants had been documented previously, whereas three frameshift variants were novel, then a pathogenicity prediction was made for all variants (Table 1).

In family 1, proband 302 carried *FAM20A* compound heterozygous variants c.406C > T (p.Arg136\*) and c.826C > T (p.Arg276\*). Her father only carried the heterozygous nonsense variant c.406C > T (p.Arg136\*), while her mother only carried another heterozygous nonsense variant c.826C > T (p.Arg276\*). According to family co-segregation, the variants of the proband were inherited from both her parents through an autosomal-recessive mode of inheritance.

In family 2, proband 748 carried *FAM20A* compound heterozygous variants c.936dupC (p.Val313Argfs\*67) and c.1483dupC (p.Leu495Profs\*44). Unfortunately, both of her parents had passed away and were unavailable for genetic screening. Her two brothers were both heterozygous, carrying the frameshift variant c.936dupC (p.Val313Argfs\*67), and had normal dentition, which was in accordance with the autosomal-recessive mode.

In family 3, proband 914 carried a *FAM20A* homozygous variant c.530\_531insGGTC (p.Ser178Valfs\*21). His parents both carried the same heterozygous variant. His family co-segregation also revealed an autosomal-recessive inheritance pattern.

### *Bioinformatics analysis indicated functional impact of FAM20A variants*

To predict the functional impact of these variants, we first searched the dbSNP and gnomAD databases, then carried out pathogenicity prediction using PROVEAN and MutationTaster. We then classified these nonsense and frameshift variants as pathogenic variants according to the ACMG classification (Table 1).

By predicting the secondary structure of *FAM20A* protein, it can be found that all the nonsense and



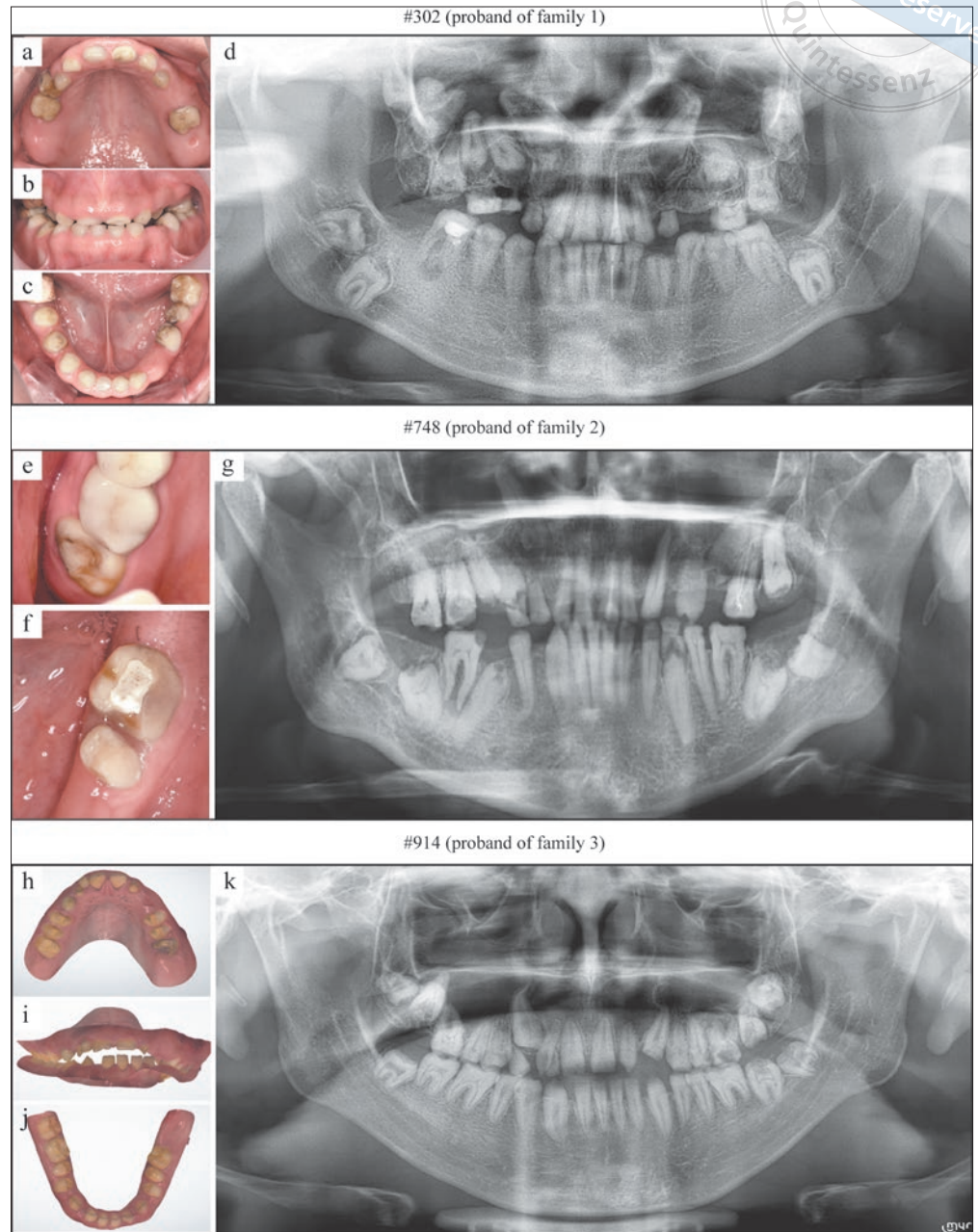


**Fig 1** Dental characteristics of the three patients. Digital photographs and panoramic radiograph of proband 302 (a to d) and proband 748 (e to g). Intraoral scan images and panoramic radiograph of proband #914 (h to k).

frameshift variants lead to the truncation of the normal protein, resulting in serious changes to the structure of FAM20A. The tertiary protein structure analysis also shows that the proteins are truncated and the spatial structures have changed (Fig 3).

*Histomorphological analyses of the clinical samples confirmed the enamel defect and ectopic mineralisation in the mucosa and dental follicle*

Three teeth were obtained from proband 302, including unerupted 25, unerupted 16 and erupted 65 with heavy

abrasion. The root morphology of tooth 16 was irregular and curved, and a developmental anomaly could be seen near the apex (Fig 4a). Tooth 65 was divided into two halves according to the buccolingual direction. Calcification of the pulp cavity was notable, and the enamel could hardly be seen on the tooth (Fig 4b).

SEM analysis of the surface of tooth 25 (Fig 4c and e) revealed a variety of features, including rough, knob-like calcifications and some relatively smooth mineral. SEM analysis of the occlusal surface of tooth 65 (Fig 4d and f) showed some larger craters suggestive of resorption lacunae.

**Table 1** Summary of FAM20A variants in the present study.

Family	Exon	Nucleotide change	Protein change	Variation type	dbSNP (AF)	gnomAD (MAF)	Provean	Mutation Taster	ACMG classification (evidence of pathogenicity)
Family1	2	c.406C>T	p.R136*	Nonsense	rs144411158 (0.000000)	0.000003979	Neutral	Disease-causing	PVS1+PS3+PM2+PM4+ PP1+PP4+PP5 Pathogenic
Family1	6	c.826C>T	p.R276*	Nonsense	rs387907215 (0.000000)	---	Deleterious	Disease-causing	PVS1+PS3+PM2+PM4+ PP1+PP4+PP5 Pathogenic
Family2	11	c.1483dupC	p.L495Pfs*44	Frameshift	/	---	/	Disease-causing	PVS1+PS3+PM2+PM4+ PP1+PP4 Pathogenic
Family2	7	c.936dupC	p.V313Rfs*67	Frameshift	/	---	/	Disease-causing	PVS1+PM2+PM4+PP1+PP4 Pathogenic
Family3	2	c.530_531insGGTC	p.S178Vfs*21	Frameshift	/	---	/	Disease-causing	PVS1+PS3+PM2+PM4+ PP1+PP4 Pathogenic

–, Variant was not found in ExAC; /, Variant cannot be predicted in dbSNP or Provean.

A small piece of the oral gingival mucosa and the dental follicle were obtained from proband 302. Upon HE staining, they both presented ectopic psammomatoid calcifications (Fig 4g and h).

#### *In vitro experiments revealed changes in subcellular localisation of FAM20A variants*

To evaluate the subcellular localisation of the FAM20A variants, we determined the subcellular localisation of the five mutated proteins by immunofluorescence. The results showed that wild-type FAM20A was located in the cytoplasm, but the localisation of the FAM20A variants R136\*, R276\*, L495Pfs\*44 and S178Vfs\*21 was altered. GFP-R136\*, GFP-R276\* and GFP-S178Vfs\*21 were located in the whole cytoplasm with weak expression in the nucleus (Fig 5c-c", d-d" and e-e"). Notably, GFP-L495Pfs\*44 was scattered in the nucleus and densely clumped in the nucleolus (Fig 5g-g"), which was very different from the wild-type. The results indicated that R136\*, R276\*, L495Pfs\*44 and S178Vfs\*21 severely affected the subcellular localisation of FAM20A, which might contribute to the pathogenic process in these patients. On the other hand, the V313Rfs\*67 variant seemed to be located in the same place in the cell as the wild type (Fig 5f-f"), but without local condensation in the cytoplasm, suggesting that the V313Rfs\*67 may lead to developmental anomalies in a different way compared with the other four variants.

#### *Co-immunoprecipitation (Co-IP) and immunoblotting illustrate reduced binding of mutant FAM20A protein to FAM20C*

Based on the results, FAM20A protein is shown to have the ability to bind to FAM20C protein in vitro. The five mutants also have a weakened binding tendency compared to the wild-type (Fig 6). The molecular weights of the mutant proteins were all reduced to varying degrees, further supporting the aforementioned predictions for the proteins; however, no comparisons were made between the variants to determine the severity of the reduction in binding capacity.

#### Discussion

AI generally refers to inherited enamel malformations that may include other local defects such as delayed tooth eruption and misshapen roots.<sup>24,29</sup> In the case of enamel-renal syndrome (ERS)<sup>25</sup>, the dental problems may appear prior to any evidence of kidney disease, perhaps because kidney ultrasound examinations are rarely performed on AI patients. Proband 302 in family 1 described herself as having bilateral medullary nephrosis with small calcifications in both kidneys, but did not provide the results of her renal examination. For patients diagnosed with bi-allelic FAM20A variants, it is advisable that the kidney be examined regularly to achieve early diagnosis and treatment. The proband of family 1 carried FAM20A complex heterozygous variants c.406C > T (p.Arg136\*) and c.826C > T (p.Arg276\*). Although these two nonsense variants have been pre-

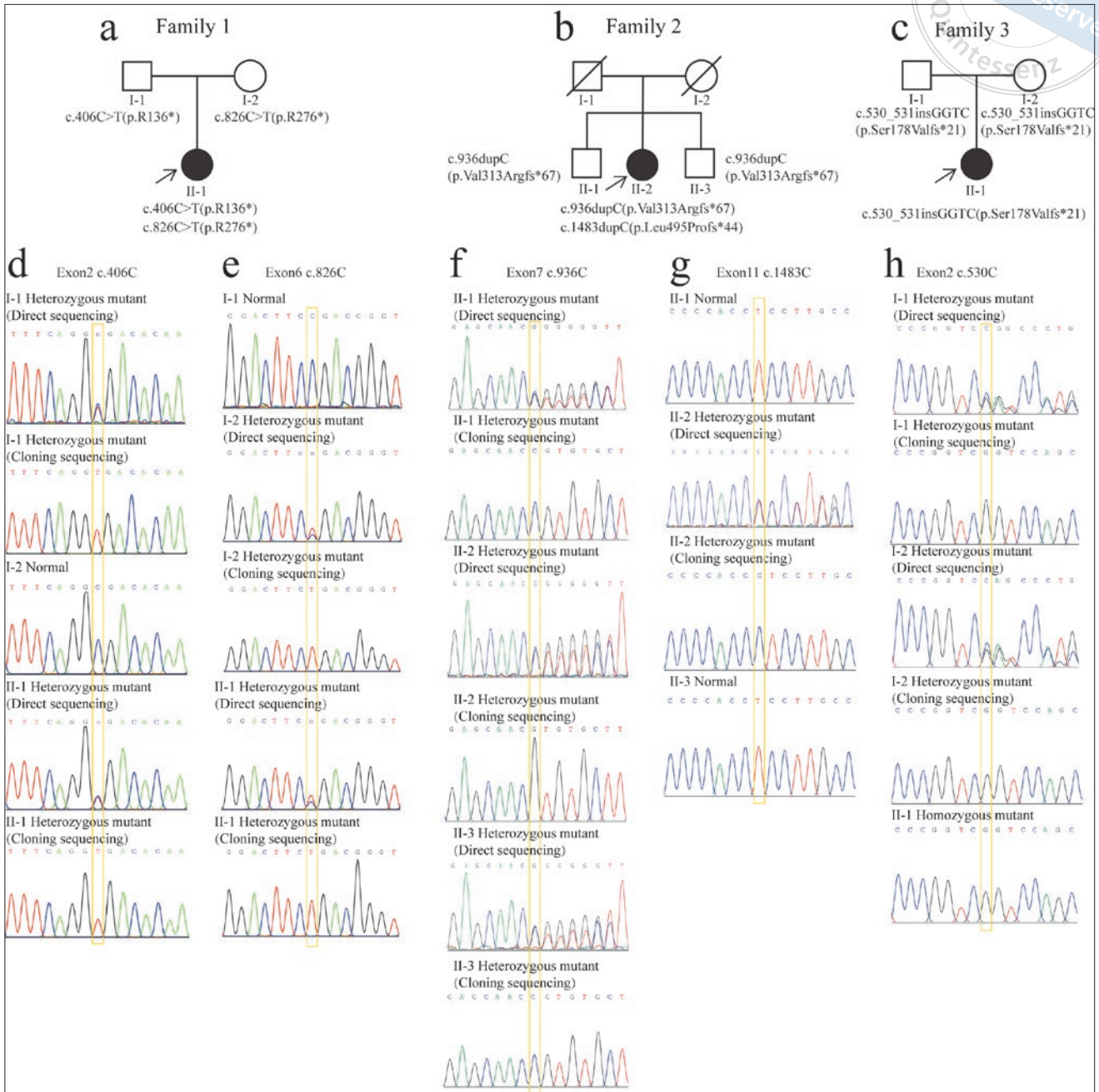


**Fig 2** Pedigree and sequencing chromatograms of the three families. Pedigree of family 1 (a), family 2 (b) and family 3 (c). DNA sequencing chromatogram showing a heterozygous *FAM20A* variant of c.406C > T (p.Arg136\*) in proband 302 (II-1) and her father (I-1) (d). DNA sequencing chromatogram showing a heterozygous *FAM20A* variant of c. 826C > T (p.Arg276\*) in proband 302 (II-1) and her mother (I-2) (e). DNA sequencing chromatogram showing a heterozygous *FAM20A* variant of c.936dupC (p.Val313Argfs\*67) in proband 748 (II-2) and her two brothers (I-1, II-3) (f). DNA sequencing chromatogram showing a heterozygous *FAM20A* variant of c.1483dupC (p.Leu495Profs\*44) in proband 748 (II-2) (g). DNA sequencing chromatogram showing a homozygous *FAM20A* variant of c.530\_531insGGTC (p.Ser178Valfs\*21) in proband 914 (II-2) and the same heterozygous *FAM20A* variant in his parents (I-1, I-2) (h).

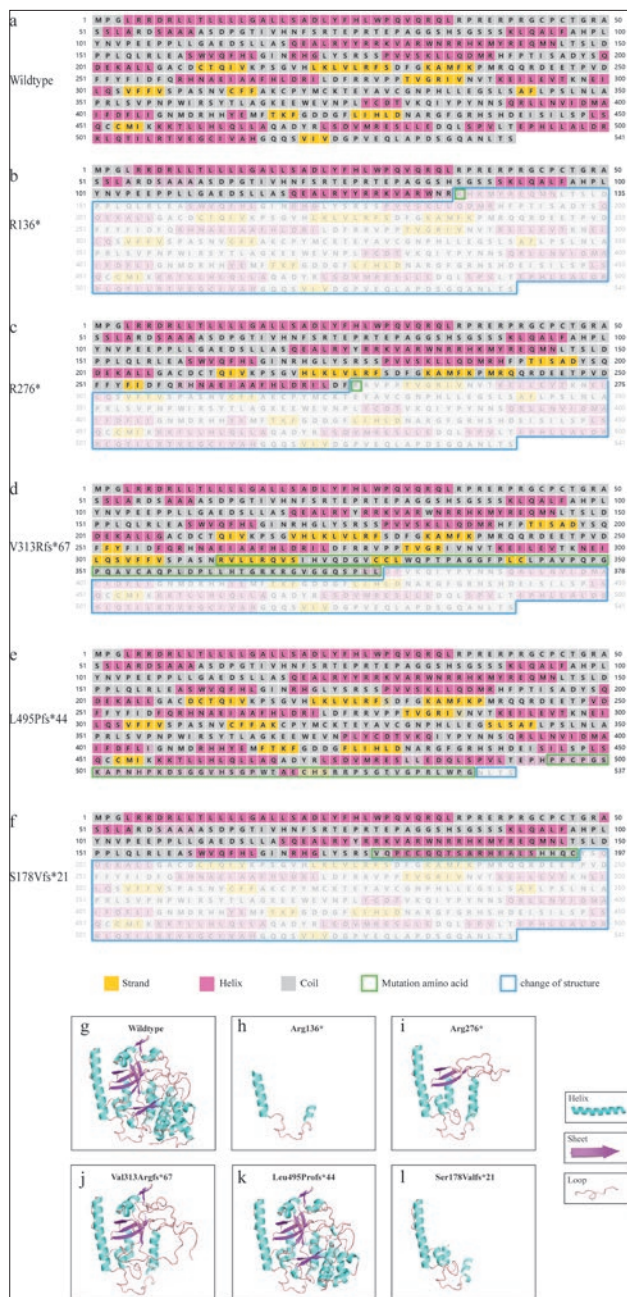
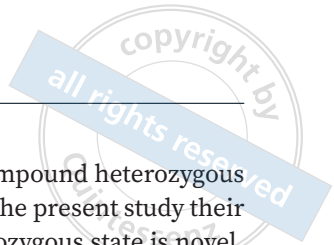


**Fig 3** Bioinformatics analysis of the FAM20A variants. The predicted secondary structure of the wild-type FAM20A protein (a). The predicted secondary structure of five mutated FAM20A proteins. Sites of variants are indicated by green squares. The structural changes in these mutated proteins compared to the wild-type FAM20A are shown as blue squares,  $\alpha$ -Helices are represented as pink squares, strands are represented as yellow squares, and while coils are represented as grey squares (b to f). Tertiary structural modelling of the FAM20A protein (g). Predicted tertiary structural changes in the five altered proteins (h to l).

viously reported separately in compound heterozygous states with other variants<sup>22,30</sup>, in the present study their presence in the compound heterozygous state is novel. We found that the root development of the unerupted molar was abnormal and the root apex of tooth 16 was curved, which was consistent with previous literature.<sup>25</sup> SEM analysis revealed a rough calcified nodule area and a relatively smooth mineral area on the crown surface, which was consistent with previous literature.<sup>25</sup> Through HE staining, the dental follicle and gingival mucosa of proband 302 displayed psammomatoid calcifications, and the ectopic mineralisation in the dental follicle and gingival mucosa was in accordance with previous literature.<sup>23,24</sup> This reoccurrence of clinical findings from different studies further confirmed the phenotypes related with FAM20A variants.

Proband 748 from family 2 carried FAM20A complex heterozygous variants c.936dupC (p.Val313Argfs\*67) and c.1483dupC (p.Leu495Profs\*44). These are both novel variants that have not been reported before, and both of which lead to truncation of the protein and functional impairment of FAM20A protein. Interestingly, variant Leu495Profs\*44 is changed from the 495th amino acid near the end of the protein, while wildtype FAM20A has 541 amino acids. However, the change in its intracellular localisation was the most significant among the five variants found in the present study. The Leu495Profs\*44 variant is restricted densely in the nucleolus. An intact signal sequence is necessary for secretion of FAM20A and that secretion is accompanied by prominent localisation of the protein to the ER.<sup>14</sup> If the highly conserved C-terminal putative kinase domain of FAM20A is mutated, the original signal sequence is lost, which may lead to re-entry from the endoplasmic reticulum into the nucleus.<sup>14</sup> The variant Leu495Profs\*44 is predicted to disrupt the signal sequence without grossly altering the other structure. The subcellular localisation results of the present study confirmed the structure prediction, and this result provided new evidence for the function of FAM20A subdomains.

Proband 914 carried a FAM20A homozygous variant, c.530\_531insGGTC (p.Ser178Valfs\*21), which was novel and led to severe protein truncation. His parents both carried the rare heterozygous variant, but denied consanguineous marriage. He showed anterior open bite, which could be attributed to the eruption disorder related to FAM20A variant. This speculation needs to be confirmed further with future clinical and functional studies.

Based on the Co-IP results, we can see that all five variants weaken the ability to bind to FAM20C, affecting

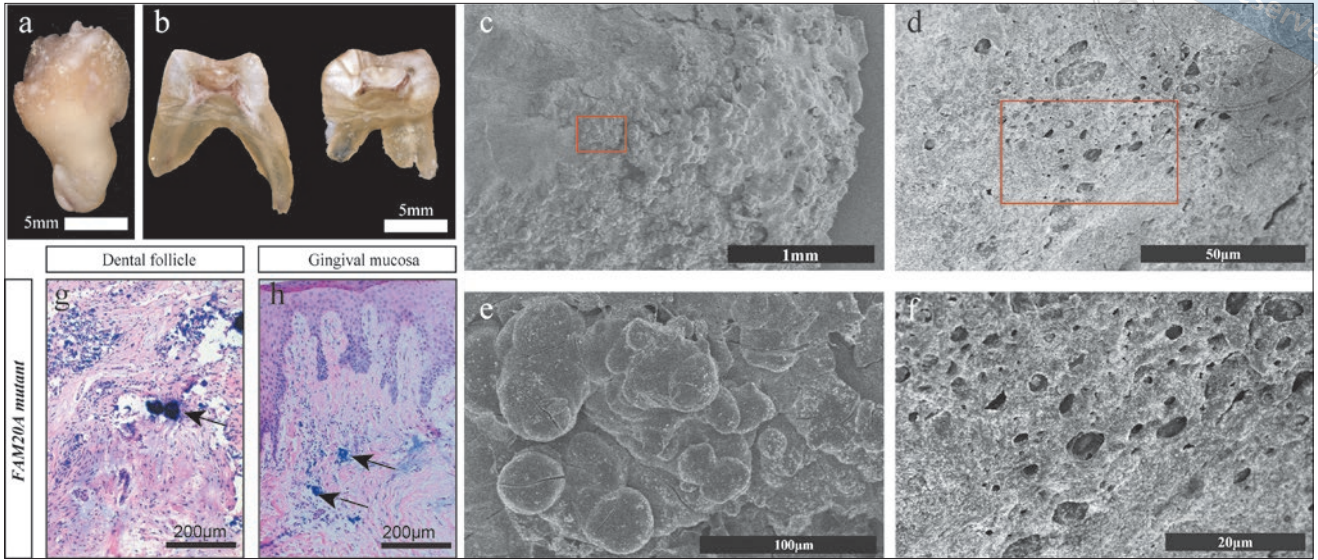


**Fig 4** Histological features of proband 302's teeth, dental follicle and gingival mucosa. Photograph of tooth 16 (a). Photograph of tooth 16 shows curved roots and poorly developed root morphology (b). Photograph of tooth 65 cut in a buccolingual direction with thin enamel (c). Low magnification view of the occlusal surface of tooth 65 for SEM analysis (d). Higher magnification of the box in panel c (e). Higher magnification of the box in panel d (f). HE section showing dental follicle tissue, with the arrow indicating ectopic psammomatoid calcification (g). HE section showing gingiva mucosa, arrows indicating ectopic psammomatoid calcification (h).

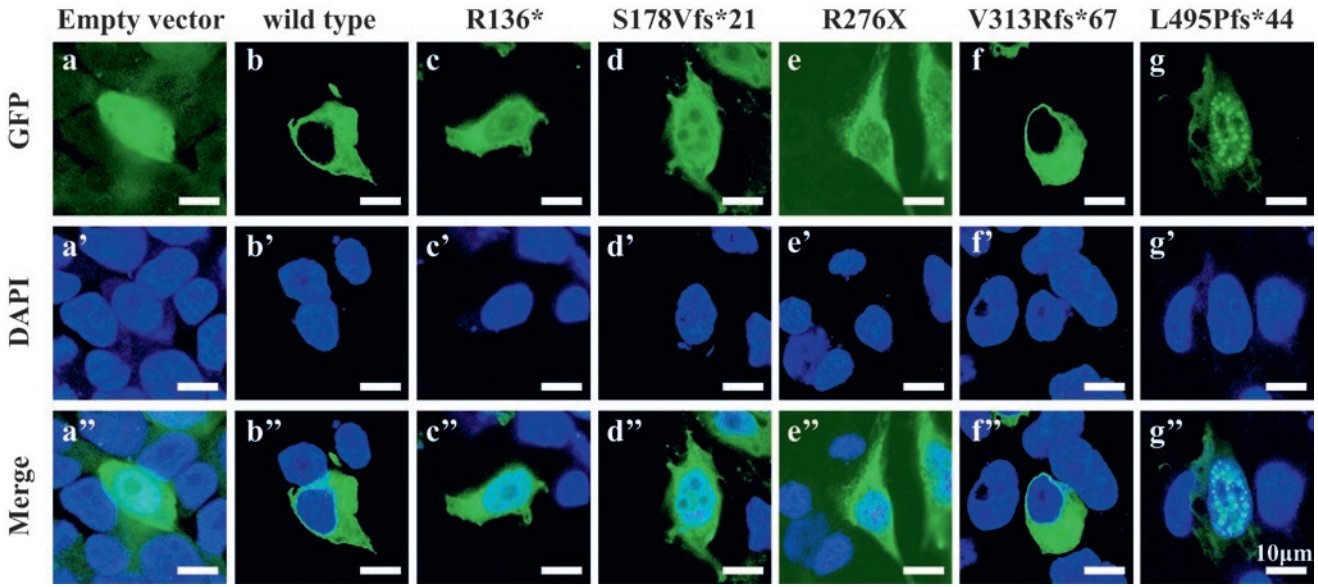


**Fig 5** Expression and subcellular localisation of wild-type and mutated FAM20A proteins. Subcellular localisation of wild-type or mutated FAM20A. Cells transfected with GFP-R136\*, GFP-R276\* and GFP-S178Vfs\*21 show expression in the entire cytoplasm with weak expression in the nucleus. GFP-V313Rfs\*67 is located in the same location as the wild type, yet without local condensation in the cytoplasm. GFP-L495Pfs\*44 shows densely clumped distributions within the nucleus. The empty vector with GFP was transfected into 293T cells as a negative control (a to g). Nuclei staining by DAPI, 4,6-diamino-2-phenylindole (a' to g'). Merge of GFP and DAPI (a'' to g''). FAM20A (GFP, green); nuclei (DAPI, blue)

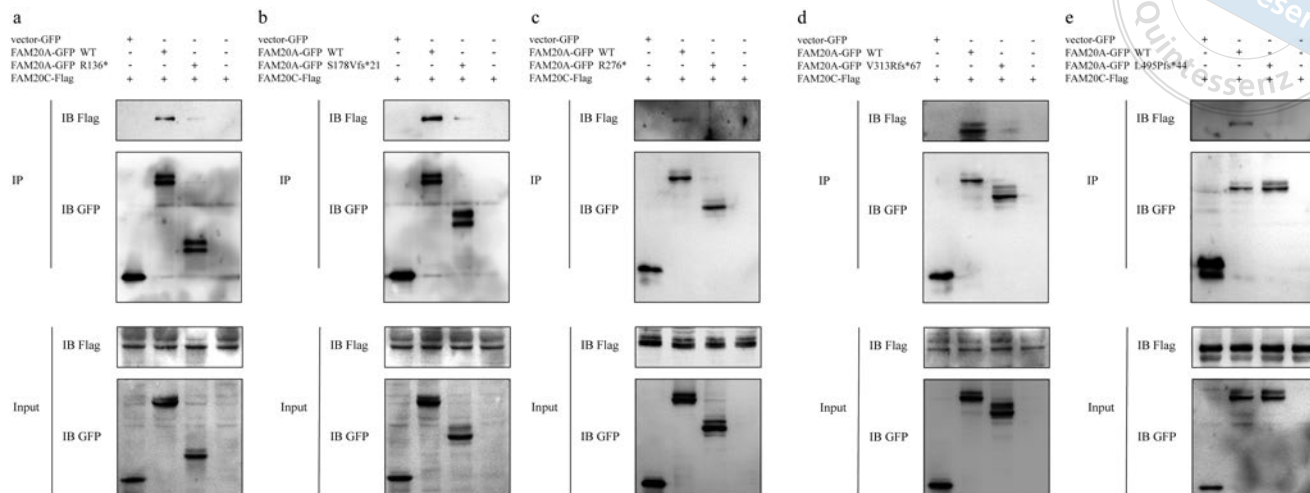


**Fig 6** Co-immunoprecipitation of the variants. FAM20A variant R136\* has a reduced ability to bind to FAM20C (a). FAM20A variant S178Vfs\*21 has a reduced ability to bind to FAM20C (b). FAM20A variant R276\* has a reduced ability to bind to FAM20C (c). FAM20A variant V313Rfs\*67 has a reduced ability to bind to FAM20C (d). FAM20A variant L495Pfs\*44\* has a reduced ability to bind to FAM20C (e).

the downstream function of the FAM20A-FAM20C complex, which leads to the development of AI. The present findings are also consistent with those from previous literature.<sup>18,25</sup>

## Conclusion

The present authors identified five *FAM20A* variants, three of which were novel, in three patients with AI, and verified the functional impacts with in vitro experiments. The clinical and histological features were also recorded. This study broadened the variant spectrum of *FAM20A* and will facilitate in-depth investigation in the future.

## Conflicts of interest

The authors declare no conflicts of interest related to this study.

## Author contribution

Dr Jia Nan DING contributed to the data acquisition, analysis, interpretation and manuscript draft; Drs Miao YU, Hao Chen LIU and Kai SUN contributed to the data acquisition and interpretation; Drs Jing WANG and Xiang Liang XU assisted in the experiments; Dr Yang LIU contributed to the study design and manuscript draft and critical revision; Dr Dong HAN contributed to the conception and critical revision of the manuscript;

All authors gave final approval for the manuscript.

(Received Jun 30, 2023; accepted Nov 23, 2023)

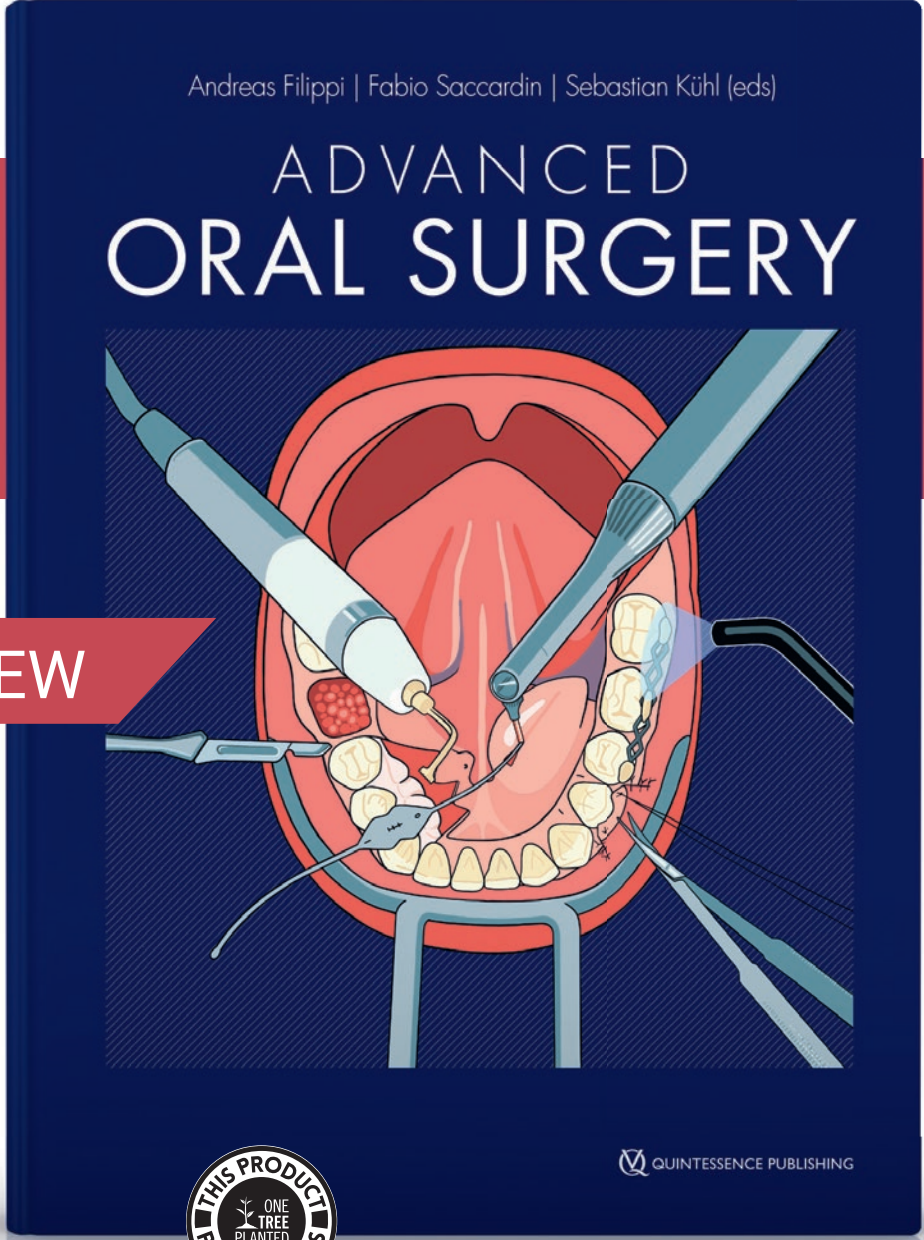
## References

1. He XY, Sun K, Xu RS, et al. Spatial signalling mediated by the transforming growth factor- $\beta$  signalling pathway during tooth formation. *Int J Oral Sci* 2016;8:199–204.
2. Xiong Y, Fang Y, Qian Y, et al. Wnt production in dental epithelium is crucial for tooth differentiation. *J Dent Res* 2019;98:580–588.
3. Tziafas D, Kodonas K. Differentiation potential of dental papilla, dental pulp, and apical papilla progenitor cells. *J Endod* 2010;36:781–789.
4. Mahdee AF, Ali AH, Gillespie JI. Structural and functional relations between the connective tissue and epithelium of enamel organ and their role during enamel maturation. *J Mol Histol* 2021;52:975–989.
5. Zeng L, He H, Sun M, et al. Runx2 and Nell-1 in dental follicle progenitor cells regulate bone remodeling and tooth eruption. *Stem Cell Res Ther* 2022;13:486.
6. Wang H, Pan M, Ni J, et al. CIC-7 deficiency impairs tooth development and eruption. *Sci Rep* 2016;6:19971.
7. Mitsui SN, Yasue A, Masuda K, et al. Novel PAX9 mutations cause non-syndromic tooth agenesis. *J Dent Res* 2014;93:245–249.
8. Brook AH. Multilevel complex interactions between genetic, epigenetic and environmental factors in the aetiology of anomalies of dental development. *Arch Oral Biol* 2009;54(suppl 1):S3–S17.
9. de la Dure-Molla M, Quentric M, Yamaguti PM, et al. Pathognomonic oral profile of enamel renal syndrome (ERS) caused by recessive FAM20A mutations. *Orphanet J Rare Dis* 2014;9:84.
10. Robinson C, Kirkham J, Brookes SJ, Bonass WA, Shore RC. The chemistry of enamel development. *Int J Dev Biol* 1995;39:145–152.

11. Li L, Saiyin W, Zhang H, et al. FAM20A is essential for amelogenesis, but is dispensable for dentinogenesis. *J Mol Histol* 2019;50:581–591.
12. Suchancova B, Holly D, Janska M, et al. Amelogenesis imperfecta and the treatment plan - Interdisciplinary team approach. *Bratisl Lek Listy* 2014;115:44–48.
13. Witkop CJ Jr. Amelogenesis imperfecta, dentinogenesis imperfecta and dentin dysplasia revisited: problems in classification. *J Oral Pathol* 1988;17:547–553.
14. Nalbant D, Youn H, Nalbant SI, et al. FAM20: An evolutionarily conserved family of secreted proteins expressed in hematopoietic cells. *BMC Genomics* 2005;6:11.
15. Cui J, Zhu Q, Zhang H, et al. Structure of Fam20A reveals a pseudokinase featuring a unique disulfide pattern and inverted ATP-binding. *Elife* 2017;6:e23990.
16. Wang SK, Reid BM, Dugan SL, et al. FAM20A mutations associated with enamel renal syndrome. *J Dent Res* 2014;93:42–48.
17. Ohyama Y, Lin JH, Govitvattana N, et al. FAM20A binds to and regulates FAM20C localization. *Sci Rep* 2016;6:27784.
18. Wang SK, Zhang H, Wang YL, et al. FAM20A mutations and transcriptome analyses of dental pulp tissues of enamel renal syndrome. *Int Endod J* 2023;56:943–954.
19. Zhang H, Zhu Q, Cui J, et al. Structure and evolution of the Fam20 kinases. *Nat Commun* 2018;9:1218.
20. Worby CA, Mayfield JE, Pollak AJ, et al. The ABCs of the atypical Fam20 secretory pathway kinases. *J Biol Chem* 2021;296:100267.
21. Zuo H, Yang D, Wan Y. Fam20C regulates bone resorption and breast cancer bone metastasis through Osteopontin and BMP4. *Cancer Res* 2021;81:5242–5254.
22. Hung CY, Rodriguez M, Roberts A, Bauer M, Mihalek I, Bodamer O. A novel FAM20C mutation causes a rare form of neonatal lethal Raine syndrome. *Am J Med Genet A* 2019;179:1866–1871.
23. Simancas Escorcía V, Diarra A, Naveau A, et al. Lack of FAM20A, ectopic gingival mineralization and chondro/osteogenic modifications in enamel renal syndrome. *Front Cell Dev Biol* 2020;8:605084.
24. Dourado MR, Dos Santos CRR, Dumitriu S, et al. Enamel renal syndrome: A novel homozygous FAM20A founder mutation in 5 new Brazilian families. *Eur J Med Genet* 2019;62:103561.
25. Wang SK, Aref P, Hu Y, et al. FAM20A mutations can cause enamel-renal syndrome (ERS). *PLoS Genet* 2013;9:e1003302.
26. Prasad MK, Geoffroy V, Vicaire S, et al. A targeted next-generation sequencing assay for the molecular diagnosis of genetic disorders with orodental involvement. *J Med Genet* 2016;53:98–110.
27. Rey T, Tarabeux J, Gerard B, et al. Protocol GenoDENT: Implementation of a new NGS panel for molecular diagnosis of genetic disorders with orodental involvement. *Methods Mol Biol* 2019;1922:407–452.
28. Richards S, Aziz N, Bale S, et al. Standards and guidelines for the interpretation of sequence variants: A joint consensus recommendation of the American College of Medical Genetics and Genomics and the Association for Molecular Pathology. *Genet Med* 2015;17:405–424.
29. Kantaputra PN, Bongkochwilawan C, Lubinsky M, et al. Periodontal disease and FAM20A mutations. *J Hum Genet* 2017;62:679–686.
30. Cho SH, Seymen F, Lee KE, et al. Novel FAM20A mutations in hypoplastic amelogenesis imperfecta. *Hum Mutat* 2012;33:91–94.



# NOW... THE SECOND VOLUME



Andreas Filippi | Fabio Saccardin  
Sebastian Kühl (Eds)

### Advanced Oral Surgery

incl 26 Videos, 312 pages, 450 illus.  
ISBN 978-1-78698-133-2  
€128

This book follows on from *Basic Oral Surgery*. It is aimed at advanced practitioners who frequently perform oral surgery procedures in their practices and want to update and develop their skills. It is also aimed at current and prospective specialists in oral and maxillofacial surgery. Like the first volume, it is designed as an atlas rather than a textbook: the clinical chapters in particular contain short theoretical texts and follow a similar structure. Numerous photographs and videos linked via QR codes supplement the text. The content and scope of the book are based on advanced training programs and the range of clinical advanced training in oral surgery provided by university departments.

NEW



QUINTESSENCE PUBLISHING

QUINTESSENCE PUBLISHING



[www.quint.link/advanced-surgery](http://www.quint.link/advanced-surgery)

[books@quintessenz.de](mailto:books@quintessenz.de)

+49 (0)30 761 80 667

QUINTESSENCE PUBLISHING



# Integrative Multi-omics Analysis Identifies Genetic Variants Contributing to Non-syndromic Cleft Lip with or without Cleft Palate

Shu LOU<sup>1,2,3,4,#</sup>, Jing YANG<sup>1,#</sup>, Gui Rong ZHU<sup>1,#</sup>, Dan Dan LI<sup>1,2,3,4</sup>, Lan MA<sup>1,3,4</sup>, Lin WANG<sup>1,2,3,4</sup>, Yong Chu PAN<sup>1,2,3,4</sup>

**Objective:** To provide novel insights into the aetiology of non-syndromic cleft lip with or without cleft palate (NSCL/P) by integrating multi-omics data and exploring susceptibility genes associated with NSCL/P.

**Methods:** A two-stage genome-wide association study (GWAS) of NSCL/P was performed, involving a total of 1,069 cases and 1,724 controls. Using promoter capture Hi-C (pChI-C) datasets in human embryonic stem cells (hESC) and chromatin immunoprecipitation sequencing (ChIP-seq) in craniofacial tissues, we filtered out single nucleotide polymorphisms (SNPs) with active cis-regulation and their target genes. Additionally, we employed expression quantitative trait loci (eQTL) analysis to identify candidate genes.

**Results:** Thirteen SNPs were identified as cis-regulation units associated with the risk of NSCL/P. Five of these were proven to be active in chromatin states in early human craniofacial development (rs7218002: odds ratio [OR] 1.50,  $P = 8.14E-08$ ; rs835367: OR 0.78,  $P = 3.48E-05$ ; rs77022994: OR 0.55,  $P = 1.05E-04$ ; rs961470: OR 0.73,  $P = 1.38E-04$ ; rs17314727: OR 0.73,  $P = 1.85E-04$ ). Additionally, pChI-C and eQTL analysis prioritised three candidate genes (rs7218002: *NTN1*, rs835367: *FGGY*, *LINC01135*). *NTN1* and *FGGY* were expressed in mouse orofacial development. Deficiencies in *NTN1*, *FGGY* and *LINC01135* were associated with cleft palate and cleft lip, abnormal facial shape and bifid uvula, and abnormality of the face, respectively.

**Conclusion:** Our study identified five SNPs (rs7218002, rs835367, rs77022994, rs961470 and rs17314727) and three susceptibility genes (*NTN1*, *FGGY* and *LINC01135*) associated with NSCL/P. These findings contribute to a better understanding of the genetic factors involved.

**Keywords:** ChIP-seq, expression quantitative trait loci, non-syndromic cleft lip, pChI-C  
*Chin J Dent Res* 2024;27(1):65–73; doi: 10.3290/j.cjdr.b5136745

1 Jiangsu Key Laboratory of Oral Diseases, Nanjing Medical University, Nanjing, P.R. China.

2 Department of Orthodontics, Affiliated Hospital of Stomatology, Nanjing Medical University, Nanjing, P.R. China.

3 State Key Laboratory of Reproductive Medicine, Nanjing Medical University, Nanjing, P.R. China.

4 Jiangsu Province Engineering Research Center of Stomatological Translational Medicine, Nanjing Medical University, Nanjing, P.R. China.

# These authors contributed equally to this study.

**Corresponding authors:** Dr Yong Chu PAN and Dr Lin WANG, Jiangsu Key Laboratory of Oral Diseases, Nanjing Medical University, 136 Hanzhong Road, Nanjing 210029, P.R. China. Tel: 86-25-86862025. Email: panyongchu@njmu.edu.cn; lw603@njmu.edu.cn

Non-syndromic cleft lip with or without cleft palate (NSCL/P) is one of the most common human birth defects, occurring in 1 in 700 live births and imposing heavy health and financial burdens on individuals.<sup>1</sup>

This work was supported by the National Natural Science Foundation of China (82270496, 81830031, 81970969, 82001088, 82101054), the Natural Science Foundation of Jiangsu Province (BK20220309), the Natural Science Foundation of the Jiangsu Higher Education Institutions of China (22KJB320003, 22KJA320002), the Chinese Postdoctoral Science Foundation (2022M721677), the Young Talents Project of the Orthodontics Committee of the Chinese Stomatological Association (COS-B2021-09), Jiangsu Province Capability Improvement Project through Science, Technology and Education-Jiangsu Provincial Research Hospital Cultivation Unit (YJXYJSDW4), and Jiangsu Provincial Medical Innovation Center (CXZX202227).

These defects arise during the embryonic period, specifically between the sixth and twelfth weeks, when there is a failure of fusion between the maxillary and medial nasal prominences, followed by the primary palate with the two lateral palatal shelves.<sup>2</sup>

In recent years, numerous genome-wide association studies (GWASs) have identified thousands of genetic variants associated with various phenotypes and diseases.<sup>1,3-5</sup> So far, at least 190 single nucleotide polymorphisms (SNPs) have been discovered to be related to NSCL/P according to the GWAS catalogue. Nevertheless, caution must be exercised when interpreting these associations, as GWAS findings often include both true driver variants that contribute to disease and passenger variants that are merely correlated with the SNPs susceptible to disease.<sup>6,7</sup> To gain a deeper understanding of the functional mechanisms underlying these associations, it is crucial to integrate genetic, transcriptional, epigenetic and other datasets systematically.

Promoter capture Hi-C (pChI-C) is a recent technique that utilises sequence capture to enrich interactions between gene promoters and long-range cis-regulatory elements, such as enhancers, thereby providing robust evidence for interactions between distal regulatory elements and target genes.<sup>8-11</sup> By combing pChI-C with GWAS data, it becomes possible to elucidate the functions of non-coding variants and establish potential links between SNPs and disease-related genes. For instance, Montefiori et al<sup>12</sup> employed pChI-C maps of cardiomyocytes to associate 1,999 SNPs related to cardiovascular diseases with 347 target genes. Li et al<sup>13</sup> integrated pChI-C data with GWAS data on systemic sclerosis and successfully identified four susceptibility loci interacting with differentially methylated CpG sites.

Chromatin immunoprecipitation sequencing (ChIP-seq) is another widely used approach to investigate genome-wide protein-DNA interactions and predict gene regulatory mechanisms.<sup>14</sup> Combining ChIP-seq with pChI-C data can help shed light on the underlying mechanisms by identifying which regulatory elements mediate these interactions.<sup>9</sup> Deoxyribonuclease I (DNase I)-hypersensitive sites (DNase) serve as markers of chromatin accessibility and play a critical role in discovering various types of cis-regulatory elements, including enhancers, promoters and silencers.<sup>15</sup> Histone modifications, such as H3K4me1 and H3K27ac, are associated with distal enhancers, with H3K27ac specifically indicating active enhancers that also possess H3K4me1 modifications.<sup>16</sup> Additionally, H3K4me3 is typically found at gene promoter regions with active transcriptional activity.<sup>17</sup>

In the present study, to gain comprehensive insights into the mechanisms underlying NSCL/P, we integrated GWAS data with pChI-C data obtained from human embryonic stem cells (hESCs) and incorporated chromatin modifications of craniofacial tissues (CTs) at different developmental stages to identify potential risk SNPs. By utilising pChI-C and expression quantitative trait loci (eQTL) analysis, we prioritised candidate target genes associated with NSCL/P development.

## Materials and methods

### *Study populations*

In the present study, we carried out a two-stage GWAS of NSCL/P. The discovery stage included 504 NSCL/P cases and 455 controls in Stage I, and the replication stage was performed in an additional 565 unrelated NSCL/P cases and 1,269 controls in Stage II. All participants were recruited from the Chinese population and were examined by two experienced oral surgeons. Patients with an underlying syndrome were excluded. Written consent was collected from all participants. Basic information on the age and sex of the subjects was collected, and peripheral blood samples were obtained in the clinical laboratory. The study was approved by the institutional ethics committee of Nanjing Medical University (NJMUERC [2008] No.20).

### *DNA extraction*

From each subject, 2 ml whole blood was collected using an anticoagulant tube. The blood samples were centrifuged at 3,000 rpm at 4°C for 5 minutes to separate them into plasma and cell parts. TIANamp Genomic DNA Kit (Tiangen Biotech, Beijing, China) was used to extract partial genomic DNA of cells following the manufacturer's instructions.

### *Genotyping, quality control and imputation of GWAS data*

Genotyping was used by Affymetrix Axiom Genome-Wide CHB1 and CHB2 Array Plates in Stage I and by Illumina Infinium Asian Screening Array (ASA) v1.0 in Stage II. SNPs and samples that did not meet the criteria were excluded before imputation as previously described.<sup>18</sup> SNPs with a call rate < 95%, minor allele frequency (MAF) < 0.05 or  $P \leq 1E-04$  for Hardy-Weinberg equilibrium (HWE) were excluded. Samples with a call rate < 95%, sex discrepancy and extreme heterozygosity

(> 6 standard deviation from the mean) were excluded. The 1,000 Genomes Project (<https://www.1000genomes.org>, phase1, release3) was used as a reference and imputation was performed based on SHAPEIT (SHAPEIT\_v2) and IMPUTE2 ([https://mathgen.stats.ox.ac.uk/impute/impute\\_v2.html](https://mathgen.stats.ox.ac.uk/impute/impute_v2.html), imputation step). SNPs with a call rate < 0.95, imputation quality info  $\leq$  0.8, MAF < 0.05 and HWE in controls  $\leq$  1E-04 were excluded from the analysis.

### *Selection of SNPs with cis-regulation*

We selected SNPs with  $P < 0.01$  in both GWAS studies, along with association direction consistency in both GWAS datasets for subsequent analysis. SNPs in cis-regulatory units of genes in hESC sequenced by pChIP-C maps in the Gene Expression Omnibus (GEO) database (<https://www.ncbi.nlm.nih.gov/geo>, acc=GSE86821) and without linkage disequilibrium (LD,  $r^2 < 0.4$ ) were identified for study. To further identify regulatory mechanisms of SNPs for human craniofacial development, we utilised ChIP-seq of four histone modifications across multiple stages (CS13, CS14, CS15, CS17) in CTs in the GEO database (acc = GSE97752) and eliminated SNPs in quiescent states.<sup>19</sup>

### *In silico functional annotation of SNPs and genes*

After identifying these susceptibility loci, several annotation approaches were used, including HaploReg v4 (<http://compbio.mit.edu/HaploReg>) and RegulomeDB (<https://regulome.stanford.edu/regulome-search>) for functional annotation. The authors then integrated pChIP-C data and eQTL analysis to highlight potential candidate genes, and based on 3DSNP (<http://biotech.bmi.ac.cn/3dsnp/>), a database for linking SNPs to their interacting genes in three dimensions and the 3D Genome Browser (<http://3dgenome.org>), a database for visualising chromatin interaction data by Hi-C to verify functional interactions between SNPs and these candidate genes.<sup>20,21</sup> To observe their expression in orofacial development, the GEO database (acc = GSE67985) and FaceBase (<https://www.facebase.org/>) were analysed among E10.5 (acc = FB00000662.01), E11.5 (acc = FB00000663.01), E12.5 (acc = FB00000664.01), E13.5 (acc = FB00000665.01) and E14.5 (acc = FB00000666.01). The phenotypes of the candidate genes in humans were assessed using the Database of Genomic Variation and Phenotype in Humans using Ensemble Resources (DECIPHER, <https://decipher.sanger.ac.uk/>).<sup>22</sup>

### *Statistical analysis*

GWASs were analysed using SNPTEST (version 2.5.6), PLINK (version 1.09) and R software (version 3.6.2).<sup>23,24</sup> In two-stage GWAS, the association between each SNP and NSCL/P risk was evaluated using odds ratios (ORs) and 95% confidence intervals (CIs) in logistic regression analysis under an additive model. The cumulative effects of five risk loci on NSCL/P susceptibility were assessed by calculating the number of risk alleles per subject and categorising pooled variables in unconditional logistic regression analysis (0 to 4 as a reference, 5 to 6, 7, 8 and 9 to 10).<sup>25</sup> Epigenetic annotation for SNPs was completed in WashU Epigenome Browser.<sup>25,26</sup> Statistical figures were performed using GraphPad Prism5 (GraphPad Software, San Diego, CA, USA).

## **Results**

### *Genome-wide association of SNPs with NSCL/P risk*

The workflow for identifying risk SNPs associated with NSCL/P is shown in Fig 1. To find susceptibility variants for NSCL/P in the Chinese population, we conducted a two-stage analysis, including 1,069 cases and 1,724 controls (Supplementary Table 1, provided on request). A total of 6,206,820 SNPs were identified in GWAS Stage I and 3,806,365 were filtered out in GWAS Stage II after quality control. A Manhattan plot displaying the results of the genome-wide association analysis is presented in Fig 2. Ultimately, 411 SNPs with  $P < 0.01$  and consistent association direction in both GWAS datasets were extracted.

### *SNPs with active cis regulation associated with NSCL/P*

After combing pChIP-C maps in hESC (Supplementary Table 2, provided on request) with two-stage GWAS, 13 SNPs located in these units were identified after excluding strong linkage disequilibrium. Five of these were identified as having different histone modifications and were associated with active chromatin states in human craniofacial tissues at various developmental stages (Table 1 and Supplementary Table 2). Rs7218002 (OR 1.50, 95% CI 1.35–1.64,  $P_{\text{meta}} = 8.14\text{E-}08$ ) was in a bivalent promoter or repressed polycomb state. Rs835367 (OR 0.78, 95% CI 0.71–0.85,  $P_{\text{meta}} = 3.48\text{E-}05$ ) and rs961470 (OR 0.73, 95% CI 0.58–0.89,  $P_{\text{meta}} = 1.38\text{E-}04$ ) were in active TSS state, whereas rs77022994 (OR 0.55, 95% CI 0.35–0.85,  $P_{\text{meta}} = 1.05\text{E-}04$ ) was in transcription state

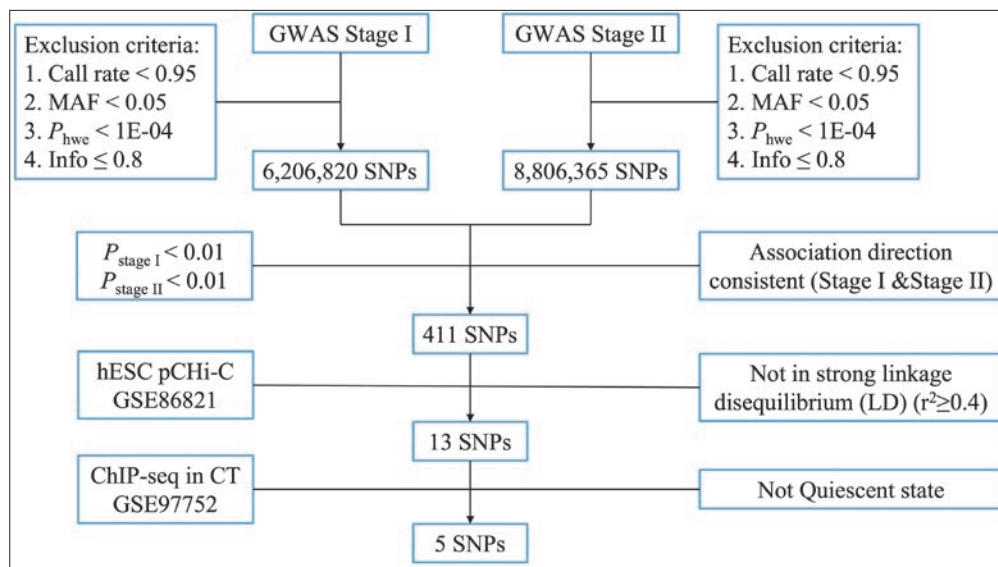


**Fig 1** Workflow for identifying the susceptible SNPs with active cis-regulatory elements involved in non-syndromic orofacial cleft. ChIP-seq, chromatin immunoprecipitation sequence; CTs, craniofacial tissues; GWAS, genome-wide association studies; hESC, human embryonic stem cell; HWE, Hardy-Weinberg equilibrium; MAF, minor allele frequency; pChIP-C, promoter capture Hi-C.

**Table 1** Five SNPs with active cis-regulatory elements involved in non-syndromic orofacial cleft.

SNP	CHR	BP (hg19)	Alleles	MAF <sup>a</sup>	Stage I			Stage II			Meta analysis	
					MAF (control/case)	OR (95% CI)	P <sup>b</sup>	MAF (control/case)	OR (95% CI)	P <sup>b</sup>	OR (95% CI)	P
rs7218002	17	8923718	T/A	0.19	0.18/0.26	1.62 (1.38–1.86)	7.46E-05	0.19/0.24	1.42 (1.24–1.61)	2.05E-04	1.50 (1.35–1.64)	8.14E-08
rs835367	1	59762468	A/G	0.44	0.48/0.40	0.71 (0.62–0.83)	8.44E-04	0.42/0.38	0.81 (0.72–0.93)	7.74E-03	0.78 (0.71–0.85)	3.48E-05
rs77022994	11	125255402	T/C	0.03	0.06/0.03	0.51 (0.04–0.98)	5.35E-03	0.05/0.03	0.59 (0.20–0.97)	6.26E-03	0.55 (0.35–0.85)	1.05E-04
rs961470	1	119530133	G/A	0.18	0.22/0.16	0.71 (0.47–0.96)	6.68E-03	0.17/0.13	0.75 (0.54–0.96)	7.01E-03	0.73 (0.58–0.89)	1.38E-04
rs17314727	5	93228046	C/T	0.13	0.18/0.15	0.69 (0.43–0.95)	5.90E-03	0.15/0.12	0.75 (0.54–0.97)	9.91E-03	0.73 (0.56–0.89)	1.85E-04

Alleles, minor allele/major allele; BP, base-pair position; CHR, chromosome.

<sup>a</sup>Minor allele frequency in 1000 Genomes Project (CHB+JPT);

<sup>b</sup>P value was adjusted by logistic regression in SNPTEST including sex and PCA as covariates.

and rs17314727 (OR 0.73, 95% CI 0.56–0.89, P<sub>meta</sub> = 1.85E-04) was in a weak enhancer state. We demonstrated that rs835367 was in DNase chromatin and had abundant H3K4me3 and H3K27ac. Rs961470 was also present in DNase chromatin and was marked by H3K4me1, H3K4me3 and H3K27ac. Additionally, rs17314727 was surrounded by H3K4me3 and H3K27ac marks (Fig 3a).

*Cumulative effects of risk loci on NSCL/P subgroups*

The cumulative effects of five significant SNPs according to the risk alleles (rs7218002 T, rs835367 G, rs77022994 C, rs961470 A and rs17314727 T) are assessed in Table 2. Compared with individuals with 0 to 4 risk alleles, those carrying 7, 8 or 9 to 10 risk alleles had ORs of 1.53 (95% CI 0.79–2.95), 2.12 (95% CI 1.07–4.20) or 4.28 (95% CI 1.89–9.74) in Stage I. We found individuals with mul-

**Fig 2** Manhattan plot of genome-wide association analysis illustrating the level of statistical significance (y-axis), as measured by the negative log of the corresponding  $P$  value in Stage I (a) and Stage II (b), for each single nucleotide polymorphism (SNP). Each typed SNP is indicated by a grey or blue dot. SNPs are arranged by chromosomal location (x-axis). The red line represents the genome-wide level ( $P = 5E-08$ ) and the blue line represents the suggestive significant level ( $P = 1E-05$ ).

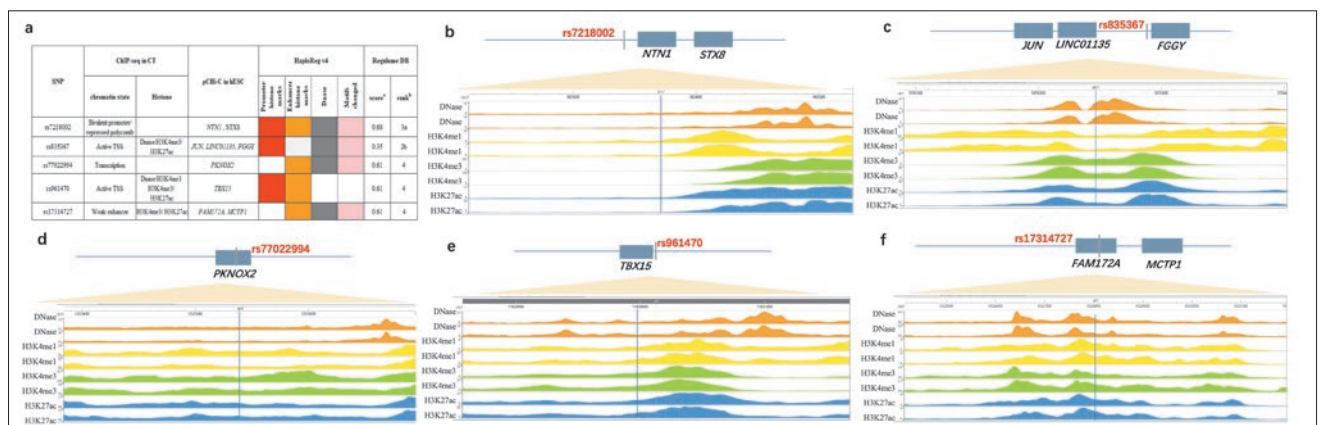
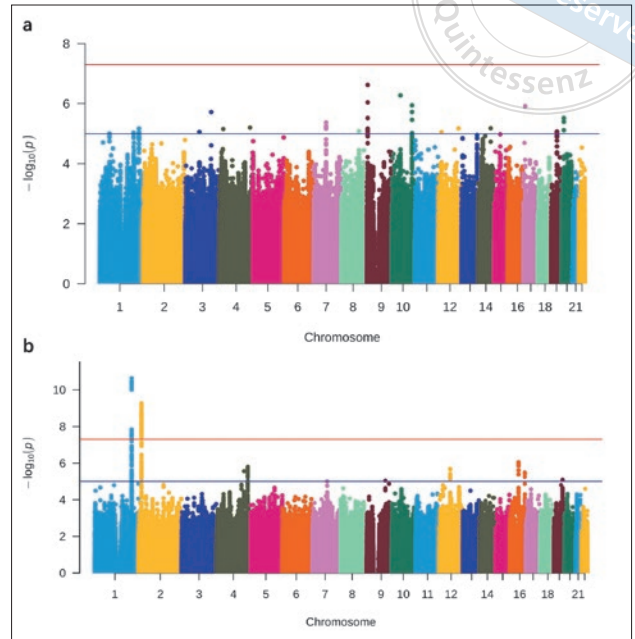


**Fig 3** Functional annotation of five risk SNPs with active cis-regulatory elements involved in non-syndromic cleft lip with or without cleft palate. Annotation of five SNPs with active cis-regulatory elements involved in non-syndromic orofacial cleft according to HaploReg v4 and Regulome DB (a). Annotation of five SNPs with active cis-regulatory elements involved in non-syndromic orofacial cleft according to ChIP-seq in CT and pChIP-C in hESC (b to f). The data were obtained from GEO Project (GSE97752), including active histone modification (H3k4me1, H3K4me3, H3k27ac) as well as DNase. Orange represented DNase chromatin accessibility, yellow indicated histone H3k4me1, green represented histone H3K3me3 and blue indicated histone H3K27ac. The nearest gene and interaction genes of five SNPs were shown in grey rectangles from pChIP-C datasets (GSE86821). ChIP-seq, chromatin immunoprecipitation sequence; CTs, craniofacial tissues; hESC, human embryonic stem cell; pChIP-C, promoter capture Hi-C. <sup>a</sup>The Regulome DB probability score ranges from 0 to 1 and 1 is most likely to be a regulatory variant. <sup>b</sup>2b means TF binding + any motif + DNase Footprint + DNase peak, 3a means TF binding + any motif + DNase peak, and 4 means TF binding + DNase peak.

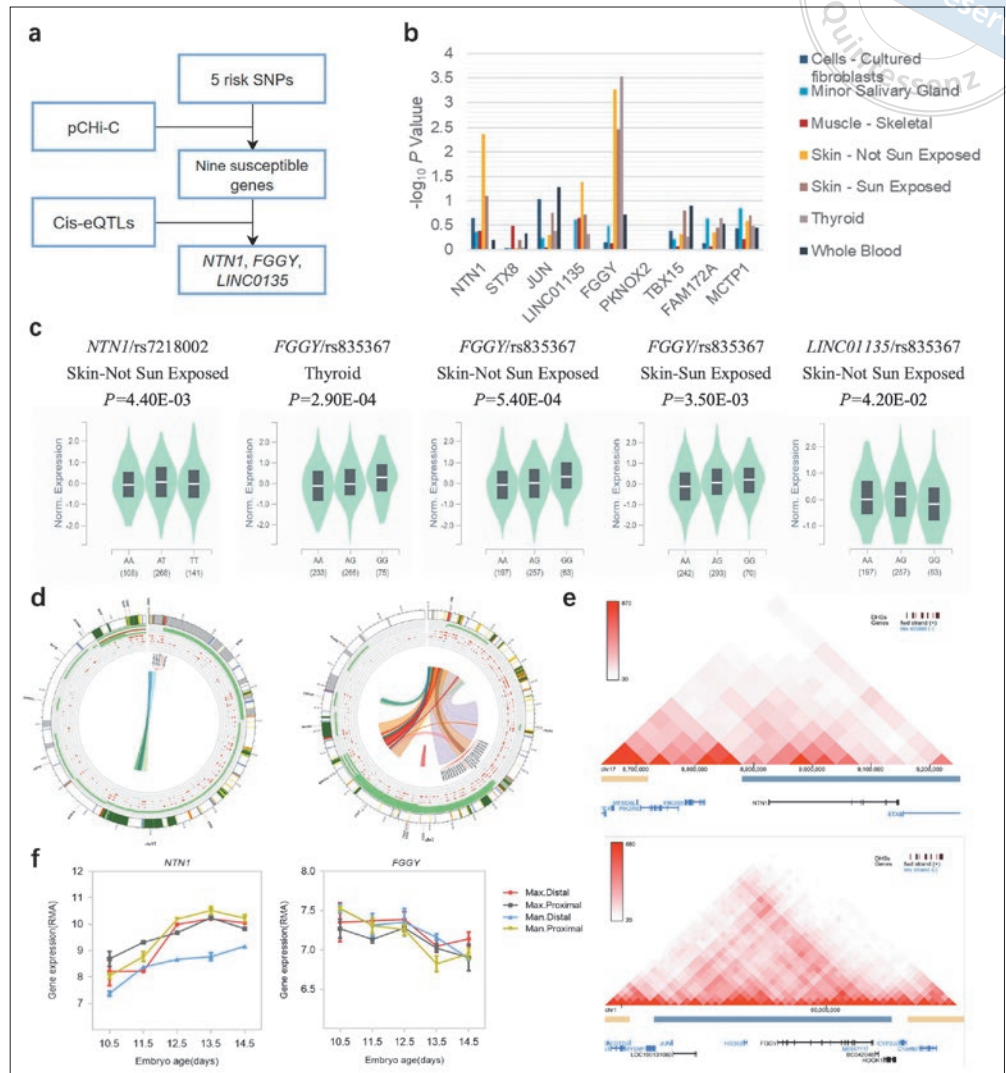
multiple risk alleles had a higher risk of NSCL/P, and similar results were also observed in Stage II. We stratified all NSCL/P cases into cleft lip only (CLO) and cleft lip and cleft palate (CLP) subgroups and observed that the risk increased in a dose-dependent manner with the number of risk variant alleles.

*Annotation and functional assessment of genetic variants*

HaploReg v4.1 and RegulomeDB were used to determine the function of the five significant SNPs. With prediction by HaploReg V4.1, functional annotation of rs7218002



**Fig 4** Identification of susceptible genes associated with non-syndromic orofacial cleft. A simplified diagram of the gene screening approach (a). eQTL analysis of five SNPs and correlated genes in different tissues (b and c). 3D chromatin looping of rs7218002 (left) and rs835367 (right) to their interacting genes (d). A region of the Hi-C interaction map in hESC on rs7218002 (left) and rs835367 (right). The alternating yellow and blue bars were predicted topologically associating domains (TADs) (e). Median expression levels of *NTN1* and *FGGY* in proximal and distal locations of maxilla and mandible during the 10.5th day to 14.5th day of mouse embryonic stage based on GEO datasets (GSE67985) (f). Man. Dis, mandibular distal location; Man.Pro, mandibular proximal location; Max.Dis, maxillary distal location; Max.Pro, maxillary proximal location.



included promoter histone marks, enhancer histone marks, DNase and motifs changed. Rs835367 might lead to promoter histone marks, DNase and motifs changed. Functional annotation of the other three SNPs is shown in Fig 3a. rs7218002 was in moderate linkage disequilibrium with rs4791774 ( $r^2 = 0.51$ ) and rs2944377 ( $r^2 = 0.55$ ), which were previously reported as having a risk of NSCL/P.<sup>27</sup>

Based on RegulomeDB scores, rs7218002 received a score of 3a, indicating a lesser likelihood of affecting transcription factor (TF) binding. On the other hand, rs835367 obtained a higher score of 2b, suggesting a greater potential for affecting TF binding. Rs7702294, rs961470 and rs17314724 received a RegulomeDB score of 4, indicating minimal binding ability for these SNPs.<sup>28</sup>

### Bioinformatic predictions of risk gene

A simplified diagram of the approach to identify the susceptible genes associated with NSCL/P is shown in Fig 4a. With prediction of pChI-C in hESC, we examined the interaction gene of five SNPs and found that five SNPs could link to nine genes (rs7218002: *NTN1*, *STX8*; rs835367: *FGGY*, *JUN*, *LINC01135*; rs7702294: *PKNOX2*; rs961470: *TBX15*; rs17314727: *FAM172A*, *MCTP1*) (Fig 3).

Further eQTL analysis was conducted using the GTEx database. rs7218002 was found to exhibit a significant association with expression of *NTN1* ( $P = 4.40E-03$ ) in skin not exposed to the sun. *FGGY* was associated with rs835367 in the thyroid ( $P = 2.90E-04$ ), skin not exposed to the sun ( $P = 5.40E-04$ ) and skin exposed to the sun ( $P = 3.50E-03$ ). *LINC01135* showed an association with

**Table 2** Cumulative effect of five risk SNP in non-syndromic orofacial cleft and subgroups.

GWAS	No. of risk allele	Control	Total case	OR (95% CI)	CLO	OR (95% CI)	CLP	OR (95% CI)
Stage I	0-4	23	18	Reference	9	Reference	9	Reference
	5-6	208	149	0.61 (0.32-1.18)	66	0.81 (0.36-1.84)	83	1.02 (0.45-2.30)
	7	137	164	1.53 (0.79-2.95)	65	1.21 (0.53-2.77)	99	1.85 (0.82-4.16)
	8	70	116	2.12 (1.07-4.20)	45	1.64 (0.70-3.87)	71	2.59 (1.12-5.99)
	9-10	17	57	4.28 (1.89-9.74)	20	3.01 (1.10-8.22)	37	5.56 (2.13-14.54)
Stage II	0-4	55	10	Reference	2	Reference	5	Reference
	5-6	454	202	2.45 (1.22-4.90)	62	3.76 (0.89-15.78)	106	6.42 (1.54-26.74)
	7	404	256	3.49 (1.75-6.96)	88	5.99 (1.43-25.02)	121	8.23 (1.98-34.26)
	8	278	203	4.02 (2.00-8.07)	65	6.43 (1.53-27.04)	103	10.19 (2.44-42.53)
	9-10	78	70	6.13 (2.90-12.94)	25	8.81 (2.00-38.76)	35	12.34 (2.85-53.46)

CLO, cleft lip only; CLP, cleft lip and palate.

rs835367 in skin not exposed to the sun ( $P = 4.20E-02$ ) (Fig 4b and c).

The 3D chromatin looping data demonstrated that rs7218002 interacted with *NTN1* and rs835367 could interact with *FGGY* and *LINC01135* (Fig 4d). According to the Hi-C map in hESC by 3D Genome Browser, rs7218002 and *NTN1* were located within a topologically associated domain (TAD) structure and so too were rs835367, *FGGY* and *LINC01135* (Fig 4e).

#### Gene expression in mouse craniofacial structures and phenotype in humans

Both *NTN1* and *FGGY* were expressed in the maxilla and mandible over five periods in mouse orofacial development (Fig 4f). A lack of considerable homology was detected for lncRNA *LINC01135* between humans and mice. According to DECIPHER, we found that individuals with an *NTN1* deficiency might present with multiple phenotypes like cleft palate and cleft lip. Individuals with an *FGGY* deficiency might show traits like thick lower lip vermilion, thick upper lip vermilion, abnormal facial shape and bifid uvula, and those with an *LINC01135* deficiency might present abnormalities in facial features, thick lower lip vermilion and thick upper lip vermilion.

#### Discussion

The present study investigated systematic insights into mechanisms of NSCL/P by using previously published GWAS data, pChI-C data of hESC and ChIP-seq of craniofacial tissues. The function of SNPs was assessed using HaploReg v4.1 and RegulomeDB. Candidate genes were identified based on pChI-C data and eQTL analysis, supported by 3DSNP and 3D Genome Browser. The functional roles of these genes during embryogenesis were

evaluated using FaceBase in mouse orofacial development and DECIPHER in humans.

The study identified five SNPs that may confer risk for NSCL/P, with rs7218002 exhibiting moderate linkage disequilibrium with rs4791774 and rs2944377. These two linked SNPs were reported in previous GWAS studies of NSCL/P according to the GWAS Catalogue.<sup>29</sup> By integrating various approaches, the authors found that rs7218002 could influence the gene expression of *NTN1*. Abnormal expression of *NTN1* has been implicated in the development of non-syndromic cleft lip with or without cleft palate in previous studies.<sup>27</sup> The present group generated *NTN1* knockout zebrafish models by CRISPR/Cas9 and observed relatively wider maxillo-mandibular fissures.<sup>30</sup> Complementary transcriptomic profiling was performed in embryonic chicks and demonstrated that *NTN1* was precisely expressed in the chick palate fissure margin during palate fusion.<sup>31</sup>

We identified rs835367, which lied in the promoter of *FGGY*, was associated with NSCL/P by two GWAS datasets. Our study also provided evidence that *FGGY* and *LINC01135* could be regulated by rs835367. The expression of *FGGY* decreased greatly from 10.5 to 14.5 days based on RNA-seq data of embryonic mouse tissues. Notably, previous meQTL analysis in 4,170 whole blood tissues suggested that rs835367 could regulate cg18108087, which is located near the promoter region of *FGGY* ( $P = 7.31E-24$ ).<sup>32</sup> Individuals with an *FGGY* deficiency were reported to exhibit an abnormal facial shape and bifid uvula according to DECIPHER. A bifid uvula is an anatomical variation that can be predictive of sub-mucous cleft palate, indicating that *FGGY* may contribute to the risk of NSCL/P to a certain degree.<sup>33</sup> Individuals with a *LINC01135* deficiency may exhibit abnormalities in facial features, thick lower lip vermilion and thick upper lip vermilion, suggesting that *LINC01135* may be a shared susceptibility factor for

NSCL/P. Taken together, these findings indicate that *FGGY* and *LINC01135* could be novel genes associated with NSCL/P.

## Conclusion

In the present study, a multi-omics approach was employed to provide novel insights into the aetiology of NSCL/P and identify five risk SNPs and three susceptibility genes for NSCL/P; however, further experimental studies are required to validate these results.

## Conflicts of interest

The authors declare no conflicts of interest related to this study.

## Author contribution

Drs Shu LOU and Jin YANG analysed the data and drafted the manuscript; Drs Gui Rong ZHU, Dan Dan LI and Lan MA performed the statistical analysis and revised the manuscript; Profs Lin WANG and Yong Chu PAN designed and directed the study and critically revised the manuscript.

(Received Jul 06, 2023; accepted Nov 02, 2023)

## References

- Mbuyi-Musanazayi S, Kayembe TJ, Kshal MK, et al. Non-syndromic cleft lip and/or cleft palate: Epidemiology and risk factors in Lubumbashi (DR Congo), a case-control study. *J Craniomaxillofac Surg* 2018;46:1051–1058.
- Hosseini HR, Kaklamanos EG, Athanasiou AE. Treatment outcomes of pre-surgical infant orthopedics in patients with non-syndromic cleft lip and/or palate: A systematic review and meta-analysis of randomized controlled trials. *PLoS One* 2017;12:e0181768.
- Wu MC, Kraft P, Epstein MP, et al. Powerful SNP-set analysis for case-control genome-wide association studies. *Am J Hum Genet* 2010;86:929–942.
- Horwitz T, Lam K, Chen Y, Xia Y, Liu C. A decade in psychiatric GWAS research. *Mol Psychiatry* 2019;24:378–389.
- Pathak GA, Zhou Z, Silzer TK, Barber RC, Phillips NR; Alzheimer's Disease Neuroimaging Initiative B, Prostate Cancer Cohort C, Alzheimer's Disease Genetics C. Two-stage Bayesian GWAS of 9576 individuals identifies SNP regions that are targeted by miRNAs inversely expressed in Alzheimer's and cancer. *Alzheimers Dement* 2020;16:162–177.
- Dogruluk T, Tsang YH, Espitia M, et al. Identification of variant-specific functions of PIK3CA by rapid phenotyping of rare mutations. *Cancer Res* 2015;75:5341–5354.
- Raimondi D, Passemiers A, Fariselli P, Moreau Y. Current cancer driver variant predictors learn to recognize driver genes instead of functional variants. *BMC Biol* 2021;19:3.
- Choy MK, Javierre BM, Williams SG, et al. Promoter interactome of human embryonic stem cell-derived cardiomyocytes connects GWAS regions to cardiac gene networks. *Nat Commun* 2018;9:2526.
- Schoenfelder S, Javierre BM, Furlan-Magaril M, Wingett SW, Fraser P. Promoter capture Hi-C: High-resolution, genome-wide profiling of promoter interactions. *J Vis Exp* 2018:57320.
- Zhang N, Mendieta-Esteban J, Magli A, et al. Muscle progenitor specification and myogenic differentiation are associated with changes in chromatin topology. *Nat Commun* 2020;11:6222.
- Sun F, Sun T, Kronenberg M, Tan X, Huang C, Carey MF. The Pol II preinitiation complex (PIC) influences Mediator binding but not promoter-enhancer looping. *Genes Dev* 2021;35:1175–1189.
- Montefiori LE, Sobreira DR, Sakabe NJ, et al. A promoter interaction map for cardiovascular disease genetics. *Elife* 2018;7:e35788.
- Li T, Ortiz-Fernández L, Andrés-León E, et al. Epigenomics and transcriptomics of systemic sclerosis CD4+ T cells reveal long-range dysregulation of key inflammatory pathways mediated by disease-associated susceptibility loci. *Genome Med* 2020;12:81.
- Jaini S, Lyubetskaya A, Gomes A, et al. Transcription factor binding site mapping Using ChIP-Seq. *Microbiol Spectr* 2014;2.
- Liu Y, Fu L, Kaufmann K, Chen D, Chen M. A practical guide for DNase-seq data analysis: From data management to common applications. *Brief Bioinform* 2019;20:1865–1877.
- Local A, Huang H, Albuquerque CP, et al. Identification of H3K4me1-associated proteins at mammalian enhancers. *Nat Genet* 2018;50:73–82.
- Zhang B, Zheng H, Huang B, et al. Allelic reprogramming of the histone modification H3K4me3 in early mammalian development. *Nature* 2016;537:553–557.
- Sun Y, Huang Y, Yin A, et al. Genome-wide association study identifies a new susceptibility locus for cleft lip with or without a cleft palate. *Nat Commun* 2015;6:6414.
- Wilderman A, VanOudenhove J, Kron J, Noonan JP, Cotney J. High-resolution epigenomic atlas of human embryonic craniofacial development. *Cell Rep* 2018;23:1581–1597.
- Lu Y, Quan C, Chen H, Bo X, Zhang C. 3DSNP: A database for linking human noncoding SNPs to their three-dimensional interacting genes. *Nucleic Acids Res* 2017;45:D643–D649.
- Wang Y, Song F, Zhang B, et al. The 3D Genome Browser: A web-based browser for visualizing 3D genome organization and long-range chromatin interactions. *Genome Biol* 2018;19:151.
- Swaminathan GJ, Bragin E, Chatzimichali EA, et al. DECIPHER: Web-based, community resource for clinical interpretation of rare variants in developmental disorders. *Hum Mol Genet* 2012;21:R37–R44.
- Purcell S, Neale B, Todd-Brown K, et al. PLINK: A tool set for whole-genome association and population-based linkage analyses. *Am J Hum Genet* 2007;81:559–575.
- Galesloot TE, van Steen K, Kiemeny LA, Janss LL, Vermeulen SH. A comparison of multivariate genome-wide association methods. *PLoS One* 2014;9:e95923.
- Pan Y, Han Y, Zhang H, et al. Association and cumulative effects of GWAS-identified genetic variants for nonsyndromic orofacial clefts in a Chinese population. *Environ Mol Mutagen* 2013;54:261–267.
- Li D, Hsu S, Purushotham D, Sears RL, Wang T. WashU Epigenome Browser update 2019. *Nucleic Acids Res* 2019;47:W158–W165.



27. Jiang S, Shi JY, Lin YS, et al. NTN1 gene was risk to non-syndromic cleft lip only among Han Chinese population. *Oral Dis* 2019;25:535-542.
28. Boyle AP, Hong EL, Hariharan M, et al. Annotation of functional variation in personal genomes using RegulomeDB. *Genome Res* 2012;22:1790-1797.
29. Buniello A, MacArthur JAL, Cerezo M, et al. The NHGRI-EBI GWAS Catalog of published genome-wide association studies, targeted arrays and summary statistics 2019. *Nucleic Acids Res* 2019;47:D1005-D1012.
30. Li D, Zhu G, Lou S, et al. The functional variant of NTN1 contributes to the risk of nonsyndromic cleft lip with or without cleft palate. *Eur J Hum Genet* 2020;28:453-460.
31. Hardy H, Prendergast JG, Patel A, et al. Detailed analysis of chick optic fissure closure reveals Netrin-1 as an essential mediator of epithelial fusion. *Elife* 2019;8:e43877.
32. Huan T, Joehanes R, Song C, et al. Genome-wide identification of DNA methylation QTLs in whole blood highlights pathways for cardiovascular disease. *Nat Commun* 2019;10:4267.
33. Feka P, Banon J, Leuchter I, La Scala GC. Prevalence of bifid uvula in primary school children. *Int J Pediatr Otorhinolaryngol* 2019;116:88-91.



# Do you already know our newsletter?

When you subscribe to our newsletter, you open the door to valuable insights and resources. Stay informed about the **latest publications**, embrace **continuing education**, plus, as a subscriber, you gain access to **special offers and promotions**, providing you with incredible value. Stay up to date in dentistry and dental technology with us! No obligation, free of charge, cancel at any time. Subscribe now.



[QUINT.LINK/LETTER](https://quint.link/letter)

# Knowledge Mapping of Cowden Syndrome: a Bibliometric Analysis

Qiao PENG<sup>1</sup>, Ning DUAN<sup>1</sup>, Xiang WANG<sup>1</sup>, Wen Mei WANG<sup>1</sup>

**Objective:** To provide a comprehensive overview of the current knowledge structure and research hotspots of Cowden syndrome via bibliometrics.

**Methods:** The articles and reviews related to Cowden syndrome were included from the Web of Science Core Collection (WoSCC) database. VOSviewer, CiteSpace and GraphPad Prism were used to conduct the bibliometric analysis.

**Results:** The number of papers focusing on Cowden syndrome was relatively low initially but increased rapidly from 1997 to 1999, and then maintained small-scale fluctuation. A total of 1,557 papers from 65 countries/regions and 1,762 institutions were identified. The USA was the most productive country, and Ohio State University was the most productive institution. In terms of the number of publications, Human Molecular Genetics ranked first, and Cancer Research was the most frequently cited journal. Eng was the most productive author, and Liaw was the most co-cited author. Phosphatase and tensin homologue (PTEN), germline mutations, gene, cancer, mutations, tumour suppressor gene and breast were high-frequency key words in this field.

**Conclusion:** This study was the first comprehensive bibliometric overview of the current state and development of Cowden disease. The mutation of PTEN and associated cancers, especially breast, thyroid and endometrial cancer, could be the focus of future research in this field.

**Keywords:** bibliometric analysis, Cowden syndrome, germline mutation, PTEN  
*Chin J Dent Res* 2024;27(1):75–82; doi: 10.3290/j.cjdr.b5136733

Cowden syndrome is a rare inherited condition in an autosomal dominant pattern, characterised by multiple hamartomas in different organs. It is also known as Cowden disease and multiple hamartoma syndrome, and is a rare multisystemic cancer predisposition disorder, with the breast, thyroid, endometrium and kidney being the most frequently involved organs.<sup>1</sup> Mucocutaneous lesions and macrocephaly are common clinical manifestations in patients with Cowden syndrome.<sup>2</sup>

Pathognomonic mucocutaneous lesions with verrucous manifestations are believed to exist in 100% of patients with Cowden syndrome by the age of 30. The verruca has different descriptions including “tricholemmomas”, “inverted follicular keratosis”, “oral papillomas” and “acral and palmoplantar keratosis” based on morphological appearances.<sup>1,3</sup> Cowden syndrome is inherited in an autosomal dominant pattern with mutations in the tumour suppressor gene phosphatase and tensin homologue (PTEN), which is categorised as a member of the spectrum of PTEN hamartoma tumour syndrome (PHTS).<sup>4</sup> The incidence of Cowden syndrome is reported to be approximately 1/200,000 individuals worldwide.<sup>5,6</sup>

Bibliometrics is a method of literature analysis that evaluates the output and status in a specific research field quantitatively and qualitatively, providing visual representations of the current research and playing an important role in the prediction of future developments.<sup>7,8</sup> Information about the publishing countries/regions, institutions, journals and co-cited journals, authors and co-authorship, citations, references, key-

1 Nanjing Stomatological Hospital, Affiliated Hospital of Medical School, Institute of Stomatology, Nanjing University, Nanjing, P.R. China.

**Corresponding author:** Dr Wen Mei WANG, Department of Oral Medicine, Nanjing Stomatological Hospital, Affiliated Hospital of Medical School, Nanjing University, #30 Zhongyang Road, Nanjing 210008, P.R. China. Tel: 86-25-83620362. Email: wenmei-wang@hotmail.com

This work was supported by the National Natural Science Foundation of China (82103304, 81870767) and the “2015” Cultivation Program for Reserve Talents for Academic Leaders of Nanjing Stomatological School, Medical School of Nanjing University.

words and the frontiers of research activities can be visualised by knowledge mapping.<sup>9,10</sup> CiteSpace and VOSviewer are commonly used software in data processing and analysis.

The application of bibliometric analysis is used widely in other fields nowadays, but to the best of the present authors' knowledge, so far, there is no relevant bibliometric analysis in the field of Cowden syndrome. Cowden syndrome, a rare disease with phenotypic variability, can easily lead to missed diagnosis and misdiagnosis. Its onset greatly affects patients' quality of life, and timely and accurate diagnosis and treatment are crucial to alleviate their pain. Thus, it is necessary to summarise and analyse the current research to help clinical physicians achieve a more comprehensive understanding of the disease. In this study, the present authors searched the Web of Science Core Collection (WoSCC) database to gather publications about Cowden syndrome from 1972 to 2023 and performed a bibliometric analysis to describe the current research progress and explore the hotspots and developmental trends in the field for future research.

## Materials and methods

### *Sources of data and search strategies*

The relevant publications related to Cowden syndrome were searched from the WoSCC database with the science citation index expanded (SCI-expanded). The search formula was (((TS = (Cowden syndrome)) OR TS = (Cowden disease)) OR TS = (multiple hamartoma syndrome)) OR TS = (face deformity-oral papillomosis syndrome). The type of publication was set to "articles" and "reviews", and the language of publication selected was English. All the data were downloaded within one day on 6 May 2023 and saved as a plain text file for further analysis.

### *Data collection and analysis*

Under these conditions, a total of 1,557 records were identified, composed of 1,258 articles and 299 reviews. Among the 1,258 articles, the top 10 medical fields in which these were found were Oncology (278), Genetics Heredity (254), Dermatology (148), Pathology (122), Biochemistry Molecular Biology (119), Clinical Neurology (101), Surgery (97), Endocrinology Metabolism (70), Cell Biology (66) and Gastroenterology Hepatology (64). The bibliometric analyses were performed using CiteSpace (version 6.2.R3), VOSviewer (version 1.6.11) and GraphPad Prism (version 9) to visualise the data.

## Results

### *Quantitative analysis of publications*

There was an overall upward trend in the number of publications released each year on Cowden syndrome from 1972 to 1999, then this continued to fluctuate within a narrow range from 2000 to 2023 (Fig 1). Specifically, the number of publications remained relatively low from 1972 to 1990, with a mean of 1.73 a year. From 1991 to 1996, a slow-growth rate was observed in the number of publications, with a mean of 10.33 a year. From 1997 to 1999, the number of relevant publications increased rapidly, with a mean of 57.33 a year. From 1999 to 2022, the number continued to fluctuate within a narrow range, with a mean of 56 a year.

### *Countries/regions and institutions*

A total of 65 countries/regions and 1,762 institutions were found to have contributed greatly to this field. We obtained a national collaboration diagram and observed close cooperation among the countries when the minimum number of documents published per country was set at 5 (Fig 2a). The top 10 countries/regions were the USA (831 publications, 53.37% of all articles), England (156, 10.02%), Japan (121, 7.77%), Italy (83, 5.33%), France (82, 5.27%), Canada (81, 5.20%), Germany (80, 5.13%), People's Republic of China (68, 4.37%), the Netherlands (48, 3.08%) and Spain (47, 2.77%) (Table 1 and Fig 2b).

The present authors set a minimum publication threshold of 10 documents per institution, which revealed the top 42 institutions and their collaborative relationship (Fig 2c). The size of the circles is proportional to the number of publications, and the lines between two circles indicate collaboration. Strong collaboration was found between Cleveland Clinic and Case Western Reserve University, and between Harvard University and the University of Cambridge. The top 10 institutions with the most publications are shown in Table 1 and Fig 2d. Ohio State University (108 publications, 6.94% of all articles) contributed the most publications, followed by Case Western Reserve University (103, 6.62%), Cleveland Clinic (100, 6.42%), Harvard University (74, 4.75%), the University of Cambridge (65, 4.17%), the National Cancer Institute (33, 2.12%), the University of Toronto (31, 1.99%), Dana-Farber Cancer Institute (26, 1.67%), Massachusetts General Hospital (26, 1.67%) and Mayo Clinic (26, 1.67%). Most of the top 10 institutions were based in the USA, except for the University of Cambridge (England) and the University of Toronto (Canada).

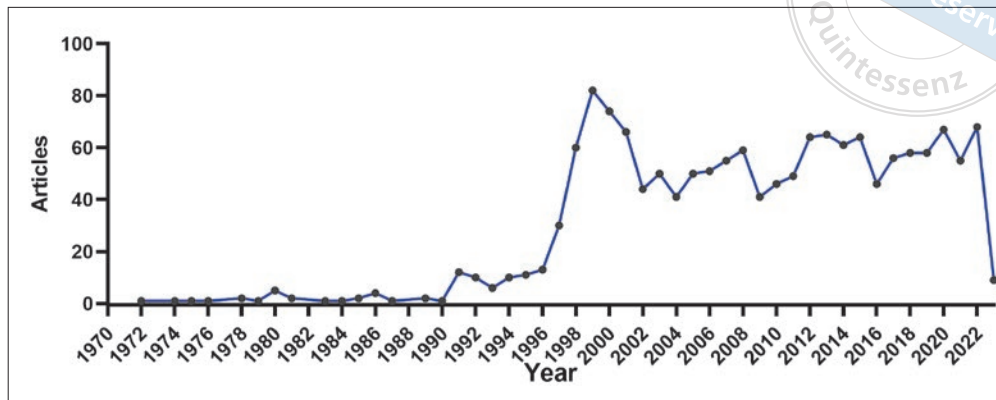


**Fig 1** Annual output and global trends in publications on Cowden syndrome from 1972 to 2023.

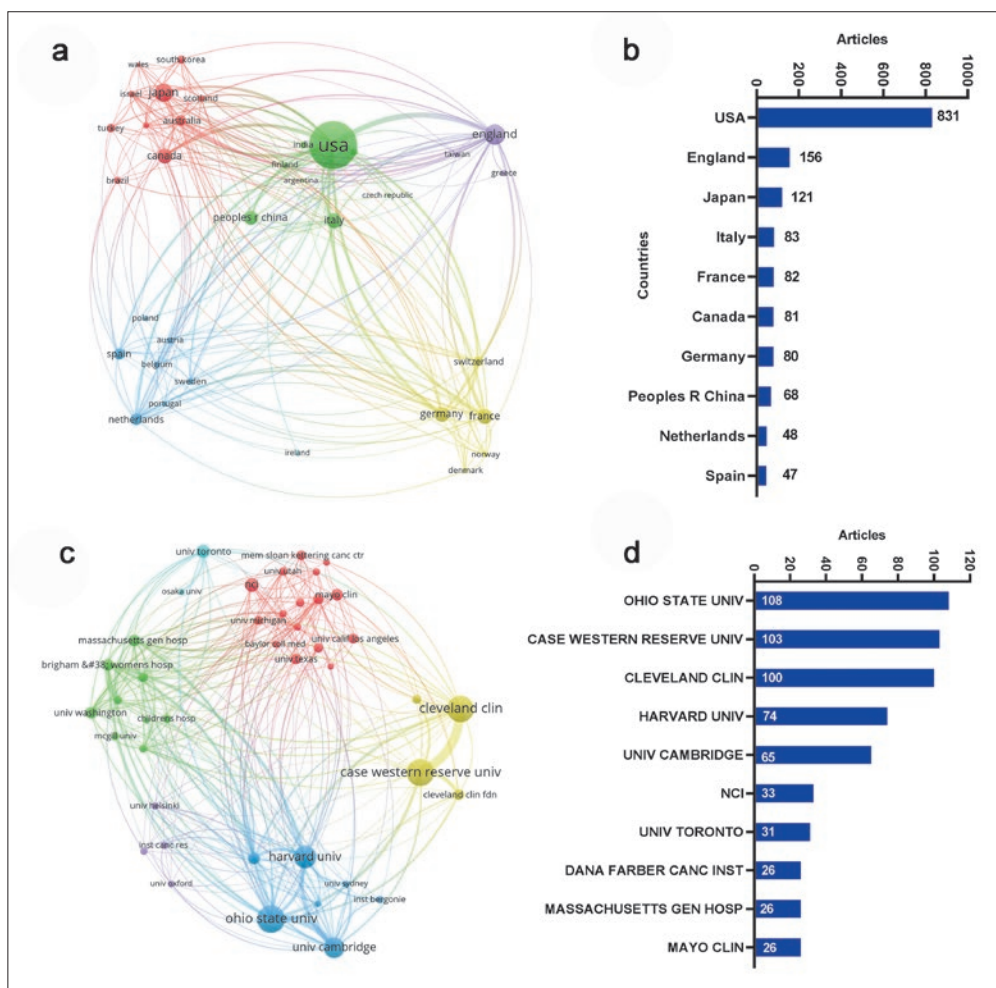


**Fig 2** Distribution of countries/regions and institutions having published articles on Cowden syndrome. Network map of countries/regions with more than five publications (a). Top 10 countries/regions with total articles (b). Network map of institutions with more than 10 publications (c). Top 10 institutions with total articles (d).

*Authors and co-cited authors*

A total of 7,415 authors were identified in the 1,557 papers. A strong collaborative network was found among these authors, contributing to this research area (Fig 3a). Eng showed strong cooperation with other researchers (Fig 3a) and was also the most productive author (190

articles), followed by Meter (27) and Zhou (20) (Fig 3b). The co-cited author is an author cited by more than two researchers simultaneously. The co-citation network is depicted in Fig 3c. The minimum number of citations was set at 100, and 44 of the total 26,322 co-cited authors met this threshold, with Liaw (204 times) ranking first, followed by Marsh (187) (Fig 3d).

**Table 1** The top 10 countries/regions and institution in publication.

Rank	Country	Total link strength	Count (%)	Institution	Total link strength	Count (%)
1	USA	377	831 (53.37)	Ohio State University (USA)	154	108 (6.94)
2	England	229	156 (10.02)	Case Western Reserve University (USA)	138	103 (6.62)
3	Japan	70	121 (7.77)	Cleveland Clinic (USA)	140	100 (6.42)
4	Italy	48	83 (5.33)	Harvard University (USA)	119	74 (4.75)
5	France	92	82 (5.27)	University of Cambridge (England)	139	65 (4.17)
6	Canada	72	81 (5.20)	National Cancer Institute (USA)	25	33 (2.12)
7	Germany	104	80 (5.13)	University of Toronto (Canada)	43	31 (1.99)
8	China	29	68 (4.37)	Dana-Farber Cancer Institute (USA)	90	26 (1.67)
9	Netherlands	81	48 (3.08)	Massachusetts General Hospital (USA)	67	26 (1.67)
10	Spain	31	47 (2.77)	Mayo Clinic (USA)	16	26 (1.67)

### Journals and co-cited journals

The 1,557 publications were found to have been published in 596 journals. With the minimum number of documents per journal set at 10, 28 journals met the threshold (Fig 4a). Among the top 10 journals, the Journal of the American Academy of Dermatology showed the highest impact factor (IF) of 15.487, followed by Cancer Research (IF<sub>2021</sub> = 13.312) and Proceedings of the National Academy of Sciences of the United States of America (IF<sub>2021</sub> = 12.779) (Table 2).

The present authors also identified 4,642 co-cited journals. When the minimum number of articles per journal was set at 200, 64 journals met the threshold (Fig 4b). The circle size is directly proportional to the number of documents, and the three colours represent three different clusters. The higher the frequency of co-citation, the greater the impact of the journal. Cancer Research was cited most frequently (3,456 citations), followed by Nature Genetics (2,920) and Journal of Medical Genetics (2,059) (Fig 4b and Table 2). Among the top 10 journals, the journal with the highest IF was Cell (IF<sub>2021</sub> = 66.85), followed by Science (IF<sub>2021</sub> = 68.832) and Nature Genetics (IF<sub>2021</sub> = 41.376). The majority of the top 10 journals and all the top 10 co-cited journals were distributed in Q1 according to the journal citation reports in 2022 (Table 2).

The dual map overlay of journals displayed the distribution of relationships between journals and cited journals, which were shown on the left and right, respectively. This citation path displayed the linkage of the different research fields. There were two main paths. The orange path suggested that papers published in molecular/biology/immunology journals commonly cited papers in molecular/biology/genetics journals, and the green path suggested that papers published in medicine/medical/clinical journals commonly cited papers in molecular/biology/genetics journals and in health/nursing/medicine journals (Fig 4c). The top 25

cited journals with the strongest citation bursts are presented in Fig 4d, among which Genetics in Medicine (strength 38.6) showed outbreak citations most recently from 2012 to 2023, followed by PLOS One (strength 33.88) and Nature Reviews Molecular Cell Biology (strength 19.02).

### Keywords

Keywords are, to some degree, the reflection of research hotspots. Thus, they help scholars to understand the research frontiers in specific fields. In this study, there were 4,927 keywords overall, 51 of which were used in more than 40 publications. In Fig 5a, the size of circles positively correlated with keyword frequency and the thickness of the line of the circle positively correlated with the strength of relationships between keywords. Germline pten, individuals and pten hamartoma tumour syndrome were newly emerging keywords. Cowden syndrome, cowden disease, pten, germline mutations, gene, cancer, mutations, diseases, tumour-suppressor gene and breast were top 10 keywords with a high frequency from 146 to 484 (Fig 5b).

A category cluster analysis was performed to generalise the keywords in the co-citation network to understand the frontier directions. These keywords were divided into nine clusters, including oncology (#0), biochemistry and molecular biology (#1), genetics and heredity (#2), clinical neurology (#3), obstetrics and gynaecology (#4), public, environmental and occupational health (#5), radiology, nuclear medicine and medical imaging (#6), surgery (#7) and paediatrics (#8) (Fig 5c). The top 20 keywords with the strongest citation burst are shown in Fig 5d. The most intense keyword was cowden syndrome (27.77), followed by cowden-disease (24.06) and hamartoma tumour syndrome (17.05). The keyword with the longest burst time was cowden syndrome, which lasted 11 years from 2012 to 2023. More meaningfully, the keywords cowden syndrome,

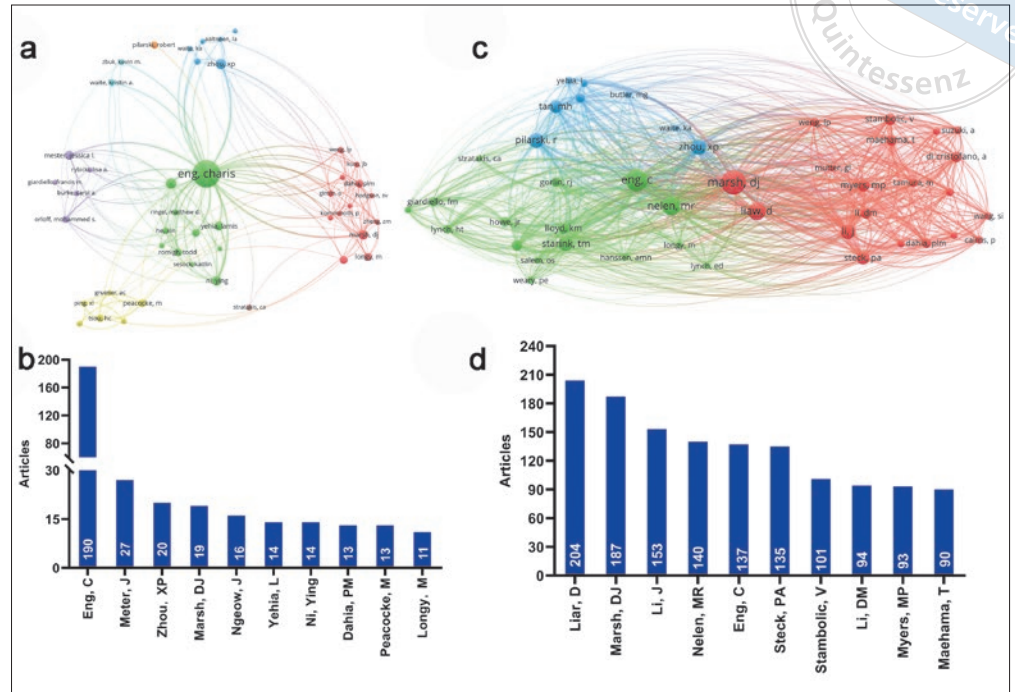


**Fig 3** Analysis of authors and co-cited authors on Cowden syndrome. Network map of co-authorship between authors with more than five articles (a). Top 10 authors with total articles (b). Network map of co-authorship between co-cited authors with more than 100 articles (c). Top 10 co-cited authors with total articles (d).

**Table 2** The top 10 most productive journals and co-cited journals.

Rank	Journal	Number of articles	IF (2021)	JCR (2021)	Co-cited journal	Number of citations	IF (2021)	JCR (2021)
1	Human Molecular Genetics	36	5.121	Q1	Cancer Research	3,456	13.312	Q1
2	Cancer Research	34	13.312	Q1	Nature Genetics	2,920	41.376	Q1
3	Oncogene	31	8.756	Q1	Journal of Medical Genetics	2,059	5.945	Q1
4	Journal of Medical Genetics	30	5.945	Q1	American Journal of Human Genetics	1,921	11.043	Q1
5	American Journal of Human Genetics	23	11.043	Q1	Proceedings of the National Academy of Sciences of the United States of America	1,873	12.779	Q1
6	American Journal of Medical Genetics Part A	22	2.578	Q3	Science	1,662	63.832	Q1
7	Journal of the American Academy of Dermatology	21	15.487	Q1	Human Molecular Genetics	1,652	5.121	Q1
8	American Journal of Dermatopathology	19	1.319	Q4	Cell	1,318	66.85	Q1
9	Journal of Cutaneous Pathology	19	1.458	Q4	Oncogene	1,191	8.756	Q1
10	Proceedings of the National Academy of Sciences of the United States of America	16	12.779	Q1	Stem Cell Research & Therapy	1,122	8.088	Q1

JCR, journal citation reports; Q, quartile in category.

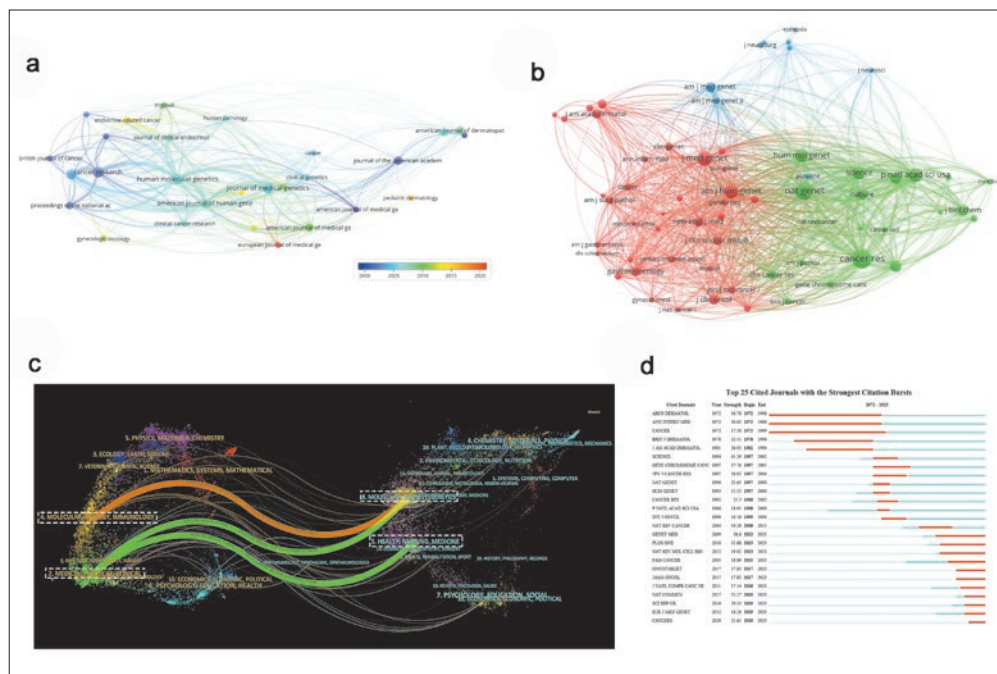


**Fig 4** Analysis of journals and co-cited journals on Cowden syndrome. Network map of journals with more than 10 documents (a). Network map of journals with a minimum of 200 citations of a source (b). Dual map overlay of journals related to research on Cowden syndrome. The coloured paths indicate the relationships between journals on the left and cited journals on the right (c). The top 25 cited journals with the strongest citation bursts (d).

germline pten, pten hamartoma tumour syndrome and mutations had outbreak citations most recently, which indicated that the link between cowden syndrome and pten might be a research hotspot in the future.

**Discussion**

This bibliometric analysis research draws scientific knowledge maps of Cowden syndrome from 1972 to 2023. In the past 20 years, the number of publications has continued to fluctuate with a narrow range, indicating the stable output in this field. The USA was the most productive country (831 publications), accounting for more than half of all the articles. The USA also showed the strongest total link strength (377), followed by England (229), suggesting close cooperation with other countries. This situation was to some degree beneficial to the advancement of the research field. From the perspective of study institutions, all the top four institutions were in the USA, namely Ohio State University, Case Western Reserve University, Cleveland Clinic and Harvard University. Taken together, these results suggest that the USA plays a leading role and influences the direction of research in this field.

With regard to authors, Eng made the largest contribution with 190 publications, far more than the next most prolific authors, Meter (27) and Zhou (20). Eng was also in the top five co-cited authors. These data indicate their great contributions to the progression of this field. In 1997, Eng published the article “Germline

mutations of the *PTEN* gene in Cowden disease, an inherited breast and thyroid cancer syndrome” in Nature Genetics, which showed the highest number of citations.<sup>11</sup> In this study, they identified the mutations of the *PTEN* gene in patients with Cowden syndrome for the first time, and proved that *PTEN* acted as a tumour suppressor gene in the germline and played a role in organising the relationship between different cell types within an organ during development.

Analysis of the top 10 most productive journals showed 70% ranked Q1 and 4 journals had an IF greater than 10, including Cancer Research (IF<sub>2021</sub> = 13.312), American Journal of Human Genetics (IF<sub>2021</sub> = 11.043), Journal of the American Academy of Dermatology (IF<sub>2021</sub> = 15.487) and Proceedings of the National Academy of Science of the United States of America (IF<sub>2021</sub> = 12.779). The results indicated that literature on Cowden syndrome is mainly published in high IF journals, and this literature was vital to reflect the overview of research in the field. It is worth noting that the literature about Cowden syndrome in its initial stage from 1972 to 1998 were mainly published in skin-related journals, such as Archives of Dermatological Research, British Journal of Dermatology and Journal of the American Academy of Dermatology. This might be due to the fact that cutaneous and mucosal lesions are the most consistent findings in patients with Cowden disease. More recently, literature has been mainly published in gene-related journals, such as Genes, Chromosomes & Cancer, Nature Genetics and Human Genetics, because



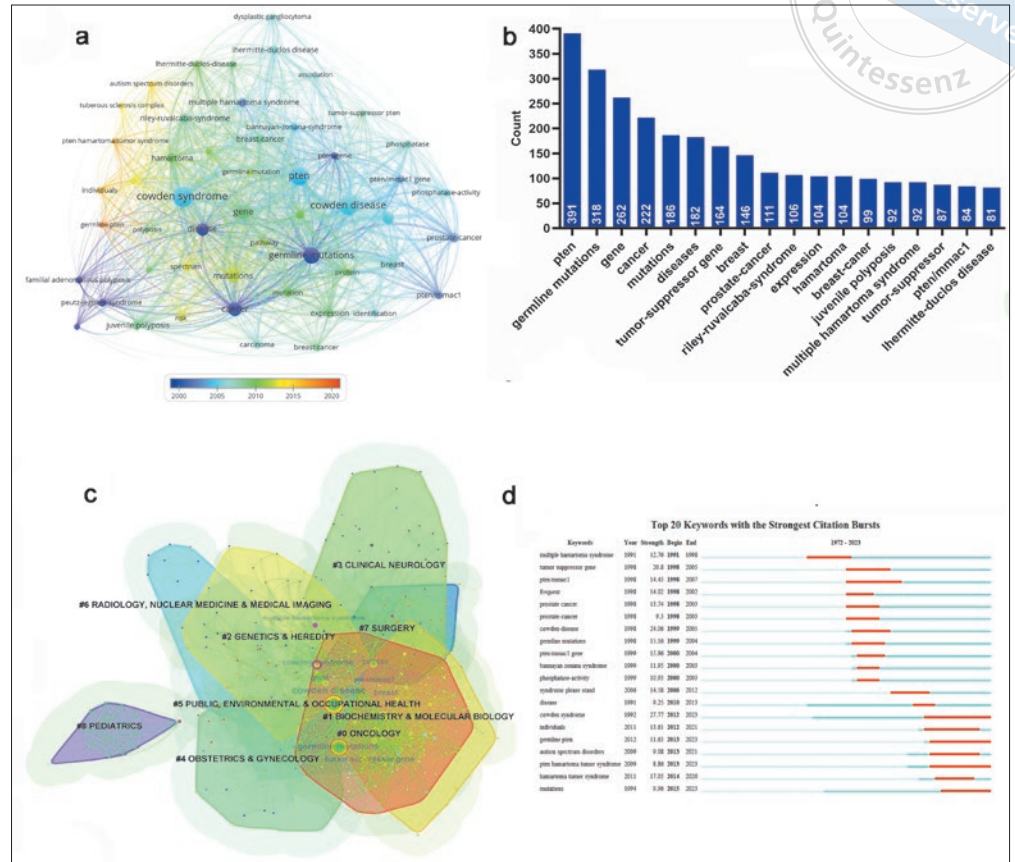


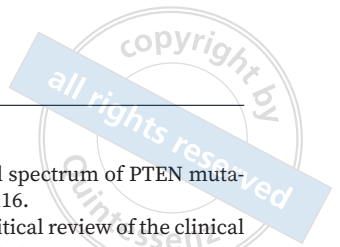
**Fig 5** Analysis of keywords on Cowden syndrome. Distribution of keywords according to average publication year (blue, earlier; red, later) (a). Mapping of keywords more than 80 counts (b). Category cluster analysis of keywords (c). Top 20 keywords with the strongest citation bursts (d).

in 1997, Eng found that it was the *PTEN* mutations that caused this syndrome.<sup>11</sup> The mutation of *PTEN*, a tumour suppressor gene, greatly elevated the incidence of tumours in different organs, which has led researchers to focus mainly on Cowden syndrome/*PTEN* hamartoma tumour syndrome. Thus, the literature nowadays is published mainly in cancer-related journals, such as *Familial Cancer*, *Oncotarget*, *JAMA Oncology*, *Journal of the National Comprehensive Cancer Network* and *Cancers*.

Keywords reflect the central theme of publications and could provide core information of research frontiers. Initially, researchers were mainly focused on the clinical syndrome with keyword “multiple hamartoma syndrome” in strong citation from 1991 to 1998. With the identification of *PTEN* mutation in Cowden syndrome by Eng in 1997, keywords then shifted to “tumour suppressor gene”, “peten/mma1” and “germline mutations”, which resulted in research on Cowden syndrome being mainly focused on its pathogenesis. In addition, germline mutations, cancer and breast are also closely associated with Cowden syndrome. The majority of patients with Cowden syndrome (80%) had germline mutations in the *PTEN* gene.<sup>12</sup> The *PTEN* gene located

on chromosome 10q22-23 is a tumour suppressor via its lipid phosphatase activity negatively regulating the phosphatidylinositol 3-kinase (PI3K) pathway, inhibiting cell survival.<sup>13,14</sup> The loss/reduction of function of *PTEN* results in activation of the PI3K/AKT/mTOR pathway, producing the opposite effect, including cell growth, protein synthesis and cell cycle progression, and ultimately manifesting as tumours. Germline mutations in the gene of *SDHB*, *SDHD* have been found for the minority of patients with Cowden syndrome without *PTEN* mutation.<sup>15</sup>

Cowden syndrome is part of PHTS, a disorder that primarily involves hamartomatous growths and cancers in multiple organs, especially the breast and thyroid.<sup>16,17</sup> Nearly 85.2% of the affected female individuals could suffer from breast cancer, with age at diagnosis ranging from 38 to 46 years.<sup>18</sup> The primary histological manifestation of breast cancer in Cowden syndrome is ductal adenocarcinoma uniquely surrounded by dense hyalinised collagen.<sup>19</sup> Thyroid carcinoma is the second most common cancer in Cowden syndrome.<sup>20</sup> The literature reports that the lifetime risk of thyroid cancer in Cowden syndrome is up to 38%, with the mean age for diagnosis at 32 years old.<sup>21</sup> Histopathologically,



follicular or papillary cancer are common types of thyroid cancer in Cowden syndrome.<sup>22</sup> Apart from breast and thyroid cancer, the risk of endometrial, renal and glial malignancies in patients with Cowden syndrome appears to be increased, but has not been quantified.

Several shortcomings still remain in this study. For example, all the relevant publications were only downloaded from the WOS database and the latest publications after 6 May 2023 were not included, which might have led to some relevant publications being missed out and thus make the analysed publications incomplete.

## Conclusion

The present authors first performed a systematical bibliometric analysis of research on Cowden syndrome to help scholars visualise the current research status. Although there are certain limitations to the present study, it still offers value, providing researchers with an intuitive and specific understanding of the field and helping to track research trends in a timely manner.

## Conflicts of interest

The authors declare no conflicts of interest related to this study.

## Author contribution

Dr Qiao PENG contributed to the study design, data collection, analysis and manuscript draft; Drs Ning DUAN, Xiang WANG and Wen Mei WANG contributed to the revision of the manuscript. All authors read and approved the final manuscript.

(Received Jun 27, 2023; accepted Nov 27, 2023)

## References

- Magaña M, Landeta-Sa AP, López-Flores Y. Cowden disease: A review. *Am J Dermatopathol* 2022;44:705–717.
- Lim A, Ngeow J. The skin in Cowden syndrome. *Front Med (Lausanne)* 2021;8:658842.
- Hammerschmidt M, Lourenço SV, Nico MMS. A clinicopathological study of the oral lesions of Cowden disease. *J Oral Pathol Med* 2017;46:637–643.
- Yehia L, Keel E, Eng C. The clinical spectrum of PTEN mutations. *Annu Rev Med* 2020;71:103–116.
- Pilarski R. Cowden syndrome: A critical review of the clinical literature. *J Genet Couns* 2009;18:13–27.
- Gammon A, Jaspersen K, Champine M. Genetic basis of Cowden syndrome and its implications for clinical practice and risk management. *Appl Clin Genet* 2016;9:83–92.
- Peng C, Kuang L, Zhao J, Ross AE, Wang Z, Ciolino JB. Bibliometric and visualized analysis of ocular drug delivery from 2001 to 2020. *J Control Release* 2022;345:625–645.
- Ge Y, Chao T, Sun J, Liu W, Chen Y, Wang C. Frontiers and hot-spots evolution in psycho-cardiology: A bibliometric analysis from 2004 to 2022. *Curr Probl Cardiol* 2022;47:101361.
- Ahmad P, Slots J. A bibliometric analysis of periodontology. *Periodontology* 2000 2021;85:237–240.
- Liu W, Wu L, Zhang Y, Shi L, Yang X. Bibliometric analysis of research trends and characteristics of oral potentially malignant disorders. *Clin Oral Investig* 2020;24:447–454.
- Liaw D, Marsh DJ, Li J, et al. Germline mutations of the PTEN gene in Cowden disease, an inherited breast and thyroid cancer syndrome. *Nat Genet* 1997;16:64–67.
- Pilarski R, Burt R, Kohlman W, Pho L, Shannon KM, Swisher E. Cowden syndrome and the PTEN hamartoma tumor syndrome: systematic review and revised diagnostic criteria. *J Natl Cancer Inst* 2013;105:1607–1616.
- Myers MP, Stolarov JP, Eng C, et al. P-TEN, the tumor suppressor from human chromosome 10q23, is a dual-specificity phosphatase. *Proc Natl Acad Sci U S A* 1997;94:9052–9057.
- Squarize CH, Castilho RM, Gutkind JS. Chemoprevention and treatment of experimental Cowden's disease by mTOR inhibition with rapamycin. *Cancer Res* 2008;68:7066–7072.
- Ni Y, Zbuk KM, Sadler T, et al. Germline mutations and variants in the succinate dehydrogenase genes in Cowden and Cowden-like syndromes. *Am J Hum Genet* 2008;83:261–268.
- Dragoo DD, Taher A, Wong VK, et al. PTEN hamartoma tumor syndrome/Cowden syndrome: Genomics, oncogenesis, and imaging review for associated lesions and malignancy. *Cancers (Basel)* 2021;13:3120.
- Gustafson S, Zbuk KM, Scacheri C, Eng C. Cowden syndrome. *Semin Oncol* 2007;34:428–434.
- Tan MH, Mester JL, Ngeow J, Rybicki LA, Orloff MS, Eng C. Lifetime cancer risks in individuals with germline PTEN mutations. *Clin Cancer Res* 2012;18:400–407.
- Farooq A, Walker LJ, Bowling J, Audisio RA. Cowden syndrome. *Cancer Treat Rev* 2010;36:577–583.
- Hall JE, Abdollahian DJ, Sinard RJ. Thyroid disease associated with Cowden syndrome: A meta-analysis. *Head Neck* 2013;35:1189–1194.
- Smerdel MP, Skytte AB, Jelsig AM, Ebbelhøj E, Stochholm K. Revised Danish guidelines for the cancer surveillance of patients with Cowden Syndrome. *Eur J Med Genet* 2020;63:103873.
- Szabo Yamashita T, Baky FJ, McKenzie TJ, et al. Occurrence and natural history of thyroid cancer in patients with Cowden syndrome. *Eur Thyroid J* 2020;9:243–246.

# Novel *PTCH1* Mutation Causes Gorlin-Goltz Syndrome

Hai Tang YUE<sup>1</sup>, Hai Yan CAO<sup>1</sup>, Miao HE<sup>1</sup>

**Objective:** To analyse the aetiology and pathogenesis of Gorlin-Goltz syndrome (GS; also known as nevoid basal cell carcinoma syndrome [NBCCS] or basal cell nevus syndrome [BCNS]) in a Chinese family.

**Methods:** Whole-exome sequencing (WES) was performed on genomic DNA samples from the subjects in a family, followed by the investigation of pathogenesis via bioinformatic approaches and conformational analysis.

**Results:** A novel heterozygous non-frameshift deletion patched 1 (*PTCH1*) [NM\_000264:c.3512\_3526del (p.1171\_1176del)] was identified by WES and further validated by Sanger sequencing. Bioinformatic and conformational analysis showed that the mutation caused altered *PTCH1* protein structure, which may be related to functional abnormalities.

**Conclusion:** This study expands the mutation spectrum of *PTCH1* in GS and facilitates the early diagnosis and screening of GS. *PTCH1* [c.3512\_3526del (p.1171\_1176del)] may cause structural abnormalities and functional disabilities, leading to GS in families.

**Keywords:** Gorlin-Goltz syndrome, mutation, nevoid basal cell carcinoma syndrome, *PTCH1*, whole-exome sequencing

*Chin J Dent Res* 2024;27(1):83–88; doi: 10.3290/j.cjdr.b5128601

Gorlin-Goltz syndrome (GS, OMIM 109400), also known as nevoid basal cell carcinoma syndrome (NBCCS), is an ecto-mesodermic polydysplasia that affects multiple organs.<sup>1</sup> It is characterised by multiple basal cell carcinomas (BCCs), multiple odontogenic keratocysts (OKCs), calcification of the falx cerebri, vertebral and rib anomalies, and palmar and/or plantar pits.<sup>2</sup> Other findings, such as other skeletal abnormalities and cleft lip with or without cleft palate, may be noted.<sup>3</sup>

GS has been reported to be related with mutations in patched 1 (*PTCH1*), suppressor of fused (*SUFU*) and *PTCH2*.<sup>4</sup> Among them, *PTCH1*, which is located on chromosome 9q22.3, is the major pathogenic gene involved in GS. It consists of 24 exons encoding *PTCH1* protein with 1447 amino acids. *PTCH1* is a 12-pass transmembrane protein that negatively regulates the Hedgehog (HH) signalling pathway.<sup>5</sup> In the unliganded state, *PTCH1* maintains Smoothed (SMO) in an unphosphorylated state, contributing to its endocytosis and degradation. Upon binding of HH ligands, the repression of *PTCH1* on SMO is relieved, leaving SMO hyperphosphorylated, capable of activating glioma-associated oncogene homologue 1 transcription factors from *SUFU* (encoded by *SUFU*) inhibition to translocate into the nucleus and stimulate the targeted gene expression.<sup>6,7</sup> The HH signalling pathway is fundamental to proliferation and differentiation during embryonic patterning and development and homeostasis. Dysregulation of this pathway leads to a wide variety of developmental deficiencies, including holoprosencephaly, brachydactyly, non-syndromic colobomatous microphthalmia and solitary median maxillary central incisor syndrome.<sup>8-12</sup> It has also been

<sup>1</sup> State Key Laboratory of Oral & Maxillofacial Reconstruction and Regeneration, Key Laboratory of Oral Biomedicine Ministry of Education, Hubei Key Laboratory of Stomatology, School & Hospital of Stomatology, Wuhan University, Wuhan, P.R. China.

**Corresponding author:** Dr Miao HE, State Key Laboratory of Oral & Maxillofacial Reconstruction and Regeneration, Key Laboratory of Oral Biomedicine Ministry of Education, Hubei Key Laboratory of Stomatology, School & Hospital of Stomatology, Wuhan University, #237 Luoyu Road, Wuhan 430079, P.R. China. Tel: 86-27-87686211. Email: hemiao@whu.edu.cn

This work was funded by the National Natural Science Foundation of China (Grant no. U22A20313 and 81970904).

involved in tumours, including BCCs, medulloblastoma, rhabdomyosarcoma, glioblastoma and breast, ovarian, prostate, colon, stomach, pancreas and lung cancers, making it a potential target for therapy.<sup>13,14</sup>

To date, over 600 *PTCH1* mutations have been identified in patients with GS, most of which are nonsense, small indels and missense, according to the Human Gene Mutation Database (<https://www.hgmd.cf.ac.uk/ac/index.php>).

In the present study, a novel heterozygous non-frameshift deletion *PTCH1* [NM\_000264: c.3512\_3526del (p.1171\_1176del)] was analysed in a 13-year-old proband and his mother with GS. The clinicopathologic characteristics of the patients and the pathogenic mechanism of the mutant were further explored.

## Materials and methods

### *Pedigree analysis and clinical diagnosis*

This study included a 13-year-old Chinese boy who presented to the Department of Oral and Maxillofacial-Head and Neck Oncology, School and Hospital of Stomatology at Wuhan University. The diagnosis of GS was based on the most frequently used criteria proposed by Kimonis et al.<sup>15</sup> The proband's 38-year-old mother had a history of surgery for OKCs and was also enrolled in the study. The study was approved by the ethics committee of the School and Hospital of Stomatology, Wuhan University (2017-09). Peripheral blood samples and clinical data were collected after obtaining informed consent.

### *Genomic DNA extraction and whole-exome sequencing (WES)*

Genomic DNA was extracted from the peripheral venous blood of the subjects using the improved salting-out method. DNA samples that passed the quality detection analyses were analysed using WES at Genesky Biotechnologies in Shanghai, China. The exons were targeted from the genomic DNA with the SureSelectXT Human All Exon Kit (Agilent, Santa Clara, CA, USA), and then the Illumina HiSeq X-TEN platform (Illumina, San Diego, CA, USA) was used for sequencing. The readings were aligned with the hg38 human genome assembly using a Burrows-Wheeler aligner. Polymerase chain reaction (PCR) duplicates were removed, and the quality of alignments was evaluated in terms of mean coverage depth, effective base, effective reads and 90×-120× coverage ratio using Picard software. The Genome Analysis Toolkit was used to analyse indels and single-nucleotide variants.<sup>16</sup>

ANNOVAR was employed for functional annotation with the KEGG pathway, OMIM, Gene Ontology, Mutation Taster, PolyPhen-2, SIFT and the Exome Aggregation Consortium browsers. The detailed and comprehensive variant analysis was performed in accordance with the workflow previously described.<sup>17-20</sup> Candidate variants were amplified by PCR and confirmed by Sanger sequencing. The PCR primers were designed as follows: forward: 5'-TGAATGTGAACTGCGGTTGG-3' and reverse: 5'-CTCAAAGCTCAAAGCACGGT-3'. PCR was performed at 95°C for 3 minutes (one cycle), 33 cycles at 95°C for 15 seconds, 55°C for 15 seconds and 72°C for 45 seconds, followed by a final extension at 72°C for 5 minutes. DNA from the proband's father and healthy individuals were used as controls. PCR products were sequenced by the forward and reverse primers at Tsingke Biotechnology (Wuhan, China).

### *Conservation and pathogenicity analysis*

The *Ptch1* sequences from HUMAN to ZEBRAFISH were downloaded from ENSEMBL. Multiple-species alignment analysis was performed using Clustal Omega (<https://www.ebi.ac.uk/Tools/msa/clustalo/>). Pathogenicity prediction of variants was conducted using the prediction tools mentioned above, in accordance with the 2015 American College of Medical Genetics and Genomics (ACMG) guidelines.

### *Structural bioinformatic analysis of PTCH1 p.1171\_1176del*

A diagram schematically displaying the distribution of mutations was generated using Domain Graph (version 2.0). 3D analysis of structural changes in the *PTCH1* mutant was performed using SWISS-MODEL (<https://swissmodel.expasy.org/>) and viewed on the basis of PyMOL 2.1.0.

## Results

### *Clinical findings and mutation screening*

The proband was born of a nonconsanguineous marriage (Fig 1a). There was no significant medical history of abnormal birth weight or premature birth. His diagnosis of GS was established based on OKCs of the jaw proven by histology (Figs 1b and c), palmar and plantar pits (Figs 1d and e), a first-degree relative with GS syndrome (three major criteria), microform cleft lip (Fig 1f) and left hand preaxial polydactyl (post-operation, Fig 1g,

**Fig 1** Clinical analyses of patients in the family. Pedigree analysis. Squares, male; circles, female; filled symbols, affected subjects; question mark, unconfirmed diagnosis; symbols with slant lines, the deceased; arrow, proband (**a**). Panoramic radiograph of the proband (**b**). Histopathological examination of the lesion revealing typical characteristics of OKCs in the proband (**c**). Palmar and plantar pits in the proband (**d and e**). Microform cleft lip in the proband (**f**). Post-preaxial polydactyl resection of the left hand in the proband (**g**). Radiograph of the skull showing cerebral falx calcification in the proband's mother (**h**).



two minor criteria). The proband underwent polydactyl resection at the age of 2 years. The proband's mother had no family history of consanguinity and was diagnosed with GS based on OKCs of the jaw proven by histology, bilamellar calcification of the falx cerebri (Fig 1h) and a first-degree relative with GS syndrome. She underwent surgical excision 6 years previously, and histological examination confirmed OKCs in her right maxilla.

WES identified a heterozygous non-frameshift deletion *PTCH1* [c.3512\_3526del (p.1171\_1176del)], which was further confirmed by Sanger sequencing (Fig 2a). This mutation was not reported in relevant databases, including 1000g, ExAC 03, esp6500, gnomAD\_genome, Hrcr1, Kaviar, dbSNP or HUABIAO project (<https://www.biosino.org/wepd/>). No pathogenic variants were found in other genes related to GS. *PTCH1* (c.3512\_3526del) resulted in the deletion of five amino acids (Pro, Val, Leu, Leu and Ser) adjacent to the C-terminal transmembrane region of *PTCH1*.

#### Conservation analysis and mutation pathogenicity

Conservative analysis using Clustal Omega showed that amino acids LPVLLS located at the mutant sites were highly conservative among many species (Fig 2b), indicating their important functions in phylogeny. In accordance with the guidelines of the 2015 ACMG, *PTCH1* [c.3512\_3526del (p.1171\_1176del)] was predicted to be likely pathogenic (PM2 + PM4 + PP1 + PP3 + PP4).

#### Characteristics of *PTCH1* mutant

Structural analysis was performed to investigate the effect of *PTCH1* p.1171\_1176del on protein function. In comparison with wild-type *PTCH1*, the mutation p.1171\_1176del was located adjacent to a transmembrane helix region, which starts at position 1149 and ends at position 1171, and caused a distinct conformation change. The conformation of the helix at residue 1167-1178 was converted into a loop in mutant p.1171\_1176del (Fig 3), which may lead to protein malfunction.

#### Discussion

GS is a rare autosomal-dominant condition, affecting 1/31,000 to 1/256,000 people in different regions, with no significant difference in morbidity between male and female patients.<sup>2,21,22</sup> It is an ecto-mesodermal dysplasia characterised by a range of clinical manifestations that affect multiple organs. Researchers have reported several diagnostic criteria, and those proposed by Kimonis et al<sup>15</sup> are the most commonly used. According to these, the diagnosis is made on the basis of either two major criteria or one major criterion together with two minor criteria listed below. The major criteria are BCCs, OKCs, palmar or plantar pit, bilamellar calcified falx cerebri, rib abnormalities and a first-degree relative with GS. The minor criteria are macrocephaly, congenital malformation, other skeletal abnormalities,

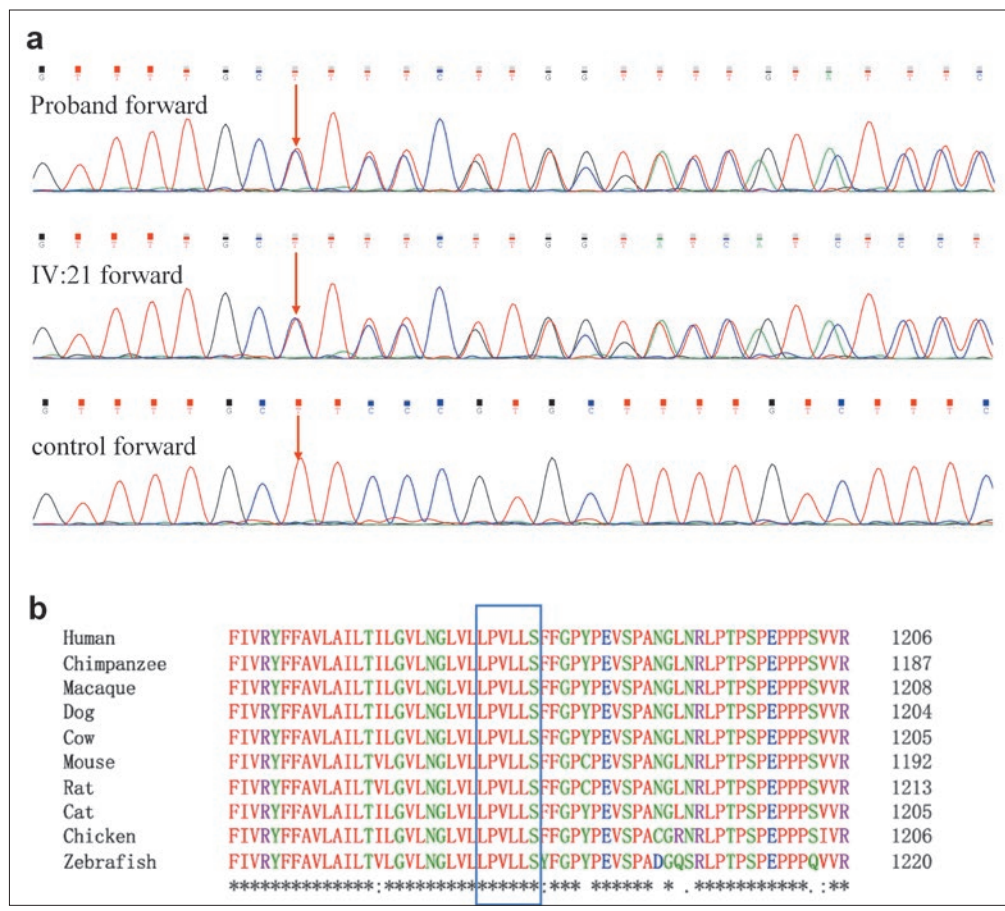


**Fig 2** Mutation and conservation analysis. Sanger sequence chromatograms revealing a novel heterozygous non-frameshift deletion *PTCH1* [c.3512\_3526del (p.1171\_1176del)] in the proband and the mother (IV:21) (a). Conservation analysis indicating p.1171\_1176 is well conserved across orthologues (b). Numbers at the end of each line denote the position of the rightmost residue.

radiological abnormalities, ovarian fibroma and medulloblastomas.<sup>2</sup>

In this study, the proband met three major criteria (histologically verified OKCs of the jaw, palmar and plantar pit, and a first-degree relative with GS), and two minor criteria (microform cleft lip and left hand preaxial polydactyl). The proband’s mother met three major criteria (histologically verified OKCs of the jaw, bilamellar calcification of the falx cerebri and a first-degree relative with GS). The proband’s mother reported another family member with GS.

The diagnosis of GS was further supported genetically by molecular analysis revealing a non-frameshift deletion *PTCH1* (c.3512\_3526del) in the proband and his mother. The deletion corresponded to codons 1171-1176 and resulted in p.1171\_1176del. *PTCH1* p.1171\_1176del probably contributes to impaired structure and function. As a ligand binding component in HH signalling pathway, structural abnormalities and dysfunctions in *PTCH1* may cause dysregulation of this pathway, leading to the GS in this family. Thus far, over 600 *PTCH1* mutations have been reported in GS. The *PTCH1* mutations identified in GS are mostly nonsense, small indels

and missense, followed by splice site mutations and large indels, which are distributed evenly along exons 2-21, with no obvious hotspots.<sup>23</sup> No obvious genotype-phenotype associations have been observed in patients with GS6. Mice heterozygous for *Ptc1* mutant showed developmental abnormalities, including hindlimb defects and medulloblastomas, which recapitulated disease phenotypes seen in patients with GS.<sup>24</sup> In addition to the major causative gene *PTCH1*, *SUFU* and *PTCH2* mutations have been reported in GS. *SUFU* is a negative regulator of the HH pathway, and loss-of-function mutations in *SUFU* were discovered in GS resulting from aberrant regulation of the HH signalling cascade.<sup>25</sup> *PTCH2* consists of 22 exons encoding transmembrane protein *PTCH2* with 1203 amino acids, which is highly homologous to the *PTCH1* product. *PTCH1* and *PTCH2* have closely associated transmembrane modules related to sterol-sensing domains that affect cholesterol modification of HH ligands.<sup>26</sup> Research indicated that *PTCH2* mutations caused inactivation of *PTCH2* inhibitory function in the HH pathway.<sup>27</sup> These studies indicated that any perturbations in the HH pathway can cause developmental abnormalities and

neoplastic lesions similar to those caused by *PTCH1* mutations. Further research is needed to uncover novel mutant genes in other components of the HH pathway in GS patients with no identified mutation. Accurate genetic diagnosis can facilitate early treatment, prevent further damage to health and improve quality of life in patients with GS.

### Conclusion

A novel heterozygous non-frameshift deletion *PTCH1* [c.3512\_3526del (p.1171\_1176del)] was identified in a family with GS. This study expands the mutation spectrum of *PTCH1* in GS. The mutation caused a distinct conformational change in *PTCH1*, which may cause protein malfunction and lead to GS in the family.

### Acknowledgements

The authors thank all the subjects for their participation in this study.

### Conflicts of interest

The authors declare no conflicts of interest related to this study.

### Author contribution

Dr Hai Tang YUE contributed to the conception, methodology, analysis and draft; Dr Hai Yan CAO contributed to the methodology, analysis and literature; Dr Miao HE contributed to the study design and supervision, manuscript draft and revision.

(Received Aug 21, 2023; accepted Nov 09, 2023)

### References

- Bakaeen G, Rajab LD, Sawair FA, Hamdan MA, Dallal ND. Nevroid basal cell carcinoma syndrome: A review of the literature and a report of a case. *Int J Paediatr Dent* 2004;14:279–287.
- Onodera S, Nakamura Y, Azuma T. Gorlin syndrome: Recent advances in genetic testing and molecular and cellular biological research. *Int J Mol Sci* 2020;21:7559.
- Lambrech JT, Kreuzsch T. Examine your orofacial cleft patients for Gorlin-Goltz syndrome. *Cleft Palate Craniofac J* 1997;34:342–350.
- Matsudate Y, Naruto T, Hayashi Y, et al. Targeted exome sequencing and chromosomal microarray for the molecular diagnosis of nevoid basal cell carcinoma syndrome. *J Dermatol Sci* 2017;86:206–211.
- Doheny D, Manore SG, Wong GL, Lo HW. Hedgehog signaling and truncated *GLI1* in cancer. *Cells* 2020;9:2114.
- Gianferante DM, Rotunno M, Dean M, et al. Whole-exome sequencing of nevoid basal cell carcinoma syndrome families and review of Human Gene Mutation Database *PTCH1* mutation data. *Mol Genet Genomic Med* 2018;6:1168–1180.
- Cherry AL, Finta C, Karlström M, et al. Structural basis of SUFU-GLI interaction in human Hedgehog signalling regulation. *Acta Crystallogr D Biol Crystallogr* 2013;69:2563–2579.
- Ming JE, Kaupas ME, Roessler E, et al. Mutations in *PATCHED-1*, the receptor for *SONIC HEDGEHOG*, are associated with holoprosencephaly. *Hum Genet* 2002;110:297–301.
- Roessler E, Belloni E, Gaudenz K, et al. Mutations in the human *Sonic Hedgehog* gene cause holoprosencephaly. *Nat Genet* 1996;14:357–360.
- McCready ME, Sweeney E, Fryer AE, et al. A novel mutation in the *IHH* gene causes brachydactyly type A1: A 95-year-old mystery resolved. *Hum Genet* 2002;111:368–375.
- Schimmenti LA, de la Cruz J, Lewis RA, et al. Novel mutation in *sonic hedgehog* in non-syndromic colobomatous microphthalmia. *Am J Med Genet A* 2003;116A:215–221.

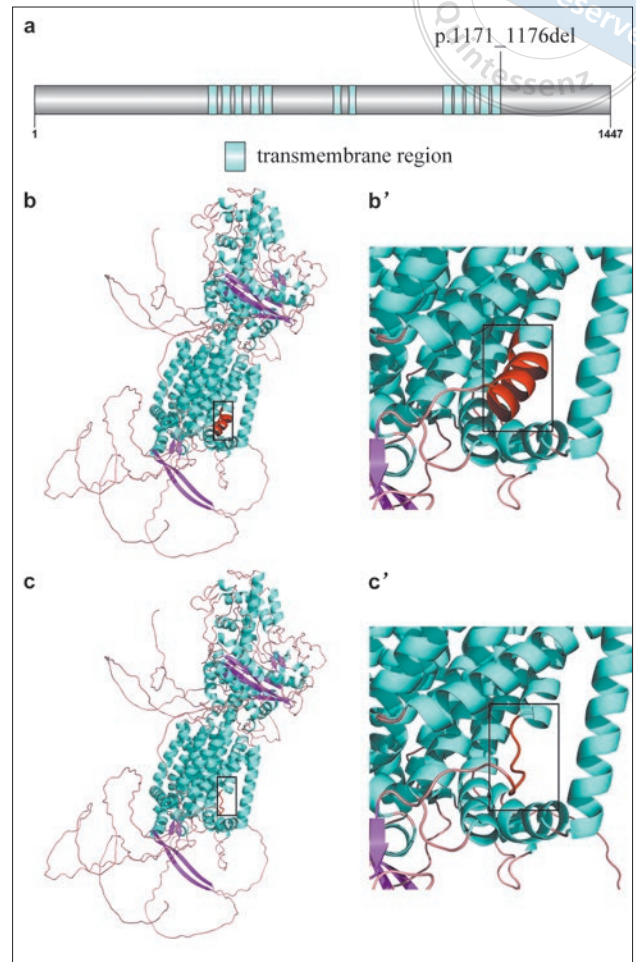


**Fig 3** Schematic presentation of the distribution of mutation (a) and structural analysis revealing conformational changes in *PTCH1* p.1171\_1176del (c and c') in comparison with wild-type *PTCH1* (b and b').

12. Garavelli L, Zanacca C, Caselli G, et al. Solitary median maxillary central incisor syndrome: Clinical case with a novel mutation of sonic hedgehog. *Am J Med Genet A* 2004;127A:93–95.
13. Atwood SX, Chang AL, Oro AE. Hedgehog pathway inhibition and the race against tumor evolution. *J Cell Biol* 2012;199:193–197.
14. Wang Y, Chen H, Jiao X, et al. PTCH1 mutation promotes anti-tumor immunity and the response to immune checkpoint inhibitors in colorectal cancer patients. *Cancer Immunol Immunother* 2022;71:111–120.
15. Kimonis VE, Goldstein AM, Pastakia B, et al. Clinical manifestations in 105 persons with nevoid basal cell carcinoma syndrome. *Am J Med Genet* 1997;69:299–308.
16. Tang S, Wang X, Li W, et al. Biallelic mutations in CFAP43 and CFAP44 cause male infertility with multiple morphological abnormalities of the sperm flagella. *Am J Hum Genet* 2017;100:854–864.
17. Han P, Wei G, Cai K, et al. Identification and functional characterization of mutations in LPL gene causing severe hypertriglyceridaemia and acute pancreatitis. *J Cell Mol Med* 2020;24:1286–1299.
18. Zhang R, Chen S, Han P, et al. Whole exome sequencing identified a homozygous novel variant in CEP290 gene causes Meckel syndrome. *J Cell Mol Med* 2020;24:1906–1916.
19. Dai Y, Liang S, Dong X, et al. Whole exome sequencing identified a novel DAG1 mutation in a patient with rare, mild and late age of onset muscular dystrophy-dystroglycanopathy. *J Cell Mol Med* 2019;23:811–818.
20. Zheng Y, Xu J, Liang S, Lin D, Banerjee S. Whole exome sequencing identified a novel heterozygous mutation in HMBS gene in a Chinese patient with acute intermittent porphyria with rare type of mild anemia. *Front Genet* 2018;9:129.
21. Endo M, Fujii K, Sugita K, Saito K, Kohno Y, Miyashita T. Nationwide survey of nevoid basal cell carcinoma syndrome in Japan revealing the low frequency of basal cell carcinoma. *Am J Med Genet A* 2012;158A:351–357.
22. Lo Muzio L. Nevoid basal cell carcinoma syndrome (Gorlin syndrome). *Orphanet J Rare Dis* 2008;3:32.
23. Ikemoto Y, Takayama Y, Fujii K, et al. Somatic mosaicism containing double mutations in PTCH1 revealed by generation of induced pluripotent stem cells from nevoid basal cell carcinoma syndrome. *J Med Genet* 2017;54:579–584.
24. Goodrich LV, Milenković L, Higgins KM, Scott MP. Altered neural cell fates and medulloblastoma in mouse patched mutants. *Science* 1997;277:1109–1113.
25. Barakat MT, Humke EW, Scott MP. Learning from Jekyll to control Hyde: Hedgehog signaling in development and cancer. *Trends Mol Med* 2010;16:337–348.
26. Fleet AJ, Hamel PA. The protein-specific activities of the transmembrane modules of Ptch1 and Ptch2 are determined by their adjacent protein domains. *J Biol Chem* 2018;293:16583–16595.
27. Fan Z, Li J, Du J, et al. A missense mutation in PTCH2 underlies dominantly inherited NBCCS in a Chinese family. *J Med Genet* 2008;45:303–308.



# Clinical and Genetic Analysis of Multiple Idiopathic Cervical Root Resorption

Yu Meng WANG<sup>1</sup>, Wen Yan RUAN<sup>1</sup>, Dan Dan CHI<sup>1</sup>, Xiao Hong DUAN<sup>1</sup>

**Objective:** To explore the genetic background and clinical phenotypes of multiple idiopathic cervical root resorption (MICRR) in a Chinese family.

**Methods:** The proband and his three family members were clinically examined and had radiographs taken with a radiovisiography (RVG) system and CBCT to define the diagnosis of MICRR. Genomic DNA (gDNA) was extracted from peripheral blood samples of the patient, his father, mother and younger sister for whole exome sequencing (WES). The pathogenicity of rare variants with minor allele frequency (MAF) less than 0.005 were analysed following possible inheritance patterns, predicted results from 12 software programs, the American College of Medical Genetics (ACMG) 2015 criteria, and information from ClinVar, OMIM and HGMD databases as well as gene function.

**Results:** The proband presented the typical MICRR phenotypes such as thin cervical pulp wall and apple core-like lesions in radiographs. Following the recessive inheritance pattern, WES analysis identified *SHROOM2*, *SYTL5*, *MAGED1* and *FLNA* with a higher chance of causing MICRR. Four genes with compound heterozygous variants and another 27 genes with *de novo* variants either in autosomal-dominant or autosomal-recessive pattern were also found to have the potential pathogenicity.

**Conclusion:** A total of 35 novel potential pathogenic genes were found to be associated with MICRR from a Chinese family through WES. The new genetic background of MICRR may be helpful for clinical and molecular diagnosis.

**Keywords:** *de novo* variants, multiple idiopathic cervical root resorption, pathogenic variant filtering, whole-exome sequencing

*Chin J Dent Res* 2024;27(1):89–99; doi: 10.3290/j.cjdr.b5128703

Root resorption is the loss of dentine, cementum and/or alveolar bone due to physiological or pathological reasons, which can occur anywhere in the tooth root. Physiological tooth absorption occurs in primary dentition and leads to exfoliation of permanent teeth; however,

root resorption in permanent teeth is largely pathological. Tooth root resorption can be divided into internal resorption and external resorption, based on position and how they progress. The former involves resorption from the pulp cavity to the root surface, whereas the latter involves resorption from the root surface to the dentine and pulp cavity. External tooth root resorption can be further divided into root surface resorption, inflammatory resorption, external cervical root resorption (ECR), replacement resorption and transient apical resorption.<sup>1</sup>

ECR is a rare and aggressive type of external root resorption, which is also known as aggressive root cervical resorption and invasive cervical external resorption. It usually occurs at the cemento-enamel junction (CEJ) of the tooth neck, and gradually destroys the cementum, dentine and pulp tissue from the root surface. As resorption progresses, it further invades the coronal direction to damage the enamel and the

<sup>1</sup> State Key Laboratory of Oral & Maxillofacial Reconstruction and Regeneration, National Clinical Research Center for Oral Disease, Shaanxi Key laboratory of Stomatology, Department of Oral Biology & Clinic of Oral Rare Diseases and Genetic Diseases, School of Stomatology, the Fourth Military Medical University, Xi'an, P.R. China.

**Corresponding author:** Dr Xiaohong Duan, Department of Oral Biology, School of Stomatology, The Fourth Military Medical University, Xi'an 710000, P.R. China. Tel: 86-29 84776174. Email: xhduan@fmmu.edu.cn

This study was funded by the National Natural Science Foundation of China (82370907, 81974145, 81771052), Key R & D plan of Shaanxi Province (2021ZDLSF02-13) and Key Project of National Oral Diseases Clinical Medicine Research Center (LCA202013, LCC202201).

root direction to damage the tooth root. The aetiology of ECR is very complex, including local factors such as orthodontic treatment, trauma, apical or periodontal inflammation, internal bleaching, tooth replantation, periodontal surgery, tumours, cysts, bruxism and impacted teeth, and systematic factors such as Paget disease, Goltz syndrome, Papillon-Lefèvre syndrome, Turner syndrome, Stevens-Johnson syndrome, hyperparathyroidism, hypoparathyroidism, kidney disease, liver disease and bad eating habits.<sup>2,3</sup> In the absence of an identifiable cause, ECR at the CEJ is termed idiopathic cervical root resorption (ICRR), and when more than three teeth are affected, ICRR is termed multiple idiopathic cervical tooth resorption (MICRR).

MICRR is an extremely rare and aggressive form of external root resorption, and current understanding of its aetiology is very limited due to the small number of cases. Possible causes of MICRR include viral infections such as pertussis<sup>4</sup>, hepatitis B<sup>5</sup> and feline viruses<sup>6</sup>; hormone changes such as thyroid hormone and progesterone<sup>7</sup>; and drug-related factors such as chemotherapy drugs and osteoporosis treatment drugs.<sup>7</sup> Most researchers believe that the occurrence of MICRR is associated with enhanced activity of osteoclasts and odontoclasts.<sup>7</sup> In 2010, Yu et al<sup>8</sup> reported a case of MICRR involving 31 permanent teeth including an impacted third molar, which indicates oral exposure and microbial infection may not be causative factors of MICRR. In addition, clinicopathological analysis of affected teeth in MICRR has shown that connective tissue in areas of resorption contains fibroblasts and fibrocytes and osteoclast-like giant cells, but without the clear presence of inflammatory cells, which indicates MICRR may be a non-inflammatory disorder but involve osteoclast-related tooth resorption.<sup>7,9,10</sup>

Family analysis of MICRR showed that three of the four affected family members had the heterozygous missense mutation (c.1219 G > A) in the *IRF8* gene. Further functional studies suggest that this mutation may inhibit the expression of IRF8 and weaken IRF8 protein function, thereby inducing osteoclastogenesis at the transcription level and increasing the risk of root resorption. These studies add to the evidence that suggests abnormal osteoclast activity could lead to the occurrence of MICRR.<sup>11</sup> Besides the above pedigree analysis, most other genetic analyses on MICRR were based on sporadic cases<sup>8,12-15</sup>, and the present authors found that most cases were sporadic except for *IRF8* mutation related MICRR in the pedigree study. The disease-causing genes in these sporadic MICRR cases were lacked solid genetic evidence in other cases. Meanwhile, these reports did not disclose the details of

the screening process of pathogenic genes, so it is difficult to determine the true harmfulness of these genes.

The present authors recruited a man with MICRR and with no other medical conditions from a Chinese family to explore possible pathogenic genes. We performed whole-exome sequencing (WES) in the pedigree, selected the genetic variants through strictly standardised steps and considered all the possible candidate pathogenic variants. Finally, we found that 35 novel variants of the proband may theoretically associate with MICRR. This study provides a new direction for the genetic aetiology of MICRR and the mechanism of its exploration.

## Patients and methods

### *Clinical information*

The proband was a 19-year-old man who was referred to the Clinic of Oral Rare Diseases and Genetic Diseases, School of Stomatology at the Fourth Military Medical University, Xi'an, China, with the chief complaint of tooth pain when chewing. He had undergone extraction of multiple teeth in his right maxilla in 2021 due to serious cervical tooth resorption that caused tooth crown fracture and tooth roots without restoration. In the 2 years before he presented to the clinic, the remaining teeth gradually developed similar symptom of cervical resorption, which resulted in tooth pain when chewing. The patient was examined and evaluated with radiographic detection, such as radiovisiography (RVG) and 3D CBCT reconstruction, to evaluate the degree of resorption and the number of affected teeth. Professional oral clinical examinations were also performed on all members of the patient's family. The study was approved by the Ethics Committee of the School of Stomatology, Fourth Military Medical University. Informed consent was obtained from each family member and from healthy controls.

### *WES*

The proband and three unaffected members of his family (I-1, I-2, II-1, II-2) included in the study underwent clinical WES. Peripheral blood samples were collected from all family members. Genomic DNA (gDNA) was extracted using QIAamp DNA Blood Mini kit (Qiagen, Valencia, CA, USA) according to the manufacturer's instructions. WES involving exome capture, high-throughput sequencing and common filtering was performed using Annoroad Gene Technology (Annoroad,

Beijing, China).<sup>16</sup> Alignment of the sequence reads, indexing of the reference genome, variant calling and annotation were carried out using the SureSelect Human All Exon V6 system (Agilent, Santa Clara, CA, USA). Valid sequencing data of WES were mapped to the human reference genome using the Maq program. The number of the human genome reference assembly was hg19.

### Bioinformatic analysis

Rare variants referred to those with an MAF less than 0.005<sup>17</sup>, which were chosen from the following databases: Exome Aggregation Consortium (<http://exac.broadinstitute.org/>), Exome Variant Server (<http://evs.gs.washington.edu/EVS>), 1000 Genomes Project (<http://browser.1000genomes.org>), dbSNP (<http://www.ncbi.nlm.nih.gov/snp>), dbVar (<http://www.ncbi.nlm.nih.gov/dbvar>), GnomAD (<http://www.gnomad-sg.org/>), NHLBI GO Exome Sequencing Project (<https://evs.gs.washington.edu/E>), Hapmap ([www.hapmap.org](http://www.hapmap.org)) and Scripps Welllderly Genome Resource (<https://www.scripps.org/>).

Following the American College of Medical Genetics (ACMG) 2015 criteria, twelve pathogenicity prediction software programs were used to predict the variants to be damaging, deleterious and disease-causing. These included the SIFT < 0.05, the MutationAssessor > 1.938, the FATHMM < -1.5, the GERP++ > 3, the PhyloP > 2.5, the PhastCons > 0.6, the PolyPhen2\_HDIV (Probably damaging  $\geq 0.957$ , possibly damaging  $0.453 \leq \text{pp2\_hdiv} \leq 0.956$ ; benign  $\leq 0.452$ ) and the PolyPhen2\_HVAR (Probably damaging  $\geq 0.909$ , possibly damaging  $0.447 \leq \text{pp2\_hdiv} \leq 0.909$ ; benign  $\leq 0.446$ ). The pathogenic variants predicted from more than two software programs were selected and analysed. Variants without patients' hereditary source were excluded. The types of variants included missense, frameshift, inframe insertion, inframe deletion, splice region, splice donor, splice acceptor, stop gained and stop lost. The predicted pathogenicity of the gene variants, especially on those genes associated with tooth resorption and development, bone development, saliva functions, odontoclasts and osteoclastogenesis, were analysed. All the variants were also verified on ClinVar, OMIM and HGMD databases.

The present authors also considered compound heterozygous variants that met the condition above. The compound heterozygous variant was found when the proband had more than two variation sites in the same gene and the different sites were inherited from his father and mother separately. If the proband's sister did not have the same compound heterozygous variants as him, the compound heterozygous variant was reserved.

Since the patient's parents and sister did not have similar phenotypes, the mode of inheritance in the family was considered autosomal recessive or X-linked inheritance. The de novo variants were also considered from the possible four inheritance patterns (Fig 1).

## Results

### Clinical findings

Upon initial diagnosis of MICRR in February 2022, the intraoral examination of the patient showed that multiple teeth (12 to 17) in the right maxilla were missing due to having been extracted previously. In addition, multiple tooth defects were detected using a dental probe in the cervical region under the CEJ, including teeth 25, 26, 27, 28, 33, 34, 35, 36, 42, 43, 44, 45, 46 and 47. Sensitivity during cervical probing of teeth was observed in teeth 42 to 47. Dental percussion examination revealed slight discomfort in teeth 34, 44, 45 and 46. Transient pulp sensitivity occurred in teeth 34, 44, 45 and 46 during cold pulp sensitivity testing and was accompanied by radiating pain in tooth 34. Furthermore, electric pulp testing of tooth 34 demonstrated a negative response. Teeth 42 to 47 had undergone gingivectomy and surgical crown lengthening to expose the subgingival defect before images were taken, so the lesion area of multiple teeth is visible and located supragingivally (Fig 2).

After further radiographic examination, many low-density areas were found in the cervical regions of teeth 26, 27, 28, 33, 34, 35, 36, 42, 43, 44, 45, 46 and 47. Teeth 45, 46, 47 exhibited severe cervical resorption and radiographs revealed typical apple core-like lesions at the CEJ. This severe resorption almost resulted in the separation of the crown and root of the tooth, which is the typical X-ray finding of MICRR (Fig 2). 3D reconstruction showed worm-eaten lacunar-like resorption on the inner surfaces of crowns and cervical resorptive regions of the affected teeth. Tooth 25 had received root canal treatment, and teeth 38 and 48 were mesially impacted. None of the remaining teeth were affected by secondary apical periodontitis.

Family history revealed that other family members had no similar phenotypes of cervical root resorption. No other identifiable cause was found for the proband such as orthodontic treatment, trauma, apical lesions or tumors or cysts. The proband had no direct or indirect contact with cats, no history of allergy to drugs/food, no habit of eating sweets or acidic foods, and no history of hereditary diseases in his family or any other systemic disease. The proband had not received radio-

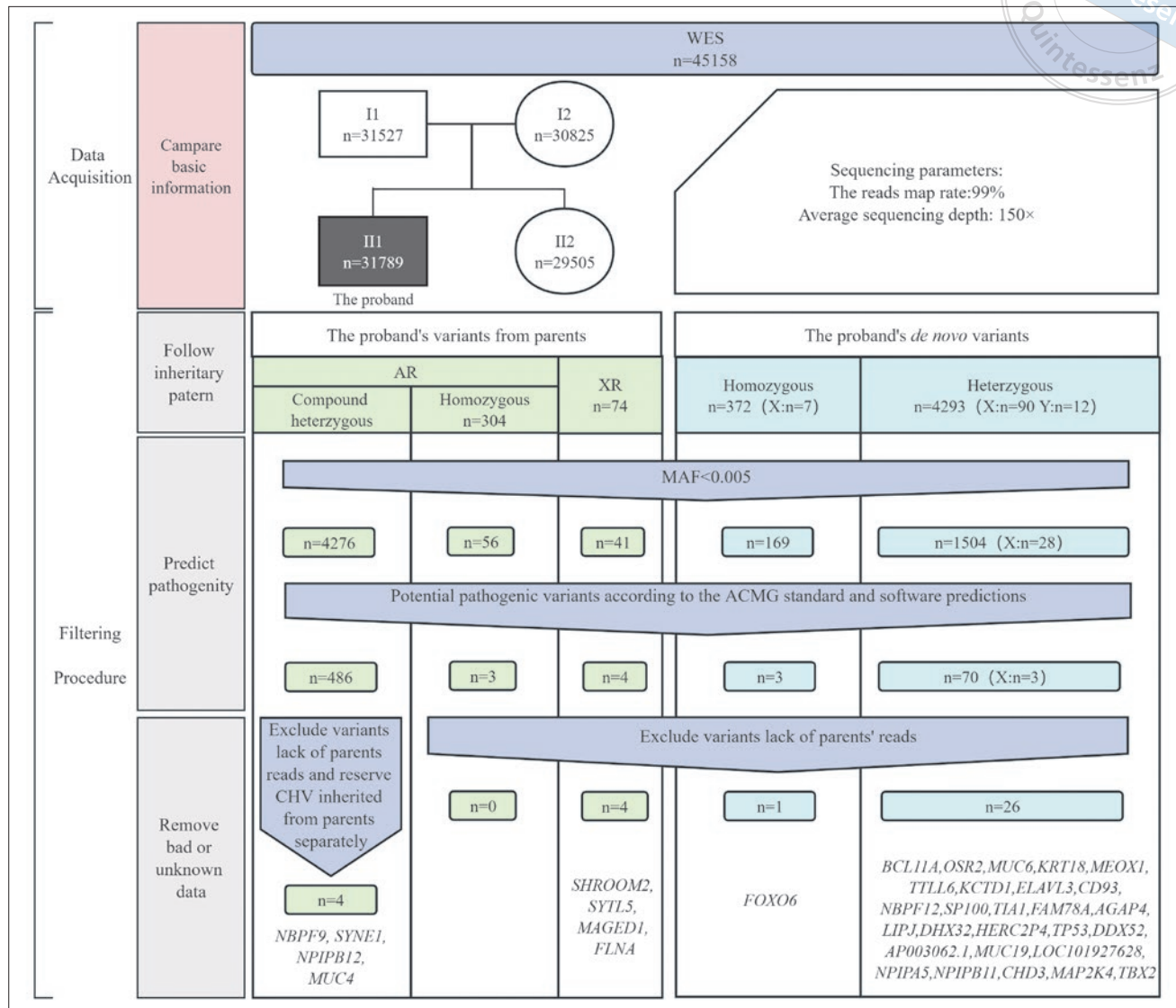


**Fig 1** The variants filtering process. AR, autosomal recessive; CHR, chromosome; CHV, compound heterozygous variants; MAF, minor allele frequency; underline, variants fit condition  $0.005 < MAF < 0.01$ ; n, number of variants; XR, X-chromosome recessive.

therapy and had good function of the salivary glands and good oral hygiene. These characteristics helped to rule out the possibility of rampant caries.

### Genetic findings

A mean coverage of > 150× for 99% of the target regions reads map indicated that the reference sequence selection was accurate and sufficient for the analysis. A total of 45,158 variants were observed among the family members, including 31,789 variants in the proband, 31,527 in his father, 30,825 in his mother and 29,505 in his sister. Based on to the inheritance pattern, 74 variants fitting X-linked recessive inheritance and 304 homozy-

gous variants fitting autosomal recessive inheritance were screened out. Additionally, there were 372 *de novo* homozygous variants in the autosomal genes and seven variants in X-linked genes. Furthermore, there were 4,293 *de novo* heterozygous variants in the autosomal genes, 90 in X-linked genes and 12 in the Y-linked genes. After initial exclusion of variants with an MAF > 0.005 in public databases (ExAC, EVS, 1KGP, dbSNP, dbVar, GnomAD, ESP, Hapmap, Welllderly and BGI internal database) further analysis, considering the variation type and software prediction, enabled a significant reduction of the candidate variants. Further evaluation considering the variant consequence, severity, and duplication of genes and unknown reads resulted in the identification

**Table 1** Pathogenic genes fitted X-linked inheritance pattern in the transmitted ways.

CHR	Variation type	Inheritance	Gene	mRNA	Protein	Annotation
X	Missense	XR	<i>SHROOM2</i>	ENST00000380913.3:c.1549C > T	p.Arg517Cys	Nasopharyngeal carcinoma
X	Missense	XR	<i>SYTL5</i>	NM_001163335.1:c.1409A > G	p.Asn470Ser	NF-κB
X	Missense	XR	<i>MAGED1</i>	NM_001005332.1:c.865G > C	p.Gly289Arg	Osteoclastogenesis; mineralisation of rEMSCs
X	Missense	XR	<i>FLNA</i>	ENST00000369856.3:c.227C > T	p.Thr76Ile	Osteogenic and osteoclastic differentiation

CHR, chromosome; rEMSCs, rat ectomesenchymal stem cells; XR, X-chromosome recessive.



**Fig 2** Intraoral image and radiographs. Black arrows indicate the cervical root resorption. 3D reconstruction showed worm-eaten lacunar resorptions in the inner surfaces of crowns and cervical resorptive regions. Red arrows in the digital radiovisiography show typical apple core-like change in the affected teeth. Teeth 42 to 47 had undergone gingivectomy and surgical crown lengthening to expose the subgingival defect before the pictures were taken.

of 35 variants (Fig 1). These were divided into 8 genes with transmitted variants and 27 genes with non-transmitted variants (de novo variants) based on the source of variation.

#### Transmitted variants

Based on X chromosomal recessive modes, variants in four genes (*SHROOM2*, *SYTL5*, *MAGED1* and *FLNA*) were identified (Table 1). No homozygous variant was found in accordance with the typical autosomal recessive inheritance mode (Fig 1). The proband had four genes (*NBPF9*, *SYNE1*, *NPIP12* and *MUC4*) with compound heterozygous variants. We filtered a compound heterozygous vari-

ant c.1077C > A/c.349 + 2T > C (p.Pro360Thr/\*) in *NBPF9*, c.14868C > A/c.599G > A (p.Ser4956Arg/p.Gly200Asp) in *SYNE1* and c.1074\_1085dupTCCACCCTCAGC/c.1838C > A (p.Pro359\_Ala362dup/p.Pro613His) in *NPIP12* (Table 2). The proband also had a compound heterozygous variant with six variation sites, of which four were inherited from his father and two from his mother, of the *MUC4* gene (Table 3).

#### Non-transmitted variants

The proband had 27 genes with non-transmitted autosomal heterozygous variants and one with a non-transmitted autosomal homozygous variant (Fig 1). The de novo

**Table 2** Compound heterozygous variants.

CHR	Gene	Variation type	mRNA	Protein	EXON	INTRON	Variants origin	Sister	Annotation
1	NBPF9	Mis-sense	NM_001277444.1:c.1077C > A	p.Pro360Thr	'8/15'	-	F	N	Mandibular prognathism
		Splice donor	ENST00000281815.8:c.349+2T > C	-	-	'11/12'	M	N	
6	SYNE1	Mis-sense	ENST00000423061.1:c.14868C > A	p.Ser4956Arg	'78/146'	-	F	N	Ataxia
		Mis-sense	NM_033071.3:c.599G > A	p.Gly200Asp	'8/146'	-	M	N	
16	NPIP12	Inframe insertion	ENST00000550665.1:c.1074_1085dupTCCACCCTCAGC	p.Pro359_ Ala362dup	'8/8'	-	F	N	NA
		Mis-sense	ENST00000354563.5:c.1838C > A	p.Pro613His	'3/3'	-	M	N	

CHR, chromosome; F, father; M, mother; N, the sister does not have the same variant as the proband; NA, not applicable.

**Table 3** Compound heterozygous variants.

CHR	Variation type	Gene	mRNA	Protein	Exon	Variants from	Sister	Annotation
3	Inframe insertion	MUC4	ENST00000477086.1:c.5037_5038insTCTCTTCCTGTCCACCAGCAC-TTCCTCAGCATCCACCGGTCACGCCACCCCTCTCCTGTCCACCGA CAATTCCTCAGTATCCACAGGT-CACGCCACC	p.Thr1679_Pro1680ins-SerLeuProVal ThrSerThrSerSerAlaSerThrGlyHisAla ThrProLeuProValThrAspAsnSerSerVal SerThrGlyHisAlaThr	'2/25'	F	N	Periodontitis
3	Inframe insertion	MUC4	XM_005269327.1:c.921delAinsGACACTTCCTCAGCATCCACAGGTCA CGCCACCCCTCTTCATGTCACCA	p.Thr292_Pro307dup	'1/3'	M	Y	
3	Inframe insertion	MUC4	XM_005269332.1:c.1162delAinsGCCCTTCCTCAGCATCCACAGGTCA CGCCACCCCTCTTCCTGTCCACCAA	p.Pro387_Met388insAla-LeuProGlnHis ProGlnVal-ThrProProLeuPheLeuSer-Pro	'3/5'	M	N	
3	Missense	MUC4	ENST00000478156.1:c.6602C > T	p.Ala2201Val	'2/24'	M	N	
3	Inframe insertion	MUC4	XM_005269327.1:c.921delAinsGACACTTCCTCAGCATCCACAGGTCA CGCCACCCCTCTTCATGTCACCA	p.Thr292_Pro307dup	'1/3'	F	Y	
3	Inframe insertion	MUC4	XM_005269331.1:c.2082delGinsTCAGTATCCACAGGTATGCCACCCCTCTTCATGTCACCGACACTCCG	p.Pro694_Gln695insGlnTyrProGlnVal MetProProLeuPheMetSerProThr-LeuPro	'5/5'	M	N	

CHR, chromosome; F, father; M, mother; N, the sister does not have the same variant as the proband; Y, the sister has the same variant as the proband.

autosomal homozygous variant is a frameshift variant in the *FOXO6* gene, whereas the other 26 de novo variants are autosomal heterozygous variants. Among these variants, there were nine genes (*BCL11A*, *OSR2*, *MUC6*, *KRT18*, *MEOX1*, *TLL6*, *KCTD1*, *ELAVL3* and *CD93*) with missense variants, eight (*NBPF12*, *FAM78A*, *AGAP4*, *LIPJ*, *DHX32*, *HERC2P4*, *TP53* and *DDX52*) with splice variants, two (*FOXO6* and *AP003062.1*) with frameshift variants, two (*MUC19* and *NPIPA5*) with inframe inser-

tions, four (*NPIP11*, *CHD3*, *MAP2K4* and *TBX2*) with inframe deletions, and one (*LOC101927628*) with a stop gained variant (Tables 4 and 5).

## Discussion

To determine the disease as a recessive inheritance mode, a large sample of pedigree separation analysis is often required.<sup>18</sup> For a small sample size, determin-

**Table 4** De novo missense and splice region variants in novel pathogenic genes.

	CHR	Inheritance	Gene	mRNA	Protein	Exon	Annotation
Missense	2	AD	<i>BCL11A</i>	ENST00000335712.6:c.1565C > G	p.Ala522Gly	'4/4'	Sickle cell disease and $\beta$ -thalassemia
	8	AD	<i>OSR2</i>	ENST00000457907.2:c.602A > G	p.Asp201Gly	'3/5'	Osteoblast function
	11	AD	<i>MUC6</i>	NM_005961.2:c.5709C > G	p.Ser1903Arg	'31/33'	Cancer
	12	AD	<i>KRT18</i>	XM_005268863.1:c.300C > G	p.Ser100Arg	'1/7'	Cancer
	17	AD	<i>MEOX1</i>	ENST00000318579.4:c.121A > C	p.Thr41Pro	'1/3'	Naegeli-Franceschetti-Jadassohn syndrome
	17	AD	<i>TTLL6</i>	NM_001130918.1:c.350G > C	p.Arg117Pro	'3/16'	Alzheimer's disease
	18	AD	<i>KCTD1</i>	NM_001142730.2:c.61G > C	p.Ala21Pro	'1/5'	Cementoblast differentiation
	19	AD	<i>ELAVL3</i>	XM_005259812.1:c.781G > C	p.Gly261Arg	'7/7'	Paraneoplastic neurologic disorders
	20	AD	<i>CD93</i>	NM_012072.3:c.346T > G	p.Trp116Gly	'1/2'	Human dental fluorosis
	CHR	Inheritance	Gene	mRNA	Protein	Intron	Annotation
Splice region	1	AD	<i>NBPF12</i>	ENST00000446760.2:c.-36+6T > G	NA	'6/28'	Triple negative breast cancer
	2	AD	<i>SP100</i>	XM_005246808.1:c.1612+3delA	NA	'18/27'	Cytomegalovirus infection
	2	AD	<i>TIA1</i>	ENST00000477044.2:c.223-3dupT	NA	'3/7'	Paget disease
	9	AD	<i>FAM78A</i>	ENST00000464831.1:c.109-4T > A	NA	'2/3'	Cancer
	10	AD	<i>AGAP4</i>	XM_005271798.1:c.382+3G > A	NA	'4/10'	Radiation exposure
	10	AD	<i>LIPJ</i>	NM_001010939.2:c.-103-3T > A	NA	'2/10'	Gestational diabetes
	10	AD	<i>DHX32</i>	ENST00000284690.3:c.850-7dupT	NA	'3/10'	Cancer
	16	AD	<i>HERC2P4</i>	ENST00000566591.1:n.232-5delT	NA	'2/6'	16p11.2-p12.2 duplication syndrome
	17	AD	<i>TP53</i>	ENST00000413465.2:c.783-6_783-5delCT	NA	'6/6'	Osteogenic differentiation of dental stem cells
	17	AD	<i>DDX52</i>	ENST00000349699.2:c.748-3delT	NA	'5/14'	Bone density in middle-aged and elderly Chinese

AD, autosomal dominant; CHR, chromosome; NA, not applicable; underline, variants fit the condition  $0.005 < \text{MAF} < 0.01$ .

ing the inheritance mode is quite difficult. The filtering process for the pathogenic gene from WES data should be very carefully. The detailed clinical phenotypes of family members are crucial for determining the genetic pattern of the disease, but the possibility of non-transmitted mutations cannot be ignored.<sup>19</sup> Unlike previous research, the filtering strategy used in the present study considered the potential for parent-derived variations as well as non-transmitted variants of the proband, and the classification of different genetic patterns provided a more complete idea of the subsequent genetic pathogenic gene filtering of core families with a small sample size.

Based on our findings, we predicted 18 missense variants including damaging, deleterious and disease-causing with 12 prediction tools (Table 6). There are many possible influences of a missense variant, including amino acid sequence, functional RNA and protein folding alterations. This mutation may have no effect on protein expression or may be beneficial; however, most of them have harmful or lethal effects.

The negative clinical phenotypes in the proband's parents and sister helped us to exclude the unrelated

variants from the possible inheritance mode, and four genes (*SHROOM2*, *SYTL5*, *MAGED1* and *FLNA*) were selected with a higher chance of causing MICRR. The proband carried variants in *SHROOM2*, *SYTL5*, *MAGED1* and *FLNA* genes from his mother. His sister carried heterozygous variants in *SHROOM2*, *SYTL5* and *MAGED1* and did not carry a variant allele in the *FLNA* gene but did not show disease. *SYTL5*, *MAGED1* and *FLNA* are related to osteoclastogenesis or osteoclast differentiation, and *SYTL5* is involved in NF- $\kappa$ B function (Table 1). Four genes (*NBPF9*, *SYNE1*, *NPIP12* and *MUC4*) with compound heterozygous variants were also considered (Tables 2 and 3); however, the bias caused by a single sample cannot be excluded. Because no other affected family members could help to narrow down the pathogenic gene<sup>11</sup>, we considered the de novo variants were not found from his parents.

Filtering genes with variants may be associated with tooth or bone development, saliva functions, odontoclasts and osteoclastogenesis (Tables 2 to 5). *FOXO6*, *OSR2*, *TP53*, *MAP2K4* and *TBX2* play important roles in osteoclast function or the osteogenic process. *OSR2*, *CHD3* and *TBX2* are involved in the tooth development

**Table 5** De novo frameshift, inframe variants and stop gained variants.

	CHR	Inheritance	Gene	mRNA	Protein	Exon	Annotation
Frameshift	1	AR	<i>FOXO6</i>	XM_002342102.5:c.1008_1009insGGGACGCCGCCTACTTCGGCGGCTGCAAGGGCGCGCCTACGGCGGGGGCGGGGGCTT	p.Gln337GlyfsTer177	'2/2'	Craniofacial complex
	11	AD	<i>AP003062.1</i>	ENST00000597621.1:c.280_314delAGTGGAGACCCAGCTTGCAGGCCATCAGAGGCTGC	p.Arg100SerfsTer285	'1/1'	Unknown
Inframe insertion	12	AD	<i>MUC19</i>	XM_003846356.2:c.14442_14443insGCT	p.Arg4814_Asn4815insAla	'55/171'	Protecting against demineralisation of teeth
	16	AD	<i>NPIPA5</i>	ENST00000360151.4:c.834delGinsTCTACCCTCAGCG	p.Ala278_Asp279insLeu-ProSerAla	'8/8'	Radioreistance
Stop gained	15	AD	<i>LOC101927628</i>	XM_005255006.1:c.46C > T	p.Arg16Ter	'1/1'	
Inframe deletion	16	AD	<i>NPIPB11</i>	ENST00000524087.1:c.1495_1620delCCTGCCGAGCATCTGCGGGGGCCGCTTCCACCCTCAGCGGATGATAATCTCAAGACACCTTCTGAGCGTCACTCCCTTCCACCCTCAGCTCCACCCTCAGCAGATGATAATATCAAGACA	p.Pro499_Thr540del	'8/8'	Psychosis
	17	AD	<i>CHD3</i>	XM_005256430.1:c.220_222delCCG	p.Pro74del	'1/34'	Tooth root development
	17	AD	<i>MAP2K4</i>	ENST00000353533.5:c.20_22delGCG	p.Gly10del	'1/11'	Osteoclastogenesis
	17	AD	<i>TBX2</i>	ENST00000419047.1:c.187_189delGCG	p.Ala63del	'1/7'	Tooth development

AD, autosomal dominant; AR, autosomal recessive; CHR, chromosome.

process, and *CHD3* may play a particularly significant role in tooth root development and subsequent cementogenesis. *KCTD1* is also possibly involved in cementoblast differentiation and mineralisation. *CD93* gene was downregulated in patients with human dental fluorosis and Kashin-Beck disease. *MUC19* and *MUC4* were related to saliva functions. There were four genes with compound heterozygous variants in which *NBPF9* was associated with mandibular prognathism (Table 2).

Here, we used the criteria for rare variants defined as having frequency < 0.5%, and common variants as having frequency > 5% according to the 1000 Genomes Project.<sup>17</sup> One article also defined rare variants as having a frequency of <1%.<sup>20</sup> If the selecting condition was changed to 1%, two more genes (*SP100* and *TIA1*) with splice variants would be reserved (Table 4). *TIA1* was associated with Paget disease which is one inducement of ECR; however, no typical phenotype of Paget disease was observed in the proband's physical examination, such as bone pain, arthropathy, deformity, fracture,

hearing loss, neurological complications or osteosarcoma. The present study showed the unreported pathogenic genes in MICRR, which enriched the genetic investigation of rare diseases.

MICRR originates from the mesial or distal CEJ and then spreads to the entire cervical region. It is mainly limited to the cervical region and less extended to the apical part.<sup>21</sup> It advances rapidly and sometimes can be accompanied by extensive gingivitis and periodontitis<sup>22,23</sup>, but there is no direct evidence of a relationship between MICRR and these two diseases. Caries are usually a chronic process that commonly occurs in pits and fissures of teeth. Rampant caries frequently occur in children. Adults suffering from rampant caries usually have some specific causes, such as an addiction to sweet foods, radiotherapy<sup>24</sup>, salivary gland dysfunction, xerostomia<sup>25</sup> or a habit of keeping cariogenic food in the mouth and then going to sleep.<sup>26</sup> However, the proband in the present study did not have a clear trigger, and the resorption progressed rapidly. Over a short period of 9



**Table 6** Prediction results of missense variants from different software.

	Variant	Type	Gene	Software prediction <sup>b</sup>											
				1	2	3	4	5	6	7	8	9	10	11	12
Variants fit XR <sup>a</sup> inheritance pattern	c.1549C > T	Mis-sense	SHROOM2	0.01	0.83	0.23	0.063963	0.003511	1.525	2.24	0.94	0.163	5.2155	0.94	0
	c.1409A > G	Mis-sense	SYTL5	0.02	0.997	0.984	0	0.9784	2.59	-0.7	5.88	1.973	15.2041	5.88	1
	c.865G > C	Mis-sense	MAGED1	0.78	0.999	0.961	0.117001	0.14329	1.04	4.07	0.442	-0.021	0.5291	0.442	0.94
	c.227C > T	Mis-sense	FLNA	0.03	0.001	0.119	0.025578	0.267632	1.725	-0.04	3.35	0.953	5.8987	3.35	0.828
De novo heterozygous variants	c.1565C > G	Mis-sense	BCL11A	0.28	0.996	0.984	0.032386	0.989977	1.7	3.34	5.46	2.563	18.9177	5.46	1
	c.602A > G	Mis-sense	OSR2	U	0.998	0.995	0	0.996931	1.795	3.39	3.42	2	9.2799	3.42	0.906
	c.5709C > G	Mis-sense	MUC6	0.11	0.998	0.993	U	U	1.735	3.37	-2.72	-0.74	1.8545	-2.72	0
	c.300C > G	Mis-sense	KRT18	0.05	0.149	0.162	0.007844	0.992958	2.05	-2.03	1.95	0.588	8.0905	1.95	1
	c.121A > C	Mis-sense	MEOX1	0.17	0.028	0.037	6.00E-06	0.642301	1.5	-2.86	3.56	1.968	4.5549	3.56	1
	c.350G > C	Mis-sense	TTLL6	0.08	0.289	0.16	0.012239	U	1.425	U	5.49	2.865	10.1692	5.49	1
	c.61G > C	Mis-sense	KCTD1	0.01	U	U	U	U	U	1.95	1.14	0.495	3.944	1.14	0.999
	c.781G > C	Mis-sense	ELAVL3	0.2	0.747	0.41	0	0.700611	1.15	2.92	3.68	2.231	3.7517	3.68	0.998
	c.346T > G	Mis-sense	CD93	0	1	1	3.60E-05	U	3.825	2.63	5.49	2.194	15.0546	5.49	1
	c.1077C > A	Mis-sense	NBPF9	0	1	1	U	0.002793	U	1.7	0.553	0.567	U	0.553	0.001
	c.6602C > T	Mis-sense	MUC4	U	0.773	0.546	U	0.000972	-0.55	3.13	U	-2.622	2.7646	0	0.002
	c.1838C > A	Mis-sense	NPIP12	0.01	0.999	0.996	U	U	U	0.3	U	U	U	U	U
	c.14868C > A	Mis-sense	SYNE1	0.47	0.546	0.13	0.001229	0.085582	1.5	1.76	-4.23	-0.853	3.894	-4.23	0.807
c.599G > A	Mis-sense	SYNE1	0.02	0.25	0.152	0.00341	0.983255	-0.04	-2.12	4.8	1.411	14.1097	4.8	0.921	

<sup>a</sup>XR, recessive variation on the X-chromosome.

<sup>b</sup>Pathogenicity of missense variants was predicted using 12 software platforms: SIFT, PolyPhen2\_HDIV, PolyPhen2\_HVAR, LRT, Mutation Taster, MutationAssessor, FATHMM, GERP\_plus, PhyloP, SiPhy, Gerp and PhastCons (from 1 to 12). Damaging, SIFT < 0.05, PolyPhen2\_HDIV (probably damaging >= 0.957, possibly damaging 0.453 <= pp2\_hdiv <= 0.956; benign <= 0.452), PolyPhen2\_HVAR (probably damaging >= 0.909, possibly damaging 0.447 <= pp2\_hdiv <= 0.909; benign <= 0.446) MutationAssessor > 1.938, FATHMM < -1.5, GERP++ > 3, PhyloP > 2.5, PhastCons > 0.6.

U, unknown.

months, most of the maxillary right teeth were lost due to rapid resorption in the tooth neck, and the rest of the teeth were widely involved in cervical resorption.

In the early stages, typical MICRR is usually asymptomatic but sometimes presents pink colour changes in the tooth neck. Resorption is usually invasive and progresses rapidly, and may form a cavity with sharp edges and a large amount of granulation tissue inside. The pulp vitality test is positive. Radiographs show a thin cervical pulp wall, a small amount of dentine

around the pulp and apple core-like lesions at the CEJ.<sup>14,22</sup> In later stages, the dentine may be resorbed completely, causing crown fracture and ultimately dentition defects.<sup>13</sup> Many studies have reported that tooth loss is closely associated with overall health.<sup>22-26</sup> Tooth loss had a positive association with accelerated aging<sup>27</sup>, new-onset Parkinson's disease<sup>28</sup>, coronary heart disease and stroke<sup>28</sup>, diabetes<sup>29</sup> and oro-digestive cancers.<sup>30</sup> Tooth loss and hypertension showed a bidirectional association.<sup>31</sup>



The pathogenic aetiology of MICRR is currently unclear. Most scholars believe it is associated with the enhanced activity of odontoclasts.<sup>6,11,13,22</sup> Numerous lysosomes containing high-density particulate surrounding mitochondrion in the granulation tissue were observed in MICRR cases.<sup>14</sup> MICRR was regarded as similar to feline odontoclastic resorptive lesions in cats.<sup>6,32</sup> Few genetic studies have been performed in MICRR cases.<sup>11,33</sup> The variants in *IRF8* and *FLNA* has been reported to be associated with MICRR.<sup>33</sup> However, the inheritance mode of the pedigree was not fully considered, and should be validated experimentally in gene-edited mice. The evidence would have been more convincing had there been experimental verification. Sanger sequencing should be performed to confirm the possible pathogenic genes in the future. The variants selected in this study were used as predictions only, which cannot explain the causal relationship between these variants and MICRR.

## Conclusion

In the present study, 35 genes were filtered and found to be potentially associated with MICRR, but no conclusion could be drawn regarding the genetic pattern of MICRR. These data will strengthen the aetiological diagnosis of MICRR, and the authors expect to increase the understanding of pathogenetic mechanisms of MICRR in the future.

## Acknowledgements

The authors thank all the subjects for their participation and all the clinicians who provided assistance in this study.

## Conflicts of interest

The authors declare no conflicts of interest related to this study.

## Author contribution

Dr Yu Meng WANG collected the clinical data, performed the bioinformatic analysis and drafted the manuscript; Dr Wen Yan RUAN revised the manuscript; Dr Dan Dan CHI collected the DNA samples and performed the original sequencing; Dr Xiao Hong DUAN designed and supervised the study and revised the manuscript.

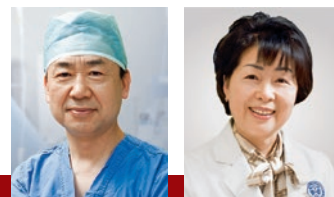
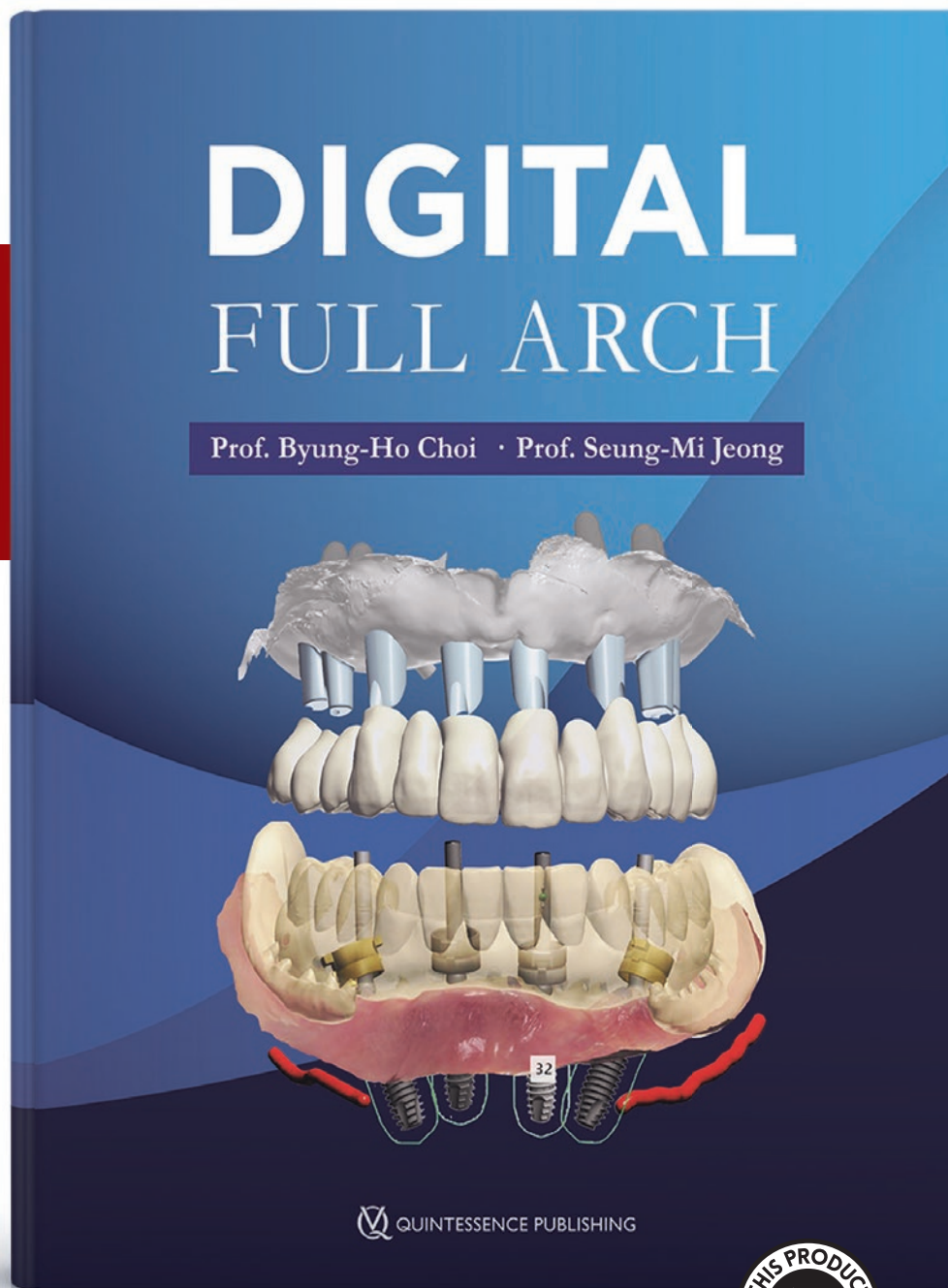
(Received Oct 12, 2023; accepted Nov 16, 2023)

## References

1. Patel S, Saberi N. The ins and outs of root resorption. *Br Dent J* 2018;224:691–699.
2. Jeng PY, Lin LD, Chang SH, et al. Invasive cervical resorption—Distribution, potential predisposing factors, and clinical characteristics. *J Endod* 2020;46:475–482.
3. Patel S, Mavridou AM, Lambrechts P, Saberi N. External cervical resorption-part 1: Histopathology, distribution and presentation. *Int Endod J* 2018;51:1205–1223.
4. Kjær I, Strøm C, Worsaae N. Regional aggressive root resorption caused by neuronal virus infection. *Case Rep Dent* 2012;2012:693240.
5. Kumar V, Chawla A, Kaur A. Multiple idiopathic cervical root resorptions in patients with hepatitis B virus infection. *J Endod* 2018;44:1575–1577.
6. Chu EY, Deeb JG, Foster BL, Hajishengallis E, Somerman MJ, Thumbigere-Math V. Multiple idiopathic cervical root resorption: A challenge for a transdisciplinary medical-dental team. *Front Dent Med* 2021;2:652605.
7. Wang N, Zhang M, Zhu J, Zhu Y, Wu J. Multiple idiopathic cervical root resorption: A systematic review. *Oral Dis* 2023;29:2409–2422.
8. Yu VSH, Messer HH, Tan KB. Multiple idiopathic cervical resorption: case report and discussion of management options. *Int Endod J* 2011;44:77–85.
9. Coyle M, Toner M, Barry H. Multiple teeth showing invasive cervical resorption—An entity with little known histologic features. *J Oral Pathol Med* 2006;35:55–57.
10. Mattar R, Pereira SA, Rodor RC, Rodrigues DB. External multiple invasive cervical resorption with subsequent arrest of the resorption. *Dent Traumatol* 2008;24:556–559.
11. Thumbigere-Math V, Foster BL, Bachu M, et al. Inactivating mutation in *IRF8* promotes osteoclast transcriptional programs and increases susceptibility to tooth root resorption. *J Bone Miner Res* 2019;34:1155–1168.
12. Samara E, Kelly E, Walker R, Borumandi F. Multiple idiopathic cervical root resorption: Case report of an unusual presentation. *Spec Care Dentist* 2021;41:98–102.
13. Mikušková K, Vaňuga P, Adamicová K, et al. Multiple idiopathic external cervical root resorption in patient treated continuously with denosumab: A case report. *BMC Oral Health* 2022;22:129.
14. Wu J, Lin LY, Yang J, et al. Multiple idiopathic cervical root resorption: A case report. *Int Endod J* 2016;49:189–202.
15. Llavayol M, Pons M, Ballester ML, Berástegui E. Multiple cervical root resorption in a young adult female previously treated with chemotherapy: A case report. *J Endod* 2019;45:349–353.
16. Duan X, Yang S, Zhang H, et al. A novel *AMELX* mutation, its phenotypic features, and skewed X inactivation. *J Dent Res* 2019;98:870–878.
17. 1000 Genomes Project Consortium; Auton A, Brooks LD, Durbin RM, et al. A global reference for human genetic variation. *Nature* 2015;526:68–74.
18. Pakkanen S, Baffoe-Bonnie AB, Matikainen MP, et al. Segregation analysis of 1,546 prostate cancer families in Finland shows recessive inheritance. *Hum Genet* 2007;121:257–267.
19. Richards S, Aziz N, Bale S, et al. Standards and guidelines for the interpretation of sequence variants: a joint consensus recommendation of the American College of Medical Genetics and Genomics and the Association for Molecular Pathology. *Genet Med* 2015;17:405–424.

20. UK10K Consortium; Walter K, Min JL, Huang J, et al. The UK10K project identifies rare variants in health and disease. *Nature* 2015;526:82–90.
21. Macaraeg K, Lee SM, Kalra L, Velasco M, Hajishengallis E. Multiple external root resorption in a pediatric patient with familial expansile osteolysis. *Pediatr Dent* 2020;42:62–65.
22. Chen X, Yu X, Yan K, Liu S, Sun Z, Li S. Multiple idiopathic cervical root resorption involving all permanent teeth. *Aust Endod J* 2020;46:263–271.
23. Liang H, Burkes EJ, Frederiksen NL. Multiple idiopathic cervical root resorption: systematic review and report of four cases. *Dentomaxillofac Radiol* 2003;32:150–155.
24. Li SS, Wu CZ, Qiao XH, Li CJ, Li LJ. Advances on mechanism and treatment of salivary gland in radiation injury [in English, Chinese]. *Hua Xi Kou Qiang Yi Xue Za Zhi* 2021;39:99–104.
25. Quilici D, Zech KN. Prevention and treatment options for medication-induced xerostomia. *Gen Dent* 2019;67:52–57.
26. Namita, Rai R. Adolescent rampant caries. *Contemp Clin Dent* 2012;3:S122–S124.
27. Xu KH, Li L, Jia SL, et al. Association of tooth loss and diet quality with acceleration of aging: Evidence from NHANES. *Am J Med* 2023;136:773–779.e774.
28. Woo HG, Chang Y, Lee JS, Song TJ. Association of tooth loss with new-onset Parkinson's disease: A nationwide population-based cohort study. *Parkinsons Dis* 2020;2020:4760512.
29. Kaur G, Holtfreter B, Rathmann W, et al. Association between type 1 and type 2 diabetes with periodontal disease and tooth loss. *J Clin Periodontol* 2009;36:765–774.
30. Al-Maweri SA, Ibraheem WI, Al-Ak'hali MS, Shamala A, Halboub E, Alhadj MN. Association of periodontitis and tooth loss with liver cancer: A systematic review. *Crit Rev Oncol Hematol* 2021;159:103221.
31. Xu K, Yu W, Li Y, et al. Association between tooth loss and hypertension: A systematic review and meta-analysis. *J Dent* 2022;123:104178.
32. von Arx T, Schawalder P, Ackermann M, Bosshardt DD. Human and feline invasive cervical resorptions: the missing link?--Presentation of four cases. *J Endod* 2009;35:904–913.
33. Qin W, Gao J, Ma S, et al. Multiple cervical root resorption involving 22 teeth: A case with potential genetic predisposition. *J Endod* 2022;48:1526–1532.

# OPTIMAL TECHNIQUES AND SOLUTIONS



Byung-Ho Choi | Seung-Mi Jeong

## Digital Full Arch

314 pages, 1,091 illus  
ISBN 978-89-85917-21-6  
€250

Full-arch rehabilitation is one of the most challenging implant-driven oral therapies. As a result, complications frequently occur. In this book, an attempt is made to find the optimal solutions to avoid these complications using digital systems, with the focus on the method that can prevent or minimize them rather than how to deal with them. The book describes definitive outcomes and scientific proof of the efficacy of various digital full-arch systems for All-on-4 and All-on-6 implant treatment as well as the proper techniques to obtain the greatest benefits. The entire digital workflow is discussed with the use of detailed photographs and supplementary videos.

QUINTESSENZ PUBLISHING



QUINTESSENZ PUBLISHING



# Hub Genes, Possible Pathways and Predicted Drugs in Hereditary Gingival Fibromatosis by Bioinformatics Analysis

Rong Xia YANG<sup>1</sup>, Fan SHI<sup>1</sup>, Shu Ning DU<sup>1</sup>, Xin Yu LUO<sup>1</sup>, Wan Qing WANG<sup>1</sup>, Zhi Lu YUAN<sup>1</sup>, Dong CHEN<sup>1</sup>

**Objective:** To explore potential pathogenic processes and possible treatments using unbiased and reliable bioinformatic tools.

**Methods:** Gene expression profiles of control and hepatocyte growth factor (HGF) samples were downloaded from CNP0000995. Analysis of differentially expressed genes (DEGs) was conducted using R software (version 4.2.1, R Foundation, Vienna, Austria). Functional enrichment analyses were performed using the Gene Ontology (GO), Kyoto Encyclopaedia of Genes and Genomes (KEGG) and Gene Set Enrichment Analysis (GSEA) databases, then the protein-protein interaction (PPI) network was constructed to screen the top 10 hub genes. Finally, five genes related to cell junctions were selected to build gene-miRNA interactions and predict small-molecule drugs.

**Results:** A total of 342 downregulated genes and 188 upregulated genes were detected. Candidate pathways include the extracellular matrix (ECM) receptor interaction pathway, the TGF- $\beta$  signalling pathway and the cell adhesion molecule (CAM) pathway, which were discovered through KEGG and GSEA enrichment studies. GO analyses revealed that these DEGs were significantly enriched in cell adhesion, the adherens junction and focal adhesion. Five hub genes (CDH1, SNAP25, RAC2, APOE and ITGB4) associated with cell adhesion were identified through PPI analysis. Finally, the gene-miRNA regulatory network identified three target miRNAs: hsa-miR-7110-5p, hsa-miR-149-3p and hsa-miR-1207-5p. Based on the gene expression profile, the small-molecule drugs zebularine, ecuronium and prostratin were selected for their demonstrated binding activity when docked with the mentioned molecules.

**Conclusion:** This study offered some novel insights into molecular pathways and identified five hub genes associated with cell adhesion. Based on these hub genes, three potential therapeutic miRNAs and small-molecule drugs were predicted, which are expected to provide guidance for the treatment of patients with HGF.

**Keywords:** CDH1, cell-cell junction, hereditary gingival fibromatosis, MiRNA, small-molecule drugs

*Chin J Dent Res* 2024;27(1):101–109; doi: 10.3290/j.cjdr.b5128671

1 Department of Stomatology, The First Affiliated Hospital of Zhengzhou University, Zhengzhou, P.R. China.

**Corresponding author:** Dr Dong CHEN, Department of Stomatology, The First Affiliated Hospital of Zhengzhou University, No.1 Jianshe East Road, Erqi District, Zhengzhou 450052, P.R. China. Tel: 86-371-66913114. Email: chendongfmmu@163.com

This study was supported by The National Natural Science Foundation of China (82170920).

Hereditary gingival fibromatosis (HGF) is an uncommon condition characterised by localised or widespread lesions on the gingiva and its cause is still unclear. It can be inherited as autosomal dominant or recessive mode and cause enlargement of the gingiva.<sup>1</sup> An excessive amount of gum tissue can cover the visible part of the teeth, leading to tooth displacement, retention of primary teeth, and difficulties with speech and chewing.<sup>2</sup> Rarely present at birth, alveolar ridge thickening often

starts when permanent teeth begin to emerge. It tends to worsen during childhood and may occasionally persist into adolescence.<sup>3</sup> Some drugs, including immunosuppressants, calcium channel blockers and antiepileptic medications, are also linked to gingival overgrowth.<sup>4</sup> It is important to establish an aetiology and develop appropriate treatment plans based on the aetiology.

The pathological manifestations of the gingiva consisted of dense connective tissue that is rich in collagen fibre bundles and infiltrated by inflammatory cells. Researchers have identified several hallmarks of epithelial-to-mesenchymal transition (EMT), including basal lamina rupture and migration of epithelial cells into connective tissue.<sup>5,6</sup> EMT is the process whereby epithelial cells transform into fibroblast-like cells associated with organ development, oral submucous fibrosis and the invasion of oral squamous cell carcinoma in oral tissue. Recently, EMT has been proposed as a new pathogenic mechanism that contributes to the development of drug-induced gingival fibrosis.<sup>7,8</sup> Cellular proliferation and the abnormal accumulation of extracellular matrix (ECM) components, including collagen, integrin, fibronectin and glycosaminoglycans, are also the causes of gingival fibrosis. The molecular processes that cause this pathogenic process, however, are not fully understood.

Current treatment options for this condition are limited to surgical procedures, such as gingivectomy and gingivoplasty, which unfortunately have a high recurrence rate.<sup>9</sup> For clinical diagnosis and treatment, it is crucial to understand the molecular and pathophysiological mechanisms of HGF. The purpose of this study is to investigate the molecular pathways associated with the HGF RNA-seq datasets obtained from the China National GeneBank Database (CNCBdb) and to explore potential therapeutic targets.

## Materials and methods

### *Data collection and processing*

We downloaded the BAM-formatted human genome RNA-seq datasets of primary fibroblasts from HGFs and normal gingival tissues, which included two HGFs and three normals (the BAM data of CNR0453836 is incomplete), from CNCBdb (<https://db.cngb.org/>). In our study, the data were first processed through a series of steps: Trim Galore was used for quality control of the CNP000099510 high-throughput data. STAR was employed to compare the reference genome and RSEM software was used to quantify gene expression.

### *Identification of differentially expressed genes (DEGs)*

The original datasets were converted into a recognisable format using R software (version 4.2.1), The “DESeq2” R package was then used to normalise and identify differentially expressed genes (DEGs). The threshold values for DEG detection were determined to be  $|\log_2(\text{fold change [FC]})| > 1$  and  $P < 0.05$ . A volcano plot was created using <http://www.sangerbox.com>.<sup>11</sup>

### *Kyoto Encyclopedia of Genes and Genomes (KEGG) and Gene Ontology (GO) analysis*

Kyoto Encyclopedia of Genes and Genomes (KEGG) pathway enrichment analysis was conducted in R software using the package “clusterProfiler”. Gene Ontology (GO) analysis, which includes enrichment for biological processes (BPs), cellular components (CCs) and molecular functions (MFs), was conducted via <http://metascape.org>.  $P < 0.05$  was considered statistically significant.

### *Further Gene Set Enrichment Analysis (GSEA) analysis*

All genomic data from both HGFs and normal gingival samples were uploaded to for Gene Set Enrichment Analysis (GSEA). Enrichments were considered significant when the NES  $> 1.0$ , the normalised  $P < 0.05$  and the FDR  $< 0.25$ .

### *Construction of protein-protein interaction (PPI) network*

The Search Tool for the Retrieval of Interacting Genes (STRING, <https://string-db.org>) was used to identify protein-protein interactions (PPI) among DEGs. The interaction score was set at 0.4. The result of the PPI network was processed and analysed using Cytoscape version 3.9.1. The key genes in the PPI network were then screened using the CytoHubb plugin.

### *Further screening of hub genes*

Hub gene-associated cell junctions according to the STRING database were further screened and the evidence was listed.

### *Gene-miRNA network construction*

Targeted miRNAs were predicted using miRWalk 3.0 (<http://mirwalk.umm.uni-heidelberg.de/>) and the miRDB database (<http://www.mirdb.org/>). The minimum seed sequence length was set to 6 mer and the

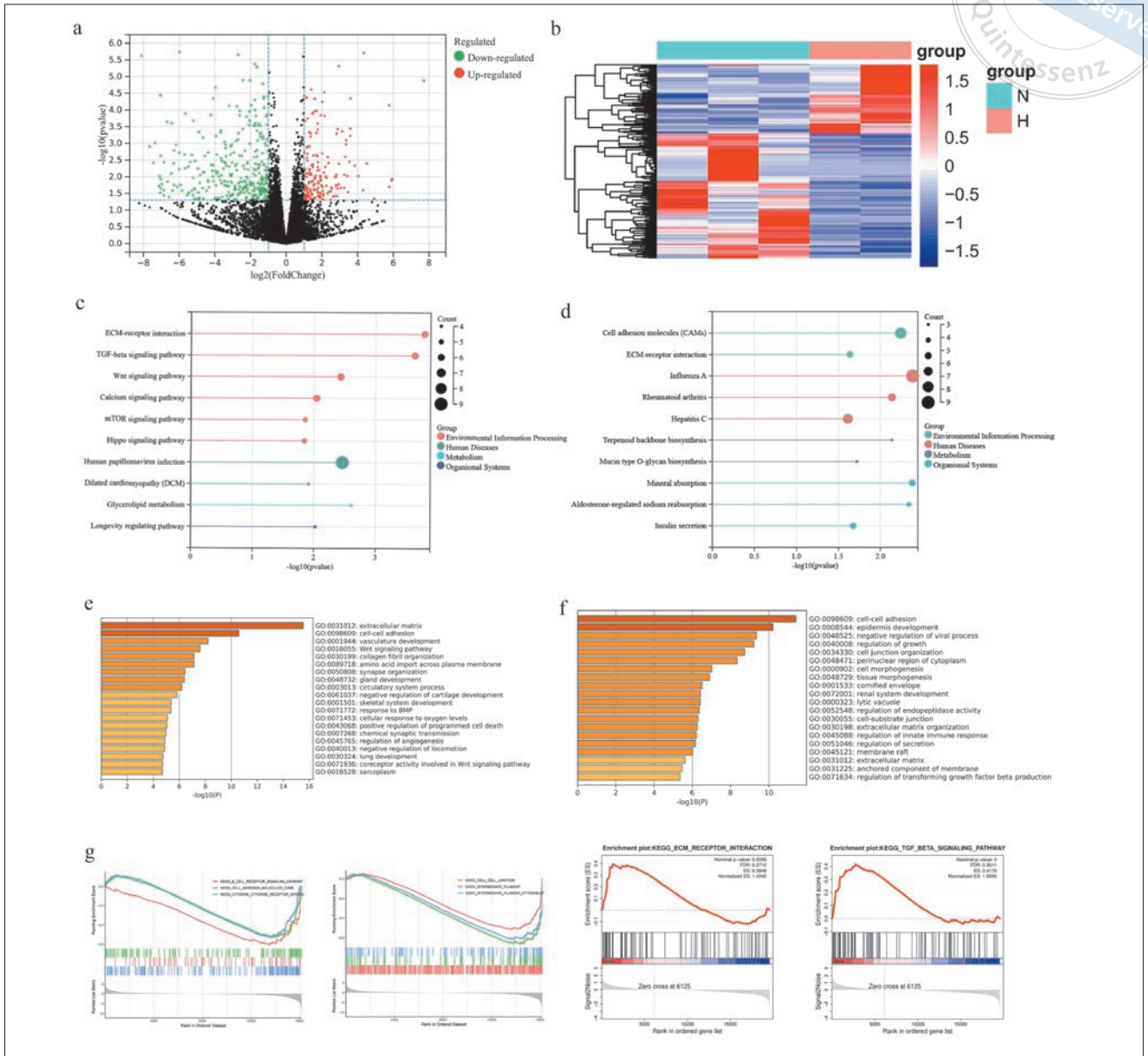


**Fig 1** Volcano plot of 530 DEGs. The black dots represent genes with no appreciable variation in expression, whereas the red and green dots represent genes that are upregulated and downregulated genes, respectively (a). Heatmap of all DEGs in the HGF group and normal group. N represents gingival fibroblasts from normal and H represents gingival fibroblasts from HGF (b). Upregulated genes as identified by KEGG, ECM receptor interaction and the TGF- $\beta$  signalling pathway are significantly enriched (c). Downregulated genes as identified by KEGG and CAMs are significantly enriched (d). Upregulated genes as identified by GO analysis and extracellular matrix are significantly enriched (e). Downregulated genes as identified by GO analysis and cell-cell adhesion are significantly enriched (f). Pathway and CC enrichment plots of GSEA showed CAMs pathways, ECM receptor interaction pathway, TGF- $\beta$  signalling pathway and cell-cell adhesion in HGF are more active than normal (g).

selection criteria were set at  $P < 0.95$ . MiRNAs that target more than two genes were selected as a result.

### *Small-molecule drug prediction*

Connectivity Map (<https://clue.io/>) is an online database of chemical reagent action expression profiles. We inputted the top 150 upregulated genes and the top 150 downregulated DEGs into the Query tool. From the results, we selected the top three small-molecule chemical medicines with the highest scores to be molecularly docked with hub genes.

### *Molecular docking*

The PDB database (<http://www.rcsb.org/>) was used to obtain the 3D structures of the protein molecules, and the PubChem database (<https://pubchem.ncbi.nlm.nih.gov/>) was employed to obtain the structures of the small-molecule medications. The 3D structure was examined using the molecular docking program AutoDock Vina1.2.0 and 3D docking pictures were generated using PyMOL 2.5.2. It is widely acknowledged that a specific binding activity between the small-molecule medication and the protein when the binding energy is less than  $-4.25$  kcal/mol. Additionally, when the binding energy is less than  $-5.0$  kcal/mol, it is deemed that the two have a strong binding activity.<sup>12</sup>

### *Statistical analysis*

All analyses were performed using R software. The “DESeq2” R package used negative binomial distribution and functional enrichment analyses used a hypergeometric test. Significance was defined as  $P < 0.05$ .

## **Results**

### *DEG analysis*

The CNP0000995 dataset contained 530 DEGs, including 188 upregulated genes and 342 downregulated genes. These DEGs were presented in a volcano plot (Fig 1a) and a heatmap (Fig 1b).

### *Enriched GO, KEGG pathway analysis of the DEGs*

For the analysis of GO and KEGG pathway enrichment, the ECM receptor interaction pathway, TGF- $\beta$  signalling pathway and cell adhesion molecule (CAM) were significantly enriched in the KEGG analysis (Fig 1c and

d). GO analysis results showed that changes in BPs of DEGs were significantly enriched in several categories, including cell-cell adhesion, cell junction organisation, extracellular matrix, regulation of transforming growth factor beta production and collagen fibril organisation. Changes in cell-substrate junctions and the extracellular matrix were primarily enriched in CCs (Fig 1e and f).

### *GSEA analysis*

GSEA analysis found that cell-cell junctions, CAMs pathways, the ECM receptor interaction pathway and TGF- $\beta$  signalling pathway were significantly enriched in the HGF group (Fig 1g).

### *Construction and analysis of the PPI network*

A PPI network was established that included upregulated and downregulated genes based on a combined score  $> 0.4$ , which was considered statistically significant. Cytoscape software (version 3.9.1) was used to visualise the integrated regulatory network and identify the high (marked in red) and low (marked in green) levels of gene expression (Fig 2a). The top 10 genes, ranked by betweenness level using the CytoHubba plugin in Cytoscape, were chosen (Fig 2b). These genes included CDH1, SNAP25, RAC2, APOE, ITGB4, SFN, AHR, CXCL12, SCN2A and CD24 (Table 1).

### *Further screening of hub genes*

Five hub genes associated with cell adhesion according to the String database were screened out, namely CDH1, SNAP25, RAC2, APOE and ITGB4 (Fig 2c), and the evidence was listed (knowledge and text mining) (Table 2).

### *Further miRNA mining and interaction network analysis*

Predicted miRNAs for five genes associated with cell adhesion and gene-miRNA interactions were visualised in Cytoscape 3.9.1 (Fig 3). Target miRNAs with a high number of gene crosslinks  $\geq 2$  were selected, including hsa-miR-7110-5p, hsa-miR-149-3p and hsa-miR-1207-5p.

### *Small-molecule drug screening*

The gene expression profile was compared and examined using the Connectivity Map database. We selected three small-molecule drugs with the potential to modify the expression profile and ranked them in order of effectiveness, from highest to lowest. First was zebular-



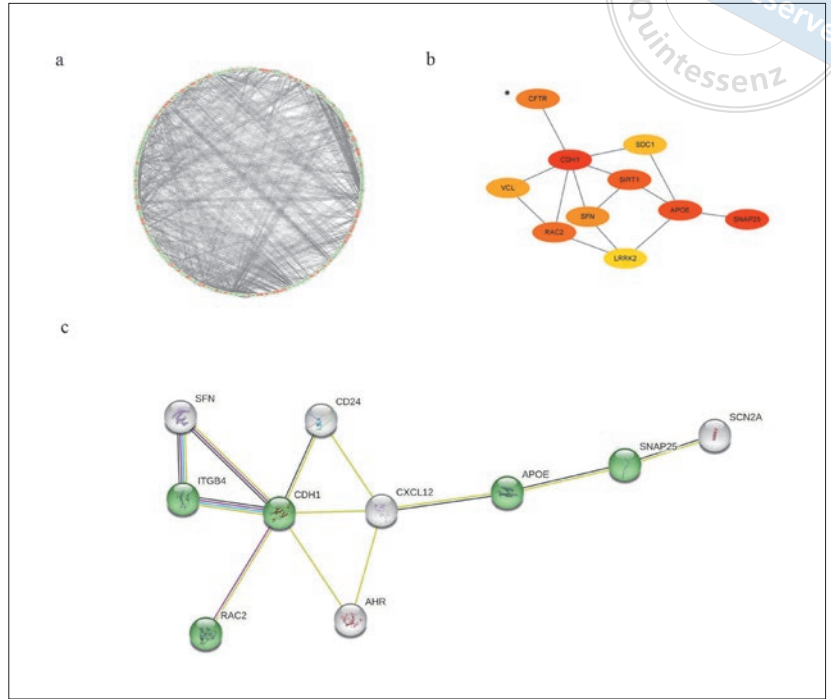


**Fig 2** PPI network of DEGs formed using Cytoscape, with red and green dots representing genes that are upregulated and downregulated, respectively (a). Ten hub genes (CDH1, SNAP25, RAC2, APOE, ITGB4, SFN, AHR, CXCL12, SCN2A and CD24) with the greatest significance were chosen in the PPI network and the colour from red to yellow indicates high to low scores (b). Five hub genes (CDH1, SNAP25, RAC2, APOE and ITGB4) associated with cell adhesion were chosen (marked in green) (c).

**Table 1** Top 10 genes in the network ranked by betweenness method.

Rank	Symbol	Up/down	Score
1	DH1	Down	84
2	SNAP25	Down	14
3	RAC2	Down	14
4	APOE	Down	10
5	ITGB4	Down	9
6	SFN	Down	9
7	AHR	Up	9
8	CXCL12	Down	9
9	SCN2A	Down	8
10	CD24	Down	8

**Table 2** Evidence for five genes.

Knowledge	Name	Source	Evidence	Confidence
Knowledge	APOE	UniProtKB	IDA/CURATED	★★★★★
	CDH1	UniProtKB	IDA	★★★★★
	ITGB4	UniProtKB	IDA/CURATED	★★★★★
Text mining	Name	Z-score	Confidence	
	CDH1	7.3	★★★★★	
	RAC2	5.2	★★★	
	SNAP25	6.2	★★★★★	

ine, a DNA methyltransferase inhibitor, with an enrichment score of -85.32. Second was vecuronium, which acts as an antagonist to the acetylcholine receptor, with

an enrichment score of -82.22, and third was prostratin, a PKC activator, with an enrichment score of -81.29 (Table 3).

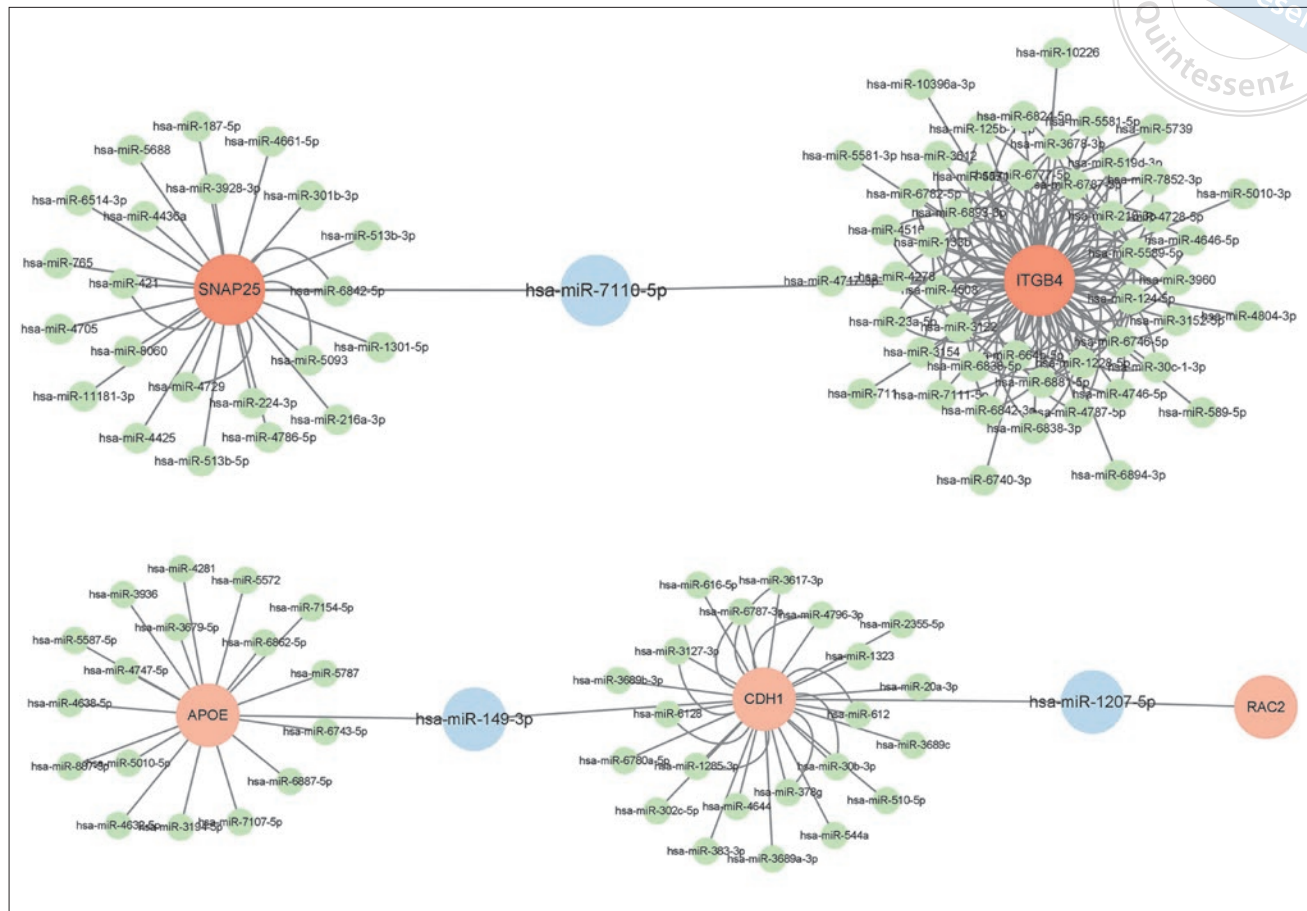


**Fig 3** Gene-miRNA interactions were constructed according to miRWalk 3.0 and the miRDB database. Genes are represented by the red dot, and target miRNAs are represented by the blue dot. Target miRNAs include hsa-miR-7110-5p, hsa-miR-149-3p and hsa-miR-1207-5p.

**Table 3** Small-molecule drug Information.

Rank	ID	Type	Name	Description	Score
a	BRD-A01145011	CP	Zebularine	DNA methyltransferase inhibitor	-85.32
b	BRD-K61341215	CP	Vecuronium	Acetylcholine receptor antagonist	-82.22
c	BRD-K91145395	CP	Prostratin	PKC activator	-81.29

CP, compound; ID, broad identity.

*Molecular docking*

We docked zebularine, vecuronium and prostratin with the five molecules (APOE, CDH1, RAC2, SNAP25 and ITGB4). Table 4 displays the data for molecular docking and binding energy. The binding site map for vecuronium and APOE is shown in Fig 4a. Through ARG-32, APOE interacts with ligands to form hydrogen bonds. The binding energy of Selumetinib with DCT is -6.18 kcal/mol, indicating high binding activity. The binding site map for vecuronium and CDH1 is presented in Fig 4b. Through ILE-146, CDH1 interacts with ligands

to form hydrogen bonds. The binding energy of Selumetinib with DCT is -4.52 kcal/mol, indicating strong binding activity. A diagram of the prostratin and CDH1 binding site is shown in Fig 4c. Through ALA-132, GLU-129 and TYR-148, CDH1 interacts with ligands via hydrogen bonds. The binding energy of Selumetinib with DCT is 4.52 kcal/mol, suggesting some binding activity. Fig 4d shows the binding site map of zebularine and RAC2. RAC2 interacts with ligands through GLN-180 and TYR-154, forming a hydrogen bond. Zebularine and RAC2 have a binding energy of -4.44 kcal/mol, suggesting that they exhibit binding activity.

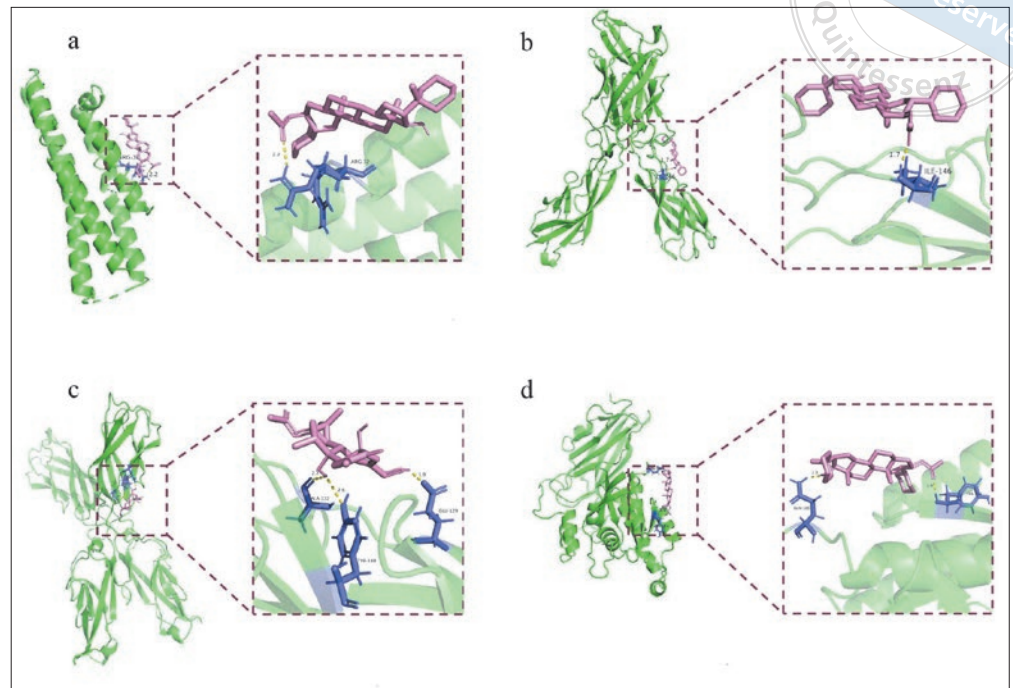


**Fig 4** Molecular docking modes according to Auto-Dock Vina1.2.0. The binding energy of APOE complexed with vecuronium was  $-6.18$  kcal/mol (a). The binding energy of CDH1 complexed with vecuronium was  $-4.52$  kcal/mol (b). The binding energy of CDH1 complexed with prostratin was  $-4.52$  kcal/mol (c). The binding energy of RAC2 complexed with zebularine was  $-4.44$  kcal/mol (d).

**Table 4** Docking parameters and results.

No.	Target	Protein	Compound	Minimum binding energy(kcal/mol)
a	APOE	Synaptosomal-associated protein 25	Vecuronium	-6.18
b	APOE	Synaptosomal-associated protein 25	Prostratin	-3.95
c	APOE	Synaptosomal-associated protein 25	Zebularine	-3.01
d	CDH1	Cadherin 1	Vecuronium	-4.52
e	CDH1	Cadherin 1	Prostratin	-4.52
f	CDH1	Cadherin 1	Zebularine	-2.14
g	RAC2	Rac Family Small GTPase 2	Vecuronium	-2.24
h	RAC2	Rac Family Small GTPase 2	Prostratin	-4.12
i	RAC2	Rac Family Small GTPase 2	Zebularine	-4.44
j	SNAP25	Synaptosome Associated Protein 25	Vecuronium	-4.23
k	SNAP25	Synaptosome Associated Protein 25	Prostratin	-2.97
l	SNAP25	Synaptosome Associated Protein 25	Zebularine	-2.15
m	ITGB4	Integrin Subunit Beta 4	Vecuronium	-3.14
n	ITGB4	Integrin Subunit Beta 4	Prostratin	-2.29
o	ITGB4	Integrin Subunit Beta 4	Zebularine	-1.89

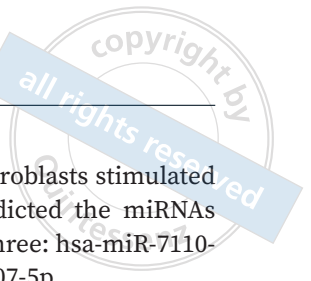
## Discussion

The present authors identified 530 DEGs, including 188 upregulated genes and 342 downregulated genes. The ECM receptor interaction pathway, TGF- $\beta$  signalling pathway and CAMs pathway were all involved in HGF, according to KEGG and GSEA enrichment studies. GO functional analysis showed that DEGs were primarily enriched in cell adhesion, the adherens junction and focal adhesion. In addition, five genes (CDH1, SNAP25, RAC2, APOE and ITGB4) associated with cell adhesion were screened. Finally, the authors made predictions of

miRNA molecules and small-molecule drugs based on these five hub genes.

The aetiology of HGF is most significant histologically in terms of increased ECM accumulation and degeneration. TGF- $\beta$ , a multifunctional cytokine that plays a key role in inflammation, wound healing and fibrosis, is an important contributor to ECM deposition and EMT processes in tissue fibrosis.<sup>13,14</sup> The findings of our bioinformatics analytics fully align with these conclusions.

In this study, we also discovered that the CAMs pathway was significantly enriched in the KEGG and GSEA



analyses. Furthermore, the GO analysis focused on cell adhesion, adherens junction and focal adhesion. Cell adhesion refers to the ability of a single cell to adhere to the surface of another cell or another inanimate object, such as ECM. To establish connections between cells or between cells and the extracellular matrix, the process of cell adhesion relies on a wide range of proteins known as CAMs, including integrins, selectins, cadherins, members of the immunoglobulin superfamily (IgSF) and mucins.<sup>15</sup> CAMs have mostly been studied in relation to tumours and can mediate the interaction between tumour cells and host cells and ECM, playing a crucial role in the multi-stage sequential process of tumour metastasis.<sup>16</sup> However, some studies also suggest that CAMs can contribute to fibrosis in different organs, such as the liver<sup>17</sup> and lungs.<sup>18</sup>

CDH1, a transmembrane adhesion receptor involved in the regulation of cell adhesion, migration and epithelial cell proliferation<sup>19</sup>, scored highest among the five hub genes. Downregulation of CDH1 is considered a crucial event in the progression of EMT. Iwano et al<sup>20</sup> found that type II EMT is the primary source of fibroblasts in connective tissue fibrosis. Another study suggests that cyclosporin A can induce type II EMT in gingiva by modifying the morphology of epithelial cells and changing the EMT markers, such as CDH1.<sup>21</sup> The pathogenic function of type II EMT in HGF, however, remains unclear. Roman-Malo et al<sup>5</sup> observed some histologic features that have been described for EMT in gingival lesions of HGF patients. Based on the above information, we hypothesise that the downregulation of CDH1 leads to the loss of intercellular adhesion, which in turn induces type II EMT and ultimately results in HGF fibrosis. Nevertheless, this is only an initial hypothesis, and more trials are required to confirm it.

The laminin receptor ITGB4, a vital structural component of the hemidesmosome in epithelial cells, was found to be downregulated in our study.<sup>22</sup> It plays a crucial role in tissue morphogenesis by regulating cell adhesion, morphology, polarity and differentiation. According to studies, renal fibrosis and herpes epidermolysis bullosa are linked to the ITGB4 gene.<sup>23,24</sup> Nevertheless, there is insufficient data regarding the connection between ITGB4 and gingival fibrosis.

MiRNAs are a type of traditional non-coding RNA that play a role in regulating various physiological and pathological functions.<sup>25</sup> Current studies have shown that microRNA may participate in the fibrosis of various organs.<sup>26</sup> In HGF, the expression of miR-355-3p is downregulated in gingival fibroblasts as well as in nor-

mally occurring human gingival fibroblasts stimulated by TGF- $\beta$ .<sup>27</sup> In this study, we predicted the miRNAs through the database, resulting in three: hsa-miR-7110-5p, hsa-miR-149-3p and hsa-miR-1207-5p.

Hsa-miR-1207-5p has been reported to be closely associated with cancer development and metastasis. It may function as a novel EMT-negative regulator inhibiting the invasion and metastasis of cancer cells in nasopharyngeal, gastric, lung and oral cancers.<sup>28-30</sup> MiR-149-3p has been proven to be closely associated with liver and lung fibrosis and may be involved in the EMT process in tumour cells. However, no study has shown that the aforementioned miRNA molecules are associated with therapeutic treatments for gingival fibrosis. This association needs to be confirmed through further trials.

The present study has certain limitations because the sample size is small, which restricts the scope of analysis. In the absence of experimental confirmation, further fundamental studies are required to validate the results and identify the crucial genes and pathways. Additionally, further research must be conducted to investigate whether small-molecule medications and the miRNAs discovered can serve as potential therapeutic targets for HGF.

## Conclusion

The present authors found potential pathogenic pathways, such as the CAMs pathway and ECM receptor interaction pathway. GO analysis suggested that cell adhesion may potentially play a role in HGF. The authors also screened hub genes involved in cell adhesion, including CDH1, SNAP25, RAC2, APOE and ITGB4.

## Conflicts of interest

The authors declare no conflicts of interest related to this study.

## Author contribution

Drs Rong Xia YANG, Fan SHI, Shu Ning DU, Xin Yu LUO, Wan Qing WANG and Zhi Lu YUAN contributed to the data analysis; Dr Rong Xia YANG contributed to the manuscript draft; Dr Dong CHEN contributed to the study conception and manuscript revision.

(Received Jun 30, 2023; accepted Nov 23, 2023)

## References

1. Strzelec K, Dziedzic A, Łazarz-Bartyzel K, et al. Clinics and genetic background of hereditary gingival fibromatosis. *Orphanet J Rare Dis* 2021;16:492.
2. Afonso RA, Godinho GV, Silva CA, Silva EJ, Volpato LE. Hereditary gingival fibromatosis and developmental anomalies: A case report. *Cureus* 2022;14:e24219.
3. Resende EP, Xavier MT, Matos S, Antunes AC, Silva HC. Non-syndromic hereditary gingival fibromatosis: Characterization of a family and review of genetic etiology. *Spec Care Dentist* 2020;40:320–328.
4. Bakshi SS, Choudhary M, Agrawal A, Chakole S. Drug-induced gingival hyperplasia in a hypertensive patient: A case report. *Cureus* 2023;15:e34558.
5. Roman-Malo L, Bullon B, de Miguel M, Bullon P. Fibroblasts collagen production and histological alterations in hereditary gingival fibromatosis. *Diseases* 2019;7:39.
6. Bawazir M, Islam MN, Cohen DM, Fitzpatrick S, Bhattacharyya I. Gingival fibroma: An emerging distinct gingival lesion with well-defined histopathology. *Head Neck Pathol* 2021;15:917–922.
7. Hazzaa HH, Gouda OM, Kamal NM, et al. Expression of CD163 in hereditary gingival fibromatosis: A possible association with TGF- $\beta$ 1. *J Oral Pathol Med* 2018;47:286–292.
8. Kamal NM, Hamouda MA, Abdelgawad N. Expression of TGF- $\beta$  and MMP-2 in hereditary gingival fibromatosis epithelial cells. A possible contribution of the epithelium to its pathogenesis. *J Oral Biol Craniofac Res* 2022;12:617–622.
9. Bektaş-Kayhan K, Selvi F, Koca-Ünsal RB. Surgical treatment of hereditary gingival fibromatosis by diode laser: Report of five rare cases in the same family. *Spec Care Dentist* 2023;43:539–545.
10. Wu J, Chen D, Huang H, et al. A novel gene ZNF862 causes hereditary gingival fibromatosis. *Elife* 2022;11:e66646.
11. Shen W, Song Z, Zhong X, et al. Sangerbox: A comprehensive, interaction-friendly clinical bioinformatics analysis platform. *iMeta* 2022;1:e36.
12. Li C, Shi Y, Zuo L, et al. Identification of biomarkers associated with cancerous change in oral leukoplakia based on integrated transcriptome analysis. *J Oncol* 2022;2022:4599305.
13. Budi EH, Schaub JR, Decaris M, Turner S, Derynck R. TGF- $\beta$  as a driver of fibrosis: Physiological roles and therapeutic opportunities. *J Pathol* 2021;254:358–373.
14. Walton KL, Johnson KE, Harrison CA. Targeting TGF- $\beta$  mediated SMAD signaling for the prevention of fibrosis. *Front Pharmacol* 2017;8:461.
15. Samanta D, Almo SC. Nectin family of cell-adhesion molecules: Structural and molecular aspects of function and specificity. *Cell Mol Life Sci* 2015;72:645–658.
16. Harjunpää H, Lloret Asens M, Guenther C, Fagerholm SC. Cell adhesion molecules and their roles and regulation in the immune and tumor microenvironment. *Front Immunol* 2019;10:1078.
17. Hintermann E, Christen U. The many roles of cell adhesion molecules in hepatic fibrosis. *Cells* 2019;8:1503.
18. Hu Q, Saleem K, Pandey J, Charania AN, Zhou Y, He C. Cell adhesion molecules in fibrotic diseases. *Biomedicines* 2023;11:1995.
19. Meigs TE, Fedor-Chaiken M, Kaplan DD, Brackenbury R, Casey PJ. Galpha12 and Galpha13 negatively regulate the adhesive functions of cadherin. *J Biol Chem* 2002;277:24594–24600.
20. Iwano M, Plieth D, Danoff TM, Xue C, Okada H, Neilson EG. Evidence that fibroblasts derive from epithelium during tissue fibrosis. *J Clin Invest* 2002;110:341–350.
21. Fu MM, Chin YT, Fu E, et al. Role of transforming growth factor-beta1 in cyclosporine-induced epithelial-to-mesenchymal transition in gingival epithelium. *J Periodontol* 2015;86:120–128.
22. Du X, Yuan L, Yao Y, et al. ITGB4 deficiency in airway epithelium aggravates RSV infection and increases HDM sensitivity. *Front Immunol* 2022;13:912095.
23. Luo C, Yang L, Huang Z, et al. Case report: A case of epidermolysis bullosa complicated with pyloric atresia and a literature review. *Front Pediatr* 2023;11:1098273.
24. Wee LWY, Tan EC, Bishnoi P, et al. Epidermolysis bullosa with pyloric atresia associated with compound heterozygous ITGB4 pathogenic variants: Minimal skin involvement but severe mucocutaneous disease. *Pediatr Dermatol* 2021;38:908–912.
25. Ho PTB, Clark IM, Le LTT. MicroRNA-based diagnosis and therapy. *Int J Mol Sci* 2022;23:7167.
26. Ghafouri-Fard S, Abak A, Talebi SF, et al. Role of miRNA and lncRNAs in organ fibrosis and aging. *Biomed Pharmacother* 2021;143:112132.
27. Gao Q, Yang K, Chen D, et al. Antifibrotic potential of MiR-335-3p in hereditary gingival fibromatosis. *J Dent Res* 2019;98:1140–1149.
28. Chen L, Lü MH, Zhang D, et al. miR-1207-5p and miR-1266 suppress gastric cancer growth and invasion by targeting telomerase reverse transcriptase. *Cell Death Dis* 2014;5:e1034.
29. Alvarez ML, Khosroheidari M, Eddy E, Kiefer J. Role of microRNA 1207-5P and its host gene, the long non-coding RNA Pvt1, as mediators of extracellular matrix accumulation in the kidney: Implications for diabetic nephropathy. *PLoS One* 2013;8:e77468.
30. Dang W, Qin Z, Fan S, et al. miR-1207-5p suppresses lung cancer growth and metastasis by targeting CSF1. *Oncotarget* 2016;7:32421–32432.

# Chinese Journal of Dental Research

The Official Journal of the Chinese Stomatological Association (CSA)

## GUIDELINES FOR AUTHORS

*Chinese Journal of Dental Research* is a peer-reviewed general dental journal published in English by the Chinese Stomatological Association. The Journal publishes original articles, short communications, invited reviews, and case reports. Manuscripts are welcome from any part of the world. The Journal is currently published quarterly and distributed domestically by CSA and internationally by Quintessence Publishing Co Ltd.

All authors are asked to adhere to the following guidelines.

### Manuscript submission

ScholarOne Manuscripts for *Chinese Journal of Dental Research* (CJDR) has been launched.

To submit your outstanding research results more quickly, please visit: <http://mc03.manuscriptcentral.com/cjdr>

Any questions, please contact:

4F, Tower C, Jia 18#, Zhongguancun South Avenue, HaiDian District, 100081, Beijing, P.R. China. E-mail: [editor@cjdrca.com](mailto:editor@cjdrca.com);  
Tel: 86-10-82195785; Fax: 86-10-62173402.

Submitted manuscripts must be unpublished original papers that are not under consideration for publication elsewhere. Submissions that have been published with essentially the same content will not be considered. This restriction does not apply to results published as an abstract. The submission of a manuscript by the authors means that the authors automatically agree to assign exclusive licence to the copyright to CSA if and when the manuscript is accepted for publication.

Manuscripts must be accompanied by a letter from all authors or from one author on behalf of all the authors containing a statement that the manuscript has been read and approved by all the authors and the criteria for authorship have been met. It should also contain the following statement: "The attached (enclosed) paper entitled ... has not been published and is not being submitted for publication, in whole or in part, elsewhere".

Manuscripts that reveal a lack of proper ethical consideration for human subjects or experimental animals will not be accepted for publication. The Journal endorses the Recommendations from the Declaration of Helsinki.

### Format of Papers

#### Preparation of manuscripts

The manuscript should be written clearly and concisely and be double-spaced on 21 x 29 cm white paper with at least 2.5 cm margin all around. All pages should be numbered, beginning from section of title page, and followed by abstract, introduction, materials and methods, results, discussion, acknowledgements, references, figure legends and figures/tables. Non-standard abbreviations should be defined when first used in the text. Use a standard font such as Times New Roman or Arial to avoid misrepresentation of your data on different computers that do not have the unusual or foreign language fonts. For units, the Journal recommends the use of the International System of Units (SI Units). For authors whose native language is not English, the Journal strongly recommends improving the English in the manuscript by consulting an English-speaking scientist before submission.

**Title page** should include: full title (a brief declarative statement of the major findings of the research), full names of authors, professional affiliations and complete postal address, telephone and fax number, and email address of the corresponding author. If the work was supported by a grant, indicate the name of the supporting organisation and the grant number.

**Abstract and keywords:** 250 words presented in a concise form and including the purpose, general methods, findings, and conclusions of the research described in the paper. A list of 5 keywords or short phrases (a few words per phrase) suitable for indexing should be typed at the bottom of the abstract page. Avoid vague or overly general terms. If necessary, the keywords will be adjusted to the standards of the Journal by the editors without consulting the authors.

**Introduction:** should begin with a brief introduction of background related to the research and should be as concise as possible. The rationale of the study should be stated.

**Materials and Methods:** should be described clearly and referenced in sufficient detail. Description should be such that the reader can judge the accuracy, reproducibility, reliability, etc. of the work.

**Results:** should present the experimental data in tables and figures with suitable descriptions and avoid extended discussions of its relative significance.

**Discussion:** should focus on the interpretation and significance of the findings with concise objective comments. Speculation is to be based on data only. The text should be written with a logical connection between the introduction and conclusions.

**Acknowledgements:** should only recognise individuals who provided assistance to the project.

**References:** should be cited in the text using superscript numbers and typed in numerical order following a style below:

1. Sorensen JA, Engleman MT, Torres TJ, Avera SP. Shear bond strength of composite resin to porcelain. *Int J Prosthodont* 1991;4:17-23.
2. Renner RP, Boucher LJ. Removable Particle Dentures. Chicago: Quintessence, 1987:24-30.
3. White GE, Johson A van Noort R, Northeast SE, Winstanley B. The quality of cast metal ceramic crowns made for the NHS [abstract 48]. *J Dent Res* 1990;69(special issue):960.
4. Jones DW. The strength and strengthening mechanisms of dental ceramics. In: McLean JW (ed). *Dental ceramics: Proceedings of the First International Symposium on Ceramics*. Chicago: Quintessence, 1983:83-41.
5. Rosenstiel S. *The Marginal Reproduction of Two Elasto meric Impression Materials* [Master's thesis]. Indianapolis: Indiana University, 1997.

**Figures and Tables:** should be numbered consecutively with Arabic numerals, with each one displayed on a separate page. Photographs should be of excellent quality with a width of 8 cm or 17 cm. All figures and tables should be cited in the text. Please refer to a current volume of this Journal for general guidance.

**Legends for all figures,** including charts and graphs, must be typed together on a separate page and should be understandable without reference to the text, including a title highlighting the key results and a key for any symbols or abbreviations used in the figure.

#### Case reports

Authors should describe one to three patients or a single family. The text is limited to no more than 2500 words, and up to 15 references.

#### Revised Manuscripts

All revisions must be accompanied by a cover letter to the Editor. The letter must detail on a point-by-point basis the contributors' disposition of each of the referees' comments, and certify that all contributors approve of the revised content.

# GET A HANDLE ON EVERYTHING

Perfect training with Quintessence e-books:  
compact, portable, always available

Copyright by  
all rights reserved  
Quintessenz



We offer our e-books on numerous platforms (including Apple Books, Google Play Books, Amazon Kindle Store). So you can read our e-books on the device of your choice: smartphone, tablet, e-reader, laptop or PC. You can find all our e-books here: [www.quint.link/e-books](http://www.quint.link/e-books).

